THE FETAL ORIGINS OF METABOLIC DISORDERS

EDITED BY: Takahiro Nemoto, Tomoko Aoyama and Hiroaki Itoh
PUBLISHED IN: Frontiers in Endocrinology

frontiers Research Topics

ISSN 1664-8714
ISBN 978-2-88976-664-2
DOI 10.3389/978-2-88976-664-2

About Frontiers

Frontiers is more than just an open-access publisher of scholarly articles: it is a pioneering approach to the world of academia, radically improving the way scholarly research is managed. The grand vision of Frontiers is a world where all people have an equal opportunity to seek, share and generate knowledge. Frontiers provides immediate and permanent online open access to all its publications, but this alone is not enough to realize our grand goals.

Frontiers Journal Series

The Frontiers Journal Series is a multi-tier and interdisciplinary set of open-access, online journals, promising a paradigm shift from the current review, selection and dissemination processes in academic publishing. All Frontiers journals are driven by researchers for researchers; therefore, they constitute a service to the scholarly community. At the same time, the Frontiers Journal Series operates on a revolutionary invention, the tiered publishing system, initially addressing specific communities of scholars, and gradually climbing up to broader public understanding, thus serving the interests of the lay society, too.

Dedication to Quality

Each Frontiers article is a landmark of the highest quality, thanks to genuinely collaborative interactions between authors and review editors, who include some of the world's best academicians. Research must be certified by peers before entering a stream of knowledge that may eventually reach the public - and shape society; therefore, Frontiers only applies the most rigorous and unbiased reviews.
Frontiers revolutionizes research publishing by freely delivering the most outstanding research, evaluated with no bias from both the academic and social point of view. By applying the most advanced information technologies, Frontiers is catapulting scholarly publishing into a new generation.

What are Frontiers Research Topics?

Frontiers Research Topics are very popular trademarks of the Frontiers Journals Series: they are collections of at least ten articles, all centered on a particular subject. With their unique mix of varied contributions from Original Research to Review Articles, Frontiers Research Topics unify the most influential researchers, the latest key findings and historical advances in a hot research area! Find out more on how to host your own Frontiers Research Topic or contribute to one as an author by contacting the Frontiers Editorial Office: frontiersin.org/about/contact

THE FETAL ORIGINS OF METABOLIC DISORDERS

Topic Editors:
Takahiro Nemoto, Nippon Medical School, Japan
Tomoko Aoyama, University of Auckland, New Zealand
Hiroaki Itoh, Hamamatsu University School of Medicine, Japan

Citation: Nemoto, T., Aoyama, T., Itoh, H., eds. (2022). The Fetal Origins of Metabolic Disorders. Lausanne: Frontiers Media SA. doi: 10.3389/978-2-88976-664-2

Table of Contents

frontiers | Frontiers in Endocrinology

EDITORIAL
published: 04 July 2022
doi: 10.3389/fendo.2022.942256

Editorial: A Half-Century History of Nutritional Guidance for Pregnant Women in Japan: A Promising Research Target of the DOHaD Study

Hiroaki Itoh[1]*, *Tomoko Aoyama*[2,3], *Yukiko Kohmura-Kobayashi*[1] and *Takahiro Nemoto*[4]

[1] Department of Obstetrics and Gynecology, Hamamatsu University School of Medicine, Hamamatsu, Japan, [2] Liggins Institute, University of Auckland, Auckland, New Zealand, [3] National Institutes of Biomedical Innovation, Health and Nutrition, Tokyo, Japan, [4] Department of Bioregulatory Science (Physiology), Nippon Medical School, Tokyo, Japan

Keywords: developmental origins of health and disease (DOHaD), Japan, low birthweight, weight gain in pregnancy, nutrition

Editorial on the Research Topic

The Fetal Origins of Metabolic Disorders

INTRODUCTION

The Research Topic of 'The Fetal Origins of Metabolic Disorders' was based on the concept of the Developmental Origins of Health and Disease (DOHaD) theory (1). DOHaD theory connects metabolic disorders of offspring with environmental disruptions during the early critical developmental period. DOHaD theory was devised from the findings of three well-known cohort studies: British (2) and Finnish (3) studies that demonstrated adult health deterioration of low birthweight babies (less than 2,500 g), and a Dutch study (4) of increased risk of adult lifestyle diseases in the people who experienced severe undernourishment *in utero* during the 'Dutch Famine' in World War II.

Since the early 1980s in Japan, the rate of low birthweight infants has increased and has remained high at about 10% (**Figure 1**). In this editorial, we introduce the origins and changes of Japanese nutritional guidance for pregnant women and discuss the possible importance of follow-up studies of the offspring to compare health prognoses.

THE HISTORY OF NUTRITIONAL MANAGEMENT OF PREGNANT WOMEN IN JAPAN GOES BACK TO EPIDEMIOLOGICAL RESEARCH DURING WORLD WAR II

At the end of World War II, there was extreme famine around Amsterdam, the so-called 'Dutch Famine'. During the famine, pregnant women had low incidence rates of preeclampsia (5) and decreased blood pressure during labour (6). Based on a clinical study (7), the Japan Society of Obstetrics and Gynecology (JSOG) officially recommended energy intake restrictions for pregnant women who developed preeclampsia in 1981 (**Figure 1**) (8). In consideration of the effect of this treatment policy, the Perinatal Committee of JSOG aimed to prevent preeclampsia for general

OPEN ACCESS

Edited and reviewed by:
Cunming Duan,
University of Michigan, United States

***Correspondence:**
Hiroaki Itoh
ihiroaki@hama-med.ac.jp

Specialty section:
This article was submitted to Experimental Endocrinology, a section of the journal Frontiers in Endocrinology

Received: *12 May 2022*
Accepted: *16 May 2022*
Published: *04 July 2022*

Citation:
Itoh H, Aoyama T, Kohmura-Kobayashi Y and Nemoto T (2022) Editorial: A Half-Century History of Nutritional Guidance for Pregnant Women in Japan: A Promising Research Target of the DOHaD Study. Front. Endocrinol. 13:942256. doi: 10.3389/fendo.2022.942256

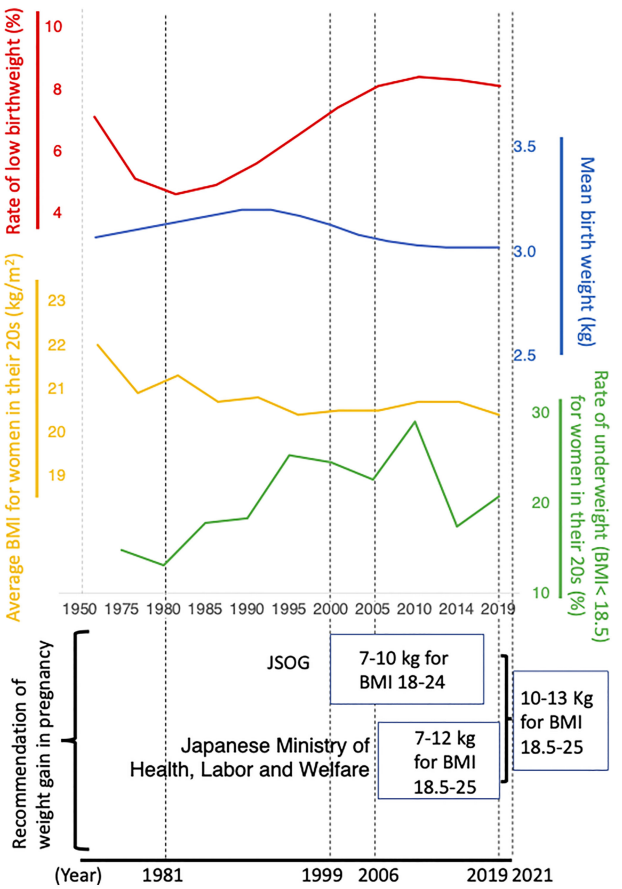

FIGURE 1 | Comparison of the longitudinal changes of rate of low birthweight (%), mean birthweight (kg), average BMI for women in their 20s (kg/m^2), rate of being underweight (BMI < 18.5) for women in their 20s (%), and recommendation of weight gain in pregnancy at that time in Japan. BMI; body mass index (kg/m^2). JSOG; Japan Society of Obstetrics and Gynecology. Web data used for **Figure 1** is summarized in **Supplemental Table 1**.

pregnant women and formulated a guideline for maternal weight gain in pregnancy in 1997 that was published in 1999 (**Figure 1**) (9). This guideline recommended weight gain of 7-10 kg during pregnancy for pregnant women with a BMI of 18-24 kg/m^2 (**Figure 1**) (9).

Independently, the Japanese Ministry of Health, Labour and Welfare published the 'Optimal weight gain chart during pregnancy' in 2006, which recommended aiming for a birth weight of 2,500 g to 4,000 g and a weight gain of 7-12 kg during pregnancy for women with a BMI of 18.5 to 25 kg/m^2 (**Figure 1**) (10). It was a serious problem at that time that there were two different guidelines, JSOG 1999 and Ministry of Health, Labour and Welfare 2006, that were enforced in parallel in Japan (**Figure 1**). Moreover, the purpose of the recommendation was different between the two guidelines (prevention of preeclampsia, and aiming for an appropriate birth weight of 2,500 g to 4,000 g, respectively).

Hytten and Leitch, performed metabolic analysis on pregnant Caucasian women of normal physique and calculated physiological weight gain due to pregnancy to be 12.5 kg (11). It is suggested that the weight gain recommendation of JSOG 1999 as well as Ministry of Health, Labour and Welfare 2006 may be less than the physiological weight gain of pregnant women; however, there is no report that performed an exact metabolic analysis of Japanese pregnant women.

WITHDRAWAL OF 1999 JSOG RECOMMENDATIONS OF WEIGHT GAIN IN PREGNANCY

Based on the DOHaD theory, an article by Normile (2018) in 'Science' reported that the rate of low birthweight since the early 1980s had increased in Japan and may induce serious health problems in future generations, and that there was considerable involvement of the recommendation of strict weight gain during pregnancy by JSOG 1981 in the continuous decrease of birthweight since the early 1980s in Japan (12). However, JSOG 1981 recommended the restriction of calorie intake only to pregnant women complicated with eclampsia (8), whereas the recommendation of strict weight gain restrictions for general pregnant women for the purpose of preventing preeclampsia was published in 1999 (9) (**Figure 1**), when a decrease in Japanese birthweight had already been occurring for two decades (13). However, this may have had a contribution to this trend.

It is also noted that young Japanese women have a strong desire to be thin (14) and their BMI has continued to decline (**Figure 1**), which may be one of important candidates causing a decrease in Japanese birthweight (13). Nevertheless, in consideration of the 'Science' article, the JSOG Perinatal Committee acknowledged that the 1999 JSOG recommendation of weight gain in pregnancy was below the physiological increase and may be harmful for fetuses especially concerning long-term health outcomes, and that there had been little evidence supporting its preventive effect for preeclampsia. Therefore, they decided to officially withdraw the 1999 JSOG recommendation (15).

2021 FORMULATION OF NEW RECOMMENDATIONS OF WEIGHT GAIN IN PREGNANCY

From the background described in the previous chapter, a new 'JSOG reference value for weight gain during pregnancy 2021' was formulated (16). For pregnant women with a BMI of 18.5 to 25 kg/m^2, the recommended value for weight gain due to pregnancy was 10-13 kg (16), which was quite a large amount compared to that of JSOG 1999 (7-10 kg for BMI of 18 to 24 kg/m^2) (9) or Japanese Ministry of Health, Labour and Welfare 2006 (7-12 kg for BMI of 18.5 to 25 kg/m^2) (10) (**Figure 1**). The Japanese Ministry of Health, Labour and Welfare withdrew the 2006 recommendation and officially accepted that of JSOG 2021 (17).

IMPACT OF FUTURE LONG-TERM COHORT STUDIES IN JAPAN AS A UNIQUE MODEL OF DOHAD POPULATION STUDY

In Japan, mean birthweight decreased and the rate of low birthweight increased from the early 1980s. Rather strict restrictions were recommended between 1991 and 2019 (**Figure 1**); however, this was followed by a sudden increase of the weight gain recommendation in 2021. The average BMI of the childbearing generation has decreased (**Figure 1**). These characteristic changes may indicate distinct differences in intrauterine nutritional conditions between the different generations. Therefore, it is an interesting and valuable research target to investigate the long-term prognosis of Japanese offspring of the different generations and possible associations with maternal dietary conditions.

CONTRIBUTIONS OF THE ARTICLES PUBLISHED ON THE RESEARCH TOPIC

The Research Topic of 'The Fetal Origins of Metabolic Disorders' fundamentally consists of: 1) environmental disruption in the early critical period, 2) resultant phenotypic and/or metabolic disorders in the offspring, and 3) programming. As for environmental disruption in the early critical period, Ishiyama et al. reported that there were embryonal nutritional effects, Molle et al. described thrifty eating behavior, Lundy et al. reported vitamin D deficiency, and Nemoto et al. demonstrated the effects of nicotine exposure. Regarding resultant phenotypic and/or metabolic disorders in the offspring, Huang et al. and Ikenoue et al. reported changes of fetal growth or composition, and Suzuki et al. and Zhang et al. reported changes in adipose tissue. Regarding programming, Yang et al., Sato et al., and Liu et al. investigated fibroblast growth factor 19, ghrelin, and fatty acid binding protein 4, respectively; Itoh et al. focused on chronic inflammation, (metaflammation); and Kasuga et al. reported epigenetic changes.

AUTHOR CONTRIBUTIONS

All authors contributed to the drafting and editing of this editorial and approved the final version.

FUNDING

This work was supported by JSPS KAKENHI Grant Numbers JP20H03823, JP20K09666, and JP20K16886, and AMED under Grant Number JP21gm1310009.

SUPPLEMENTARY MATERIAL

The Supplementary Material for this article can be found online at: https://www.frontiersin.org/articles/10.3389/fendo.2022.942256/full#supplementary-material

REFERENCES

1. Gluckman PD, Hanson MA. *Developmental Origins of Health and Disease*. Cambridge, United Kingdom: Cambridge University Press (2006).
2. Barker DJP. Mothers, Babies and Health in Later Life. *Edinburgh: Churchill Livingstone* (1998).
3. Eriksson JG. Early Growth, and Coronary Heart Disease and Type 2 Diabetes: Experiences From the Helsinki Birth Cohort Studies. *Int J Obes (Lond)* (2006) 30 Suppl 4:S18–22. doi: 10.1038/sj.ijo.0803515
4. de Rooij SR, Painter RC, Holleman F, Bossuyt PM, Roseboom TJ. The Metabolic Syndrome in Adults Prenatally Exposed to the Dutch Famine. *Am J Clin Nutr* (2007) 86(4):1219–24. doi: 10.1093/ajcn/86.4.1219
5. Smith CA. The Effect of Wartime Starvation in Holland Upon Pregnancy and its Product. *Am J Obstet Gynecol* (1947) 53(4):599–608. doi: 10.1016/0002-9378(47)90277-9
6. Ribeiro MD, Stein Z, Susser M, Cohen P, Neugut R. Prenatal Starvation and Maternal Blood Pressure Near Delivery. *Am J Clin Nutr* (1982) 35(3):535–41. doi: 10.1093/ajcn/35.3.535
7. Kido K, Aso T, Hatyashi S, Murata M, Yamada Y, Inoue T, et al. Low Calorie Therapy for Toxemia of Pregnancy. *Acta Obstet Gynaecol Japonica* (1977) 29(10):1305–13.
8. Furuya H, Sugawa H, Fukuda T, Ichizyou M, Nakayama M, Honda H, et al. Revision of Guideline of Nutritional Management in Toxemia of Pregnancy in Annual Report of the Committee of Nutrition and Metabolism. *Acta Obstet Gynaecol Japonica* (1981) 33(5):730.
9. Nakabayashi M. Guideline of Nutritional Management in Toxemia of Pregnancy. *Acta Obstet Gynaecol Japonica* (1999) 51(12):N–507-N-10.
10. Japanese Ministry of Health, Labour and Welfare. *Optimal Weight Gain Chart During Pregnancy* (2006). Available at: https://www.mhlw.go.jp/houdou/2006/02/dl/h0201-3a4.pdf.
11. Hytten FE, Leitch I. *The Physiology of Human Pregnancy*. London: Blackwell (1971).
12. Normile D. Staying Slim During Pregnancy Carries a Price. *Science* (2018) 361 (6401):440. doi: 10.1126/science.361.6401.440
13. Itoh H, Khomura-Kobayashi Y, Kawai K, Kanayama N. Multiple Causative Factors Underlie Low Birthweight. *Science (eLetters)* (2018) 361(6401):440. doi: 10.1126/science.361.6401.440.
14. Inokuchi M, Matsuo N, Takayama JI, Hasegawa T. Trends in Thin Body Stature Among Japanese Female Adolescents, 2003-2012. *Ann Hum Biol* (2015) 42(6):533–7. doi: 10.3109/03014460.2014.975280
15. Itoh H, Itakura A, Kanayama N, Ikeda T. Withdrawal of the 1999 JSOG Recommendation of Weight Gain Restriction During Pregnancy (Commentary of the JSOG Perinatal Committee). *J Obstet Gynaecol Res* (2019) 45(11):2302. doi: 10.1111/jog.14080
16. Itakura A, Aoki S, Umazume T, Zagoh H, Matsunaga K, Masuyama H, et al. Guidelines for Weight Gain During Pregnancy(Commentary of the JSOG Perinatal Committee). *Acta Obstet Gynaecol Japonica* (2021) 73(6):678–9.
17. Japanese Ministry of Health, Labour and Welfare. *Dietary Guidelines During Pregnancy and After Childbirth* (2021). Available at: https://www.mhlw.go.jp/seisakunitsuite/bunya/kodomo/kodomo_kosodate/boshi-hoken/ninpu-02.html.

Conflict of Interest: The authors declare that the research was conducted in the absence of any commercial or financial relationships that could be construed as a potential conflict of interest.

this article, or claim that may be made by its manufacturer, is not guaranteed or endorsed by the publisher.

frontiers in Endocrinology

ORIGINAL RESEARCH
published: 09 June 2021
doi: 10.3389/fendo.2021.694336

Prenatal Nicotine Exposure Induces Low Birthweight and Hyperinsulinemia in Male Rats

Takahiro Nemoto[1]*, *Hisae Ando*[2], *Mototsugu Nagao*[2], *Yoshihiko Kakinuma*[1] and *Hitoshi Sugihara*[2]

[1] Department of Bioregulatory Science (Physiology), Nippon Medical School, Tokyo, Japan, [2] Department of Endocrinology, Diabetes and Metabolism, Nippon Medical School, Tokyo, Japan

Smoking during pregnancy is one of the causes of low birthweight. Ingestion of nicotine during pregnancy has various metabolic impacts on the fetus and offspring. According to the developmental origins of health and disease theory, low birthweight is a risk factor for developing various non-communicable diseases, including diabetes. We hypothesized that when nicotine-induced low-birthweight rats, when exposed to a high-fat diet (HFD) after growth, are predisposed to glucose intolerance as a result of a mismatch between the eutrophic environment and small body size. Therefore, we investigated whether hyperinsulinemia was caused by exposure of nicotine-induced low-birthweight rats to HFD, including whether this phenomenon exhibited possible sex differences. The average birthweight and body weight at weaning day of offspring from nicotine-administered dams was lower than those of controls. The offspring from nicotine-administered dams did not show rapid fat accumulation after exposure to HFD, and weight and body fat ratio of these animals did not differ from those of the controls. Blood glucose levels did not differ between the groups, but insulin levels increased only in male HFD-exposed offspring from nicotine-administered dams. Similarly, only in HFD-exposed male from nicotine-administered dams showed decreases in the insulin receptor expression in the liver. We conclude that male rats subjected to prenatal nicotine exposure develop hyperinsulinemia when exposed to HFD after growth. Our results suggest that decreased expression of insulin receptors in the liver may be involved in the mechanism underlying hyperinsulinemia in low-birthweight offspring, a phenomenon that appeared to exhibit a sex-specific bias.

Keywords: nicotine, insulin, DOHaD (development origins of health and disease), sex-specificity, prenatal

OPEN ACCESS

Edited by:
Takashi Yazawa,
Asahikawa Medical University, Japan

Reviewed by:
Ken Fujiwara,
Kanagawa University, Japan
Hsien-Hui Chung,
Kaohsiung Veterans General Hospital, Taiwan

***Correspondence:**
Takahiro Nemoto
taknemo@nms.ac.jp

Specialty section:
This article was submitted to Experimental Endocrinology, a section of the journal Frontiers in Endocrinology

Received: *13 April 2021*
Accepted: *24 May 2021*
Published: *09 June 2021*

Citation:
Nemoto T, Ando H, Nagao M, Kakinuma Y and Sugihara H (2021) Prenatal Nicotine Exposure Induces Low Birthweight and Hyperinsulinemia in Male Rats. Front. Endocrinol. 12:694336. doi: 10.3389/fendo.2021.694336

INTRODUCTION

There are various etiologies of low birthweight (1), and smoking by pregnant mothers is one such causes (2, 3). Smoking by pregnant mothers remains a major public health concern. Nicotine is the major psychoactive component in tobacco and believed to be the driving force for tobacco consumption. Maternal nicotine exposure is likely to have serious adverse consequences including demonstrated effect on fetal development in both humans (4) and mice (5). Fetuses

exposed to nicotine are prone to some lifelong health problems, including dysfunctions in the endocrine (6, 7), respiratory (8), cardiovascular (9, 10), and nervous systems (11).

Gillman et al. have developed DOHaD (Developmental Origins of Health and Disease) into a theory intended "to recognize the broader scope of developmental cues, extending from the oocyte to the infant and beyond, and the concept that the early life environment has widespread consequences for later health" (12). At present, environmental factors at various developmental stages (including fertilization and periods of embryonic, fetal and infant development) have been shown to be associated with the health of adults and the elderly, as well as pathophysiology of various non-communicable diseases (NCDs); these effects are mediated through epigenetic alterations, and thus have come to be considered risk factors for a variety of health issues (13–15). According to the DOHaD theory, low birthweight presents an increased risk of developing various NCDs, including abnormal glucose metabolism (16). We hypothesized that exposure of nicotine-induced low-birthweight rats to a high-fat diet (HFD) after growth predisposes such animal to the development of glucose intolerance, an effect caused by a mismatch between the eutrophic environment and small body size.

Indeed, an inverse correlation has been demonstrated between birthweight and the risk of developing of type 2 diabetes (17). In addition, the association between birthweight and increased risk of type 2 diabetes is greater in low-birthweight women compared to low-birthweight men, independently of body mass index at the time of diagnosis (18). In this study, fasting blood glucose levels and hemoglobin A1c levels exhibited a strong inversely association with birthweight, with all glycemic abnormalities occurring at higher rates in low-birthweight women compared to low-birthweight men. Therefore, we also investigated whether there is a sex difference in hyperinsulinemia caused by exposure of nicotine-induced low-birthweight rats to HFD.

METHODS

Animals

Wistar rats were maintained at 23 ± 2°C with a 12-h:12-h light-dark cycle (lights on at 0800 h, off at 2000 h). They were allowed *ad libitum* access to standard chow (rodent diet CE-2, CLEA) and sterile water. All experimental procedures were reviewed and approved by the Laboratory Animals Ethics Review Committee of Nippon Medical School (#27-067). All experiments were performed in accordance with relevant guidelines and regulations.

Female rats (9 weeks old) were anesthetized by isoflurane inhalation, and an incision was made in each animal to permit subcutaneous (s.c.) insertion of an osmotic minipumps (#2004, Alzet, Los Angeles, CA). Pumps were loaded with nicotine (Wako Pure Chemical Industries, Ltd., Kyoto, Japan), formulated in saline, at a concentration designed to deliver the drug at an initial dose rate of 3 mg nicotine/kg bodyweight/day for 28 days (starting from one week before the projected mating day through the day of delivery). Several previous papers have reported administration of nicotine to pregnant rat dams at doses ranging from 1 to 5 mg/kg bodyweight/day (19–21). For the present study, we selected a nicotine dose level of 3 mg nicotine/kg bodyweight/day per pregnant rat dams based on preliminary experiments at various dose level; notably, these data (not shown) are not detected a difference in mean food intake, and gestational age between dams maintained on vehicle compared to those maintained on nicotine at 3 mg nicotine/kg bodyweight/day. Each of control dams was implanted with an osmotic pump filled with saline and delivering the vehicle at an equivalent rate to that of the nicotine solution.

One week after pump implantation, a total of forty (20 each dosed with and without nicotine) proestrous female rats (age, 10 weeks) were mated with normal male rats. Dams were housed individually with free access to water and were divided into two groups. Twelve to twenty pups were obtained from each of 12 dams of each group. We excluded rat pups born with a body weight of more than 6.0 g, which is the mean - 2 standard deviations (SDs) body weight of the offspring of normal dams. No surrogate mothers were used, and 10 rat pups (randomly selected from a given litter) were left with each birth mother to be raised by that dam. Postnatal mother rats were fed a standard diet *ad libitum*. On the weaning day, 8 rats (randomly selected from each group) were decapitated between 09:00 am to 11:00 am and blood was collected to measure the blood GH and IGF-1 concentrations. Then, the liver was sampled to measure the expression level of IGF-1-encoding mRNA (*Igf1*). After weaning, the rat pups of different litters were mixed. Rats were divided into two groups at 5 weeks of age; one group was placed on a high-fat diet (fat-based 45kcal/fat, D12451, Research Diet), and the other on a standard diet (4.5kcal/fat, CE-2, CLEA). At 15 weeks of age, body composition was measured, blood and organs were collected, and gene and protein expression and hormone levels were analyzed. Body composition of rats was evaluated through multifrequency bioelectrical impedance analysis performed using an ImpediVet (ImpediMed, Brisbane, QLD, Australia) according to the manufacturer's instructions (22).

Glucose Tolerance Test

Rats were fasted for 18 hours and then subjected to glucose loading (2 g/100g bodyweight glucose) using a gastric sonde. Blood was collected from the tail vein, and the blood glucose levels before and after 15 min glucose challenge were measured (LAB Gluco glucose sensor, Filgen, Aichi, Japan).

RNA Extraction and Real-Time Reverse Transcription-Polymerase Chain Reaction (RT-PCR)

We performed mRNA quantification as previously reported (23). Total RNA was extracted from the liver using RNAiso Plus (Takara, Shiga, Japan). The absorbance of each sample at 260 nm and 280 nm was assayed, and RNA purity was judged as the 260/280 nm ratio (The 260/280 nm ratios of all samples used in this study exceeded 1.7). First-strand cDNA was generated using 250 ;ng of denatured total RNA; the reaction mixture was incubated at 37°C for 15 min, 84°C for 5 sec, and 4°C for

5 min using a PrimeScript® RT reagent kit with gDNA Eraser (Takara). PCR was performed for 40 cycles of denaturation at 94°C for 5 sec and annealing-extension at 60°C for 30 sec using SYBR premix Ex Taq (Takara) and primer sets specific for the transcripts encoding rat IGF-1 (*Igf1*; RA028844, Takara), rat insulin receptor (*Insr*; RA0.53014, Takara) and glyceraldehyde phosphate dehydrogenase (GAPDH; encoded by *Gapgh*; RA015380, Takara). To normalize each sample for RNA content, mRNA expression levels were normalized to those of *Gapdh*, a housekeeping gene. The 2nd derivative method was used as the standard method for calculating C_t values, respectively (24).

Western Blotting

We performed western blotting quantification as previously reported (25). Protein samples from rat liver were extracted using cOmplete lysis-M (Roche, Mannheim, Germany). The protein concentrations of lysate samples were determined using the Pierce 660 nm Protein assay (Thermo Scientific, Rockford, IL). Aliquots containing 5 μg of total protein each were electrophoresed on a 5-20% gradient SuperSep™ SDS-polyacrylamide gel (FUJIFILM Wako Pure Chemical Corporation, Osaka, Japan) and transferred to a nitrocellulose membrane. The transfer membranes were blocked with 5% skim milk and then incubated with an anti-insulin receptor (Insr) antibody (1:1,000, Abcam, Cambridge, UK, Cat# ab131238, RRID: AB_11155955) for 1 h at room temperature. The transfer membranes were washed with Tris-Buffered Saline with 0.05% Tween 20 (TBS-T, pH7.6) and further incubated with horseradish peroxidase (HRP)-labeled anti-rabbit IgG (1:5,000, Jackson ImmunoResearch Labs, West Grove, PA, Cat#711035152, RRID: AB_10015282) for 1 h at room temperature. The signals were detected using SuperSignal West Dura extended duration substrate (Thermo Scientific). Following detection, the membranes were stripped of the antibody using Restore PLUS Western Blot Stripping Buffer (Thermo Scientific). The stripped blots then were re-probed using THE™ [HRP]-labeled anti-β-actin antibody (1:1,000, GeneScript, Piscataway, NJ, Cat# A00730-40),. The expression levels of Insr were normalized to those of the β-actin signal.

Measurement of Blood GH, IGF-1 and Insulin Levels

Hormone levels were measured using serum derived from blood obtained from decapitated rats. Serum GH and IGF-1 were analyzed using a Rat GH ELISA kit (Shibayagi, Co, Ltd., Gunma, Japan) and a Mouse/Rat IGF-1 Immunoassay kit (R&D Systems, Minneapolis, MN), respectively. Insulin was measured using a rat insulin EIA kit (Macrodia AB, Uppsala, Sweden).

Statistical Analysis

Unpaired *t* tests, a one-way analysis of variance (ANOVA) followed by Tukey's *post hoc* test for multiple comparisons, or ANOVA were used for each statistical analysis. All analyses were performed as two-tailed test. Prism 9 software (GraphPad Software, Inc., La Jolla, CA) was used for all calculations. Real-time RT-PCR and western blot data are expressed as percent ± SEM with the control defined as 100%. $p < 0.05$ was considered statistically significant.

RESULTS

During pregnancy, there were no statistically significant differences in food intake and during pregnancy between the nicotine-administered (7.0 ± 1.1g/100g b.w.; mean ± SEM, n=10) and saline-treated groups (7.7 ± 0.6g/100g b.w., $p \geq 0.05$, n=10). Similarly, changes in bodyweight during pregnancy were not significantly different between nicotine-administered dams and control dams ($p > 0.05$, n=10 of each dams). Litter size was equivalent between groups. The mean bodyweights of the pups on the day of birth were 5.38 ± 0.03 g (n=118) and 7.33 ± 0.04 g (n=108) for offspring of the nicotine-administered dams and the control dams, respectively (**Figure 1A**). The body length and the bodyweight at weaning day (at 21 days of age) of male rats were significantly lower in offspring from nicotine-administered dams than in offspring from control dams (**Figures 1B, C**). Similarly, the body length and the bodyweight at weaning day of female rats were significantly lower in offspring from nicotine-administered dams than in offspring from control dams (**Figures 1B, C**). The pups' serum GH levels at the weaning day did not differ significantly between the groups (**Figure 1D**), but serum IGF-1 levels (**Figure 1E**) and the expression levels of *Igf1* mRNA in the liver (**Figure 1F**) were significantly lower in both male and female offspring from nicotine-administered dams than in offspring from control dams.

At 5 weeks of age, the pups were randomly divided into two groups; and maintained on either HFD or standard diet. Body weight before HFD exposure was significantly lower in offspring from nicotine-administered dams than that in offspring from control dams (**Figures 2A, B**). HFD significantly increased the bodyweight of the offspring from both the nicotine-administered dams and the control dams, but there was no significant difference between the offspring from the nicotine-administered dams and those from control dams (**Figures 2C, D**). In addition, HFD significantly increased the body fat ratio in both males and females, but there was no significant difference in the magnitude of these increase between offspring from the nicotine-administered dams and those from control dams (**Figures 2E, F**).

There was no significant difference in fasting blood glucose among the groups (**Figures 3A, B**). Fasting blood insulin levels were significantly higher in HFD-exposed male offspring of both the nicotine-administered dams and of control dams than in standard chow-fed offspring of each set of dams. In contrast, there was no significant difference in blood insulin levels between the standard diet-fed offspring of nicotine-administered dams and of control dams (**Figure 3C**). Among females, fasting insulin levels were higher in offspring from the nicotine-administered

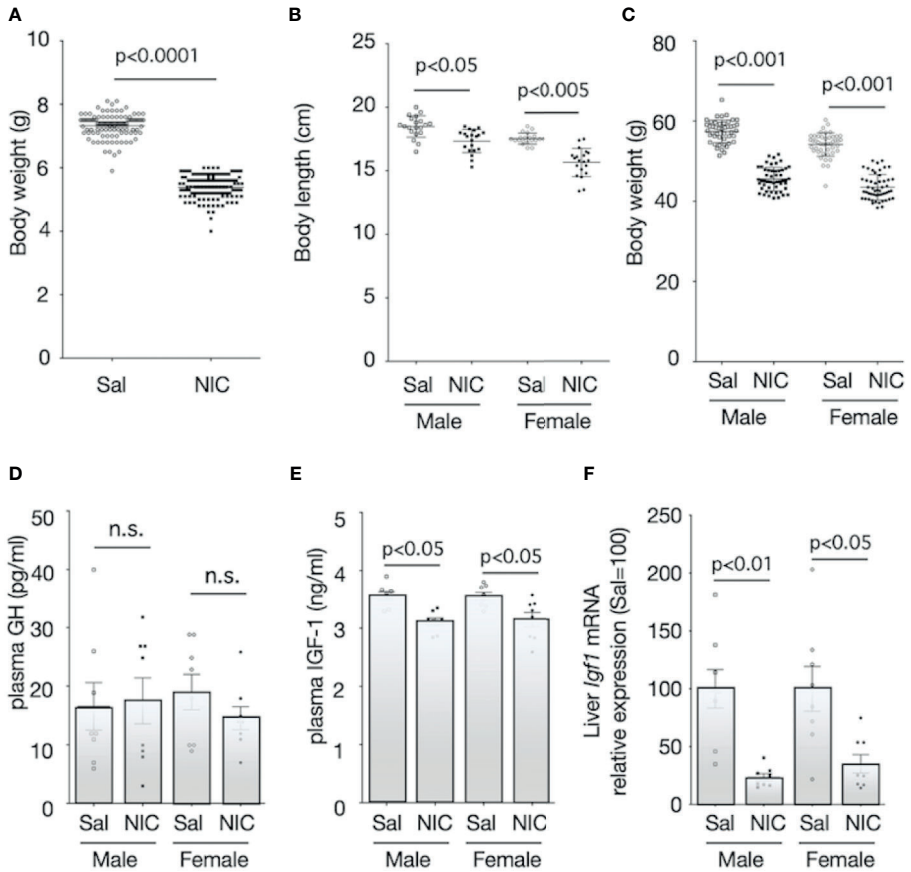

FIGURE 1 | Body size and plasma concentrations of GH and IGF-1, and expression of IGF-1 mRNA in the liver. Bodyweight at birthday **(A)**, body length **(B)** and bodyweight at weaning day (3-week-old) **(C)** were measured. Plasma concentrations of growth hormone (GH) **(D)** and insulin-like growth factor (IGF)-1 **(E)** of offspring from nicotine-administered dams (NIC) and saline-treated dams (Sal) were measured. The mRNA expression levels of *Igf1* in the liver of offspring from nicotine-administered dams (NIC) and saline-treated dams (Sal) were quantified **(F)**. The mRNA expression levels were normalized to *Gapdh* levels and then to that in Sal, which was defined as 100%. Values are presented as means ± SEM (n=8). Statistical analysis was performed using unpaired-T test **(A)** and one-way ANOVA followed by Tukey's *post hoc* test for multiple comparisons **(B–F)**. n.s., not significant ($p \geq 0.05$).

dams than in offspring of controls dams. Among the offspring of control dams, fasting insulin levels were significantly higher in the HFD-exposed rats than in standard chow-fed rats; in contrast, no significant diet-associated difference was observed in offspring of nicotine-administered dams (**Figure 3D**).

Oral glucose challenge (2g/100g b.w.) did not reveal significant differences between HFD exposed rats and standard chow-fed rats or between offspring of nicotine-administered and control dams when blood glucose levels were assessed 15 minutes post-challenge (**Figures 4A, B**). Among male HFD-exposed rats, blood insulin levels in response to glucose challenge were significantly higher in offspring of nicotine-administered dams than in offspring of control dams. Moreover, among offspring from nicotine-administered dams, the blood insulin concentration in response to glucose challenge was significantly higher in HFD-exposed rats than in standard chow-fed rats (**Figure 4C**). However, there were no significant differences in insulin levels in female rats when comparing between the groups based on dams or based on diet (**Figure 4D**).

The liver expressions levels of the *Insr* mRNA and Insr protein were significantly lower in HFD-exposed offspring than in standard chow-fed offspring from nicotine-administered dams and control dams (**Figures 5A, C**). As seen with blood insulin levels, there was no significant difference in the *Insr* mRNA and Insr protein expression in female rats when comparing between the groups based on dams or based on diet (**Figures 5B, D**).

DISCUSSION

In this study, offspring from nicotine-administered dams delivered low-birthweight offspring, and those offspring failed to "catch up" in growth by the weaning day. Among the pups, there was no significant difference in GH at the weaning day, and the levels of Igf1 mRNA on the liver and of IGF-1 in serum were lower in low-birthweight rats delivered from nicotine-administered dams (compared to those in pups delivered from control dams). It has been reported that, in the offspring of dams

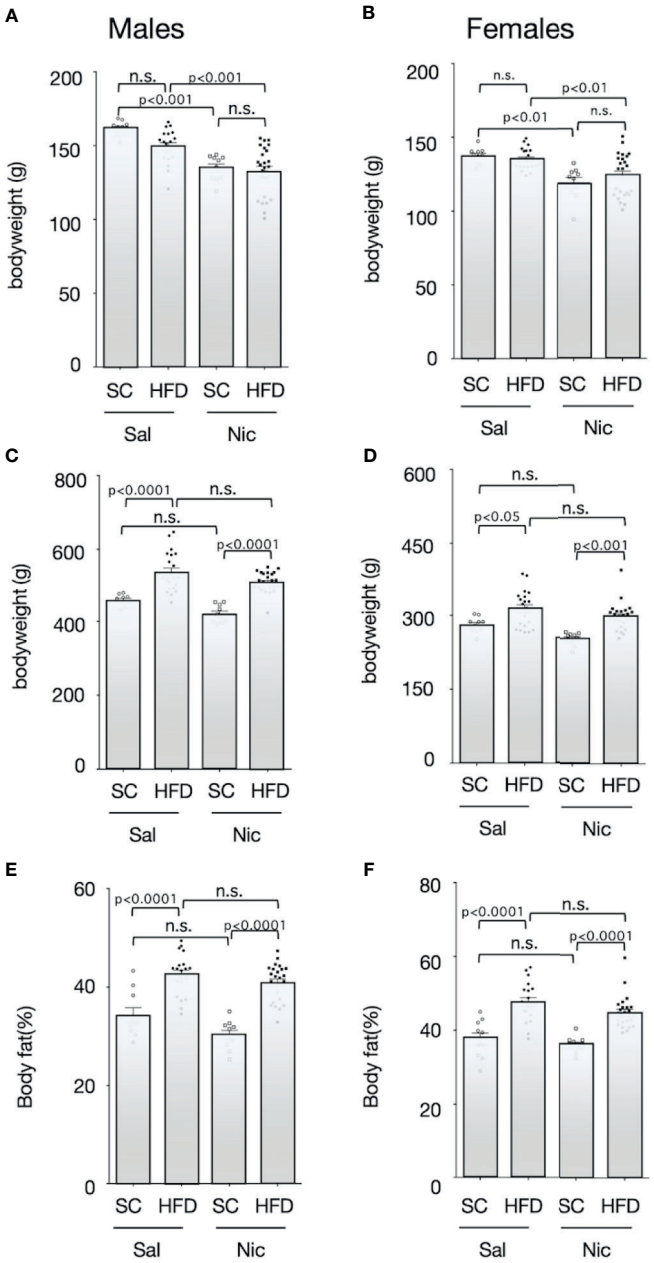

FIGURE 2 | Bodyweights and body fat ratio. Plots of the bodyweight before (5-week-old) (**A** for males and **B** for females) and after (13-week-old) (**C** for males and **D** for females) exposure to the high-fat diet (HFD) or standard chow (SC), and the body fat percentage after exposure to the HFD or SC (13-week-old) (**E** for males and **F** for females) are shown. Values are presented as means ± SEM. Statistical analysis was performed using one-way ANOVA followed by Tukey's *post hoc* test for multiple comparisons. n.s., not significant ($p \geq 0.05$).

in which the uterine arteries were ligated in the last trimester, blood IGF-1 levels decrease during weaning; epigenetic changes in the *Igf1* promoter region are thought to be involved in the decrease in IGF-1 production (26). Although we did not analyze epigenetic changes in the *Igf1* gene as part of the model used here, the changes in the epigenome may have reduced *Igf1* mRNA expression levels. In fact, Ernst, et al. reviewed possible evidence that nicotine activates maternal peripheral nicotinic acetylcholine receptors, resulting in increased catecholamine release, followed by vasoconstriction and decreased placental blood flow, causing fetal hypoxia, which can further impair fetal growth (**Figure 6**) (27). These authors explained that nicotine tends to disrupt the function of the placenta. The activation of placental cholinergic systems by nicotine is known to suppresses

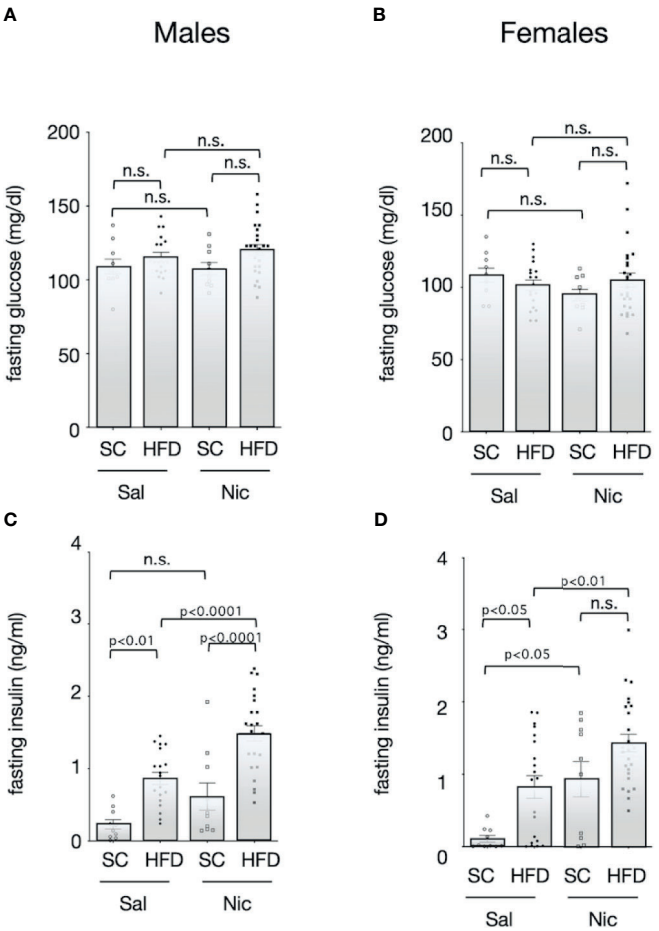

FIGURE 3 | Fasting blood sugar and insulin levels. Plasma concentrations of glucose (**A** for males and **B** for females) and insulin (**C** for males and **D** for females) of standard chow-fed (SC) offspring or high fat diet (HFD)-exposed offspring from nicotine-administered dams (NIC) or saline-treated dams (Sal) were measured (13-week-old). Values are presented as means ± SEM. Statistical analysis was performed using one-way ANOVA followed by Tukey's *post hoc* test for multiple comparisons. n.s., not significant ($p \geq 0.05$).

transplacental amino acid transport. This reduction of placental amino acid transport may contribute to fetal intrauterine growth retardation. Thus, we postulate that the decreases in umbilical cord blood flow and nutrient transport due to nicotine exposure in dams decreases IGF-1 production in offspring and may impaired catch-up growth.

In the present study, we showed that exposure to a HFD of male offspring from nicotine-administered dams significantly increased blood insulin levels in response to glucose challenge without associated rapid accumulation of body fat. However, we observed that low-birthweight female offspring from nicotine-administered dams did not exhibit increased blood insulin levels after oral glucose challenge, even when exposed to an HFD. The expression level of insulin receptor in the liver also was decreased in HFD-exposed male offspring from nicotine-administered dams, but not in HFD-exposed female rats. These results suggested that there are sex differences in the effects of nicotine exposure on fetal programming. Namely, in our prenatal nicotine-exposed rat model, males may have a higher predisposition to develop insulin resistance than females. Indeed, in humans, type 2 diabetes develops slightly more frequently in males, and males develop the disease at a younger age than do females (28, 29). On the other hand, female-specific changes in the pathophysiological mechanism of human diabetes also have been clarified. A large genome-wide association studies (GWAS) meta-analysis in individuals of European descent identified genetically coded sexual dimorphisms for metabolic characteristics and outcomes, including female-specific effects on type 2 diabetes (30). It is becoming clear that not only are there sex differences in the onset of the disease, but also that the onset of the disease in the offspring is affected by the uterine environment; sex differences in dysregulation of gene expression have been demonstrated in numerous animal models. Both male and female offspring from type 1 diabetes dams showed reduced insulin secretion responded to oral glucose. However, in that model, only female rats (but not males) showed decreased insulin secretion in response to intravenous glucose infusion (31). Another model

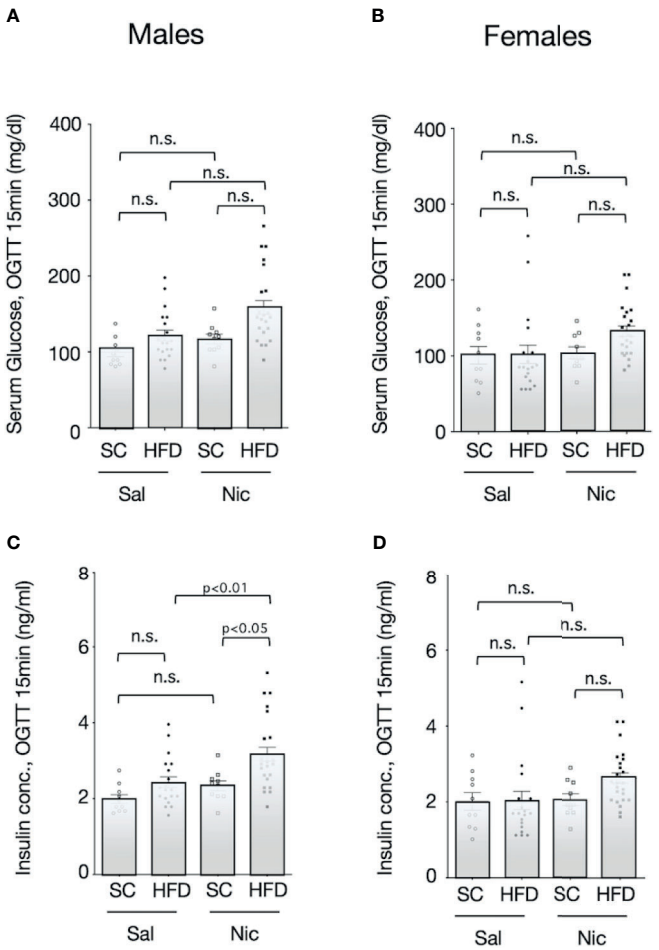

FIGURE 4 | Blood sugar and insulin levels after oral glucose challenge. Blood samples were collected 15 min after glucose solution (2g/100g b.w.) ingestion. Their plasma concentrations of glucose (**A** for males and **B** for females) and insulin (**C** for males and **D** for females) of standard chow-fed (SC) offspring or high fat diet (HFD)-exposed offspring from nicotine-administered dams (NIC) or saline-treated dams (Sal) were measured. Values are presented as means ± SEM. Statistical analysis was performed using one-way ANOVA followed by Tukey's *post hoc* test for multiple comparisons. n.s., not significant ($p \geq 0.05$).

demonstrated that HFD combined with maternal vitamin D deficiency disrupted glucose homeostasis and adiposity in male offspring but not in females. The authors of that work showed that such phenotypes were associated with different transcriptomic profiles in adipose tissue, which could be related to differential modulation of plasma 17ß-estradiol concentrations (32). In fact, insulin sensitivity and beta cell function are known to be higher in females than in males (33). Mechanistically, estrogens have been reported to protect against insulin resistance through activation of the estrogen receptor (ER) α pathway in insulin-sensitive tissues (34, 35). Also, ERα signaling in hepatocytes mediates protective effects against steatosis and insulin resistance in HFD-exposed female mice (36). On the other hand, it has been reported that growth-restricted in males are resistant to impaired glucose homeostasis, whereas growth-restricted females are susceptible to metabolic dysfunction regardless of postnatal diet (37). The difference in these results suggests that the cause of growth retardation may be malnutrition or other factors. In the present work, we observed that low-birthweight male rats (but not females) resulting from embryonic nicotine exposure had elevated blood insulin levels when exposed to an HFD. In this study, chronic neonatal nicotine exposure did not produce sex-specific differences in changes of body weight, or overall growth pattern. Therefore, we postulate that there was a difference in predisposition to glucose intolerance after birth attributable to the protective effect of estrogen, and not as a result of the effect of the decrease in GH and/or IGF-1 levels due to fetal programming by nicotine (**Figure 6**). Further studies using ovariectomized rats or aged female rats are needed to investigate the protective effect of estrogen on glucose tolerance in nicotine-exposed low-birthweight rats.

In the present study, there were no significant differences in fasting blood glucose, nor in mRNA and protein expression

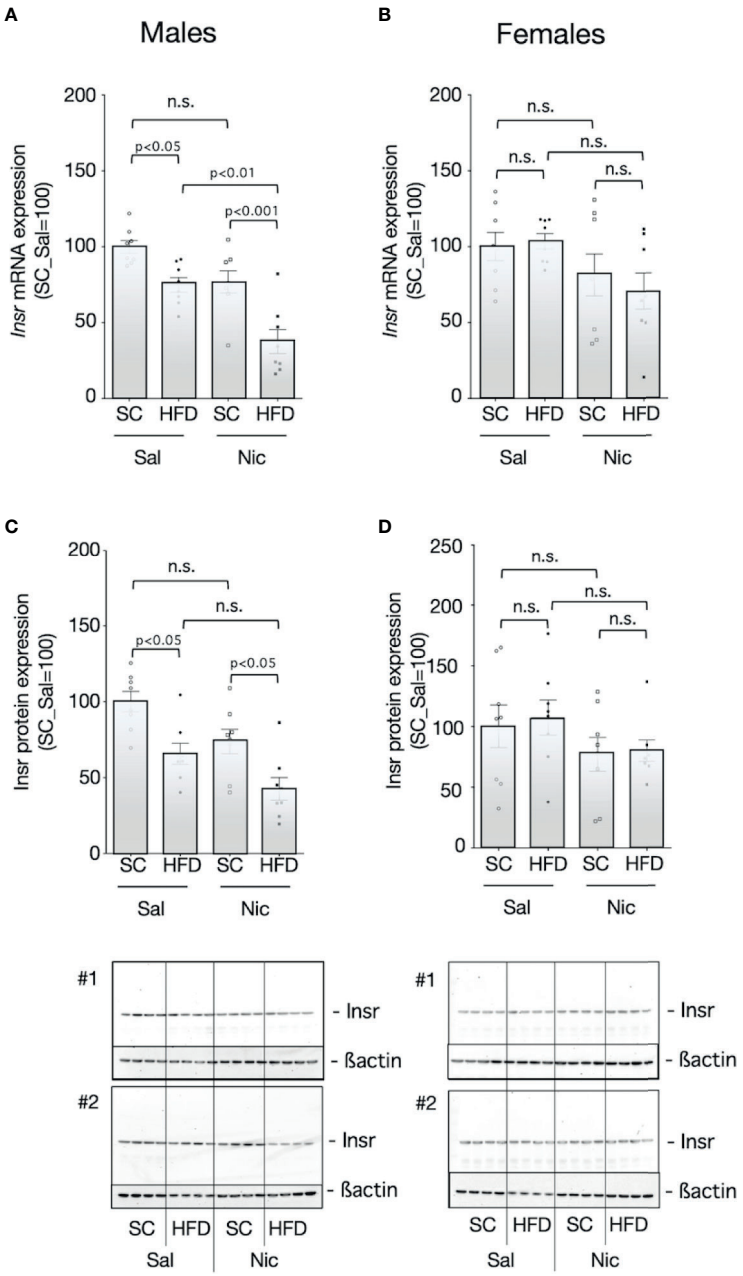

FIGURE 5 | Expression of insulin receptor (Insr) in the liver. *Insr* mRNA expression levels (**A** for males and **B** for females) and Insr protein expression levels (**C** for males and **D** for females) in the liver of standard chow-fed (SC) offspring or high fat diet (HFD)-exposed offspring from nicotine-administered dams (NIC) or saline-treated dams (Sal) were quantified. The mRNA expression levels were normalized to Gapdh levels and then to that in Sal, which was defined as 100%. The protein expression levels were normalized to that of ß-actin and then to that in Sal, which was defined as 100%. Values are presented as means ± SEM (n=8). Statistical analysis was performed using one-way ANOVA followed by Tukey's *post hoc* test for multiple comparisons. n.s., not significant ($p \geq 0.05$).

levels of the insulin receptor in the liver, when comparing between the standard diet-fed low-birthweight rats and the standard diet-fed control rats. The concept of the DOHaD suggests that adverse influences early in development, particularly during the intrauterine stage, may result in changes in the physiological and metabolic responses of the fetus, which in turn may result in an increased risk of NCDs after growth. Understanding of the underlying molecular mechanisms of fetal malnutrition and the impact of low birthweight on the development of NCDs in later years is incomplete. Organisms have an evolved ability to respond to environmental changes by adjusting their phenotype during development. Therefore, a fetus

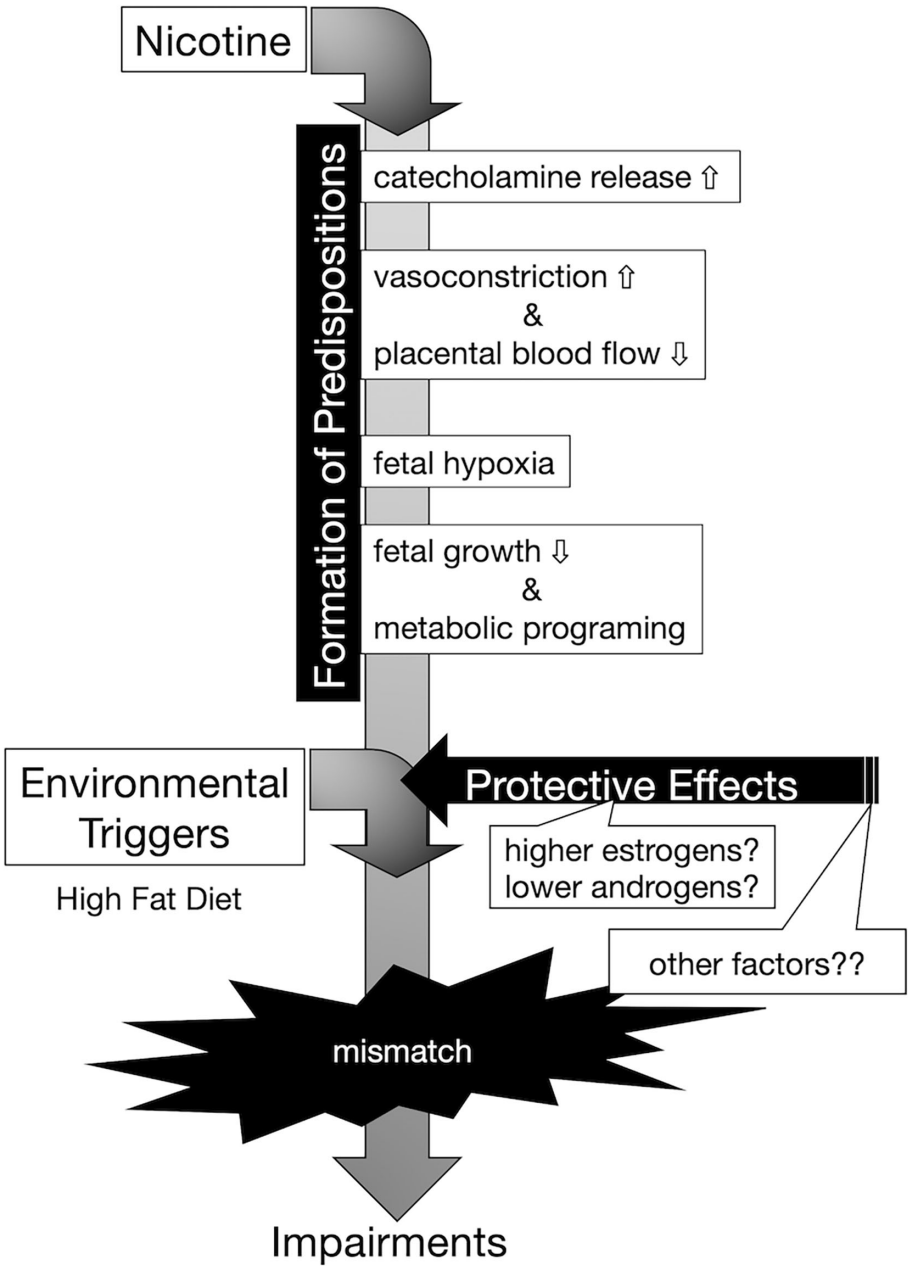

FIGURE 6 | Conceptual diagram of the onset of hyperinsulinemia due to embryonic nicotine exposure. Exposure to nicotine in dams causes a decrease in uterine blood flow, and metabolic programming due to hypoxia and malnutrition in the fetus is assumed. Nicotine may directly affect the egg *via* cord blood, but the effect is unknown in this study. According to DOHaD theory, the mismatch between the predispositions acquired by low-birthweight offspring and the post-growth environment increases the risk of developing the disease. Female hormones (estrogens) may act protectively in the development of diabetes. In our experimental model, it is possible that the decrease in the expression of insulin receptors in the liver was blocked in the female rats compared to that of male rats, but since there was no difference in the DNA methylation of the insulin receptor gene, further analyses are needed to clarify the mechanism underlying the sex-specificity in the future.

exposed to a signal that the fetus interprets as reflecting undernourishment or maternal chemical exposure is expected to result in an adaptation of the prenatal metabolic systems to suit the environment. Subsequent maladaptation occurs when the postnatal environment does not match the prenatal environment, leading to obesity and type 2 diabetes (38). In humans, the combination of low birthweight and rapid growth in childhood is associated with later insulin resistance (39). In this study, there were no statistical differences between fasting and blood glucose levels after the oral glucose challenge. This means that glucose tolerance remains normal although insulin sensitivity is reduced in the offspring from nicotine-

administered dams. Furthermore, the initial secretion of insulin after the oral glucose challenge was not reduced in high-fat diet exposed offspring from nicotine-administered dams, indicating that pancreatic β-cells were maintained normally even when the fetus is exposed to the nicotine. Thus, the DOHaD theory suggests that the onset of NCDs is triggered by a two-step process involving a combination of the embryonic environment and the postnatal environment, and that its onset takes time. The results of the present study indicate that impaired glucose tolerance due to fetal nicotine exposure manifests as a result of a second hit of HFD exposure. In other words, embryonic programming by nicotine exposure may affect the gene expression regulation mechanism. The expression level of the insulin receptor in the livers of our embryonic nicotine-exposed rats was decreased in HFD-exposed rats. The induction of altered phenotypes during development in response to environmental stimuli is accompanied by epigenetic changes. Epigenetic factors include DNA methylation and histone modifications. Epigenetic changes, especially DNA methylation, provide a "memory" of developmentally plastic responses to the early environment and are central to phenotypic generation and their stability throughout the life course (40, 41). Animal studies have reported that changes in gene promoter methylation induced in the F1 generation by maternal protein restriction during pregnancy are transmitted to the F2 generation. This result represents a mechanism of phenotypic induction of transmitted between generations (42). In humans, it has been reported that increased DNA methylation is involved in decreased insulin receptor expression in the adipose tissue of infants born to mother with gestational diabetes (43). However, the degree of change in DNA methylation is very small. In fact, we also quantified DNA methylation (using bisulfate sequencing) in the promoter region of *Insr* in rat liver, but the observed differences contributed only a few percent of the eligible nucleotides (data not shown in figures). Therefore, it is possible that something other than DNA methylation (i.e., methylation of histone H3 K27, which is known to affect transcription elongation) may be involved. Clearly, further research will be needed to address the mechanism of the effect observed in the present study.

As shown in this study, embryonic nicotine-exposed rats exhibit hyperinsulinemia when exposed to an HFD after growth. Our results suggest that decreased expression of insulin receptors in the liver may be involved in the formation of predisposition of insulin resistance; notably, the observed effects revealed a sex-specific difference in the developmental outcomes among fetal nicotine-exposed low-birthweight offspring. Hence, moderation of fat and sugar intake may be warranted in those, especially males, born with low birthweight, especially for males, to ensure minimal risk for type 2 diabetes.

DATA AVAILABILITY STATEMENT

The raw data supporting the conclusions of this article will be made available by the authors, without undue reservation.

ETHICS STATEMENT

The animal study was reviewed and approved by the Laboratory Animals Ethics Review Committee of Nippon Medical School.

AUTHOR CONTRIBUTIONS

TN designed the work, acquired data, analyzed data, and drafted the manuscript. HA performed western blot analysis of the liver. MN designed the work and drafted the manuscript. YK and HS interpreted the data and substantively revised the manuscript. All authors contributed to the article and approved the submitted version.

FUNDING

This work was supported in part by the Smoking Research Foundation of Japan (grant ID: 2014G003).

REFERENCES

1. Arima K, Kasai Y, Sugimoto M, Marui E, Minematsu K. Risk Factors for Low Birth Weight Infants in Japanese Pregnancies: A One-Year Study of 2551 Cases in Tokyo. *Int J Pediatr Neonatal Care* (2017) 3:IJPNC-122.. doi: 10.15344/2455-2364/2017/122
2. Ko TJ, Tsai LY, Chu LC, Yeh SJ, Leung C, Chen CY, et al. Parental Smoking During Pregnancy and its Association With Low Birth Weight, Small for Gestational Age, and Preterm Birth Offspring: A Birth Cohort Study. *Pediatr Neonatol* (2014) 55:20–7. doi: 10.1016/j.pedneo.2013.05.005
3. Harrod CS, Reynolds RM, Chasan-Taber L, Fingerlin TE, Glueck DH, Brinton JT, et al. Quantity and Timing of Maternal Prenatal Smoking on Neonatal Body Composition: The Healthy Start Study. *J Pediatr* (2014) 165:707–12. doi: 10.1016/j.jpeds.2014.06.031
4. Kyrklund-Blomberg NB, Granath F, Cnattingius S. Maternal Smoking and Causes of Very Preterm Birth. *Acta Obstet Gynecol Scand* (2005) 84:572–7. doi: 10.1111/j.0001-6349.2005.00848.x
5. Rowell PP, Clark MJ. The Effect of Chronic Oral Nicotine Administration on Fetal Weight and Placental Amino Acid Accumulation in Mice. *Toxicol Appl Pharmacol* (1982) 66:30–8. doi: 10.1016/0041-008X(82)90058-8
6. Al Mamun A, Lawlor DA, Alati R, O'Callaghan MJ, Williams GM, Najman JM. Does Maternal Smoking During Pregnancy Have a Direct Effect on Future Offspring Obesity? Evidence From a Prospective Birth Cohort Study. *Am J Epidemiol* (2006) 164:317–25. doi: 10.1093/aje/kwj209
7. Raum E, Kupper-Nybelen J, Lamerz A, Hebebrand J, Herpertz-Dahlmann B, Brenner H. Tobacco Smoke Exposure Before, During, and After Pregnancy and Risk of Overweight at Age 6. *Obes (Silver Spring)* (2011) 19:2411–7. doi: 10.1038/oby.2011.129
8. Hollams EM, de Klerk NH, Holt PG, Sly PD. Persistent Effects of Maternal Smoking During Pregnancy on Lung Function and Asthma in Adolescents. *Am J Respir Crit Care Med* (2014) 189:401–7. doi: 10.1164/rccm.201302-0323OC
9. Geerts CC, Grobbee DE, van der Ent CK, de Jong BM, van der Zalm MM, van Putte-Katier N, et al. Tobacco Smoke Exposure of Pregnant Mothers and Blood Pressure in Their Newborns: Results From the Wheezing Illnesses Study Leidsche Rijn Birth Cohort. *Hypertension* (2007) 50:572–8. doi: 10.1161/HYPERTENSIONAHA.107.091462

10. Cohen G, Jeffery H, Lagercrantz H, Katz-Salamon M. Long-Term Reprogramming of Cardiovascular Function in Infants of Active Smokers. *Hypertension* (2010) 55:722–8. doi: 10.1161/HYPERTENSIONAHA.109.142695
11. Muneoka K, Ogawa T, Kamei K, Muraoka S, Tomiyoshi R, Mimura Y, et al. Prenatal Nicotine Exposure Affects the Development of the Central Serotonergic System as Well as the Dopaminergic System in Rat Offspring: Involvement of Route of Drug Administrations. *Brain Res Dev Brain Res* (1997) 102:117–26. doi: 10.1016/S0165-3806(97)00092-8
12. Gillman MW, Barker D, Bier D, Cagampang F, Challis J, Fall C, et al. Meeting Report on the 3rd International Congress on Developmental Origins of Health and Disease (Dohad). *Pediatr Res* (2007) 61:625–9. doi: 10.1203/pdr.0b013e3180459fcd
13. El Hajj N, Schneider E, Lehnen H, Haaf T. Epigenetics and Life-Long Consequences of an Adverse Nutritional and Diabetic Intrauterine Environment. *Reproduction* (2014) 148:R111–20. doi: 10.1530/REP-14-0334
14. Fall CHD, Kumaran K. Metabolic Programming in Early Life in Humans. *Philos Trans R Soc Lond B Biol Sci* (2019) 374:20180123. doi: 10.1098/rstb.2018.0123
15. Goyal D, Limesand SW, Goyal R. Epigenetic Responses and the Developmental Origins of Health and Disease. *J Endocrinol* (2019) 242: T105–19. doi: 10.1530/JOE-19-0009
16. Oya J, Nakagami T, Kurita M, Yamamoto Y, Hasegawa Y, Tanaka Y, et al. Association of Birthweight With Diabetes and Insulin Sensitivity or Secretion in the Japanese General Population. *J Diabetes Investig* (2015) 6:430–5. doi: 10.1111/jdi.12325
17. de Lauzon-Guillain B, Balkau B, Charles MA, Romieu I, Boutron-Ruault MC, Clavel-Chapelon F. Birth Weight, Body Silhouette Over the Life Course, and Incident Diabetes in 91,453 Middle-Aged Women From the French Etude Epidemiologique De Femmes De La Mutuelle Generale De l'education Nationale (E3n) Cohort. *Diabetes Care* (2010) 33:298–303. doi: 10.2337/dc09-1304
18. Rich-Edwards JW, Colditz GA, Stampfer MJ, Willett WC, Gillman MW, Hennekens CH, et al. Birthweight and the Risk for Type 2 Diabetes Mellitus in Adult Women. *Ann Intern Med* (1999) 130:278–84. doi: 10.7326/0003-4819-130-4_Part_1-199902160-00005
19. Chen WJ, Kelly RB. Effect of Prenatal or Perinatal Nicotine Exposure on Neonatal Thyroid Status and Offspring Growth in Rats. *Life Sci* (2005) 76:1249–58. doi: 10.1016/j.lfs.2004.08.022
20. Chen CM, Chou HC, Huang LT. Maternal Nicotine Exposure During Gestation and Lactation Induces Kidney Injury and Fibrosis in Rat Offspring. *Pediatr Res* (2015) 77:56–63. doi: 10.1038/pr.2014.148
21. Zhou J, Zhu C, Luo H, Shen L, Gong J, Wu Y, et al. Two Intrauterine Programming Mechanisms of Adult Hypercholesterolemia Induced by Prenatal Nicotine Exposure in Male Offspring Rats. *FASEB J* (2019) 33:1110–23. doi: 10.1096/fj.201800172R
22. Moon JR, Smith AE, Tobkin SE, Lockwood CM, Kendall KL, Graef JL, et al. Total Body Water Changes After an Exercise Intervention Tracked Using Bioimpedance Spectroscopy: A Deuterium Oxide Comparison. *Clin Nutr* (2009) 28:516–25. doi: 10.1016/j.clnu.2009.04.025
23. Nemoto T, Kakinuma Y, Shibasaki T. Impaired miR449a-induced Downregulation of Crhr1 Expression in Low-Birth-Weight Rats. *J Endocrinol* (2015) 224:195–203. doi: 10.1530/JOE-14-0537
24. Nolan T, Hands RE, Bustin SA. Quantification of mRNA Using Real-Time RT-PCR. *Nat Protoc* (2006) 1:1559–82. doi: 10.1038/nprot.2006.236
25. Nemoto T, Kakinuma Y. Fetal Malnutrition-Induced Catch Up Failure is Caused by Elevated Levels of miR-322 in Rats. *Sci Rep* (2020) 10:1339. doi: 10.1038/s41598-020-58392-x
26. Fu Q, Yu X, Callaway CW, Lane RH, McKnight RA. Epigenetics: Intrauterine Growth Retardation (IUGR) Modifies the Histone Code Along the Rat Hepatic IGF-1 Gene. *FASEB J* (2009) 23:2438–49. doi: 10.1096/fj.08-124768
27. Ernst M, Moolchan ET, Robinson ML. Behavioral and Neural Consequences of Prenatal Exposure to Nicotine. *J Am Acad Child Adolesc Psychiatry* (2001) 40:630–41. doi: 10.1097/00004583-200106000-00007
28. Glumer C, Jorgensen T, Borch-Johnsen KS. Inter. Prevalences of Diabetes and Impaired Glucose Regulation in a Danish Population: The Inter99 Study. *Diabetes Care* (2003) 26:2335–40. doi: 10.2337/diacare.26.8.2335
29. Ben Romdhane H, Ben Ali S, Aissi W, Traissac P, Aounallah-Skhiri H, Bougatef S, et al. Prevalence of Diabetes in Northern African Countries: The Case of Tunisia. *BMC Public Health* (2014) 14:86. doi: 10.1186/1471-2458-14-86
30. Morris AP, Voight BF, Teslovich TM, Ferreira T, Segre AV, Steinthorsdottir V, et al. Large-Scale Association Analysis Provides Insights Into the Genetic Architecture and Pathophysiology of Type 2 Diabetes. *Nat Genet* (2012) 44:981–90. doi: 10.1038/ng.2383
31. Gautier JF, Fetita LS, Riveline JP, Ibrahim F, Porcher R, Abi Khalil C, et al. Sex Difference in the Effect of Fetal Exposure to Maternal Diabetes on Insulin Secretion. *J Endocr Soc* (2018) 2:391–7. doi: 10.1210/js.2017-00482
32. Seipelt EM, Tourniaire F, Couturier C, Astier J, Loriod B, Vachon H, et al. Prenatal Maternal Vitamin D Deficiency Sex-Dependently Programs Adipose Tissue Metabolism and Energy Homeostasis in Offspring. *FASEB J* (2020) 34:14905–19. doi: 10.1096/fj.201902924RR
33. Kautzky-Willer A, Brazzale AR, Moro E, Vrbikova J, Bendlova B, Sbrignadello S, et al. Influence of Increasing BMI on Insulin Sensitivity and Secretion in Normotolerant Men and Women of a Wide Age Span. *Obes (Silver Spring)* (2012) 20:1966–73. doi: 10.1038/oby.2011.384
34. Handgraaf S, Riant E, Fabre A, Waget A, Burcelin R, Liere P, et al. Prevention of Obesity and Insulin Resistance by Estrogens Requires ERalpha Activation Function-2 (EralphaAF-2), Whereas ERalphaAF-1 is Dispensable. *Diabetes* (2013) 62:4098–108. doi: 10.2337/db13-0282
35. Riant E, Waget A, Cogo H, Arnal JF, Burcelin R, Gourdy P. Estrogens Protect Against High-Fat Diet-Induced Insulin Resistance and Glucose Intolerance in Mice. *Endocrinology* (2009) 150:2109–17. doi: 10.1210/en.2008-0971
36. Zhu L, Brown WC, Cai Q, Krust A, Chambon P, McGuinness OP, et al. Estrogen Treatment After Ovariectomy Protects Against Fatty Liver and may Improve Pathway-Selective Insulin Resistance. *Diabetes* (2013) 62:424–34. doi: 10.2337/db11-1718
37. Intapad S, Dasinger JH, Johnson JM, Brown AD, Ojeda NB, Alexander BT. Male and Female Intrauterine Growth-Restricted Offspring Differ in Blood Pressure, Renal Function, and Glucose Homeostasis Responses to a Postnatal Diet High in Fat and Sugar. *Hypertension* (2019) 73:620–9. doi: 10.1161/HYPERTENSIONAHA.118.12134
38. Eriksson JG, Forsen TJ, Osmond C, Barker DJ. Pathways of Infant and Childhood Growth That Lead to Type 2 Diabetes. *Diabetes Care* (2003) 26:3006–10. doi: 10.2337/diacare.26.11.3006
39. Eriksson JG, Osmond C, Kajantie E, Forsen TJ, Barker DJ. Patterns of Growth Among Children Who Later Develop Type 2 Diabetes or its Risk Factors. *Diabetologia* (2006) 49:2853–8. doi: 10.1007/s00125-006-0459-1
40. Jones PA, Takai D. The Role of DNA Methylation in Mammalian Epigenetics. *Science* (2001) 293:1068–70. doi: 10.1126/science.1063852
41. Bird A. DNA Methylation Patterns and Epigenetic Memory. *Genes Dev* (2002) 16:6–21. doi: 10.1101/gad.947102
42. Burdge GC, Slater-Jefferies J, Torrens C, Phillips ES, Hanson MA, Lillycrop KA. Dietary Protein Restriction of Pregnant Rats in the F0 Generation Induces Altered Methylation of Hepatic Gene Promoters in the Adult Male Offspring in the F1 and F2 Generations. *Br J Nutr* (2007) 97:435–9. doi: 10.1017/S0007114507352392
43. Ott R, Melchior K, Stupin JH, Ziska T, Schellong K, Henrich W, et al. Reduced Insulin Receptor Expression and Altered DNA Methylation in Fat Tissues and Blood of Women With GDM and Offspring. *J Clin Endocrinol Metab* (2019) 104:137–49. doi: 10.1210/jc.2018-01659

Conflict of Interest: The authors declare that the research was conducted in the absence of any commercial or financial relationships that could be construed as a potential conflict of interest.

frontiers in Endocrinology

ORIGINAL RESEARCH
published: 29 June 2021
doi: 10.3389/fendo.2021.690648

Epigenetic Changes in Neonates Born to Mothers With Gestational Diabetes Mellitus May Be Associated With Neonatal Hypoglycaemia

Yoshifumi Kasuga[1,2], Tomoko Kawai[2], Kei Miyakoshi[1], Yoshifumi Saisho[3], Masumi Tamagawa[1], Keita Hasegawa[1,2], Satoru Ikenoue[1], Daigo Ochiai[1], Mariko Hida[4], Mamoru Tanaka[1] and Kenichiro Hata[2]**

[1] Department of Obstetrics and Gynecology, Keio University School of Medicine, Tokyo, Japan, [2] Department of Maternal-Fetal Biology, National Research Institute for Child Health and Development, Tokyo, Japan, [3] Department of Internal Medicine, Keio University School of Medicine, Tokyo, Japan, [4] Department of Pediatrics, Keio University School of Medicine, Tokyo, Japan

OPEN ACCESS

Edited by:
Takahiro Nemoto,
Nippon Medical School, Japan

Reviewed by:
Kazuki Yasuda,
Kyorin University, Japan
Koshi Hashimoto,
Dokkyo Medical University
Koshigaya Hospital, Japan

***Correspondence:**
Kenichiro Hata
hata-k@ncchd.go.jp
Tomoko Kawai,
kawai-tm@ncchd.go.jp

Specialty section:
This article was submitted to Pediatric Endocrinology, a section of the journal Frontiers in Endocrinology

Received: 03 April 2021
Accepted: 01 June 2021
Published: 29 June 2021

Citation:
Kasuga Y, Kawai T, Miyakoshi K, Saisho Y, Tamagawa M, Hasegawa K, Ikenoue S, Ochiai D, Hida M, Tanaka M and Hata K (2021) Epigenetic Changes in Neonates Born to Mothers With Gestational Diabetes Mellitus May Be Associated With Neonatal Hypoglycaemia. Front. Endocrinol. 12:690648. doi: 10.3389/fendo.2021.690648

The detection of epigenetic changes associated with neonatal hypoglycaemia may reveal the pathophysiology and predict the onset of future diseases in offspring. We hypothesized that neonatal hypoglycaemia reflects the *in utero* environment associated with maternal gestational diabetes mellitus. The aim of this study was to identify epigenetic changes associated with neonatal hypoglycaemia. The association between DNA methylation using Infinium HumanMethylation EPIC BeadChip and neonatal plasma glucose (PG) level at 1 h after birth in 128 offspring born at term to mothers with well-controlled gestational diabetes mellitus was investigated by robust linear regression analysis. Cord blood DNA methylation at 12 CpG sites was significantly associated with PG at 1 h after birth after adding infant sex, delivery method, gestational day, and blood cell compositions as covariates to the regression model. DNA methylation at two CpG sites near an alternative transcription start site of *ZNF696* was significantly associated with the PG level at 1 h following birth (false discovery rate-adjusted $P < 0.05$). Methylation levels at these sites increased as neonatal PG levels at 1 h after birth decreased. In conclusion, gestational diabetes mellitus is associated with DNA methylation changes at the alternative transcription start site of *ZNF696* in cord blood cells. This is the first report of DNA methylation changes associated with neonatal PG at 1 h after birth.

Keywords: gestational diabetes mellitus, epigenetics, DNA methylation, umbilical cord blood, neonatal hypoglycaemia

INTRODUCTION

Gestational diabetes mellitus (GDM) is an important perinatal problem because it can promote the development of intra-uterine foetal death, shoulder dystocia, macrosomia, and/or neonatal hypoglycaemia in offspring. A recent report indicated that epigenetic modifications associated with maternal hyperglycaemia during pregnancy can predispose offspring to develop metabolic

disorders, and that the in utero environment during maternal GDM is associated with changes in foetal DNA methylation at CpG sites in genes related to metabolic function (1–7). Environmental interactions with the genome can cause epigenetic modifications, which have been investigated as mechanisms related to the development of type 1 diabetes and type 2 diabetes (8, 9). In mice, GDM alters DNA methylation in the pancreatic genome of offspring, suggesting an association with the development of abnormalities in glycolipid metabolism, type 2 diabetes susceptibility, and future obesity (10). However, no methods are available for directly measuring in utero hyperglycaemic conditions, and no associations between the degree of hyperglycaemia and methylation have been shown.

Neonates born to mothers with GDM frequently present with hypoglycaemia. Because maternal glucose traverses the placenta, fetus born to mothers with GDM develop hyperinsulinemia to decrease plasma glucose (PG) levels. However, maternal glucose is shut down after birth, which often develop hypoglycaemia in neonates who were hyperinsulinemia in utero. The presence of hypoglycaemia in neonates immediately after birth is predictive of the future development of obesity or metabolic disorders (11). Furthermore, neonates that develop hypoglycaemia, which is associated with neurodevelopmental outcomes (i.e., developmental delay at an older age), should be treated as soon as possible (12–14). Infants with hypoglycaemia can be born even to women with well-controlled GDM (15). It indicates that early-pregnancy high glucose (before GDM diagnosis) may be involved in neonatal hypoglycaemia and influence adverse foetal tissue development. Furthermore, higher maternal dietary glycaemic index and glycaemic load during early pregnancy are associated with a larger foetal abdominal circumference in late-pregnancy or offspring fat mass, even at the age of 4–6 years (16, 17). Besides, fluctuating glucose and insulin concentrations during early pregnancy are associated with childhood glucose and insulin levels (18). Therefore, neonatal hypoglycaemia may be associated with epigenetic changes in cord blood cells.

In this study, we tested the hypothesis that neonatal hypoglycaemia can reflect foetal hyperinsulinemia due to maternal early-pregnancy hyperglycaemia and that offspring cord blood epigenetics may be associated with neonatal hypoglycaemia. To this end, we examined the associations between the DNA methylation status in umbilical cord blood samples and neonatal PG at 1 h after birth.

MATERIALS AND METHODS

Ethics Approval and Consent to Participate

The study was approved by the Keio University School of Medicine Ethics Committee (20100154, 20110321, 20150103, and 20150168) and the Institutional Review Board of the National Research Institute for Child Health and Development (406) and was conducted in accordance with the ethical standards outlined in the 1964 Declaration of Helsinki and later amendments. All subjects provided written informed consent.

Study Population

We collected samples of cord blood from 132 offspring born at term to mothers with GDM and under neonatal care at Keio University Hospital between 2012 and 2016. Neonatal PG was routinely measured at 1 h after birth by the nursing staff, and neonatal hypoglycaemia was diagnosed according to glucose concentrations <2.6 mmol/L (47 mg/dL). GDM was diagnosed using the oral glucose tolerance test with 75 g of glucose (75 g-OGTT) according to criteria established by the International Association of Diabetes and Pregnancy Study Group (19). This required achieving one or more of the following threshold values: fasting PG, 5.1 mmol/L (92 mg/dL); 1 h PG levels during 75 g-OGTT (1 h-PG), 10.0 mmol/L (180 mg/dL); and 2 h PG levels during 75 g-OGTT (2 h-PG), 8.5 mmol/L (153 mg/dL). Each subject was evaluated based on the OGTT results. As described in our previous report, all mothers with GDM were on defined diets and self-monitored their blood glucose measurements at our hospital. Physicians analysed the blood glucose levels of all mothers every 2–3 weeks. Insulin was administered when dietary management did not result in the expected glucose levels (i.e., fasting PG level <5.6 mmol/L [100 mg/dL] or 2 h PG <6.7 mmol/L [120 mg/dL]) (20). The exclusion criteria included multiple pregnancy, preterm birth (gestational age at delivery <37 weeks), hypertensive disorder during pregnancy, neonatal asphyxia (umbilical artery pH <7.100 or Apgar score at 5 min <7), foetal growth restriction as defined by the International Society of Ultrasound in Obstetrics and Gynaecology, and congenital foetal anomaly. We also excluded women with DM (i.e., type 1 or 2 diabetes) before pregnancy and overt diabetes during pregnancy. Based on standard Japanese sex- and parity-specific birth-weight percentile curves, a birth weight $\geq 90^{th}$ or $<10^{th}$ percentile was defined as large or small for gestational age, respectively (21).

DNA Methylation in Umbilical Cord Blood

Umbilical cord blood was collected from each neonate immediately after birth. Genomic DNA was extracted using the QIAsymphony DNA Midi kit (Qiagen, Hilden, Germany), followed by bisulphite treatment using the Zymo EZ-96 DNA methylation kit (Zymo Research, Irvine, CA, USA). The genome-wide DNA methylation status for >850K CpG sites was analysed using the Infinium MethylationEPIC BeadChip array (Illumina, San Diego, CA, USA). Methylation data were acquired using the iScan system (Illumina) as idat files and processed by the minfi and ChAMP packages (https://bioconductor.org/biocLite.R) in R (v.3.4.0; www.R-project.org). The background was corrected using the NOOB method in the minfi package (22). Corrected data were normalized by BMIQ in the ChAMP package (v.2.8.9) (23). The manifest file was annotated using "IlluminaHumanMethylationEPICanno.ilm10b2.hg19." We removed 11,800 probes with detection P-values >0.01 in at least one sample, 3,125 probes with a bead count <3 in at least 5% of samples, and 2,894 non-CpG targeting probes.

Additionally, we filtered 17,124 probes located on either the X or Y chromosome, 49 multi-hit probes (24), and 77,589 single-nucleotide polymorphism (SNP)-related probes (25) using ChAMP. This yielded 754,255 autosomal probes from 132 samples. We used the Beta-value (β), which represents the ratio of the methylated probe intensity and overall intensity (sum of methylated and unmethylated probe intensities). The cell composition of each cord blood sample (i.e., 'Bcell', 'CD4T', 'CD8T', 'Gran', 'Mono', 'NK', and 'nRBC') was analysed using "FlowSorted.CordBlood.450k" in the minfi package (26). We confirmed that the same sample had not been measured twice as clustering samples by using methylation levels of 1,297 probes with a minor allele frequency of the target CpG site >0.4 (**Supplementary Figure 1A**).

Statistical Analysis

Perinatal information was retrospectively obtained from medical records at our hospital. The significance of associations between PG at 1 h after birth and each blood cell composition or each medical record estimated using the minfi package was examined by Pearson's association test. Significant differences in PG at 1 h after birth according to the neonatal sex or effects of caesarean section (CS) were examined by Welch's two-sample *t* test. Eventually, we included whole-cell types, except granulocytes, in addition to gestational age, CS, and neonatal sex as covariates. Additionally, we determined whether associations between DNA methylation and PG at 1 h after birth were influenced by genetic variants. We also evaluated significant 12 CpG sites according to a reference meQTL dataset described by Hannon et al. (27).

We assessed raw and normalized β values from the 132 samples using principal component analysis to exclude the outliers (**Supplementary Figures 1B, C**), resulting in exclusion of four samples. There were no differences in maternal characteristics between included and excluded cases (**Supplementary Table 1**). First, we analysed associations between neonatal PG at 1 h after birth and blood cell composition or medical characteristics by linear regression analysis. Associations between neonatal PG at 1 h after birth and cord blood DNA methylation in the 128 samples were assessed by robust linear regression (rlm) using the R MASS package [rlm(model, method="M", psi = psi.hampel, init = "lts")] with White's estimator [coeftest(rlm, vcov=vcovHC(rlm, type="HC"))] using the R 'sandwich' package. The variance inflation factor of PG at 1 h after birth or each estimated cell composition was as follows: PG at 1 h after birth (1.15), 'Bcell' (5.56), 'CD4T' (33.23), 'CD8T' (6.19), 'Gran' (55.35), 'Mono' (5.29), 'NK' (2.47), and 'nRBC' (4.70). Because the variance inflation factor of 'Gran' was the largest in this study, we removed the 'Gran' fractions from the covariates. After removing 'Gran', the covariates were PG at 1 h after birth (1.14), 'Bcell' (1.16), 'CD4T' (1.47), 'CD8T' (1.14), 'Mono' (1.25), 'NK' (1.23), and 'nRBC' (1.20). Other cell types were added to the rlm model as separate covariates. Additionally, we evaluated the rlm model by adding either cell type individually. The genomic inflation factor (λ) and quantile–quantile plots were used to compare the genome-wide distribution of P-values with the expected null distribution. The P-value was adjusted by λ and used to normalize the expected proportion of false-positives in the dataset (i.e., false discovery rate) and correct for multiple testing rounds using the Benjamini–Hochberg method. For maternal and neonatal characteristics, continuous data were compared between groups using the Mann–Whitney *U*, test and categorical variables were analysed using Fisher's exact test using JMP software (v15.0; SAS Institute, Cary, NC, USA). A $P < 0.05$ was considered to indicate significant results.

RESULTS

We collected PG at 1 h after birth samples from 128 term neonates born to mothers with GDM (**Table 1**). The median gestational age at delivery and birth weight were 39 weeks (range: 37–41 weeks) and 3,022 g (range: 2,352–3,834 g), respectively. Among the 128 neonates, 63 were female (49%) and 45 exhibited hypoglycaemia (36%). The median PG at 1 h after birth was 2.8 mmol/L (range: 1.2–7.6 mmol/L). Among 45 neonates with hypoglycaemia, 12 were born to mothers with GDM who received insulin therapy during pregnancy, and 24 were born to mothers with GDM whose GDM was diagnosed before 24 gestational weeks. Maternal insulin therapy and GDM diagnosed before 24 gestational weeks were not associated with neonatal hypoglycaemia ($P = 1.00$ and 0.82, respectively).

The association between PG at 1 h after birth and blood cell composition or medical characteristics is shown in **Table 2**. Although there was less collinearity between cell types and 1-h PG (**Supplementary Figure 2**), 'CD4T', 'Gran', and 'NK' were significantly correlated with PG at 1 h after birth. For medical characteristics, gestational age at birth was significantly associated with PG at 1 h after birth; however, the antepartum OGTT or metabolic features were not associated with PG at 1 h after birth. Although there was no difference in PG at 1 h after birth between female and male new-borns (2.8 mmol/L *vs.*

TABLE 1 | Characteristics of 128 neonates born to Japanese mothers with gestational diabetes and monitored 1 h after birth.

	Inclusion Group (n = 128)	
Maternal age at delivery (years)	37	(26–47)
Maternal pregravid BMI (kg/m^2)	20.4	(16.9–32.9)
Maternal insulin use during pregnancy	33	(26%)
Maternal gestational weight gain (kg)	8.2	(-5.2–18)
GDM diagnosis before 24 gestational weeks	71	(55%)
Gestational age at delivery (weeks)	39	(37–41)
Caesarean section	45	(35%)
Female neonates	63	(49%)
Birth weight (g)	3,022	(2,352–3,834)
PG at 1 h after birth (mmol/L)	2.8	(1.2–7.6)
Hypoglycaemia (PG <2.6 mmol/L)	45	(35%)
Umbilical artery pH	7.31	(7.13–7.44)
Apgar score		
1 min	8	(7–10)
5 min	9	(7–10)
Placenta weight (g)	560	(310–910)

BMI, body mass index; GDM, gestational diabetes mellitus; PG, plasma glucose level. Data are presented as median (range) or n (%).

TABLE 2 | Correlation between plasma glucose level at 1 h after birth and blood cell composition or medical records.

	Trend	P-value
Cell composition of blood sample		
B cell	-0.128255	0.15
T cell, CD4	-0.279375	0.0014
T cell, CD8	0.1179542	0.18
Granulocyte	0.187439	0.034
Monocyte	0.0227967	0.80
NK cell	0.2066989	0.019
Red blood cell	0.0408877	0.65
Maternal age at delivery	-0.016684	0.85
Maternal antepartum OGTT		
Fasting PG	-0.016684	0.85
1-h PG	0.119382	0.18
2-h PG	-0.090744	0.31
Fasting IRI	-0.111603	0.21
1-h IRI	0.0194941	0.83
2-h IRI	-0.057849	0.52
HOMA-IR	-0.047058	0.60
IS_{OGTT}	-0.007299	0.93
Insulinogenic index	0.0995087	0.27
ISSI-2	-0.004584	0.96
Gestational age at birth	0.2761861	0.0016
Birthweight	-0.030745	0.73
Neonatal PG	1	0

OGTT, oral glucose tolerance test; PG, plasma glucose level; IRI, immunoreactive insulin; HOMA-IR, homeostasis model assessment for insulin resistance; IS_{OGTT}: Insulin sensitivity index from OGTT; ISSI-2, Insulin Secretion-Sensitivity Index-2.

2.8 mmol/L, $P = 0.63$), the PG at 1 h after birth in those born *via* CS was lower than that in new-borns born *via* vaginal delivery (2.7 *vs.* 2.8 mmol/L, $P = 0.024$).

We then performed rlm analysis of DNA methylation of cord blood cells and continuous neonatal 1-h PG of 128 samples by adding four covariates: sex, CS, gestational age, and blood cell components. This model resulted in a λ of 1.22 (**Supplementary Figure 3**). Therefore, we corrected the P-value by adjusting λ to 1.1, which we considered as an acceptable value (28). This revealed that the methylation level at 12 CpG sites was individually associated with PG at 1 h after birth (false discovery rate-adjusted $P < 0.05$) (**Table 3** and **Figure 1**). Differences in the new-born DNA methylation beta value per 1 mmol/L increase in PG at 1 h after birth at these 12 CpG sites were -0.033–0.011. Of these 12 CpG sites, two (cg11388673 and cg08799779) were on the same CpG island (chr8:144371446-144372076) in *ZNF696* and associated with GDM according to the EWAS Atlas database. We confirmed that cell heterogeneity was not a major confounder in the associations of these two CpG sites, by adding and comparing each cell type individually as a covariate and based on the results without cell type covariates (**Supplementary Figure 4**). However, neonatal gender was a major confounder of these two CpG sites. Regression analysis between only the DNA methylation status and neonatal PG at 1 h after birth did not reveal these two CpG sites as significant (**Supplementary Table 2** and **Supplementary Figure 5**). Interestingly, previous reports have shown that these two CpG sites are associated with sex (**Table 4**) (29, 30); therefore, we examined the associations between each DNA methylation level in five array probes within the same CpG island and neonatal PG according to neonatal sex (**Figure 2**). Of the five probes, four were associated with neonatal PG at 1 h after birth in both male and female infants ($P < 0.05$) (**Table 5**). Among the four probes, sites cg11388673 and cg08799779 were significantly associated with neonatal PG at 1 h after birth according to rlm after considering the covariates and confounders (**Table 3**).

The sites cg11388673 and cg08799779 in *ZNF696* were −67 and +119 proximal to the alternative transcription start site (TSS), respectively. The transcript starting from this location (i.e., ENST00000523891) encodes a protein isoform of *ZNF696* (UniProt: E5RJV3_112 aa) with 96 amino acids of the C-terminus perfectly matching those of the N-terminus of another major isoform (UniProt: Q9H7X3_374 aa). DNA methylation in the proximity of the TSS of the major isoform (ENST00000330143) was not associated with PG at 1 h after birth (**Supplementary Figure 6**). We identified 46 transcription factors that bind the TSS of the major isoform, whereas only ELF1 and RUNX3 were confirmed to bind the alternative TSS in the human lymphoblastoid cell line GM12878 according to the ENCODE 3 TFBS Track (32), which is available in UCSC Genome Browser on Humans February 2009 (GRCh37/hg19) Assembly (**Supplementary Figure 7**). ELF1 and RUNX3 binding was not observed in any of the other 10 CpG sites.

TABLE 3 | Methylation sites where neonatal plasma glucose level was associated with offspring new-born blood methylation.

Target ID	CHR	Position	Coefficient[a]	SE	Raw p-value	FDR-corrected P value
cg08694578	2	241835147	0.007079794	0.001208394	4.66E-09	0.02163268
cg11388673	8	144371779	-0.033161507	0.005901354	1.92E-08	0.038674577
cg22424746	1	117753313	0.004865795	0.000888525	4.34E-08	0.042628046
cg14419205	14	103534883	0.009046023	0.001674679	6.60E-08	0.042628046
cg14126408	10	44705342	0.009221915	0.00171699	7.83E-08	0.042628046
cg26151761	1	203025885	0.004951642	0.000922286	7.92E-08	0.042628046
cg09818265	1	57917333	0.009563449	0.001787176	8.74E-08	0.042628046
cg12217831	8	40958960	0.008928346	0.001675977	9.97E-08	0.042628046
cg08799779	8	144371965	-0.032174481	0.006116658	1.44E-07	0.048566746
cg09399476	12	9838211	0.006667227	0.001272616	1.61E-07	0.048566746
cg27052152	12	55027176	0.010687028	0.002041143	1.64E-07	0.048566746
cg18158709	2	235598570	0.001918437	0.000367827	1.83E-07	0.049131149

CHR, chromosome; FDR, false discover rate; SE, standard error.

[a]*Differences in DNA methylation beta value per 1 mmol/L increase in PG at 1 h after birth.*

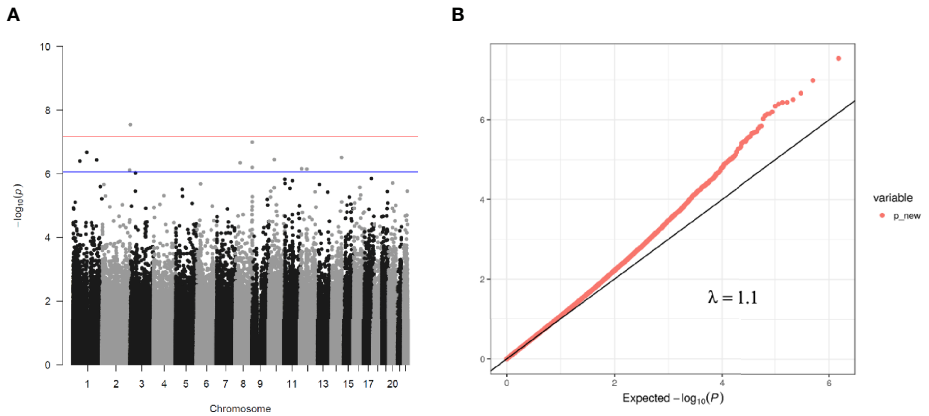

FIGURE 1 | **(A)** Manhattan plot of EWAS between PG at 1 h after birth and DNA methylation levels of 754,255 CpG sites. **(B)** QQ plot of EWAS p-values.

TABLE 4 | Outputs from mQTL database and EWAS Atlas for identified 12 CpGs.

chr	CpG site	position (hg19)	position (hg38)	Annotation	Gene Name	Location	meQTL SNP (hg38)	meQTL Beta value	meQTL P-value	EWAS Atlas (We checked on August 24,2020)
1	cg09818265	57917333	57451661	intron 3 of 16 (NM_021080)	DAB1	OpenSea				
1	cg22424746	117753313	117210691	intron 1 of 4 (NM_001253850)	VTCN1	OpenSea				Multiple sclerosis
1	cg26151761	203025885	203056757	intron 18 of 29 (NM_001304331)	PPFIA4	OpenSea				IL-13 treatment
2	cg18158709	235598570	234689926	intron 1 of 2 (NR_132376)	LINC01173	OpenSea				
2	cg08694578	241835147	240895730	exon 1 of 5 (NM_001085437)	C2orf54	OpenSea				
8	cg12217831	40958960	41101441	Intergenic	–	OpenSea				
8	cg11388673	144371779	143289609	Promoter-TSS (ENST 00000523891)	ZNF696	Island	chr8.143289197	-0.053828385	8.96E-20	Gender, GDM, Primary Sjogren's Syndrome, Klinefelter syndrome
8	cg08799779	144371965	143289795	Promoter-TSS (ENST 00000523891)	ZNF696	Island	chr8.143289818	-0.053782588	4.02E-22	Gender
10	cg14126408	44705342	44209894	Intergenic	–	S_Shelf				Crohn's disease, Pretem birth
12	cg09399476	9838211	9685615	intron 2 of 5 (NM_001004419)	CLEC2D	OpenSea	chr12.9206399	0.01062681	2.18307E-10	
							chr12.9361655	0.01149018	4.47186E-13	
							chr12.9663833	0.01600185	3.98094E-23	
							chr12.9673426	-0.04524827	2.72462E-92	
							chr12.9764510	-0.01051047	4.44425E-09	
12	cg27052152	55027176	54633392	intron 1 of 4 (NM_033277)	LACRT	OpenSea	chr12.54615029	-0.028313087	1.34E-57	Ancestry
14	cg14419205	103534883	103068546	Intergenic	0	OpenSea				

chr, chromosome; SNP, single nucleotide polymorphism.

Methylation levels at the 12 CpG sites continuously changed in association with neonatal 1 h PG level after birth. However, these epigenetic changes may be related to genetic variations concentrated in neonates in whom methylation levels at any of the 12 CpG sites were either in the higher or lower range. Evaluation of this possibility using the DNA-methylated quantitative trait locus (meQTL) database (25) confirmed the presence of eight meQTL SNPs related to methylation levels at four CpG sites out of the 12 CpG sites (**Table 4**). None of eight SNPs have been reported to be associated with any traits in the

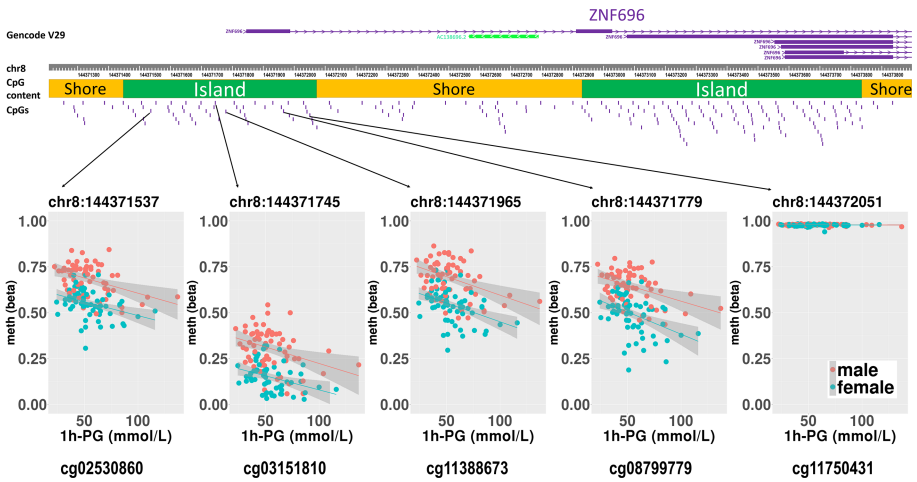

FIGURE 2 | Rlm analysis of DNA methylation and 1-h PG after birth in each of five CpG sites located in the same CpG island in the *ZNF696* promoter. DNA methylation of the 5′ region of four CpG sites was associated with PG at 1 h after birth after birth. Only cg11388673 and cg08799779 were significant after considering covariates and confounders.

TABLE 5 | The association with DNA methylation at 5 CpG sites within alternative TSS of *ZNF696* and neonatal PG at 1h after birth by neonatal sex.

CGI [chr8:144371446-144372076]	Male			Female		
	Coefficient	SE	Pr(>|z|)	Coefficient	SE	Pr(>|z|)
cg02530860 (8:144371537)	-0.025	0.007	2.7.E-04	-0.027	0.007	2.7.E-04
cg03151810* (8:144371745)	-0.029	0.009	1.3.E-03	-0.029	0.008	1.6.E-04
cg11388673* (8:144371779)	-0.028	0.007	1.3.E-05	-0.043	0.010	3.3.E-05
cg08799779 (8:144371965)	-0.031	0.008	7.2.E-05	-0.036	0.010	2.1.E-04
cg11750431 (8:144372051)	-3.4.E-04	7.4.E-04	0.64	7.0.E-04	4.3.E-04	0.10

chr, chromosome; SE, standard error.
Rlm was performed adding 3 covariates; cesarean section delivery, gestational age, and cell components (-Gran).
**indicates the probes that reported to be hyper-methylated in infants cord blood born to GDM (31).*

GWAS Catalog. The minor allelic frequency (MAF) of the eight SNPs was 0.290–0.490 in the Genome Aggregation Database (gnomAD; https://gnomad.broadinstitute.org). Next, to determine whether unexamined genetic variants associated with neonatal hypoglycaemia can alter methylation of the 12 CpG sites identified in our study, we referred to the GWAS Catalog. Among the six reported GDM-associated variants, none of the variants could be *cis*-meQTL within 1 Mb of the 12 CpG sites (30, 32). There were 549 significant genome-wide associations ($P < 5 \times 10^{-8}$) between 384 common SNPs within 1 Mb of 12 CpG sites and any trait. Of the 549 associations, SNPs associated with body mass index, fasting blood glucose, and T2DM were identified within 1 Mb of four (cg09818265, cg26151761, cg27052152, and cg14419205), one (cg12217831), and two (cg22424746 and cg14419205) of the 12 CpG sites, respectively. We cannot rule out the possibility that these meQTL- and GWAS-identified genetic variants are involved in methylation changes observed in the 12 CpG sites in a neonatal period-specific manner without evaluating the genetic variants in our subjects.

DISCUSSION

In this study, we measured genome-wide DNA methylation levels in umbilical cord blood and PG levels in neonates born to women with GDM. The results revealed an association between methylation at CpG sites proximal to an alternative TSS of *ZNF696* and PG at 1 h after birth.

We hypothesized that postnatal blood glucose levels reflect the degree of foetus-individual response to *in utero* hyperglycaemia, and that neonatal epigenetics and hypoglycaemia are associated. In this study, about half of the mothers were diagnosed with GDM after 24 gestational weeks. However, since we thought they might have had potential hyperglycaemia from the early stages of pregnancy according to previous reports (16–18), the DNA methylation status in cord blood cells was associated with neonatal PG at 1 h after birth. This is the first study investigating the possible association between the offspring epigenome with hypoglycaemia in neonates born to mothers with GDM. We identified two CpG sites associated with neonatal PG on the same CpG island

(chr8:144371446–144372076) and in the vicinity of the alternative TSS of *ZNF696*. Moreover, another two CpG sites within the same CpG island were associated with DNA methylation and PG at 1 h after birth (**Figure 2**). A previous report indicated that a CpG site in this region is associated with GDM according to genome-wide DNA methylation analysis of offspring born to mothers with GDM (31). Although the function of *ZNF696* remains unknown, a previous study reported that this gene is involved in acquired paclitaxel resistance in nasopharyngeal carcinoma cells (33). In the present study, DNA methylation at two CpG sites within *ZNF696* showed associations with neonatal 1-h PG. Although the method used to detect DNA methylation had a limited ability to detect all CpGs in the genome, the findings using array probes suggested strong epigenetic regulation. Yamamoto et al. reported that in-target intrapartum glucose control in mothers with GDM was not associated with neonatal hypoglycaemia after adjusting for neonatal factors and considering gestational age, preterm delivery, and infant sex as confounders of neonatal factors (34). This suggests that neonatal hypoglycaemia does not occur because of temporal maternal glycaemic dysregulation during intrapartum. Therefore, the association between changes in DNA methylation identified in the present study and neonatal hypoglycaemia suggests that both epigenetic regulation and hypoglycaemia are ascribed to effects related to maternal hyperglycaemia. Furthermore, epigenetic changes to the *ZNF696* promoter may regulate blood cell function along with neonatal hypoglycaemia.

We confirmed eight meQTL SNPs, which have been reported for four CpG sites among the 12 CpG sites (**Table 4**). Whether our results were affected by these reported genetic variants and if these reported genetic variants alone were associated with the changes in the methylation at four CpG sites remain unclear. Undefined SNPs may affect neonatal methylation at the identified 12 CpG sites in *cis* or *trans* manner to synergistically interact with maternal hyperglycaemia. Further studies are needed to clarify these possibilities. The TF ChIP-seq database revealed that ELF1 and RUNX3 bind the alternative TSS of *ZNF696* based on information obtained using the human lymphoblastoid cell line GM12878 (32). These two transcription factors do not reportedly bind to other regions that are associated with the remained 10 CpG sites. This may be related to the results that showed that among the 12 significant CpG sites, methylation changes at the two CpG sites in the *ZNF696* alternative TSS alone are negatively associated with postnatal 1-h PG. Targeting of alternative TSSs is related to developmental stage (35, 36) or cell differentiation (37). This suggests that the synergistic effects of the *in utero* environment and foetal glucose tolerance are driven by DNA methylation at the alternative TSS of *ZNF696*. Furthermore, Yamamoto et al. reported that male sex was significantly associated with neonatal hypoglycaemia in children born to mothers with type 1 diabetes and GDM (34). In the present study, neonatal gender was unrelated to PG at 1 h after birth; however, we only observed an association between DNA methylation at *ZNF696* and PG at 1 h after birth when neonatal sex was added as a covariate. Moreover, hypermethylation was observed in CpG sites in the alternative TSS of *ZNF696* in males and in neonatal hypoglycaemia (**Figure 2**), suggesting differential isoform transcription at this location between genders. Similar epigenetic regulation may occur in various tissues and affect the control of blood glucose depending on the neonatal sex.

Hyperinsulinemia, insulin resistance, and metabolic syndrome reportedly alter the blood cell composition (38). We identified a significant correlation between neonatal PG and the percentage of 'CD4T', 'Gran', and 'NK' components in cord blood cells, respectively. This indicates that *in utero* hyperinsulinemia affects cord blood cell differentiation.

This study has several limitations. First, PG at 1 h after birth was determined only in neonates born to mothers with GDM at our hospital and not in those delivered from mothers without GDM. In addition, we did not determine the neonatal plasma insulin level. Furthermore, as neonatal hyperinsulinemia is the major reason for neonatal hypoglycaemia in offspring born to mothers with GDM, the neonatal plasma insulin level may better reflect the *in utero* environment compared to PG. However, we did not determine plasma insulin levels in neonates. To overcome this limitation, we examined the methylation beta value of cord blood from 60 new-borns born to mothers with normal glucose tolerance (NGT) but whose neonatal PG at 1 h after birth was not evaluated. Neonatal hypoglycaemia may occur not only in new-borns born to mothers with GDM but also in those who are preterm or are small or large for their gestational age (38). Our 60 NGT subjects were all born after 37 gestational weeks. Four new-borns of our 60 subjects had -1.5 SD birth weight and four had +1.5 SD birth weight compared to subjects born at the same gestational age. We predicted that neonatal hypoglycaemia had not occurred in our 60 subjects with NGT based on the following results. The methylation levels in the 60 subjects with NGT should be higher than those in 128 subjects with GDM at the 10 CpG sites whose regression coefficients for neonatal PG levels showed positive values in our analysis, and vice versa for the remaining 2 CpG sites. As shown in **Supplementary Figure 8**, the median methylation levels of NGT were higher than those of GDM at cg08694578 and cg27052152 in both sexes. Student's *t*-test revealed significant methylation differences between NGT and GDM at cg27052152 only in males ($p = 0.035$). The median methylation levels at cg11388673 and cg08799779, which are in the alternative TSS of *ZNF696*, were decreased in NGT compared to in GDM as predicted, although they were not significantly different. The differences were more obvious in males. These results regarding to at least four of the 12 identified CpG sites support our speculation that methylation changes at the identified CpG sites could be markers for *in utero* hyperglycaemia, even after including NGT subjects. Further experiments are warranted to confirm these results by recruiting subjects with NGT, whose neonatal PG is evaluated at 1 h after birth. Second, the sample size was small. When calculating multiple regression power with a medium effect size and at the false discovery rate-corrected significance level, the power of our sample size was 0.024. Without adjusting the 5% significance level using multiple test

correction, the power was 0.86. However, we performed association analysis between DNA methylation and neonatal PG by adding four covariates, including sex, CS, gestational age, and blood cell components. Furthermore, aside from GDM and preterm birth, maternal obesity, poor or excessive nutrition, and adiposity are associated with neonatal hypoglycaemia (39). Given that a previous study reported that umbilical cord blood was associated with PG after birth in neonates (40), analysis of the relationship between neonatal PG and DNA methylation may be more effective than examining the relationship with GDM to identify epigenetic mechanisms related to the development of neonatal hypoglycaemia. Nevertheless, further investigation using a larger cohort is necessary to identify other epigenetic mechanisms related to neonatal hypoglycaemia. We attempted to verify our results using the Asian cohort study GUSTO (41). However, in this previous study, data on cord blood DNA methylation was obtained from only 65 of 211 mothers with GDM, limiting our ability to interpret the findings in this small sample. Third, since hyperinsulinemia in mothers with GDM might be often attributed to excessive insulin therapy, we cannot deny the possibility that insulin therapy during pregnancy influenced DNA methylation in cord blood samples. However, maternal insulin therapy was not significantly associated with neonatal hypoglycaemia in our neonates. In addition, since we have introduced self-monitored blood glucose measurements for all GDM cases, we believe that extra insulin therapy did not occur in our subjects. Fourth, overt diabetes might be more strongly influenced by DNA methylation compared to GDM because maternal hyperglycaemia in overt diabetes mothers might be more prominent than that in mothers with GDM. However, in this study, only one mother developed overt DM, and we could not analyse the association between neonatal hypoglycaemia and DNA methylation in cord blood samples among neonates born to overt diabetes mothers. We have to consider further research using larger samples.

In summary, we identified DNA methylation at two CpG sites near an alternative TSS of *ZNF696* and found that they were significantly associated with PG at 1 h after birth. Methylation levels at these sites increased as neonatal PG levels at 1 h after birth decreased, suggesting that neonatal hypoglycaemia driven by the GDM status of mothers alters access to an alternative TSS of *ZNF696* in cord blood cells, which may be related to abnormal blood cell differentiation. Furthermore, epigenetic variations in offspring related to exposure to maternal hyperglycaemia, especially during early pregnancy, may reflect neonatal PG levels at 1 h after birth.

DATA AVAILABILITY STATEMENT

Data supporting the results of this article are available in the Gene Expression Omnibus repository (GSE122086, https://www.ncbi.nlm.nih.gov/geo/query/acc.cgi?acc=GSE122086 and GSE122288, https://www.ncbi.nlm.nih.gov/geo/query/acc.cgi?acc=GSE122288). Methylation data and analytical conditions are available upon request.

ETHICS STATEMENT

The studies involving human participants were reviewed and approved by The Keio University School of Medicine Ethics Committee The Institutional Review Board of the National Research Institute for Child Health and Development. The patients/participants provided their written informed consent to participate in this study.

AUTHOR CONTRIBUTIONS

YK and KM collected the data; YK performed experiments; YK and TK performed statistical analyses, wrote the manuscript, contributed to the discussion, and reviewed/edited the manuscript; KM contributed to the discussion and wrote and reviewed/edited the manuscript; YS, SI, DO, MH, MTam, and KHas, MTan and KHat contributed to the discussion and reviewed/edited the manuscript. All authors contributed to the article and approved the submitted version.

FUNDING

This study was supported by the Japan Agency for Medical Research and Development (18ek0109278h0002, 18ek0109290h0002, and 18mk0102093s0402), Japan Society for the Promotion of Science KAKENHI (17K19535 and 19K09761), and NCCHD of Japan research grant (2020B-21).

ACKNOWLEDGMENTS

The authors thank the medical staff in the perinatal care unit of Keio University Hospital for excellent patient care. We thank Editage (www.editage.jp) for English language editing. We thank Dr. Jonathan Huang of Singapore Institute for Clinical Sciences for providing information about GUSTO.

SUPPLEMENTARY MATERIAL

The Supplementary Material for this article can be found online at: https://www.frontiersin.org/articles/10.3389/fendo.2021.690648/full#supplementary-material

Supplementary Figure 1 | Quality evaluation of methylation data. **(A)** The results of cluster analysis of DNA methylation profiles in 132 neonates. **(B)** PCA was performed to confirm b values for the 132 samples to exclude outliers, resulting in exclusion of four samples.

Supplementary Figure 2 | Collinearity assessment between blood cell types and PG at 1 h after birth. **(A)** The percentage of variances in each principal component were plotted following PCA of cell types and PG at 1 h after birth. The first principal component (PC1) explained 33.9% of the variations. **(B)** The contribution of each factor to the principal components is shown in the circled area. 'Gran' and 'NK' contributed the most to PC1, and PG at 1 h after birth contributed to PC3. Cell types contributed to different PCs. **(C)** Variable association plots. PG at 1 h after birth was positively associated with 'Gran' and 'NK' and negatively associated with 'CD4T'.

Supplementary Figure 3 | Correction of the genomic inflation factor (l). P-values were plotted using a Manhattan plot. QQ plots were plotted to show genomic inflation. Rlm analysis of DNA methylation in cord blood cells and continuous neonatal PG at 1 h after birth in 128 samples. Adding four covariates resulted in a l of 1.22. We considered PG at 1 h after birth to be significantly associated with DNA methylation sites after correcting the P-values with l (corrected to 1.1) (see **Figure 1B**).

Supplementary Figure 4 | Association for each cell type with PG at 1 h after birth associated methylation sites. **(A)** Verification of the P-values for associations with DNA methylation at each of four CpG sites in the CpG island chr8:144371446–144372076 (hg19) and PG at 1 h after birth by adding each blood cell type individually as a covariate. Cell types not affecting the significance of the association between DNA methylation at cg11388673 and cg08799779. **(B)** QQ plots of analyses performed in **(A)**. Upper and lower rows indicate QQ plots before and after correction, respectively. **(C)** P-values following adjustment for the inflation factor and plotted with Manhattan plots. Data were derived from rlm analysis and adding individual cord blood cell types as covariates.

Supplementary Figure 5 | The effect of each covariate on associations between DNA methylation and PG at 1 h after birth. Each Manhattan plot shows the P-values derived from rlm analysis after correcting with the inflation factor and the addition of each covariate confounder (neonatal sex, gestational age, and C-section) individually. The corrected inflation factor for each analysis is shown as a QQ plot. Neonatal sex was a major confounder of the association between DNA methylation at CpG sites in chr8:144371446–144372076 (hg19) and PG at 1 h after birth.

Supplementary Figure 6 | The association between DNA methylation in 12 CpG sites proximal to the TSS of the ZNF696 isoform (ENST00000330143) and PG at 1 h after birth. Associations are shown according to neonatal sex.

Supplementary Figure 7 | Reference data for TF ChIP-seq peaks from ENCODE3 data. Forty-six TFs bind the TSS of the ZNF696 isoform, whereas only ELF1 and RUNX3 were confirmed to bind the alternative TSS in the GM12878 cell line according to ENCODE3 data.

Supplementary Figure 8 | Methylation values distribution at the 12 CpG sites in GDM and NGT were shown in box plot by neonatal sex. The 10 CpG sites whose methylation showed positive association with neonatal PG at 1 h after birth were indicated in upper panels above a dash line. The 2 CpG sites which showed negative association arrayed below a dashed line. Significant methylation value difference between GDM and NGT were analyzed by t-test (* $p < 0.05$).

REFERENCES

1. Quilter CR, Cooper WN, Cliffe KM, Skinner BM, Prentice PM, Nelson L, et al. Impact on Offspring Methylation Patterns of Maternal Gestational Diabetes Mellitus and Intrauterine Growth Restraint Suggest Common Genes and Pathways Linked to Subsequent Type 2 Diabetes Risk. *FASEB J* (2014) 28 (11):4868–79. doi: 10.1096/fj.14-255240
2. Ruchat SM, Houde AA, Voisin G, St-Pierre J, Perron P, Baillargeon JP, et al. Gestational Diabetes Mellitus Epigenetically Affects Genes Predominantly Involved in Metabolic Diseases. *Epigenetics* (2013) 8(9):935–43. doi: 10.4161/epi.25578
3. Finer S, Mathews C, Lowe R, Smart M, Hillman S, Foo L, et al. Maternal Gestational Diabetes Is Associated With Genome-Wide DNA Methylation Variation in Placenta and Cord Blood of Exposed Offspring. *Hum Mol Genet* (2015) 24(11):3021–9. doi: 10.1093/hmg/ddv013
4. Wu P, Farrell WE, Haworth KE, Emes RD, Kitchen MO, Glossop JR, et al. Maternal Genome-Wide DNA Methylation Profiling in Gestational Diabetes Shows Distinctive Disease-Associated Changes Relative to Matched Healthy Pregnancies. *Epigenetics* (2018) 13(2):122–8. doi: 10.1080/15592294.2016.1166321
5. Haertle L, El Hajj N, Dittrich M, Muller T, Nanda I, Lehnen H, et al. Epigenetic Signatures of Gestational Diabetes Mellitus on Cord Blood Methylation. *Clin Epigenet* (2017) 9:28. doi: 10.1186/s13148-017-0329-3
6. Kang J, Lee CN, Li HY, Hsu KH, Lin SY. Genome-Wide DNA Methylation Variation in Maternal and Cord Blood of Gestational Diabetes Population. *Diabetes Res Clin Pract* (2017) 132:127–36. doi: 10.1016/j.diabres.2017.07.034
7. Moen GH, Sommer C, Prasad RB, Sletner L, Groop L, Qvigstad E, et al. Mechanisms IN Endocrinology: Epigenetic Modifications and Gestational Diabetes: A Systematic Review of Published Literature. *Eur J Endocrinol* (2017) 176(5):R247–67. doi: 10.1530/EJE-16-1017
8. Dang MN, Buzzetti R, Pozzilli P. Epigenetics in Autoimmune Diseases With Focus on Type 1 Diabetes. *Diabetes Metab Res Rev* (2013) 29(1):8–18. doi: 10.1002/dmrr.2375
9. Ling C, Groop L. Epigenetics: A Molecular Link Between Environmental Factors and Type 2 Diabetes. *Diabetes* (2009) 58(12):2718–25. doi: 10.2337/db09-1003
10. Zhu Z, Chen X, Xiao Y, Wen J, Chen J, Wang K, et al. Gestational Diabetes Mellitus Alters DNA Methylation Profiles in Pancreas of the Offspring Mice. *J Diabetes Complicat* (2019) 33(1):15–22. doi: 10.1016/j.jdiacomp.2018.11.002
11. Fetita LS, Sobngwi E, Serradas P, Calvo F, Gautier JF. Consequences of Fetal Exposure to Maternal Diabetes in Offspring. *J Clin Endocrinol Metab* (2006) 91(10):3718–24. doi: 10.1210/jc.2006-0624
12. Brody SC, Harris R, Lohr K. Screening for Gestational Diabetes: A Summary of the Evidence for the U.S. Preventive Services Task Force. *Obstet Gynecol* (2003) 101(2):380–92. doi: 10.1097/00006250-200302000-00027
13. Group HSCR, Metzger BE, Lowe LP, Dyer AR, Trimble ER, Chaovarindr U, et al. Hyperglycemia and Adverse Pregnancy Outcomes. *N Engl J Med* (2008) 358(19):1991–2002. doi: 10.1056/NEJMoa0707943
14. Catalano PM, McIntyre HD, Cruickshank JK, McCance DR, Dyer AR, Metzger BE, et al. The Hyperglycemia and Adverse Pregnancy Outcome Study: Associations of GDM and Obesity With Pregnancy Outcomes. *Diabetes Care* (2012) 35(4):780–6. doi: 10.2337/dc11-1790
15. Voormolen DN, de Wit L, van Rijn BB, DeVries JH, Heringa MP, Franx A, et al. Neonatal Hypoglycemia Following Diet-Controlled and Insulin-Treated Gestational Diabetes Mellitus. *Diabetes Care* (2018) 41(7):1385–90. doi: 10.2337/dc18-0048
16. Okubo H, Crozier SR, Harvey NC, Godfrey KM, Inskip HM, Cooper C, et al. Maternal Dietary Glycemic Index and Glycemic Load in Early Pregnancy are Associated With Offspring Adiposity in Childhood: The Southampton Women's Survey. *Am J Clin Nutr* (2014) 100(2):676–83. doi: 10.3945/ajcn.114.084905
17. Wahab RJ, Scholing JM, Gaillard R. Maternal Early Pregnancy Dietary Glycemic Index and Load, Fetal Growth, and the Risk of Adverse Birth Outcomes. *Eur J Nutr* (2021) 60(3):1301–11. doi: 10.1007/s00394-020-02327-9
18. Wahab RJ, Voerman E, Jansen PW, Oei EHG, Steegers EAP, Jaddoe VWV, et al. Maternal Glucose Concentrations in Early Pregnancy and Cardiometabolic Risk Factors in Childhood. *Obes (Silver Spring)* (2020) 28 (5):985–93. doi: 10.1002/oby.22771
19. Minakami H, Maeda T, Fujii T, Hamada H, Iitsuka Y, Itakura A, et al. Guidelines for Obstetrical Practice in Japan: Japan Society of Obstetrics and Gynecology (JSOG) and Japan Association of Obstetricians and Gynecologists (JAOG) 2014 Edition. *J Obstet Gynaecol Res* (2014) 40(6):1469–99. doi: 10.1111/jog.12419
20. Akiba Y, Miyakoshi K, Ikenoue S, Saisho Y, Kasuga Y, Ochiai D, et al. Glycemic and Metabolic Features in Gestational Diabetes: Singleton Versus Twin Pregnancies. *Endocr J* (2019) 66(7):647–51. doi: 10.1507/endocrj.EJ18-0575
21. Itabashi K, Miura F, Uehara R, Nakamura Y. New Japanese Neonatal Anthropometric Charts for Gestational Age at Birth. *Pediatr Int* (2014) 56 (5):702–8. doi: 10.1111/ped.12331
22. Aryee MJ, Jaffe AE, Corrada-Bravo H, Ladd-Acosta C, Feinberg AP, Hansen KD, et al. Minfi: A Flexible and Comprehensive Bioconductor Package for the Analysis of Infinium DNA Methylation Microarrays. *Bioinformatics* (2014) 30 (10):1363–9. doi: 10.1093/bioinformatics/btu049
23. Morris TJ, Butcher LM, Feber A, Teschendorff AE, Chakravarthy AR, Wojdacz TK, et al. ChAMP: 450k Chip Analysis Methylation Pipeline. *Bioinformatics* (2014) 30(3):428–30. doi: 10.1093/bioinformatics/btt684
24. Nordlund J, Backlin CL, Wahlberg P, Busche S, Berglund EC, Eloranta ML, et al. Genome-Wide Signatures of Differential DNA Methylation in Pediatric Acute Lymphoblastic Leukemia. *Genome Biol* (2013) 14(9):r105. doi: 10.1186/gb-2013-14-9-r105

25. Zhou W, Laird PW, Shen H. Comprehensive Characterization, Annotation and Innovative Use of Infinium DNA Methylation BeadChip Probes. *Nucleic Acids Res* (2017) 45(4):e22. doi: 10.1093/nar/gkw967
26. Bakulski KM, Feinberg JI, Andrews SV, Yang J, Brown S, LM S, et al. DNA Methylation of Cord Blood Cell Types: Applications for Mixed Cell Birth Studies. *Epigenetics* (2016) 11(5):354–62. doi: 10.1080/15592294.2016.1161875
27. Hannon E, Gorrie-Stone TJ, Smart MC, Burrage J, Hughes A, Bao Y, et al. Leveraging DNA-Methylation Quantitative-Trait Loci to Characterize the Relationship Between Methylomic Variation, Gene Expression, and Complex Traits. *Am J Hum Genet* (2018) 103(5):654–65. doi: 10.1016/j.ajhg.2018.09.007
28. Howe CG, Cox B, Fore R, Jungius J, Kvist T, Lent S, et al. Maternal Gestational Diabetes Mellitus and Newborn Dna Methylation: Findings From the Pregnancy and Childhood Epigenetics Consortium. *Diabetes Care* (2020) 43(1):98–105. doi: 10.2337/dc19-0524
29. Yousefi P, Huen K, Dave V, Barcellos L, Eskenazi B, Holland N. Sex Differences in DNA Methylation Assessed by 450 K BeadChip in Newborns. *BMC Genomics* (2015) 16:911. doi: 10.1186/s12864-015-2034-y
30. McCartney DL, Zhang F, Hillary RF, Zhang Q, Stevenson AJ, Walker RM, et al. An Epigenome-Wide Association Study of Sex-Specific Chronological Ageing. *Genome Med* (2019) 12(1):1. doi: 10.1186/s13073-019-0693-z
31. Weng X, Liu F, Zhang H, Kan M, Wang T, Dong M, et al. Genome-Wide DNA Methylation Profiling in Infants Born to Gestational Diabetes Mellitus. *Diabetes Res Clin Pract* (2018) 142:10–8. doi: 10.1016/j.diabres.2018.03.016
32. Consortium EP, Moore JE, Purcaro MJ, Pratt HE, Epstein CB, Shoresh N, et al. Expanded Encyclopaedias of DNA Elements in the Human and Mouse Genomes. *Nature* (2020) 583(7818):699–710. doi: 10.1038/s41586-020-2493-4
33. Li W, You Y, Zhang X, Song Y, Xiang H, Peng X, et al. Amplification of Chromosome 8q21-qter Associated With the Acquired Paclitaxel Resistance of Nasopharyngeal Carcinoma Cells. *Int J Clin Exp Pathol* (2015) 8(10):12346–56.
34. Yamamoto JM, Donovan LE, Mohammad K, Wood SL. Severe Neonatal Hypoglycaemia and Intrapartum Glycaemic Control in Pregnancies Complicated by Type 1, Type 2 and Gestational Diabetes. *Diabetes Med* (2020) 37(1):138–46. doi: 10.1111/dme.14137
35. Davis WJr., Schultz RM. Developmental Change in TATA-Box Utilization During Preimplantation Mouse Development. *Dev Biol* (2000) 218(2):275–83. doi: 10.1006/dbio.1999.9486
36. Steinthorsdottir V, Stefansson H, Ghosh S, Birgisdottir B, Bjornsdottir S, Fasquel AC, et al. Multiple Novel Transcription Initiation Sites for NRG1. *Gene* (2004) 342(1):97–105. doi: 10.1016/j.gene.2004.07.029
37. Pozner A, Lotem J, Xiao C, Goldenberg D, Brenner O, Negreanu V, et al. Developmentally Regulated Promoter-Switch Transcriptionally Controls Runx1 Function During Embryonic Hematopoiesis. *BMC Dev Biol* (2007) 7:84. doi: 10.1186/1471-213X-7-84
38. van Kempen A, Eskes PF, Nuytemans D, van der Lee JH, Dijksman LM, van Veenendaal NR, et al. Lower Versus Traditional Treatment Threshold for Neonatal Hypoglycemia. *N Engl J Med* (2020) 382(6):534–44. doi: 10.1056/NEJMoa1905593
39. Henriksen T. Nutrition and Pregnancy Outcome. *Nutr Rev* (2006) 64(5 Pt 2):S19–23; discussion S72-91. doi: 10.1301/nr.2006.may.S19-S23
40. Kennedy LML, Crawford TM, Andersen CC, Stark MJ. Does Umbilical Cord Blood Glucose Extraction Discriminate the Risk of Early Neonatal Hypoglycaemia in At-Risk Newborns? *J Paediatr Child Health* (2019) 55(12):1476–80. doi: 10.1111/jpc.14473
41. Soh SE, Chong YS, Kwek K, Saw SM, Meaney MJ, Gluckman PD, et al. Insights From the Growing Up in Singapore Towards Healthy Outcomes (GUSTO) Cohort Study. *Ann Nutr Metab* (2014) 64(3-4):218–25. doi: 10.1159/000365023

Conflict of Interest: The authors declare that the research was conducted in the absence of any commercial or financial relationships that could be construed as a potential conflict of interest.

frontiers in Endocrinology

MINI REVIEW
published: 22 July 2021
doi: 10.3389/fendo.2021.708767

Newer Insights Into Fetal Growth and Body Composition

Satoru Ikenoue, Yoshifumi Kasuga, Toyohide Endo, Mamoru Tanaka and Daigo Ochiai*

Department of Obstetrics and Gynecology, Keio University School of Medicine, Tokyo, Japan

Based on epidemiological and experimental evidence, the origins of childhood obesity and early onset metabolic syndrome can be extended back to developmental processes during intrauterine life. It is necessary to actively investigate antecedent conditions that affect fetal growth by developing reliable measures to identify variations in fetal fat deposition and body composition. Recently, the resolution of ultrasonography has remarkably improved, which enables better tissue characterization and quantification of fetal fat accumulation. In addition, fetal fractional limb volume has been introduced as a novel measure to quantify fetal soft tissue volume, including fat mass and lean mass. Detecting extreme variations in fetal fat deposition may provide further insights into the origins of altered fetal body composition in pathophysiological conditions (i.e., fetal growth restriction or fetal macrosomia), which are predisposed to the metabolic syndrome in later life. Further studies are warranted to determine the maternal or placental factors that affect fetal fat deposition and body composition. Elucidating these factors may help develop clinical interventions for altered fetal growth and body composition, which could potentially lead to primary prevention of the future risk of metabolic dysfunction.

Keywords: DOHaD, fetal ultrasound, fetal body composition, fetal subcutaneous fat, fractional limb volume, fetal growth restriction, macrosomia, predisposition

OPEN ACCESS

Edited by:
Hiroaki Itoh, Hamamatsu University School of Medicine, Japan

Reviewed by:
Noriko Sato, Tokyo Medical and Dental University, Japan
Takahiro Nemoto, Nippon Medical School, Japan

****Correspondence:***
Satoru Ikenoue
sikenoue.a3@keio.jp

Specialty section:
This article was submitted to Pediatric Endocrinology, a section of the journal Frontiers in Endocrinology

Received: *12 May 2021*
Accepted: *28 June 2021*
Published: *22 July 2021*

Citation:
Ikenoue S, Kasuga Y, Endo T, Tanaka M and Ochiai D (2021) Newer Insights Into Fetal Growth and Body Composition. Front. Endocrinol. 12:708767. doi: 10.3389/fendo.2021.708767

INTRODUCTION

Fetal growth is an important predictor of perinatal outcomes. Previous studies have also shown that birth weight is associated with future risk of obesity and metabolic dysfunction in the offspring. Barker et al. reported that low birthweight infants are predisposed to cardiovascular disease in adulthood (1). Maternal undernutrition during pregnancy leads to increased risks of cardiovascular disease in the offspring in later life (2). Meanwhile, the infants of mothers with gestational diabetes have increased adiposity (3). Large-for-gestational age (LGA) neonates born to mothers with gestational diabetes are predisposed to early onset metabolic syndrome (4).

These experimental and epidemiological evidence have shown that the origins of early onset metabolic syndrome can be extended back to developmental processes during intrauterine life (Developmental Origins of Health and Disease) (5–7). Therefore, it is necessary to actively investigate the antecedent conditions that affect fetal growth by developing reliable measures to identify variations in fetal growth and body composition.

BODY WEIGHT AND BODY COMPOSITION

Total body weight and height has been traditionally used as the gold standard for the measurement of body size and nutritional status. Recently, the concept of body composition has been introduced, which is composed of fat mass, lean mass, and bone mineral content.

Neonatal Body Composition

Previous studies on infant body size have mainly relied on height- and weight-based measures (i.e. weight for length, body mass index, or ponderal index). However, these parameters are indirect measures of fat mass or lean mass, and only moderately correlate with percent body fat (8). Newborns with decreased percentage body fat are reported to be at risk of hypoglycemia and short-term morbidity (9). Small-for-gestational age (SGA) newborns, who are supposed to be predisposed to thrifty phenotype, have lower body fat percentage compared to appropriate-for-gestational age infants (10). Higher neonatal body fat percentage is also associated with increased adiposity in childhood (11). These reports suggest that neonatal body composition and body fat percentage could be a more specific marker of future risk of metabolic syndrome as compared with birth weight (11, 12).

The body fat percentage of neonates is higher in humans than in other mammals. It is important for human neonates to prioritize adipose tissue accumulation because adipose tissue is an important buffer against limited nutrient supply soon after birth, and could be utilized as one of the brain's energy resources (13). Indeed, the infant brain requires approximately half of the total energy needs, and ketone bodies derived from adipose tissue can provide a quarter of this requirement (14). Consequently, although neonatal fat mass constitutes only 14% of birth weight, it accounts for a larger variation (46%) in birth weight (15, 16). In contrast, the ponderal index explains only 22% of the variation in birth weight and correlates poorly with body fat percentage (16).

Dual-energy X-ray absorptiometry and air displacement plethysmography have recently been used as gold standards for measuring body composition and body fat percentage in infants (17).

Ultrasound-Based Measures of Fetal Weight

Fetal ultrasonography is commonly used to evaluate fetal growth in clinical practice, and most studies use conventional biometry (estimated fetal weight). Estimated fetal weight has been reported to be a useful predictor of fetal macrosomia (18), or fetal growth restriction with decreased percent body fat (19). However, the estimated fetal weight can fluctuate by approximately 15% compared to the actual weight and has poor accuracy, especially for fetuses with growth restriction or macrosomic infants (20). A possible explanation is that the estimated fetal weight is an indirect measure of fat mass or lean mass, and has only a modest association with newborn adiposity (21). However, few studies have incorporated fetal fat mass or lean mass measures into formulas that estimate fetal weight. There have recently been remarkable improvements in the resolution of fetal ultrasonography, which enables better tissue characterization and quantification of fetal fat mass and lean mass. Several studies have been conducted to assess fetal body composition (22) and its correlation with newborn adiposity (**Table 1**).

Ultrasound-Based Measures of Fetal Body Composition

Histologically, fetal fat is observed in early gestation (29). However, measures of fetal fat mass or lean mass by ultrasonography are mostly obtained after 20 weeks of gestation because enlargement and accumulation of adipocytes accelerate in the second half of pregnancy (30). Since 70-90% of total body fat in human infants is subcutaneous and not visceral (31), subcutaneous fat mass is measured for evaluating fetal adiposity. Fetal fat mass can be reliably and reproducibly measured using ultrasonography at the mid-upper arm, mid-thigh, and abdomen (32).

Fetal Fat Mass Measures in the Upper-Arm and Thigh

In 1985, Jeanty et al. reported the measurement of subcutaneous fat thickness in the arm and thigh (33). This method yields substantial measurement error because the subcutaneous fat thickness in the limb is not continuous around the limb. In 1997, Bernstein et al. measured the fat area on the arm and thigh, instead of the fat thickness at term gestation. The fat area on the arm and thigh were quantified by subtracting the lean mass area from the total cross-sectional area at the midpoint of the humerus or femur. They reported a significant correlation between the fat area of the limb and newborn fat mass (28).

Fetal Fat Mass Measures in the Abdomen

In previous studies, abdominal subcutaneous fat thickness was measured as the hyperechoic region anterior to the margins of the ribs. The widest point was selected in the anterior third of the abdominal circumference (34). In 1997, Petrikovsky et al. reported that anterior abdominal wall thickness is useful for ruling out fetal macrosomia (35). Subsequently, in 1999, Gardeil et al. measured anterior abdominal wall thickness as a predictor of fetal growth restriction (34). An increasing amount of evidence has been gathered over the last 20 years in the assessment of fetal body composition and fat mass (22).

Fetal Fat Mass Measures in Other Parts

In addition to the three major sites (upper-arm, thigh and abdomen), fetal fat is deposited in other areas such as the cheek, ribs, and buttocks (22, 36, 37). Abramowicz et al. has reported that fetal cheek-to-cheek diameter is useful in the prediction of birth weight and mode of delivery (36, 38, 39). Matsumoto et al. reported the fetal nutrition score, derived from fetal subcutaneous tissue present at face, ribs and buttocks. The fetal nutrition score significantly correlated with neonatal nutrition score derived from face, ribs, thigh and buttocks (37). However, the accuracy of quantitative measurement of fat mass in these areas has not been validated.

Fetal Fractional Limb Volume

3D ultrasonography refers specifically to the volume rendering of ultrasound data, and is now widely used in the clinical practice including prenatal diagnosis. Fetal fractional limb volume measured by three-dimensional ultrasonography was

TABLE 1 | Fetal fat mass measures predicting newborn adiposity.

Author, publication year	N	Newborn adiposity measures		Gestational age at fetal ultrasonography	Fetal biometry	Correlation coefficient	p value	Covariates
		Parameter	Device					
Ikenoue et al. (23)	109	%BF	DXA	20, 30 weeks	Arm percent fat area (30 weeks)	0.45	p<0.001	GA, Parity, BMI, GWG, SES, Ethnicity, Obstetrical complications
					Thigh percent fat area (30 weeks)	0.26	p<0.05	
					FAST (30 weeks)	0.21	p<0.05	
O'Connor et al. (24)	62	Fat mass	ADP	28, 33, 38 weeks	FAST (38 weeks)	–	p<0.001	smoking
					Thigh fat thickness (38weeks)	–	p=0.004	
					Thigh fat thickness (28weeks)	–	p=0.023	
Buhling et al. (25)	172	Skinfold thickness	Anthropometry*	37– weeks	FAST	0.58	p<0.001	BMI, placental site, amniotic fluid volume
					Thigh fat thickness	0.64	p<0.001	
Knight et al. (26)	106	%BF	ADP	36–40 weeks	Arm fat area	–	p<0.001	–
Lee et al. (27)	87	%BF	ADP	38 weeks (mean)	Fractional thigh volume	0.68	p<0.001	Age, parity, GA, sex, ethnicity, Obstetrical complications
					Fractional arm volume	0.62	–	
					Estimated fetal weight	0.55	–	
					Abdominal circumference	0.50	–	
Moyer-Mileur et al. (21)	47	%BF	ADP	35 week	Estimated fetal weight	0.33	p<0.05	Parity, BMI, GWG, SES
					Abdominal circumference	0.37	p<0.05	
Bernstein et al. (28)	36	%BF	Anthropometry*	19–40 weeks	Thigh fat area	0.63	p<0.001	Age, Parity, BMI, GA, GWG, sex
					Arm fat area	0.45	p<0.05	

%BF, percent body fat; DXA, Dual-energy X-ray absorptiometry; ADP, air displacement plethysmography; FAST, fetal abdominal subcutaneous tissue; GA, gestational age; BMI, body mass index; GWG, gestational weight gain, SES, socioeconomical status.

**Sum of subcutaneous skinfold thickness.*

introduced by Lee et al., defined as the cylindrical limb subvolume based on the central 50% of the total humeral or femoral length (40). It is a reproducible measure for quantifying fetal soft tissue volume, including fat mass and lean mass (41, 42). Usually, before starting fractional limb volume measures, sonographers are required to measure 20-30 training data sets. The learning curve for technically satisfactory measurements of fractional limb volume is quickly achieved without difficulty (43). Recently, automated fractional limb volume measures has also been investigated (44). Fractional limb volume is useful to improve birth weight estimation (43) and accounts for a greater proportion of variation in neonatal body fat percentage than conventional fetal measures such as estimated fetal weight (27). The growth trajectory of fetal soft tissue volume (especially fat mass) accelerates early in the third trimester (45, 46), which coincides with the accelerated growth of fractional limb volume around 30 weeks of gestation (44, 47, 48). We recently reported greater fetal fractional arm volume among mothers with gestational diabetes in late gestation (49).

Maternal-Fetal Factors That Affect Fetal Body Composition

Maternal pregravid body mass index (BMI) and diabetes are well known determinants of fetal growth, in particular fetal adiposity (50, 51). Infants born to women with higher BMI have increased percentage body fat as compared to infants born to women with normal BMI (52, 53). Overweight or obese women with normal glucose tolerance levels still have infants with increased adiposity (50). Maternal gestational weight gain and presence of gestational diabetes have been associated with increased fetal abdominal subcutaneous fat thickness (54). Moreover, several biomarkers (maternal systemic interleukin-6, cord blood leptin and insulin-like growth factor) potentially affect fetal body composition (55, 56).

Fetal Liver Blood Flow Volume and Infant Body Composition

Fetal liver blood flow volume has recently emerged as one of the determinants of fetal growth and subsequent infant body composition (57, 58). The fetal liver is the primary site where nutrient interconversion and *de novo* synthesis occur (59). Hence, variation in the relative distribution of umbilical venous blood flow shunting either through the ductus venosus or through the fetal liver has been proposed as a mechanism of fetal adaptation to intrauterine conditions (23, 60, 61).

Several studies have been conducted investigating the association between fetal liver blood flow volume and maternal pregravid BMI (62), gestational weight gain (63), serum glucose

level (64–66), and fetal growth restriction (67). More recent report showed the correlation between fetal liver blood flow volume and placental corticotrophin releasing hormone, which is a paracrine determinant of the placental vasculature (68). Considering these previous reports, assessing fetal liver blood flow volume may help better understand the mechanisms influencing fetal growth and body composition.

FUTURE PERSPECTIVES

Further studies are warranted to determine the association between ultrasound-based measures of fetal body composition and metabolic dysfunction in later life. It is also important to investigate the factors (maternal demographic background, metabolic status including dyslipidemia and dysglycemia, and placental transporters of the nutrients) that affect fetal body composition and fat deposition (69).

Fetal fat mass and fractional limb volume could also be surrogate markers of fetal nutritional status, to distinguish constitutionally small/large fetus from malnourished/overnourished fetus. Physiological diversity and heterogeneity in fetal growth velocity patterns (especially in the third trimester of gestation) has been reported (70). Additionally. the growth trajectory of fetal soft tissue volume (especially fat mass) accelerates early in the third trimester (45, 46). Based on these, sequential measures of fetal fat mass and fractional limb volume in the third trimester (e.g. every 2-4 weeks) could be clinically useful to distinguish constitutionally small/large fetus from malnourished/overnourished fetus. These can help better understand the "thrifty" or "drifty" phenotype of the fetus, both of which are predisposed to the metabolic syndrome in later life. Further studies should be conducted to evaluate how these findings translate into clinical interventions for altered fetal growth and body composition. This could potentially lead to the primary prevention of future risk of metabolic dysfunction.

CONCLUSION

An ultrasound-based measure of fetal fat mass has been established that provides new insights into the evaluation of fetal growth and body composition, and its relationship with newborn adiposity. The ability to detect extreme variations in fetal fat deposition may help understand alterations in fetal body composition in pathophysiological conditions, such as fetal growth restriction or fetal macrosomia. Further studies are warranted to elucidate the maternal or placental factors that affect fetal fat deposition and newborn body composition. Elucidating these factors could help develop clinical intervention strategies for altered fetal growth and body composition, which potentially lead to primary prevention of the metabolic dysfunction in later life.

AUTHOR CONTRIBUTIONS

SI researched data, wrote the manuscript. SI, YK, TE, MT, and DO contributed to discussion and reviewed the manuscript. All authors contributed to the article and approved the submitted version.

FUNDING

This work was funded by the Japan Society for the Promotion of Science, KAKENHI Grant Number 20K18231.

REFERENCES

1. Barker DJ, Winter PD, Osmond C, Margetts B, Simmonds SJ. Weight in Infancy and Death From Ischaemic Heart Disease. *Lancet* (1989) 2 (8663):577–80. doi: 10.1016/S0140-6736(89)90710-1
2. Roseboom T, de Rooij S, Painter R. The Dutch Famine and Its Long-Term Consequences for Adult Health. *Early Hum Dev* (2006) 82(8):485–91. doi: 10.1016/j.earlhumdev.2006.07.001
3. Hapo Study Cooperative Research Group. Hyperglycemia and Adverse Pregnancy Outcome (HAPO) Study: Associations With Neonatal Anthropometrics. *Diabetes* (2009) 58(2):453–9. doi: 10.2337/db08-1112
4. Boney CM, Verma A, Tucker R, Vohr BR. Metabolic Syndrome in Childhood: Association With Birth Weight, Maternal Obesity, and Gestational Diabetes Mellitus. *Pediatrics* (2005) 115(3):e290–6. doi: 10.1542/peds.2004-1808
5. Oken E, Gillman MW. Fetal Origins of Obesity. *Obes Res* (2003) 11(4):496–506. doi: 10.1038/oby.2003.69
6. Entringer S, Buss C, Swanson JM, Cooper DM, Wing DA, Waffarn F, et al. Fetal Programming of Body Composition, Obesity, and Metabolic Function: The Role of Intrauterine Stress and Stress Biology. *J Nutr Metab* (2012) 632548. doi: 10.1155/2012/632548
7. Gluckman PD, Hanson MA. Living With the Past: Evolution, Development, and Patterns of Disease. *Science (New York N Y)* (2004) 305(5691):1733–6. doi: 10.1126/science.1095292
8. Schmelzle HR, Quang DN, Fusch G, Fusch C. Birth Weight Categorization According to Gestational Age Does Not Reflect Percentage Body Fat in Term and Preterm Newborns. *Eur J Pediatr* (2007) 166(2):161–7. doi: 10.1007/s00431-006-0209-x
9. Shaw M, Lutz T, Gordon A. Does Low Body Fat Percentage in Neonates Greater Than the 5th Percentile Birthweight Increase the Risk of Hypoglycaemia and Neonatal Morbidity? *J Paediatr Child Health* (2019) 55 (12):1424–8. doi: 10.1111/jpc.14433
10. Kuriyan R, Naqvi S, Bhat KG, Ghosh S, Rao S, Preston T, et al. The Thin But Fat Phenotype Is Uncommon at Birth in Indian Babies. *J Nutr* (2020) 150 (4):826–32. doi: 10.1093/jn/nxz305
11. Catalano PM, Farrell K, Thomas A, Huston-Presley L, Mencin P, de Mouzon SH, et al. Perinatal Risk Factors for Childhood Obesity and Metabolic Dysregulation. *Am J Clin Nutr* (2009) 90(5):1303–13. doi: 10.3945/ajcn.2008.27416
12. Lowe WLJr., Scholtens DM, Kuang A, Linder B, Lawrence JM, Lebenthal Y, et al. Hyperglycemia and Adverse Pregnancy Outcome Follow-Up Study (HAPO FUS): Maternal Gestational Diabetes Mellitus and Childhood Glucose Metabolism. *Diabetes Care* (2019) 42(3):372–80. doi: 10.2337/dc18-1646
13. Kuzawa CW, Chugani HT, Grossman LI, Lipovich L, Muzik O, Hof PR, et al. Metabolic Costs and Evolutionary Implications of Human Brain Development. *Proc Natl Acad Sci USA* (2014) 111(36):13010–5. doi: 10.1073/pnas.1323099111
14. Bougneres PF, Lemmel C, Ferre P, Bier DM. Ketone Body Transport in the Human Neonate and Infant. *J Clin Invest* (1986) 77(1):42–8. doi: 10.1172/JCI112299
15. Chen LW, Tint MT, Fortier MV, Aris IM, Shek LP, Tan KH, et al. Which Anthropometric Measures Best Reflect Neonatal Adiposity? *Int J Obes* (2018) 42(3):501–6. doi: 10.1038/ijo.2017.250
16. Catalano PM, Tyzbir ED, Allen SR, McBean JH, McAuliffe TL. Evaluation of Fetal Growth by Estimation of Neonatal Body Composition. *Obstet Gynecol* (1992) 79(1):46–50.

17. de Knegt VE, Carlsen EM, Bech Jensen JE, Lade Rasmussen AM, Pryds O. DXA Performance in a Pediatric Population: Precision of Body Composition Measurements in Healthy Term-Born Infants Using Dual-Energy X-Ray Absorptiometry. *J Clin Densitom* (2015) 18(1):117–23. doi: 10.1016/j.jocd.2014.08.004
18. Moraitis AA, Shreeve N, Sovio U, Brocklehurst P, Heazell AEP, Thornton JG, et al. Universal Third-Trimester Ultrasonic Screening Using Fetal Macrosomia in the Prediction of Adverse Perinatal Outcome: A Systematic Review and Meta-Analysis of Diagnostic Test Accuracy. *PloS Med* (2020) 17 (10):e1003190. doi: 10.1371/journal.pmed.1003190
19. Law TL, Korte JE, Katikaneni LD, Wagner CL, Ebeling MD, Newman RB. Ultrasound Assessment of Intrauterine Growth Restriction: Relationship to Neonatal Body Composition. *Am J Obstet Gynecol* (2011) 205(3):255.e1-6. doi: 10.1016/j.ajog.2011.06.027
20. Coomarasamy A, Connock M, Thornton J, Khan KS. Accuracy of Ultrasound Biometry in the Prediction of Macrosomia: A Systematic Quantitative Review. *BJOG* (2005) 112(11):1461–6. doi: 10.1111/j.1471-0528.2005.00702.x
21. Moyer-Mileur LJ, Slater H, Thomson JA, Mihalopoulos N, Byrne J, Varner MW. Newborn Adiposity Measured by Plethysmography Is Not Predicted by Late Gestation Two-Dimensional Ultrasound Measures of Fetal Growth. *J Nutr* (2009) 139(9):1772–8. doi: 10.3945/jn.109.109058
22. Schwartz J, Galan H. Ultrasound in Assessment of Fetal Growth Disorders: Is There a Role for Subcutaneous Measurements? *Ultrasound Obstet Gynecol* (2003) 22(4):329–35. doi: 10.1002/uog.887
23. Ikenoue S, Waffarn F, Ohashi M, Sumiyoshi K, Ikenoue C, Buss C, et al. Prospective Association of Fetal Liver Blood Flow at 30 Weeks Gestation With Newborn Adiposity. *Am J Obstet Gynecol* (2017) 217(2):204.e1–8. doi: 10.1016/j.ajog.2017.04.022
24. O'Connor C, Doolan A, O'Higgins A, Segurado R, Sheridan-Pereiraet M, Turner MJ, et al. Fetal Subcutaneous Tissue Measurements in Pregnancy as a Predictor of Neonatal Total Body Composition. *Prenat Diagn* (2014) 34:1-4. doi: 10.1002/pd.4400
25. Buhling KJ, Doll I, Siebert G, Catalano PM. Relationship Between Sonographically Estimated Fetal Subcutaneous Adipose Tissue Measurements and Neonatal Skinfold Measurements. *Ultrasound Obstet Gynecol* (2012) 39(5):558-62. doi: 10.1002/uog.10092
26. Knight CL, Rueda S, Noble JA, Papageorghiou AT. Fetal Arm Fat: An In Utero Marker of Body Composition? *Ultrasound Obstet Gynecol* (2012) 40 (S1):106.
27. Lee W, Balasubramaniam M, Deter RL, Hassan SS, Gotsch F, Kusanovic JP, et al. Fetal Growth Parameters and Birth Weight: Their Relationship to Neonatal Body Composition. *Ultrasound Obstet Gynecol* (2009) 33(4):441–6. doi: 10.1002/uog.6317
28. Bernstein IM, Goran MI, Amini SB, Catalano PM. Differential Growth of Fetal Tissues During the Second Half of Pregnancy. *Am J Obstet Gynecol* (1997) 176 (1):28–32. doi: 10.1016/S0002-9378(97)80006-3
29. Poissonnet CM, Burdi AR, Garn SM. The Chronology of Adipose Tissue Appearance and Distribution in the Human Fetus. *Early Hum Dev* (1984) 10 (1-2):1–11. doi: 10.1016/0378-3782(84)90106-3
30. Sparks JW. Human Intrauterine Growth and Nutrient Accretion. *Semin Perinatol* (1984) 8(2):74–93.
31. Fields DA, Teague AM, Short KR, Chernausek SD. Evaluation of DXA vs. MRI for Body Composition Measures in 1-Month Olds. *Pediatr Obes* (2015) 10(5):e8–10. doi: 10.1111/ijpo.12021
32. Ikenoue S, Waffarn F, Sumiyoshi K, Ohashi M, Ikenoue C, Buss C, et al. Association of Ultrasound-Based Measures of Fetal Body Composition With Newborn Adiposity. *Pediatr Obes* (2017) 12 Suppl 1:86–93. doi: 10.1111/ijpo.12198
33. Jeanty P, Romero R, Hobbins JC. Fetal Limb Volume: A New Parameter to Assess Fetal Growth and Nutrition. *J Ultrasound Med* (1985) 4(6):273–82. doi: 10.7863/jum.1985.4.6.273
34. Gardeil F, Greene R, Stuart B, Turner MJ. Subcutaneous Fat in the Fetal Abdomen as a Predictor of Growth Restriction. *Obstet Gynecol* (1999) 94 (2):209–12. doi: 10.1097/00006250-199908000-00010
35. Petrikovsky BM, Oleschuk C, Lesser M, Gelertner N, Gross B. Prediction of Fetal Macrosomia Using Sonographically Measured Abdominal Subcutaneous Tissue Thickness. *J Clin Ultrasound* (1997) 25(7):378–82. doi: 10.1002/(sici)1097-0096(199709)25:7<378::aid-jcu5>3.0.co;2-7
36. Abramowicz JS, Rana S, Abramowicz S. Fetal Cheek-to-Cheek Diameter in the Prediction of Mode of Delivery. *Am J Obstet Gynecol* (2005) 192(4):1205–11; discussion 11-3. doi: 10.1016/j.ajog.2005.01.008
37. Matsumoto M, Yanagihara T, Hata T. Three-Dimensional Qualitative Sonographic Evaluation of Fetal Soft Tissue. *Hum Reprod* (2000) 15 (11):2438–42. doi: 10.1093/humrep/15.11.2438
38. Abramowicz JS, Sherer DM, Woods JRJr. Ultrasonographic Measurement of Cheek-to-Cheek Diameter in Fetal Growth Disturbances. *Am J Obstet Gynecol* (1993) 169(2 Pt 1):405–8. doi: 10.1016/0002-9378(93)90097-3
39. Abramowicz JS, Robischon K, Cox C. Incorporating Sonographic Cheek-to-Cheek Diameter, Biparietal Diameter and Abdominal Circumference Improves Weight Estimation in the Macrosomic Fetus. *Ultrasound Obstet Gynecol* (1997) 9(6):409–13. doi: 10.1046/j.1469-0705.1997.09060409.x
40. Lee W, Deter RL, Ebersole JD, Huang R, Blanckaert K, Romero R. Birth Weight Prediction by Three-Dimensional Ultrasonography: Fractional Limb Volume. *J Ultrasound Med* (2001) 20(12):1283–92. doi: 10.7863/jum.2001.20.12.1283
41. Lee W. A Commentary About the Importance of Fetal and Neonatal Soft-Tissue Assessment. *BJOG* (2018) 125(12):1567. doi: 10.1111/1471-0528.15303
42. Roelants JA, Vermeulen MJ, Koning IV, Groenenberg IAL, Willemsen SP, Hokken-Koelega ACS, et al. Foetal Fractional Thigh Volume: An Early 3D Ultrasound Marker of Neonatal Adiposity. *Pediatr Obes* (2017) 12 Suppl 1:65–71. doi: 10.1111/ijpo.12231
43. Lee W, Mack LM, Sangi-Haghpeykar H, Gandhi R, Wu Q, Kang L, et al. Fetal Weight Estimation Using Automated Fractional Limb Volume With 2-Dimensional Size Parameters: A Multicenter Study. *J Ultrasound Med* (2020) 39(7):1317–24. doi: 10.1002/jum.15224
44. Mack LM, Kim SY, Lee S, Sangi-Haghpeykar H, Lee W. Automated Fractional Limb Volume Measurements Improve the Precision of Birth Weight Predictions in Late Third-Trimester Fetuses. *J Ultrasound Med* (2017) 36 (8):1649–55. doi: 10.7863/ultra.16.08087
45. Pereira GR. Nutritional Assessment. In: RA Polin, WW Fox, SH Abman, editors. *Fetal and Neonatal Physiology*. Philadelphia: Elsevier/Saunders (2011). p. 341–51.
46. Ikenoue S, Akiba Y, Endo T, Kasuga Y, Yakubo K, Ishii R, et al. Defining the Normal Growth Curve of Fetal Fractional Limb Volume in a Japanese Population. *J Clin Med* (2021) 10(3):485. doi: 10.3390/jcm10030485
47. Sharma KA, Das D, Dadhwal V, Deka D, Singhal S, Vanamail P. Two-Dimensional Fetal Biometry Versus Three-Dimensional Fractional Thigh Volume for Ultrasonographic Prediction Of Birthweight. *Int J Gynecol Obstet* (2019) 145(1):47–53. doi: 10.1002/ijgo.12770
48. Lee W, Balasubramaniam M, Deter RL, Hassan SS, Gotsch F, Kusanovic JP, et al. Fractional Limb Volume – A Soft Tissue Parameter of Fetal Body Composition: Validation, Technical Considerations and Normal Ranges During Pregnancy. *Ultrasound Obstet Gynecol* (2009) 33(4):427–40. doi: 10.1002/uog.6319
49. Akiba Y, Ikenoue S, Endo T, Kasuga Y, Ochiai D, Miyakoshi K, et al. Differences in Fetal Fractional Limb Volume Changes in Normal and Gestational Diabetic Pregnancies: An Exploratory Observational Study. *BJOG* (2021) 128(2):329–35. doi: 10.1111/1471-0528.16265
50. Sewell MF, Huston-Presley L, Super DM, Catalano P. Increased Neonatal Fat Mass, Not Lean Body Mass, Is Associated With Maternal Obesity. *Am J Obstet Gynecol* (2006) 195(4):1100–3. doi: 10.1016/j.ajog.2006.06.014
51. Catalano PM, Thomas A, Huston-Presley L, Amini SB. Increased Fetal Adiposity: A Very Sensitive Marker of Abnormal In Utero Development. *Am J Obstet Gynecol* (2003) 189(6):1698–704. doi: 10.1016/s0002-9378(03)00828-7
52. Bennett AE, Kearney JM. Maternal Sociodemographic and Health Behaviours Associated With Adiposity in Infants as Measured by Air Displacement Plethysmography. *Early Hum Dev* (2019) 140:104887. doi: 10.1016/j.earlhumdev.2019.104887
53. Breij LM, Steegers-Theunissen RP, Briceno D, Hokken-Koelega AC. Maternal and Fetal Determinants of Neonatal Body Composition. *Horm Res Paediatr* (2015) 84(6):388–95. doi: 10.1159/000441298
54. Rohl J, Huston-Presley L, Amini S, Stepanchak B, Catalano P. Factors Associated With Fetal Growth and Body Composition as Measured by Ultrasound. *Am J Obstet Gynecol* (2001) 185(6):1416–20. doi: 10.1067/mob.2001.118846

55. Radaelli T, Uvena-Celebrezze J, Minium J, Huston-Presley L, Catalano P, Hauguel-de Mouzon S. Maternal Interleukin-6: Marker of Fetal Growth and Adiposity. *J Soc Gynecol Invest* (2006) 13(1):53–7. doi: 10.1016/j.jsgi.2005.10.003
56. Christou H, Connors JM, Ziotopoulou M, Hatzidakis V, Papathanassoglou E, Ringer SA, et al. Cord Blood Leptin and Insulin-Like Growth Factor Levels Are Independent Predictors of Fetal Growth. *J Clin Endocrinol Metab* (2001) 86(2):935–8. doi: 10.1210/jcem.86.2.7217
57. Tchirikov M, Kertschanska S, Sturenberg HJ, Schroder HJ. Liver Blood Perfusion as a Possible Instrument for Fetal Growth Regulation. *Placenta* (2002) 23 Suppl A:S153–8. doi: 10.1053/plac.2002.0810
58. Kessler J, Rasmussen S, Godfrey K, Hanson M, Kiserud T. Venous Liver Blood Flow and Regulation of Human Fetal Growth: Evidence From Macrosomic Fetuses. *Am J Obstet Gynecol* (2011) 204(5):429.e1–7. doi: 10.1016/j.ajog.2010.12.038
59. Seifter S, Englard S. Energy Metabolism. In: IM Arias, editor. *The Liver: Biology and Pathobiology*. New York: Raven Press (1994). p. 323–64.
60. Godfrey KM, Haugen G, Kiserud T, Inskip HM, Cooper C, Harvey NC, et al. Fetal Liver Blood Flow Distribution: Role in Human Developmental Strategy to Prioritize Fat Deposition Versus Brain Development. *PloS One* (2012) 7(8):e41759. doi: 10.1371/journal.pone.0041759
61. Kuzawa CW. Fetal Origins of Developmental Plasticity: Are Fetal Cues Reliable Predictors of Future Nutritional Environments? *Am J Hum Biol* (2005) 17(1):5–21. doi: 10.1002/ajhb.20091
62. Haugen G, Hanson M, Kiserud T, Crozier S, Inskip H, Godfrey KM. Fetal Liver-Sparing Cardiovascular Adaptations Linked to Mother's Slimness and Diet. *Circ Res* (2005) 96(1):12–4. doi: 10.1161/01.RES.0000152391.45273.A2
63. Kessler J, Rasmussen S, Godfrey K, Hanson M, Kiserud T. Longitudinal Study of Umbilical and Portal Venous Blood Flow to the Fetal Liver: Low Pregnancy Weight Gain Is Associated With Preferential Supply to the Fetal Left Liver Lobe. *Pediatr Res* (2008) 63(3):315–20. doi: 10.1203/PDR.0b013e318163a1de
64. Opheim GL, Moe Holme A, Blomhoff Holm M, Melbye Michelsen T, Muneer Zahid S, Paasche Roland MC, et al. The Impact of Umbilical Vein Blood Flow and Glucose Concentration on Blood Flow Distribution to the Fetal Liver and Systemic Organs in Healthy Pregnancies. *FASEB J* (2020) 34(9):12481–91. doi: 10.1096/fj.202000766R
65. Lund A, Ebbing C, Rasmussen S, Kiserud T, Kessler J. Maternal Diabetes Alters the Development of Ductus Venosus Shunting in the Fetus. *Acta Obstet Gynecol Scand* (2018) 97(8):1032–40. doi: 10.1111/aogs.13363
66. Haugen G, Bollerslev J, Henriksen T. Human Fetoplacental and Fetal Liver Blood Flow After Maternal Glucose Loading: A Cross-Sectional Observational Study. *Acta Obstet Gynecol Scand* (2014) 93(8):778–85. doi: 10.1111/aogs.12419
67. Bellotti M, Pennati G, De Gasperi C, Bozzo M, Battaglia FC, Ferrazzi E. Simultaneous Measurements of Umbilical Venous, Fetal Hepatic, and Ductus Venosus Blood Flow in Growth-Restricted Human Fetuses. *Am J Obstet Gynecol* (2004) 190(5):1347–58. doi: 10.1016/j.ajog.2003.11.018
68. Ikenoue S, Waffarn F, Ohashi M, Tanaka M, Gillen DL, Buss C, et al. Placental Corticotrophin Releasing Hormone Is a Modulator of Fetal Liver Blood Perfusion. *J Clin Endocrinol Metab* (2021) 106(3):646–53. doi: 10.1210/clinem/dgaa908
69. Delhaes F, Giza SA, Koreman T, Eastabrook G, McKenzie CA, Bedell S, et al. Altered Maternal and Placental Lipid Metabolism and Fetal Fat Development in Obesity: Current Knowledge and Advances in Non-Invasive Assessment. *Placenta* (2018) 69:118–24. doi: 10.1016/j.placenta.2018.05.011
70. Sato N, Miyasaka N. Heterogeneity in Fetal Growth Velocity. *Sci Rep* (2019) 9(1):11304. doi: 10.1038/s41598-019-47839-5

Conflict of Interest: The authors declare that the research was conducted in the absence of any commercial or financial relationships that could be construed as a potential conflict of interest.

frontiers in Endocrinology

ORIGINAL RESEARCH
published: 21 September 2021
doi: 10.3389/fendo.2021.740902

Sex Dimorphic Associations of Gestational Diabetes Mellitus With Cord Plasma Fatty Acid Binding Protein 4 and Estradiol

Xin Liu[1,2†], Tao Zheng[3†], Ya-Jie Xu[1], Meng-Nan Yang[1], Wen-Juan Wang[1], Rong Huang[2], Guang-Hui Zhang[4], Yu-Na Guo[5], Jun Zhang[1], Fengxiu Ouyang[1], Fei Li[1,6] and Zhong-Cheng Luo[1,2*] for the Shanghai Birth Cohort*

[1] Ministry of Education-Shanghai Key Laboratory of Children's Environmental Health, Early Life Health Institute, Department of Developmental and Behavioral Pediatric & Child Primary Care, Xinhua Hospital, Shanghai Jiao Tong University School of Medicine, Shanghai, China, [2] Lunenfeld-Tanenbaum Research Institute, Prosserman Centre for Population Health Research, Department of Obstetrics and Gynecology, Mount Sinai Hospital, Institute of Health Policy, Management and Evaluation, Dalla Lana School of Public Health, Faculty of Medicine, University of Toronto, Toronto, ON, Canada, [3] Department of Obstetrics and Gynecology, Xinhua Hospital, Shanghai Jiao-Tong University School of Medicine, Shanghai, China, [4] Department of Clinical Assay Laboratory, Xinhua Hospital, Shanghai Jiao-Tong University School of Medicine, Shanghai, China, [5] Department of Obstetrics and Gynecology, International Peace Maternity and Child Health Hospital, Shanghai Jiao-Tong University School of Medicine, Shanghai, China, [6] Brain and Behavioral Research Unit, Shanghai Institute of Pediatric Research, Xinhua Hospital, Shanghai Jiao Tong University School of Medicine, Shanghai, China

OPEN ACCESS

Edited by:
Sally Radovick, The State University of New Jersey, United States

Reviewed by:
Hirotaka Hamada, University of Toronto, Canada
Satoru Ikenoue, Keio University, Japan

***Correspondence:**
Zhong-Cheng Luo
zcluo@lunenfeld.ca
Fei Li
feili@shsmu.edu.cn

[†]These authors have contributed equally to this work

Specialty section:
This article was submitted to Pediatric Endocrinology, a section of the journal Frontiers in Endocrinology

Received: *13 July 2021*
Accepted: *03 September 2021*
Published: *21 September 2021*

Citation:
Liu X, Zheng T, Xu Y-J, Yang M-N, Wang W-J, Huang R, Zhang G-H, Guo Y-N, Zhang J, Ouyang F, Li F and Luo Z-C (2021) Sex Dimorphic Associations of Gestational Diabetes Mellitus With Cord Plasma Fatty Acid Binding Protein 4 and Estradiol. Front. Endocrinol. 12:740902. doi: 10.3389/fendo.2021.740902

Fatty acid binding protein 4 (FABP4) has been associated with insulin resistance. Gestational diabetes mellitus (GDM) impairs fetal insulin sensitivity. Female newborns are more insulin resistant than male newborns. We sought to evaluate the association between GDM and cord blood FABP4, and explore potential sex dimorphic associations and the roles of sex hormones. This was a nested case-control study in the Shanghai Birth Cohort, including 153 pairs of newborns in GDM *vs*. euglycemic pregnancies matched by infant sex and gestational age at delivery. Cord plasma FABP4, leptin, total and high-molecular-weight adiponectin, testosterone and estradiol concentrations were measured. Adjusting for maternal and neonatal characteristics, cord plasma FABP4 (Mean ± SD: 27.0 ± 19.6 *vs*. 18.8 ± 9.6 ng/mL, P=0.045) and estradiol (52.0 ± 28.6 *vs*. 44.2 ± 26.6, ng/mL, P=0.005) concentrations were higher comparing GDM *vs*. euglycemic pregnancies in males, but similar in females (all P>0.5). Mediation analyses showed that the positive association between GDM and cord plasma FABP4 in males could be partly mediated by estradiol (P=0.03), but not by testosterone (P=0.72). Cord plasma FABP4 was positively correlated with total adiponectin in females (r=0.17, P=0.053), but the correlation was in the opposite direction in males (r=-0.11, P=0.16) (test for difference in r, P=0.02). Cord plasma FABP4 was not correlated with leptin in both sexes. The study is the first to demonstrate sex-dimorphic associations between GDM and cord plasma FABP4 or estradiol, and between FABP4 and adiponectin in newborns. GDM may affect fetal circulating FABP4 and estradiol levels in males only.

Keywords: gestational diabetes mellitus (GDM), fatty acid binding protein 4 (FABP4), adiponectin, testosterone, estradiol (E2), sex dimorphism

INTRODUCTION

Gestational diabetes mellitus (GDM) is characterized by glucose intolerance with first recognition in the 2nd half of pregnancy, affecting 3%-25% of pregnancies worldwide (1, 2). The offspring of mothers with gestational diabetes are at elevated risks of insulin resistance and type 2 diabetes (3, 4). The mechanisms linking GDM in early life "programming" the vulnerability to type 2 diabetes remain unclear.

A number of adipokines are involved in the regulation of insulin sensitivity, most notably leptin and adiponectin (5). GDM has been associated with impaired insulin sensitivity, elevated leptin and decreased adiponectin concentrations in the newborns (6–9). However, little is known about whether GDM may affect circulating levels of other adipokines in early life.

Fatty acid binding protein 4 (FABP4) is an adipokine involved in the transport of fatty acids to specific organelles in the cell (8). It has been shown that FABP4 deficiency ameliorates insulin resistance and prevents atherosclerosis in apolipoprotein E-deficient mice (10, 11). It remains unknown whether FABP4 is correlated with leptin or adiponectin in early life. Human studies have associated elevated circulating FABP4 levels with obesity, insulin resistance, type 2 diabetes (12, 13). It remains unclear whether GDM affects fetal FABP4 levels. We are aware of only three studies on the association between GDM and fetal/cord blood FABP4, and the findings have been inconsistent (7, 14, 15). The discrepant results may be partly related to the small to moderate sample sizes in these studies (GDM, all n<100), and thus the relative vulnerability to chance findings.

Females are more insulin resistant than males at birth (16). Clinical studies have reported higher circulating FABP4 levels in females *vs.* males in adulthood (17, 18). It is unknown whether any association between GDM and fetal circulating FABP4 may vary by sex. Sex hormones (estradiol and testosterone) play a critical role in fat deposition contributing to sex difference in insulin resistance (19, 20), and have been associated with the risks of metabolic syndrome and type 2 diabetes (21, 22). It is unknown whether sex hormones may be related to any potential sex dimorphic association between GDM and fetal FABP4.

In view of the above-discussed knowledge gaps, we sought to evaluate the association between GDM and cord blood FABP4, and explore potential sex dimorphic associations and the roles of sex hormones.

METHODS

Study Design, Subjects, and Specimens

This was a nested matched case control study based on the recently developed Shanghai Birth Cohort (SBC) (23). In the SBC cohort, a total of 4127 pregnant women at preconception or early pregnancy care were recruited from six urban university affiliated tertiary obstetric care hospitals in Shanghai between 2013 and 2016. The women were followed up at the second and third trimesters of pregnancy and delivery. Data and specimens were collected at each study visit. All collected cord blood samples were kept on ice, stored temporarily in a 4°C refrigerator and centrifuged within 2 hours after the specimen collection. Serum and EDTA plasma samples were stored in multiple aliquots at −80°C until assays. The study was approved by the research ethics boards of Shanghai Xinhua Hospital (the coordination center, approved on August 23, 2013, ref no. M2013-010) and all participating hospitals. Written informed consent was obtained from all study participants.

GDM was diagnosed according to the International Association of Diabetes and Pregnancy Study Groups (IADPSG)criteria (24); if any one of the blood glucose values was at or above the following thresholds in the 75 g oral glucose tolerance test at 24-28 weeks of gestation: fasting 5.1 mmol/L, 1-hour 10.0 mmol/L and 2-hour 8.5 mmol/L.

As part of the SBC project, we conducted a nested case control study on the impacts of GDM on early life metabolic health biomarkers in the offspring (25, 26). Cases were the newborns of GDM mothers, and controls were the newborns of euglycemic mothers. Cases (n=153) and controls (n=153) were matched (1:1) by infant sex (the same) and gestational age at delivery (within 1 week) (25). Here, we reported the study data on cord blood FABP4 and sex hormones.

Biochemical Assays

In all biomarker assays, the laboratory technicians were blinded to the clinical status (GDM or not) of study subjects. Cord plasma FABP4 was measured by an ELISA kit (R&D systems, Minnesota, USA). Plasma estradiol was measured by an ELISA kit (Labor Diagnostika Nord, Germany). Plasma testosterone was measured by a chemiluminescence immunoassay kit on a UniCel DXI 800 Access Immunoassay System (Beckman Coulter, USA). The detection limits were 6.55 pg/mL for FABP4, 6.2 pg/mL for estradiol, and 0.35 nmol/L for testosterone, respectively. The intra-assay and inter-assay coefficients of variation were in the ranges of 3.4-12.7% for FABP4, 3.1-6.4% for estradiol, and 1.7-7.1% for testosterone, respectively.

As reported previously, cord plasma leptin was measured by an ELISA kit from Invitrogen (Carlsbad, CA, USA), total and high-molecular-weight (HMW) adiponectin by an ELISA kit from ALPCO (Salem, NH, USA) (26). The intra-assay and inter-assay coefficients of variation were in the range of 6.9-10.4% (26).

Statistical Analysis

Data are presented as Mean ± SD (standard deviation) and median (interquartile range) for continuous variables, and frequency (percentage) for categorical variables. Paired t-test was used in comparisons of continuous variables, and McNemar's Chi-Square test was used in comparisons of dichotomous variables between GDM and matched controls. Log-transformed biomarker data were used in t tests, correlation and regression analyses. Pearson partial correlation coefficients were calculated to evaluate the correlations between biomarkers adjusting for gestational age at delivery/cord blood sampling. Fisher's z test was used in comparisons of correlation coefficients

Abbreviations: FABP4, Fatty acid binding protein 4; GDM, Gestational diabetes mellitus; HMW, high-molecular-weight; IADPSG, International Association of Diabetes and Pregnancy Study Groups; SBC, Shanghai Birth Cohort.

between groups. Generalized linear models were applied to assess the differences in cord blood FABP4, estradiol and testosterone concentrations by GDM status or infant sex controlling for maternal and neonatal characteristics, and to assess the predictors of cord blood FABP4, and in tests for interactions. Maternal characteristics included age, ethnicity, education, parity, smoking or alcohol use during pregnancy, pre-pregnancy BMI (kg/m^2), gestational hypertension, family history of diabetes, family history of hypertension. Neonatal characteristics included infant sex, gestational age, birth weight z score [according to the 2015 Chinese sex- and gestational age-specific birthweight standards (27)] and mode of delivery (cesarean section/vaginal). Matching variables were excluded (gestational age and infant sex) in the comparisons between GDM and control groups. Only co-variables with P<0.2 were included in the parsimonious final regression models to obtain more stable effect estimates. Mediation analyses were conducted to test whether sex hormones may mediate any relationship between GDM and cord plasma FABP4 using the product ("Baron and Kenney") method (28). All statistical analyses were performed using SAS V.9.4 (SAS Institute, Cary, NC, USA). P value <0.05 was considered statistically significant in testing the difference in the primary outcome (cord plasma FABP4 concentration) between GDM and control groups. Using an online sample size and power calculator tool (http://powerandsamplesize.com/Calculators/), we calculated that with the study sample sizes (153 GDM-control pairs; 70 pairs of female newborns, 83 pairs of male newborns) and type 1 error (alpha) at 5%, the study had a power of 99% to detect a 0.5 SD or greater difference in a cord blood biomarker between GDM and control groups, and a power of >84% in sex-specific analyses.

RESULTS

Maternal and Neonatal Characteristics

Maternal and neonatal characteristics of study subjects in this matched case control study in the Shanghai Birth Cohort have been described recently (25). Briefly, there were no significant differences in maternal age, education, parity, family history of diabetes, smoking or alcohol use in pregnancy. Maternal pre-pregnancy BMI was higher (mean: 23.6 *vs*. 21.6 kg/m^2), gestational hypertension (5.2% *vs*. 0.6%) and cesarean section (57% *vs*. 36%) were more frequent in GDM *vs*. euglycemic pregnancies (all P<0.05). Birth weight z scores were higher in GDM *vs*. euglycemic pregnancies (P=0.04). Of the 306 newborns, 166 were males (83 GDM and 83 euglycemic mothers), and 140 were females (70 GDM and 70 euglycemic mothers). There were 142 cesarean section deliveries (97 elective and 45 emergency cesarean sections).

Cord Plasma FABP4, Testosterone, and Estradiol Concentrations

Adjusting for maternal and neonatal characteristics, cord plasma FABP4 and testosterone concentrations were not significantly different between GDM and euglycemic pregnancies overall, while estradiol concentrations (49.0 ± 25.6 *vs*. 45.1 ± 23.6 ng/mL) were significantly higher in GDM pregnancies (**Table 1**). Descriptive statistics on cord plasma leptin, total and adiponectin concentrations have been reported recently (26).

In sex stratified analyses adjusting for maternal and neonatal characteristics, cord plasma FABP4 concentrations were higher in GDM *vs*. euglycemic pregnancies in males (27.0 ± 19.6 *vs*. 18.8 ± 9.61 ng/mL, P=0.045), but similar in females (23.2 ± 16.4 *vs*. 25.6 ± 21.2 ng/mL, P=0.60) (test for interaction, P=0.039) (**Table 2**). GDM was associated with higher cord plasma estradiol concentrations in males (P=0.005), but not in females (P=0.56) (test for interaction, P=0.052).

There were no significant differences in cord plasma testosterone concentrations between GDM and euglycemic pregnancies in both males and females. There were no sex differences in cord plasma FABP4, estradiol and testosterone concentrations in both GDM and euglycemic pregnancies (all P>0.05, **Table 3**).

Correlations

Cord plasma FABP4 was negatively correlated with gestational age at delivery (r=-0.16, P=0.01). Adjusting for gestational age at blood sampling, cord plasma FABP4 was positively correlated to adiponectin in females (r=0.17, P=0.053), but the correlation was in the opposite direction in males (r=-0.11, P=0.16) (Fisher's z test for difference in correlation coefficients, P=0.02) (**Table 4**, **Figure 1**). Cord plasma FABP4 was positively correlated with birth weight z score, but was not correlated with estradiol, testosterone and leptin in both males and females. Cord plasma FABP4 was not correlated to leptin or adiponectin in GDM or euglycemic pregnancies (**Table 5**).

Determinants of Cord Plasma FABP4 Levels

There was a significant interaction between GDM and fetal sex in relation to cord plasma FABP4 (P=0.039). GDM was associated with a 22.5% (95% CI: 2.3-46.6%) increase in cord plasma FABP4 in males (P=0.03), but there was no association in females (**Table 6**). Higher cord plasma FABP4 levels were

TABLE 1 | Cord plasma FABP4, estradiol and testosterone concentrations in the newborns of GDM *vs*. euglycemic (control) mothers.

Cord plasma	GDM (n=153)	Control (n=153)	Crude P*	Adjusted P*
FABP4 (ng/mL)	25.4 ± 18.3 20.2 (12.3, 30.5)	22.0 ± 16.4 16.7 (12.6, 24.1)	0.12	0.19
Estradiol (ng/mL)	49.0 ± 25.6 41.2 (32.6, 59.4)	45.1 ± 23.6 38.3 (30.6, 52.7)	0.10	**0.002**
Testosterone (nmol/L)	5.1 ± 1.1 5.0 (4.5, 5.6)	5.0 ± 1.1 4.9 (4.3, 5.5)	0.45	0.24

Data presented are mean ± SD and median (inter-quartile range).
GDM, gestational diabetes mellitus; FABP-4, fatty acid binding protein 4;
**Crude P values were from paired t-tests in log-transformed biomarker data. Adjusted P values were from generalized linear models in the comparisons of log-transformed biomarker data adjusting for maternal (pre-pregnancy BMI, family history of diabetes, family history of hypertension, gestational hypertension) and neonatal (cesarean section) characteristics; other factors were excluded since they were similar and did not affect the comparisons between the two groups (all P>0.2). P values in bold, P<0.05.*

TABLE 2 | Cord plasma FABP4, testosterone and estradiol concentrations in the newborns of GDM *vs*. euglycemic (control) mothers stratified by infant sex.

	Male newborns		Crude P*	Adjusted P*	Female newborns		Crude P*	Adjusted P*
	GDM	Control			GDM	Control		
FABP4 (ng/mL)	27.0 ± 19.6	18.8 ± 9.6	**0.007**	**0.045**	23.2 ± 16.4	25.6 ± 21.2	0.71	0.60
Testosterone (nmol/L)	5.2 ± 1.3	5.0 ± 0.9	0.45	0.37	4.9 ± 0.8	4.9 ± 1.2	0.81	0.20
Estradiol (ng/mL)	52.0 ± 28.6	44.2 ± 26.6	**0.02**	**0.005**	45.3 ± 20.8	46.0 ± 19.7	0.59	0.56

Data presented are Mean ± SD. There were 166 male newborns (of 83 GDM and 83 euglycemic mothers) and 140 female newborns (of 70 GDM and 70 euglycemic mothers). GDM, gestational diabetes mellitus; FABP4, fatty acid binding protein 4.

**Crude P values were from paired t-tests in log-transformed data. Adjusted P values were from generalized linear models in the comparisons of log-transformed biomarker data between the two groups adjusting for maternal (pre-pregnancy BMI, family history of diabetes, family history of hypertension, gestational hypertension) and neonatal (cesarean section) characteristics; other factors were excluded since they were similar and did not affect the comparisons (all P>0.2). P values in bold, P<0.05.*

Tests for interaction between fetal sex and GDM: P=0.039 in the association with FABP4, P= 0.052 in the association with estradiol.

TABLE 3 | Cord plasma FABP4, testosterone and estradiol concentrations comparing male *vs*. female newborns in GDM and euglycemic (control) pregnancies.

	GDM		P*	Control		P*
	Male newborns	Female newborns		Male newborns	Female newborns	
FABP4 (ng/mL)	27.0 ± 19.6	23.2 ± 16.4	0.21	18.8 ± 9.6	25.6 ± 21.2	0.10
Testosterone (nmol/L)	5.2 ± 1.3	4.9 ± 0.8	0.41	5.0 ± 0.9	4.9 ± 1.2	0.40
Estradiol (ng/mL)	52.0 ± 28.6	45.3 ± 20.8	0.15	44.2 ± 26.6	46.0 ± 19.7	0.18

GDM, gestational diabetes mellitus; FABP4, fatty acid binding protein 4.

Data presented are mean ± SD. There were 153 newborns (83 boys and 70 girls) of GDM and 153 newborns (83 boys and 70 girls) of euglycemic (control) mothers in the analyses.

**Crude P values in the comparisons of log-transformed biomarker data between male and female newborns; no adjustments were made since all co-variables (maternal and neonatal characteristics) were similar in male and female newborns (all P>0.2) and did not affect the comparisons.*

TABLE 4 | Cord blood FABP4 in correlations with testosterone, estradiol, leptin, adiponectin and birth weight (z score) in males and females.

	All		Males		Females		*P for difference
	r	P	r	P	r	P	
Testosterone	-0.07	0.25	-0.07	0.39	-0.07	0.44	1.00
Estradiol	0.07	0.22	0.10	0.20	0.04	0.69	0.58
Leptin	0.09	0.15	0.045	0.58	0.14	0.12	0.44
Total adiponectin	0.03	0.61	-0.11	0.16	0.17	0.053	**0.02**
HMW adiponectin	0.02	0.76	-0.12	0.12	0.14	0.12	**0.03**
Birth weight z score	0.20	**<0.001**	0.22	**0.01**	0.19	**0.03**	0.80

FABP4, fatty acid binding protein 4; HMW, high molecular weight.

Data presented are Pearson partial correlation coefficients in log-transformed biomarker data adjusting for gestational age at delivery/cord blood sampling.

**P values in Fisher's z tests for differences in correlation coefficients in males and females. P values in bold, P<0.05.*

associated with family history of hypertension, cesarean section delivery and higher birth weight z scores. Cord plasma FABP4 concentrations were higher in either elective cesarean sections (27.7 ± 19.2 ng/mL, P<0.001) or emergency cesarean sections (31.1 ± 24.2 ng/mL, P<0.001) as compared to vaginal deliveries (18.8 ± 10.6 ng/mL). Higher gestational ages at delivery were associated with lower cord plasma FABP4 concentrations. Other factors were not associated with cord plasma FABP4, including family history of diabetes, maternal age, pre-pregnancy BMI, parity, education, smoking, alcohol use and fetal sex (all P>0.2). There were no significant interactions between GDM and pre-pregnancy BMI or maternal age in relation to cord plasma FABP4 (all P>0.05).

Mediation Analyses

The positive association between GDM and cord plasma FABP4 in males was partly mediated by estradiol; the mediation effect was a 7.0% (95% CI: 0.6-13.7%, P=0.03) increase in cord plasma FABP4. In contrast, there was no mediation effect by testosterone (P=0.72). The positive relationship between cord plasma FABP4 and total adiponectin in females was not mediated by estradiol (P=0.35) or testosterone (P=0.98).

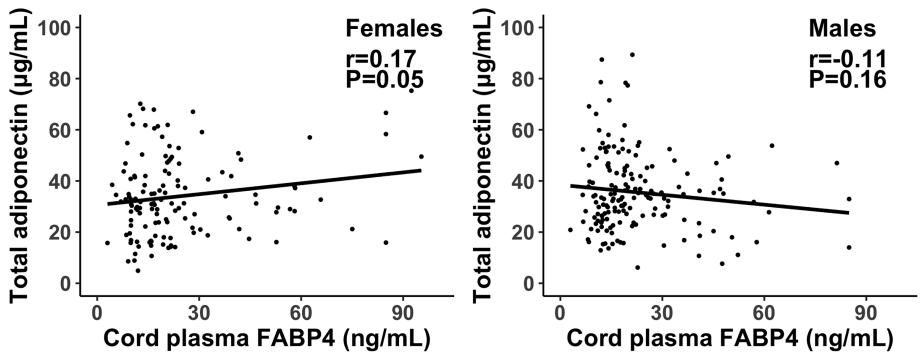

FIGURE 1 | Scatter plots illustrating the different correlations of cord plasma FABP4 with total adiponectin in female and male newborns; the interpolation represents the regression line. P=0.02 in Fisher's z test for difference in the correlation coefficients in males and females.

TABLE 5 | Cord blood FABP4 in correlations with testosterone, estradiol, leptin, adiponectin and birth weight z score in GDM and euglycemic (control) pregnancies.

	GDM		Control		*P for difference
	r	P	r	P	
Testosterone	-0.14	0.11	0.02	0.81	0.19
Estradiol	0.02	0.82	0.12	0.16	0.41
Leptin	0.08	0.35	0.11	0.19	0.79
Total adiponectin	-0.06	0.46	0.16	0.052	0.06
HMW adiponectin	-0.05	0.52	0.15	0.07	0.08
Birth weight z score	0.22	0.01	0.15	0.06	0.55

GDM, gestational diabetes mellitus; FABP4, fatty acid binding protein 4; HMW, high molecular weight.

Data presented are Pearson partial correlation coefficients adjusting for gestational age at delivery/cord blood sampling. Log-transformed biomarker data were used in the analyses.

**P values in Fisher's z tests for differences in the correlation coefficients in GDM and control groups.*

DISCUSSION

Main Findings

The study is the first to demonstrate sex dimorphic associations between GDM and cord plasma FABP4 or estradiol, and between cord plasma FABP4 and adiponectin. GDM was associated with elevated cord plasma FABP4 and estradiol concentrations in males only, and FABP4 was positively correlated with adiponectin in females only. The positive association between GDM and cord plasma FABP4 in males appears to be partly mediated by estradiol.

Data Interpretation and Comparisons to Findings in Previous Studies

Adipokines may be involved in the pathophysiology of GDM and its post-partum consequences (29). FABP4 has been associated with insulin resistance (13, 30). Studies have reported inconsistent findings on cord blood FABP4 levels in GDM (7, 14, 15). Two studies reported higher cord blood FABP4 levels (14, 15), while another study reported lower cord blood FABP4 levels in GDM *vs*. euglycemic pregnancies (7). Sample sizes in GDM pregnancies were 98, 50 and 26 in the three studies, respectively (7, 14, 15). In contrast, our study with a much larger sample size (153 GDM pregnancies) showed that GDM was associated with higher cord plasma FABP4 concentrations in males only. We could not reconcile our data against previous studies which did not report sex specific data. It should be noted that the difference would not be detected in the pooled total sample (males+females). Our comparisons were adjusted for

TABLE 6 | Determinants of cord plasma FABP4 concentrations.

	All β (95% CI)	P	Males β (95% CI)	P	Females β (95% CI)	P
GDM	9.4 (-4.8, 25.7)	0.21	22.5 (2.3, 46.6)	**0.03**	-5.4 (-24.0, 17.8)	0.62
FH of hypertension	17.5 (2.2, 35.2)	**0.02**	17.8 (-1.8, 41.3)	0.08	19.6 (-3.9, 48.8)	0.11
Gest. hypertension	-17.0 (-43.4, -21.7)	0.34	-2.6 (-36.0, 48.4)	0.90	-54.3 (-80.2, 5.5)	0.07
Cesarean section	28.8 (12.3, 47.7)	**<0.001**	22.3 (2.7, 45.6)	**0.02**	35.6 (8.6, 69.2)	**0.01**
Gestational age	-7.0 (-11.8, -1.9)	**0.01**	-6.8 (-12.8, -0.5)	**0.04**	-6.6 (-14.6, 2.1)	0.13
Birth weight z score	8.2 (1.7, 15.2)	**0.01**	9.2 (0.7, 18.5)	**0.03**	6.0 (-3.8, 16.8)	0.24

GDM, gestational diabetes mellitus; FABP4, fatty acid binding protein 4; FH, family history; Gest., gestational.

Data presented are the percentage change (95% CI) from generalized linear models, based on the regression coefficients for the outcome (FABP4 concentration) in log-transformed data. Only predictors with P<0.2 in predicting the outcome in at least one sex (male or female) group were retained in the final models. For consistency, the same set of predictors were retained in the final models for both sexes. Test for interaction with infant sex was significant for GDM only (P=0.04). Therefore, the primary effect estimates should be sex-specific for GDM, and be the effect estimates in the pooled total sample for other predictors.

P values in bold, P<0.05.

maternal and neonatal characteristics, while two previous studies did not adjust for these characteristics (14, 15), and the other study adjusted for pre-pregnancy BMI and infant sex only (7). GDM has been associated with lower cord plasma adiponectin concentrations in females only (26). The current study adds new evidence suggesting a sex dimorphic impact of GDM on circulating levels of certain adipokines in early life.

Studies in adults have reported higher circulating FABP4 levels in women *vs*. men (17, 18). Androgen may contribute to such a sex difference through affecting body fat content as fat mass is positively correlated with circulating FABP4 levels (18). Circulating testosterone and FABP4 concentrations are negatively correlated in men, but positively correlated in women (18). However, we did not observe any association between cord plasma testosterone and FABP4 in newborns. Higher cord plasma FABP4 concentrations were observed in GDM *vs*. euglycemic pregnancies in males only, suggesting that GDM may up-regulate FABP4 expression/secretion in males during fetal life. Mediation analyses indicate that this male specific positive association between GDM and cord plasma FABP4 might be partly mediated by estradiol, but not related to testosterone. A study in muscle (myotube) cells suggested that estradiol could up-regulate FABP4 expression (31). This might explain the mediation effect of estradiol on higher FABP4 levels associated with GDM in male newborns. Further studies are warranted to validate whether this is a phenomenon unique to males, and to elucidate the underlying mechanisms.

Adipose tissue produces a number of adipokines that modulate insulin response (29). There is a lack of data on the relationship between FABP4 and other adipokines in early life. Our study is the first to reveal a sex dimorphic association between cord plasma FABP4 and adiponectin. Cord plasma FABP4 and adiponectin were positively correlated in females only, and the association was unrelated to sex hormones. This novel observation requires confirmation in more independent studies.

Elective cesarean delivery is a less stressful procedure to the fetus than vaginal delivery. Cord blood cortisol levels are lower in elective cesarean deliveries compared to vaginal deliveries (32). About 50% cesarean deliveries are elective cesarean sections in Shanghai (33). Such high rates of elective cesarean sections are common in China due to maternal preference and financial incentives for hospitals (34). A study in mice reported that dexamethasone (a synthetic glucocorticoid) injection increased FABP4 mRNA expression (35), and there have been no data in humans. We observed that cord plasma FABP4 levels were higher in cesarean deliveries (elective or not) *vs*. vaginal deliveries, even though fetal cortisol levels should be lower in elective cesarean deliveries. Further studies in other independent cohorts are required to confirm this new finding.

Elevated circulating FABP4 levels have been associated with a family history of hypertension (36). Consistent with this report, we observed higher cord plasma FABP4 concentrations in subjects with a family history of hypertension. Maternal and cord blood FABP4 concentrations were not correlated, suggesting fetal tissues might be the main source of FABP4 in cord blood (7). Consistent with our data, birth weight z score was positively correlated with cord blood FABP4 levels, while gestational age was negatively correlated with cord blood FABP4 levels in previous studies (37, 38). Fetal FABP4 may be expressed at higher levels in earlier gestational ages.

Elevated circulating estrogen levels have been related to insulin resistance in pregnancy (39). After binding to the estrogen receptor, estradiol may decrease insulin sensitivity through reducing the expression of the insulin sensitive membrane transporter - glucose transporter 4 in adipose tissue and muscle (40, 41). Two studies on cord blood estradiol levels in GDM showed inconsistent findings (42, 43). Qi et al. reported decreased cord blood estradiol levels in GDM pregnancies (n=204) (42), while Jin et al. observed no significant changes in GDM pregnancies (n=48) (43). In contrast, our data showed that GDM was associated with higher cord blood estradiol concentrations in males only. The reasons for these inconsistent findings are unclear, and may be partly due to the differences in sample size and GDM diagnostic criteria. More studies in larger cohorts are warranted to clarify the association.

Strengths and Limitations

The study was based on a large birth cohort. Biochemical assays were of high quality, and study subject's clinical status was blinded to assay technicians. The study has some limitations. We could not draw conclusions regarding causality due to the observational nature of the study. The study subjects were all Chinese. More studies in other populations are required to determine the generalizability of the study findings to other ethnic groups.

CONCLUSION

Our study data suggest a sex dimorphic impact of GDM on FABP4 and estradiol levels in early life in the offspring. The male specific positive association between GDM and FABP4 appears to be partly mediated by estradiol. There may be a sex dimorphic association between FABP4 and adiponectin in early life. These new findings suggest the need for more research to illuminate the sex specific metabolic "programming" impact targets and long-term consequences that could guide the development of targeted programming interventions to reduce the vulnerability to insulin resistance and type 2 diabetes.

DATA AVAILABILITY STATEMENT

The datasets presented in this article are not readily available because access to the deidentified participant research data must be approved by the research ethics board on a case-by-case basis. Requests to access the datasets should be directed to the corresponding author (zcluo@lunenfeld.ca; feili@shsmu.edu.cn)

ETHICS STATEMENT

The studies involving human participants were reviewed and approved by the research ethics committees of the coordination center (Xinhua Hospital, reference number M2013-010) and all

participating hospitals. The patients/participants provided their written informed consent to participate in this study.

AUTHOR CONTRIBUTIONS

Z-CL, G-HZ, FL, JZ, and FO conceived the study. XL, TZ, Y-JX, M-NY, W-JW, RH, G-HZ, Y-NG, JZ, FO, FL, and Z-CL contributed to the acquisition of research data. XL and TZ conducted the literature review, data analysis, and drafted the manuscript. All authors contributed to the article and approved the submitted version.

FUNDING

This work was supported by research grants from the Ministry of Science and Technology of China (2019YFA0802501, 2017YFE0124700), the Shanghai Municipal Health Commission (2020CXJQ01), the Shanghai Science and Technology Commission (19410713500, 21410713500), the National Natural Science Foundation of China (81961128023, 81903323, 81761128035 and 81930095), the National Human Genetic Resources Sharing Service Platform (2005DKA21300), and the Canadian Institutes of Health Research (158616). The funders have no role in all aspects of the study, including study design, data collection and analysis, the preparation of the manuscript and the decision for publication.

ACKNOWLEDGMENTS

We gratefully acknowledged all research staff who had contributed to patient recruitment and data collection in the Shanghai Birth Cohort.

REFERENCES

1. American Diabetes A. Erratum. Classification and Diagnosis of Diabetes. Sec. 2. In Standards of Medical Care in Diabetes-2016. *Diabetes Care* (2016) 39 (Suppl. 1):S13–22. doi: 10.2337/dc16-er09
2. Melchior H, Kurch-Bek D, Mund M. The Prevalence of Gestational Diabetes. *Dtsch Arztebl Int* (2017) 114(24):412–8. doi: 10.3238/arztebl.2017.0412
3. Egeland GM, Meltzer SJ. Following in Mother's Footsteps? Mother-Daughter Risks for Insulin Resistance and Cardiovascular Disease 15 Years After Gestational Diabetes. *Diabetes Med* (2010) 27(3):257–65. doi: 10.1111/j.1464-5491.2010.02944.x
4. Metzger BE. Long-Term Outcomes in Mothers Diagnosed With Gestational Diabetes Mellitus and Their Offspring. *Clin Obstet Gynecol* (2007) 50(4):972–9. doi: 10.1097/GRF.0b013e31815a61d6
5. Bao W, Baecker A, Song Y, Kiely M, Liu S, Zhang C. Adipokine Levels During the First or Early Second Trimester of Pregnancy and Subsequent Risk of Gestational Diabetes Mellitus: A Systematic Review. *Metabolism* (2015) 64 (6):756–64. doi: 10.1016/j.metabol.2015.01.013
6. Okereke NC, Uvena-Celebrezze J, Hutson-Presley L, Amini SB, Catalano PM. The Effect of Gender and Gestational Diabetes Mellitus on Cord Leptin Concentration. *Am J Obstet Gynecol* (2002) 187(3):798–803. doi: 10.1067/mob.2002.125887
7. Ortega-Senovilla H, Schaefer-Graf U, Meitzner K, Abou-Dakn M, Graf K, Kintscher U, et al. Gestational Diabetes Mellitus Causes Changes in the Concentrations of Adipocyte Fatty Acid-Binding Protein and Other Adipocytokines in Cord Blood. *Diabetes Care* (2011) 34(9):2061–6. doi: 10.2337/dc11-0715
8. Trojnar M, Patro-Małysza J, Kimber-Trojnar Ż, Leszczyńska-Gorzelak B, Mosiewicz J. Associations Between Fatty Acid-Binding Protein 4–A Proinflammatory Adipokine and Insulin Resistance, Gestational and Type 2 Diabetes Mellitus. *Cells* (2019) 8(3):227. doi: 10.3390/cells8030227
9. Luo ZC, Delvin E, Fraser WD, Audibert F, Deal CI, Julien P, et al. Maternal Glucose Tolerance in Pregnancy Affects Fetal Insulin Sensitivity. *Diabetes Care* (2010) 33(9):2055–61. doi: 10.2337/dc10-0819
10. Makowski L, Boord JB, Maeda K, Babaev VR, Uysal KT, Morgan MA, et al. Lack of Macrophage Fatty-Acid-Binding Protein Ap2 Protects Mice Deficient in Apolipoprotein E Against Atherosclerosis. *Nat Med* (2001) 7(6):699–705. doi: 10.1038/89076
11. Boord JB, Maeda K, Makowski L, Babaev VR, Fazio S, Linton MF, et al. Combined Adipocyte-Macrophage Fatty Acid-Binding Protein Deficiency Improves Metabolism, Atherosclerosis, and Survival in Apolipoprotein E-Deficient Mice. *Circulation* (2004) 110(11):1492–8. doi: 10.1161/01.Cir.0000141735.13202.B6
12. Tso AW, Xu A, Sham PC, Wat NM, Wang Y, Fong CH, et al. Serum Adipocyte Fatty Acid Binding Protein as a New Biomarker Predicting the Development of Type 2 Diabetes: A 10-Year Prospective Study in a Chinese Cohort. *Diabetes Care* (2007) 30(10):2667–72. doi: 10.2337/dc07-0413
13. Xu A, Wang Y, Xu JY, Stejskal D, Tam S, Zhang J, et al. Adipocyte Fatty Acid-Binding Protein is a Plasma Biomarker Closely Associated With Obesity and Metabolic Syndrome. *Clin Chem* (2006) 52(3):405–13. doi: 10.1373/clinchem.2005.062463
14. Patro-Małysza J, Trojnar M, Kimber-Trojnar Ż, Mierzyński R, Bartosiewicz J, Oleszczuk J, et al. FABP4 in Gestational Diabetes-Association Between Mothers and Offspring. *J Clin Med* (2019) 8(3):285. doi: 10.3390/jcm8030285
15. Zhang Y, Lu JH, Zheng SY, Yan JH, Chen L, Liu X, et al. Serum Levels of Nesfatin-1 are Increased in Gestational Diabetes Mellitus. *Gynecol Endocrinol* (2017) 33(8):621–4. doi: 10.1080/09513590.2017.1306849
16. Shields BM, Knight B, Hopper H, Hill A, Powell RJ, Hattersley AT, et al. Measurement of Cord Insulin and Insulin-Related Peptides Suggests That Girls are More Insulin Resistant Than Boys at Birth. *Diabetes Care* (2007) 30 (10):2661–6. doi: 10.2337/dc06-1501
17. Djoussé L, Khawaja O, Bartz TM, Biggs ML, Ix JH, Zieman SJ, et al. Plasma Fatty Acid-Binding Protein 4, Nonesterified Fatty Acids, and Incident Diabetes in Older Adults. *Diabetes Care* (2012) 35(8):1701–7. doi: 10.2337/dc11-1690
18. Hu X, Ma X, Pan X, Luo Y, Xu Y, Xiong Q, et al. Association of Androgen With Gender Difference in Serum Adipocyte Fatty Acid Binding Protein Levels. *Sci Rep* (2016) 6:27762. doi: 10.1038/srep27762
19. Mongraw-Chaffin ML, Anderson CA, Allison MA, Ouyang P, Szklo M, Vaidya D, et al. Association Between Sex Hormones and Adiposity: Qualitative Differences in Women and Men in the Multi-Ethnic Study of Atherosclerosis. *J Clin Endocrinol Metab* (2015) 100(4):E596–600. doi: 10.1210/jc.2014-2934
20. Gates MA, Mekary RA, Chiu GR, Ding EL, Wittert GA, Araujo AB. Sex Steroid Hormone Levels and Body Composition in Men. *J Clin Endocrinol Metab* (2013) 98(6):2442–50. doi: 10.1210/jc.2012-2582
21. Agirbasli M, Agaoglu NB, Orak N, Caglioz H, Ocek T, Poci N, et al. Sex Hormones and Metabolic Syndrome in Children and Adolescents. *Metabolism* (2009) 58(9):1256–62. doi: 10.1016/j.metabol.2009.03.024
22. Rao PM, Kelly DM, Jones TH. Testosterone and Insulin Resistance in the Metabolic Syndrome and T2DM in Men. *Nat Rev Endocrinol* (2013) 9(8):479–93. doi: 10.1038/nrendo.2013.122
23. Zhang J, Tian Y, Wang W, Ouyang F, Xu J, Yu X, et al. Cohort Profile: The Shanghai Birth Cohort. *Int J Epidemiol* (2019) 48(1):21–g. doi: 10.1093/ije/dyy277
24. Metzger BE, Gabbe SG, Persson B, Buchanan TA, Catalano PA, Damm P, et al. International Association of Diabetes and Pregnancy Study Groups Recommendations on the Diagnosis and Classification of Hyperglycemia in Pregnancy. *Diabetes Care* (2010) 33(3):676–82. doi: 10.2337/dc09-1848

25. Wang WJ, Zhang L, Zheng T, Zhang GH, Du K, Yang MN, et al. Fetuin-A and Fetal Growth in Gestational Diabetes Mellitus. *BMJ Open Diabetes Res Care* (2020) 8(1):e000864. doi: 10.1136/bmjdrc-2019-000864
26. Yang MN, Chiu HC, Wang WJ, Fang F, Zhang GH, Zhu H, et al. Sex Dimorphism in the Associations of Gestational Diabetes With Cord Blood Adiponectin and Retinol-Binding Protein 4. *BMJ Open Diabetes Res Care* (2020) 8(1):e001310. doi: 10.1136/bmjdrc-2020-001310
27. Zhu L, Zhang R, Zhang S, Shi W, Yan W, Wang X, et al. Chinese Neonatal Birth Weight Curve for Different Gestational Age. *Zhonghua Er Ke Za Zhi* (2015) 53(2):97–103. doi: 10.3760/cma.j.issn.0578-1310.2015.02.007
28. VanderWeele TJ. Mediation Analysis: A Practitioner's Guide. *Annu Rev Public Health* (2016) 37:17–32. doi: 10.1146/annurev-publhealth-032315-021402
29. Fasshauer M, Blüher M, Stumvoll M. Adipokines in Gestational Diabetes. *Lancet Diabetes Endocrinol* (2014) 2(6):488–99. doi: 10.1016/s2213-8587(13)70176-1
30. Tu WJ, Guo M, Shi XD, Cai Y, Liu Q, Fu CW. First-Trimester Serum Fatty Acid-Binding Protein 4 and Subsequent Gestational Diabetes Mellitus. *Obstet Gynecol* (2017) 130(5):1011–6. doi: 10.1097/AOG.0000000000002310
31. Berio E, Divari S, Starvaggi Cucuzza L, Biolatti B, Cannizzo FT. 17β-Estradiol Upregulates Oxytocin and the Oxytocin Receptor in C2C12 Myotubes. *PeerJ* (2017) 5:e3124. doi: 10.7717/peerj.3124
32. Słabuszewska-Jóźwiak A, Włodarczyk M, Kilian K, Rogulski Z, Ciebiera M, Szymańska-Majchrzak J, et al. Does the Caesarean Section Impact on 11β HSD2 and Fetal Cortisol? *Int J Environ Res Public Health* (2020) 17(15):5566. doi: 10.3390/ijerph17155566
33. Ji H, Jiang H, Yang L, Qian X, Tang S. Factors Contributing to the Rapid Rise of Caesarean Section: A Prospective Study of Primiparous Chinese Women in Shanghai. *BMJ Open* (2015) 5(11):e008994. doi: 10.1136/bmjopen-2015-008994
34. Mi J, Liu F. Rate of Caesarean Section is Alarming in China. *Lancet* (2014) 383(9927):1463–4. doi: 10.1016/s0140-6736(14)60716-9
35. Bose SK, Hutson I, Harris CA. Hepatic Glucocorticoid Receptor Plays a Greater Role Than Adipose GR in Metabolic Syndrome Despite Renal Compensation. *Endocrinology* (2016) 157(12):4943–60. doi: 10.1210/en.2016-1615
36. Ota H, Furuhashi M, Ishimura S, Koyama M, Okazaki Y, Mita T, et al. Elevation of Fatty Acid-Binding Protein 4 is Predisposed by Family History of Hypertension and Contributes to Blood Pressure Elevation. *Am J Hypertens* (2012) 25(10):1124–30. doi: 10.1038/ajh.2012.88
37. Joung KE, Cataltepe SU, Michael Z, Christou H, Mantzoros CS. Cord Blood Adipocyte Fatty Acid-Binding Protein Levels Correlate With Gestational Age and Birth Weight in Neonates. *J Clin Endocrinol Metab* (2017) 102(5):1606–13. doi: 10.1210/jc.2016-3831
38. Papathanasiou AE, Briana DD, Gavrili S, Georgantzi S, Papathoma E, Marmarinos A, et al. Cord Blood Fatty Acid-Binding Protein-4 Levels are Upregulated at Both Ends of the Birthweight Spectrum. *Acta Paediatr* (2019) 108(11):2083–8. doi: 10.1111/apa.14826
39. Barros RP, Morani A, Moriscot A, Machado UF. Insulin Resistance of Pregnancy Involves Estrogen-Induced Repression of Muscle GLUT4. *Mol Cell Endocrinol* (2008) 295(1-2):24–31. doi: 10.1016/j.mce.2008.07.008
40. Ropero AB, Alonso-Magdalena P, Quesada I, Nadal A. The Role of Estrogen Receptors in the Control of Energy and Glucose Homeostasis. *Steroids* (2008) 73(9-10):874–9. doi: 10.1016/j.steroids.2007.12.018
41. Jambaldorj B, Terada E, Hosaka T, Kishuku Y, Tomioka Y, Iwashima K, et al. Cysteine String Protein 1 (CSP1) Modulates Insulin Sensitivity by Attenuating Glucose Transporter 4 (GLUT4) Vesicle Docking With the Plasma Membrane. *J Med Invest* (2013) 60(3-4):197–204. doi: 10.2152/jmi.60.197
42. Qi X, Gong B, Yu J, Shen L, Jin W, Wu Z, et al. Decreased Cord Blood Estradiol Levels in Related to Mothers With Gestational Diabetes. *Medicine (Baltimore)* (2017) 96(21):e6962. doi: 10.1097/md.0000000000006962
43. Jin Z, Guan X, Gao H, Shang L, Gao M, Su D, et al. The Change in Sex Hormone Binding Globulin and the Influence by Gestational Diabetes Mellitus in Fetal Period. *Gynecol Endocrinol* (2009) 25(10):647–52. doi: 10.1080/09513590903015437

Conflict of Interest: The authors declare that the research was conducted in the absence of any commercial or financial relationships that could be construed as a potential conflict of interest.

The reviewer HH declared a shared affiliation, with no collaboration, with one of the authors, XL, to the handling editor at the time of review.

Publisher's Note: All claims expressed in this article are solely those of the authors and do not necessarily represent those of their affiliated organizations, or those of the publisher, the editors and the reviewers. Any product that may be evaluated in this article, or claim that may be made by its manufacturer, is not guaranteed or endorsed by the publisher.

frontiers in Endocrinology

CASE REPORT
published: 01 October 2021
doi: 10.3389/fendo.2021.700612

Case Report: Severe Neonatal Course in Paternally Derived Familial Hypocalciuric Hypercalcemia

*Jakob Höppner[1], Sabrina Lais[2], Claudia Roll[2], Andreas Wegener-Panzer[3], Dagmar Wieczorek[4], Wolfgang Högler[5] and Corinna Grasemann[1]**

[1] Department of Pediatrics, St Josef-Hospital Bochum, Ruhr-University Bochum, Bochum, Germany, [2] Department of Neonatology, Pediatric Intensive Care and Sleep Medicine, Vestische Kinder- und Jugendklinik Datteln, University Witten/Herdecke, Datteln, Germany, [3] Department of Radiology, Vestische Kinder- und Jugendklinik Datteln, University Witten/Herdecke, Datteln, Germany, [4] Institute of Human Genetics, Medical Faculty and University Hospital Düsseldorf, Heinrich-Heine-University Düsseldorf, Düsseldorf, Germany, [5] Department of Paediatrics and Adolescent Medicine, Johannes Kepler University Linz, Linz, Austria

Familial hypocalciuric hypercalcemia (FHH, [OMIM #145980]) is recognized as a benign endocrine condition affecting PTH and calcium levels due to heterozygous inactivating mutations in the calcium sensing receptor (*CaSR*). The condition is often un- or misdiagnosed but may have a prevalence as high as 74 in 100.000. Here, the neonatal courses of two brothers with paternally inherited FHH (*CaSR* c.554G>A; p.(Arg185Gln)) are described. The older brother was born preterm at 25 weeks gestation with hypercalcemia and hyperparathyroidism. The younger brother, born full-term, had severe hyperparathyroidism, muscular hypotonia, thrombocytopenia, failure to thrive and multiple metaphyseal fractures. Treatment with cinacalcet was initiated, which resulted in subsequent reduction of PTH levels and prompt clinical improvement. While it is known that homozygous mutations in *CaSR* may lead to life-threatening forms of neonatal severe hyperparathyroidism (NSHPT), few reports have described a severe clinical course in neonates with FHH due to heterozygous mutations. However, based on the pathophysiological framework, in *de novo* or paternally transmitted FHH the differing calcium needs of mother and fetus can be expected to induce fetal hyperparathyroidism and may result in severe perinatal complications as described in this report. In summary, FHH is a mostly benign condition, but transient neonatal hyperparathyroidism may occur in affected neonates if the mutation is paternally inherited. If severe, the condition can be treated successfully with cinacalcet. Patients with FHH should be informed about the risk of neonatal disease manifestation in order to monitor pregnancies and neonates.

Keywords: familial hypocalciuric hypercalcemia, neonatal hyperparathyroidism, pregnancy, management, calcium sensing receptor (CaSR), FHH

OPEN ACCESS

Edited by:
Hiroaki Itoh, Hamamatsu University School of Medicine, Japan

Reviewed by:
Yael Levy Shraga, Edmond and Lily Safra Children's Hospital, Israel
Yoshihiko Kakinuma, Nippon Medical School, Japan

****Correspondence:***
Corinna Grasemann
corinna.grasemann@rub.de

Specialty section:
This article was submitted to Pediatric Endocrinology, a section of the journal Frontiers in Endocrinology

Received: *26 April 2021*
Accepted: *06 September 2021*
Published: *01 October 2021*

Citation:
Höppner J, Lais S, Roll C, Wegener-Panzer A, Wieczorek D, Högler W and Grasemann C (2021) Case Report: Severe Neonatal Course in Paternally Derived Familial Hypocalciuric Hypercalcemia. Front. Endocrinol. 12:700612. doi: 10.3389/fendo.2021.700612

Abbreviations: NHPT, neonatal hyperparathyroidism; CaSR, calcium-sensing receptor; NSHPT, neonatal severe hyperparathyroidism; FHH, familial hypocalciuric hypercalcemia; PTH, parathyroid hormone; TSAP, total serum alkaline phosphatase; PHPT, primary hyperparathyroidism.

INTRODUCTION

Loss-of-function mutations in the calcium-sensing and signaling pathway cause a spectrum of calcium-hyposensitivity-disorders with elevated PTH secretion (1). The resulting disorders can be summarized by inappropriately high PTH concentration despite elevated serum calcium levels.

Familial hypocalciuric hypercalcemia (FHH) comprises a genetically heterogenic group (2): FHH1 [OMIM #145980] is caused by heterozygous *inactivating* mutations in the calcium-sensing receptor (*CaSR*) gene (3). FHH2 and 3 are caused by mutations in genes encoding for proteins involved in calcium signal transduction (4–6). The CaSR is a member of the subfamily of G protein-coupled transmembrane receptors and is expressed in parathyroid chief cells and the renal tubulus (7). FHH typically presents with the biochemical triad: life-long, non-symptomatic, non-progressive hypercalcemia, normal or slightly elevated serum PTH levels and hypocalciuria (8). Thus, FHH is thought to be a mostly benign condition, with no definite association to adverse outcomes (8). Accordingly, the vast majority of patients with FHH do not require medical or surgical treatment (2, 9) and counseling of affected individuals aims to avoid future misdiagnosis and unnecessary parathyroidectomies (9, 10).

In contrast to the clinically benign course of FHH1, neonatal severe primary hyperparathyroidism (NSHPT) [OMIM #239200] is a severe rare disease associated with a high mortality and is usually caused by homozygous inactivating mutations in the CaSR gene (8, 11). Infants with NSHPT develop severe and symptomatic hypercalcemia with muscular hypotonia, respiratory distress, fractures, intestinal dysmotility, and failure to thrive in the early days of life (12–14). Milder phenotypes are summarized as neonatal hyperparathyroidism (NHPT) and refer to infants with elevated serum PTH levels and resulting bone disease, but only modest hypercalcemia, usually based on heterozygous inactivating mutations of *CaSR* (15).

Here, we present the disparate neonatal courses of two siblings with a paternally inherited FHH.

CASE PRESENTATION

Patient 1 was born in 2017 and is the first child of unrelated Caucasian parents. He was born by cesarean section at 25 weeks after premature rupture of membranes with gestational age-appropriate weight and height.

At birth, his serum calcium was 3.04 mmol/l (n: 1.90 – 2.60) and ionized calcium 1.41 mmol/l (n: 1.22 – 1.37). At day 23 of life elevated PTH (85.9 pg/ml [n: 14.9 – 56.9]) and total serum alkaline phosphatase (TSAP) (518 U/l [n: 89 – 390]) were detected while urinary calcium excretion was low (**Figure 1A**). Phosphate levels were within the normal range. He required tube-feeding with breastmilk starting day 1 of life. During the first 2 weeks, he received partial parenteral nutrition with lipids containing vitamin D3. Due to hypercalcemia routine oral vitamin D and calcium supplementation were withheld until day 42 of life.

Based on a suspected diagnosis of FHH the routine supplementation with 500 IE Vitamin D3 daily was initiated from day 42 and a calcium supplementation of 128 mg/kg BW/d (from day 48 to age 3 months) was started as appropriate for preterm infants. Calcium levels stabilized around 3.42 mmol/l and PTH remained only slightly elevated (**Figure 1A**).

At discharge at a postmenstrual age of 38 weeks renal ultrasound showed minimal nephrocalcinosis.

Molecular genetic analysis revealed the same heterozygous variant in *CaSR* NM_000388.4:c.554G>A;p.Arg185Glu; [GRCh37/hg19:chr3:g.121980436], a class V variant, that was later proven in his father. The father has been asymptomatic so far and no further diagnostic workup has been performed. To our knowledge, no other family members are affected.

Bayley Scales of Infant Development-II showed normal development at 24 months corrected age (Mental Development Index 112, Psychomotor Developmental Index 96). The boy is a currently a healthy 4-year-old with a stable serum calcium of around 3.6 mmol/l. No nephrocalcinosis is present on ultrasound.

Patient 2 is the family's second child. He was born by vaginal delivery at a gestational age of 41 weeks with normal size and Apgar scores.

At 31 and 37 weeks of gestation bowing of the right proximal femur was detected by ultrasound. Postnatally, clinical examination revealed radial deviation of both wrists.

Laboratory examination on day 1 showed thrombocytopenia (15.000/µl [n: 355.000 – 666.000/µl]) and hyperbilirubinemia (9.5 mg/dl [n: 0 – 7.0 mg/dl]). The boy received two platelet transfusions and phototherapy. Elevated serum calcium of 2.69 mmol/l and an ionized calcium with 1.54 mmol/l was present. PTH was elevated at 196.5 pg/ml, while serum phosphate and TSAP were normal. Urinary calcium was undetectable when first measured on day 21 of life (**Figure 1B**). According to national guidelines routine vitamin D3 supplementation with 500 IE/d was started on day 5.

Radiographs revealed multiple metaphyseal fractures of the long bones as well as multiple fractures at different stages of healing. Skeletal survey showed a generalized decrease in bone density with poor mineralization of the entriegeln skeleton, and at the skull wide sutures and a wormian bone was noted. (**Figure 2**).

The boy showed muscular hypotonia, limited movement of extremities, mispositioning of both wrists and the left proximal humerus with signs of discomfort.

The familial diagnosis of FHH was assumed and later confirmed. Patient 2 carries the same mutation in *CaSR* as his older brother and his father: NM_000388.4:c.554G>A;p.Arg185Glu;[GRCh37/hg19: chr3:g.121980436].

Breastfeeding was attempted, but proved difficult due to muscular hypotonia.

The patient was started on 20 mg/m² body surface/day of Cinacalcet orally given as 2.5mg twice daily on day 26. Subsequently, PTH levels decreased and urinary calcium excretion was detectable. The patient's overall clinical condition gradually improved. (**Figure 1B**).

Breastmilk was provided *via* bottle feeds and routine vitamin D supplementation was increased to 1000 IE per day during the 4th week of life.

Maternal blood test (on day 23 after delivery) showed normal levels of 25OH vitamin D at 22.0 ng/ml [n: 20 - 46] calcium (2.36 mmol/l [n: 2.20 – 2.70]), phosphate (1.31 mmol/l [n: 1.10 – 2.00]) and PTH at 18.4 pg/ml [n: 15 – 65].

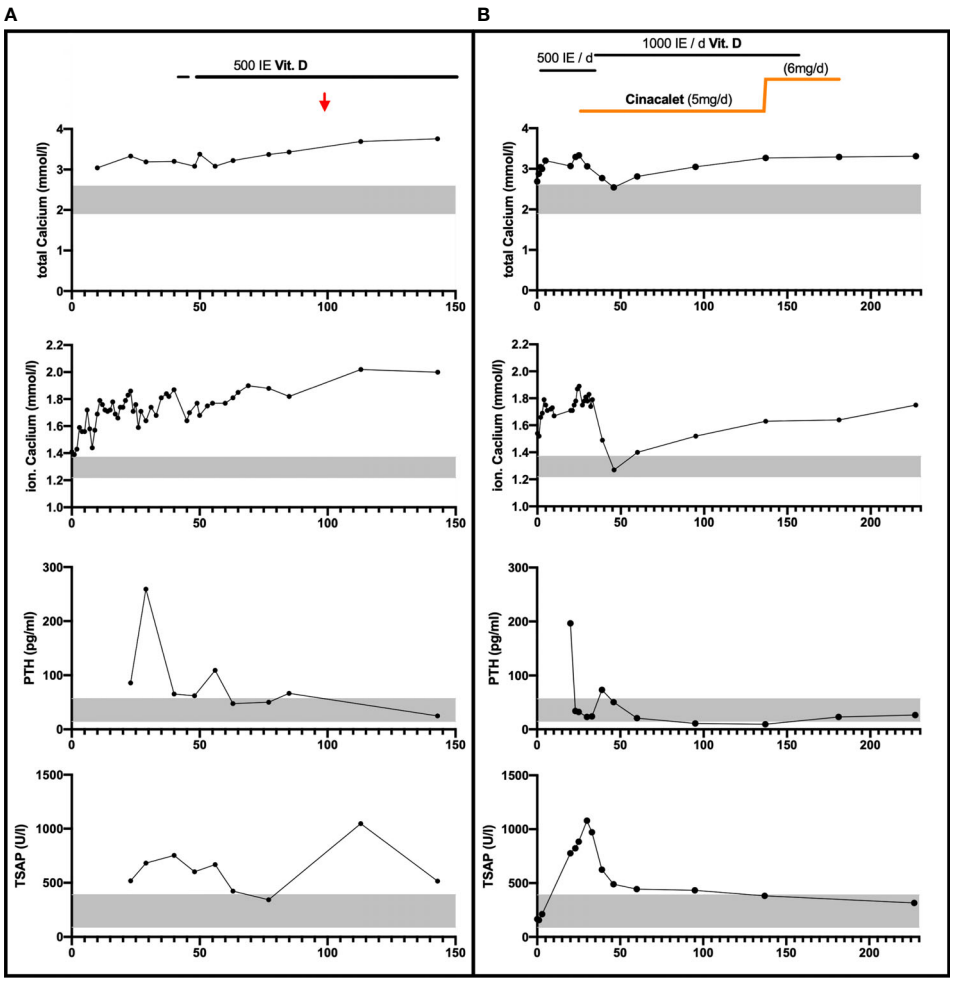

FIGURE 1 | Laboratory parameters and calcium-affecting treatments over the first 150 respectively 240 days in Patient 1 Panel **(A)** and Patient 2 Panel **(B)**. Vitamin D3 was provided orally/once daily. Cinalcacet was started in patient 2 on day 26 of life at 20 mg/m² body surface (5mg) daily and increased on day 137 of life based on increased body weight and elevated calcium levels (to 6mg). Age-appropriate normative range is indicated by the grey bar for calcium, PTH and total serum alkaline phosphate (TSAP) levels; Red arrow: estimated date of delivery.

On follow-up, the boy presented bi-weekly from 6 weeks of age until present (age 6 months). Muscular hypotonia gradually improved, as did the deformities on the left proximal humerus and the wrists. Cinacalcet was discontinued at 6 months of age and the vitamin D supplementation was reduced to 500 IE/d, to prevent oversubstitution. Serum calcium currently is 3.20 mmol/l and PTH is 26.7 pg/ml. There is no evidence for nephrocalcinosis (**Figure 1B**).

DISCUSSION

Whilst FHH1 [OMIM #145980] is thought to be a benign, typically asymptomatic condition (8), transient neonatal hyperparathyroidism later reverting to FHH has been reported, even in patients with heterozygous *CaSR* mutations, including the c.554G>A, p.Arg185Gln; R185Q variant present in the family of this report (13, 16–21). This mutation is known to result in defective receptor signaling (13, 22, 23), while the ligand binding is unaffected allowing for potential treatment with calcimimetic drugs (12, 24).

The development of neonatal hyperparathyroidism in FHH is likely modified most significantly by the parental origin of the *CaSR* mutation. In pregnancies affected by *de novo* or paternally derived mutations, the calcium setpoints of mother and fetus differ and result in conflicting regulation of calcium levels (13, 23). In these pregnancies the normocalcemic maternal environment is perceived as hypocalcemic by the fetus and thus induces fetal hyperparathyroidism to support increased fetal calcium levels at the expense of increased bone resorption. Laboratory findings in both neonates of this report resembled this situation (**Figure 1**) The demand for calcium may result in pre – and perinatal fractures, as seen in patient 2 (**Figure 2**) (16, 20). However, paternal inheritance does not always lead to NHPT but may only cause FHH, as shown in the first brother of this report (25). In contrast, in pregnancies affected by maternally derived FHH, mother and fetus share the

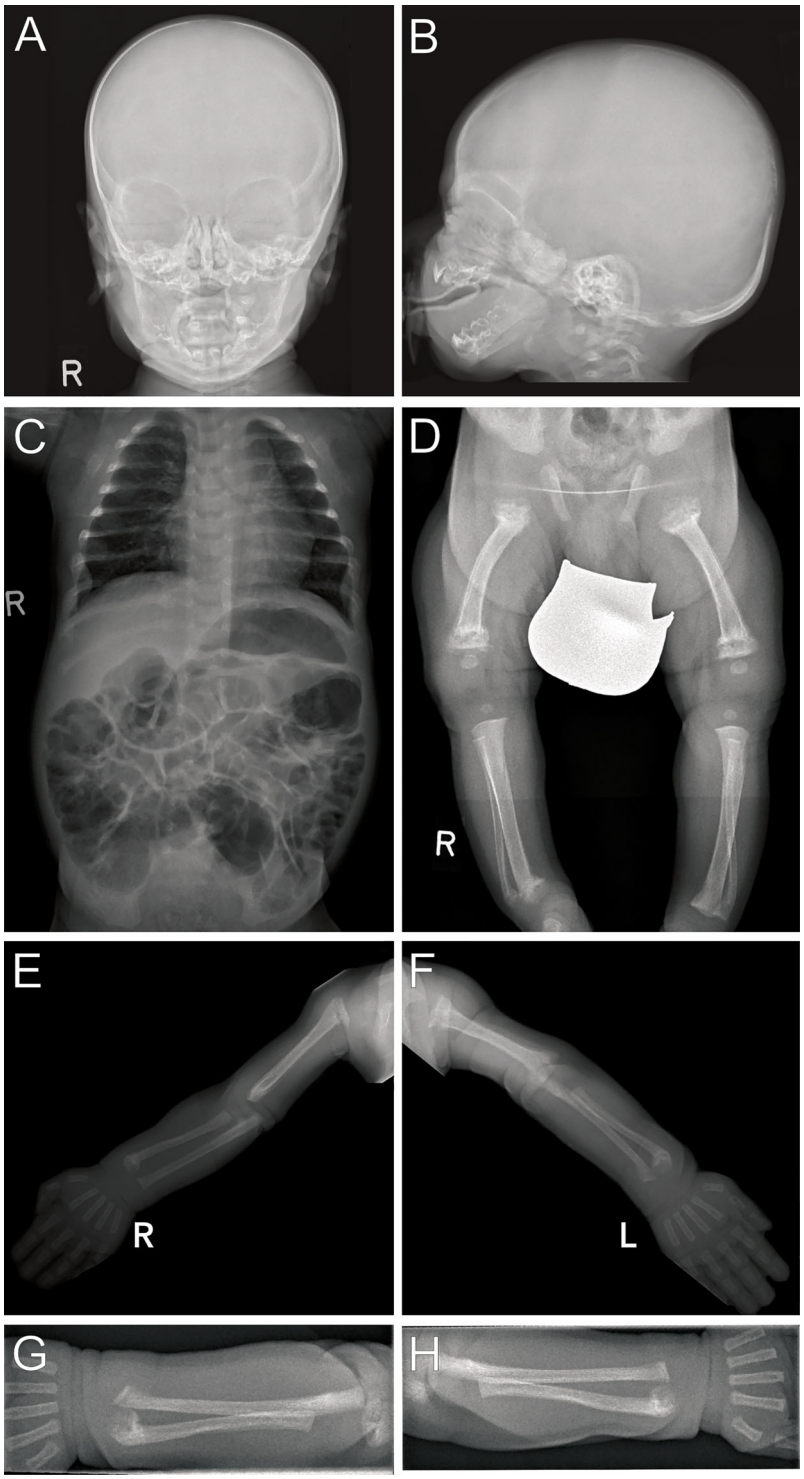

FIGURE 2 | Radiographs (Patient 2) at 3 weeks of life: Images of the skull **(A, B)** show blurred borders at the cortical/medullar bones and wide sutures with occipital intrasutural bones (Wormian bones). Poor mineralization is present in the skeleton as seen on the thoracoabdominal radiograph **(C)** arms and legs. Multiple metaphyseal fractures are present in both arms, with malalignments of the radius and ulna **(E–H)**. Distal fractures of the right tibia and fibula are present **(D)**, with internally rotated position and, to a lesser extent, likewise on the left. Fractures on the left side are close to consolidation, indicating intra uterine onset of fractures.

need for increased calcium levels and stimulation of fetal PTH is not required for calcium homeostasis (26).

In fact, the majority of the reported neonatal FHH cases are caused by de-novo or paternally derived mutations in *CaSR*, supporting the notion that maternally inherited FHH usually remains asymptomatic (11, 23, 27). Like patient 2 of this report Tonyushkina et al. reported the case of a female infant with paternally derived FHH (*CaSR* (c.1664T>C) het) who was affected by multiple fractures and bilateral femoral bowing *in utero* (28) and like the older child of this report, prematurely born infants with paternally inherited CaSR mutations were reported by Harris et al. and Fox et al. While the reason for premature delivery in patient 1 of this report was rupture of membranes (25 weeks), acute antepartum hemorrhage (27 weeks) and progressive preeclampsia (34 weeks) were reported in the other two cases (20, 29).

A modifying factor in the phenotypic variability of heterozygous *CaSR* mutations may be the maternal vitamin D status. Schwarz et al. reported the rare case of an infant with NHPT, based on a maternal heterozygous mutation in *CaSR*. (30) In this case NHPT might have risen based on insufficient calcium supply of the fetus, e.g. *via* severe maternal vitamin D deficiency (11). Consistent, Zajickova et al. presented the case of a newborn who inherited a heterozygous mutation from her father and presented with a milder phenotype. When studying the modifying effect of exogenous factors, the authors demonstrated an effect of adequate vitamin D levels in the infant, born to a healthy, yet vitamin D insufficient mother. This patient with low 25OHD level profited from an early start of vitamin D supplementation (21).

A possible reason for the different clinical presentation of the two patients of this report might be the gestational week at birth. Patient 2 was born full-term with a more severe disease and multiple fractures, which at least partly were probably present in utero. Due to the longer duration of the pregnancy, this child was longer exposed to the relatively hypocalcemic intra-uterine environment. In contrast, patient 1 was born at 25 + 6 weeks gestation and received calcium supplementation allowing for better mineralization during the third trimester. In utero, 80% of mineral is absorbed during the third trimester, resulting in an increase of trans-placenta calcium uptake from 60 mg/day of calcium at week 24 of gestation to between 300 and 350 mg/day during the last 6 weeks of the pregnancy (31, 32). Another potential mechanism for the different clinical presentation of the two patients of this report might be maternal vitamin D status during Gestation, as maternal vitamin D supply und calcium status plays a role for the clinical outcome of neonates with CaSR mutations (21).

These findings and the knowledge on the pathophysiology of FHH should have practical implications for the management of pregnancies affected by FHH and genetic counseling of patients with FHH. This becomes particularly relevant in light of the recent publication by Dershem et al. who presented results from whole exome analyses in 51,289 probands of the DiscovEHR cohort in northern USA and detected a prevalence of *CaSR* mutations of 74.1 per 100.000. Of those, 49/100.000 show a clinical FHH1 phenotype. The authors state that these results indicate a prevalence of FHH comparable to that of primary hyperparathyroidism (PHPT). If these findings can be replicated, FHH cannot be considered a rare disease anymore (33, 34). Assuming a prevalence of 74/100.000, about 580 neonates would have been affected by inherited FHH (with about 50% paternal inheritance) and an unknown number of *de novo* cases, based on the 780.000 livebirths in Germany in 2019. These numbers are difficult to interpret, given the fact that NHPT is reported so rarely in the literature.

Given the range of possible neonatal outcomes, Ghaznavi et al., recommend offering genetic counseling to all pregnant women with confirmed FHH or a partner with FHH (10). This seems reasonable, especially in the light of the data by Dershem et al. (33). Of note, no specific treatment in utero is reported or seems feasible, except for ensuring a sufficient vitamin D and calcium status in the mother.

Treatment of neonatal FHH and NHPT is not always necessary. Spontaneous clinical improvements in infants with NHPT have been reported (35). In fact, spontaneous recovery of neonates should be expected in cases of NHPT based on paternal inheritance, since the counter-regulating maternal environment is no longer influencing the fetal organism, and the neonate is allowed to achieve higher calcium levels and correct the osteopenia, if enough calcium is provided (20).

In very severe cases with clinical signs and fractures treatment with cinacalcet can be considered as in patient 2 of this report. Cinacalcet binds within the transmembrane domain and enhances CaSR sensitivity to extracellular calcium, resulting in normalization of PTH (**Figure 1A**). It is not approved for clinical use in pediatrics or FHH (36) but successful off label use in FHH has been reported previously (37–39). Based on the severe phenotype with multiple fractures, it was decided to use cinacalcet off label and discontinue the calcium treatment. The mutation in the family of this report is known to result in defective receptor signaling (13, 22, 23), while the ligand binding is unaffected allowing for potential treatment with calcimimetic drugs (12, 24). However, it remains unclear, whether the use of cinacalcet was necessary or whether a spontaneous improvement over time would have occurred, as reported by others (35).

CONCLUSION

Neonates with FHH based on paternally inherited *CaSR* mutations may present with or develop symptomatic hyperparathyroidism and fractures. This clinically relevant neonatal hyperparathyroidism may occur more frequently than currently established. Patients with FHH should be informed about this risk and careful monitoring of the pregnancy and the neonates is necessary.

DATA AVAILABILITY STATEMENT

The original contributions presented in the study are included in the article/supplementary material. Further inquiries can be directed to the corresponding author.

ETHICS STATEMENT

Ethical review and approval was not required for the study on human participants in accordance with the local legislation and institutional requirements. Written informed consent to participate in this study was provided by the participants' legal

guardian/next of kin. Written informed consent was obtained from the minor(s)' legal guardian/next of kin for the publication of any potentially identifiable images or data included in this article.

AUTHOR CONTRIBUTIONS

JH, WH, and CG conceptualized and designed the study, drafted the initial manuscript, and reviewed and revised the manuscript. SL, CR, AW-P, and DW collected data, carried out the initial analyses, and reviewed and revised the manuscript. All authors contributed to the article and approved the submitted version.

FUNDING

The authors acknowledge support by the Open Access Publication Funds of the Ruhr-University Bochum.

REFERENCES

1. Hannan FM, Kallay E, Chang W, Brandi ML, Thakker RV. The Calcium-Sensing Receptor in Physiology and in Calcitropic and Noncalcitropic Diseases. *Nat Rev Endocrinol* (2018) 15(1):33–51. doi: 10.1038/s41574-018-0115-0
2. Lee JY, Shoback DM. Familial Hypocalciuric Hypercalcemia and Related Disorders. *Best Pract Res: Clin Endocrinol Metab* (2018) 32(5):609–19. doi: 10.1016/j.beem.2018.05.004
3. Vannucci L, Brandi ML. Familial Hypocalciuric Hypercalcemia and Neonatal Severe Hyperparathyroidism. *Front Horm Res* (2018) 51:52–62. doi: 10.1159/000491038
4. Nesbit MA, Hannan FM, Howles SA, Reed AAC, Cranston T, Thakker CE, et al. Mutations in AP2S1 Cause Familial Hypocalciuric Hypercalcemia Type 3. *Nat Genet* (2013) 45(1):93–7. doi: 10.1038/ng.2492
5. Gorvin CM, Hannan FM, Cranston T, Valta H, Makitie O, Schalin-Jantti C, et al. Cinacalcet Rectifies Hypercalcemia in a Patient With Familial Hypocalciuric Hypercalcemia Type 2 (FHH2) Caused by a Germline Loss-Of-Function Gα11 Mutation. *J Bone Miner Res* (2018) 33(1):32–41. doi: 10.1002/jbmr.3241
6. Hannan FM, Babinsky VN, Thakker RV. Disorders of the Calcium-Sensing Receptor and Partner Proteins: Insights Into the Molecular Basis of Calcium Homeostasis. *J Mol Endocrinol* (2016) 57(3):R127–42. doi: 10.1530/JME-16-0124
7. Brown EM, MacLeod RJ. Extracellular Calcium Sensing and Extracellular Calcium. *Physiol Rev* (2001) 81(1):239–97. doi: 10.1152/physrev.2001.81.1.239
8. Christensen SE, Nissen PH, Vestergaard P, Mosekilde L. Familial Hypocalciuric Hypercalcaemia: A Review. *Curr Opin Endocrinol Diabetes Obes* (2011) 18(6):359–70. doi: 10.1097/MED.0b013e32834c3c7c
9. Jones AR, Hare MJ, Brown J, Yang J, Meyer C, Milat F, et al. Familial Hypocalciuric Hypercalcemia in Pregnancy: Diagnostic Pitfalls. *JBMR Plus* (2020) 4(6):1–5. doi: 10.1002/jbm4.10362
10. Ghaznavi SA, Saad NMA, Donovan LE. The Biochemical Profile of Familial Hypocalciuric Hypercalcemia and Primary Hyperparathyroidism During Pregnancy and Lactation: Two Case Reports and Review of the Literature. *Case Rep Endocrinol* (2016) 2016:1–6. doi: 10.1155/2016/2725486
11. Marx SJ, Sinaii N. Neonatal Severe Hyperparathyroidism: Novel Insights From Calcium, PTH, and the CASR Gene. *J Clin Endocrinol Metab* (2019) 105(4):1061–78. doi: 10.1210/clinem/dgz233
12. Gulcan-Kersin S, Kirkgoz T, Eltan M, Rzayev T, Ata P, Bilgen H, et al. Cinacalcet as a First-Line Treatment in Neonatal Severe Hyperparathyroidism Secondary to Calcium Sensing Receptor (CaSR) Mutation. *Horm Res Paediatr* (2020) 34899(41):313–21. doi: 10.1159/000510623
13. Reh CMS, Hendy GN, Cole DEC, Jeandron DD. Neonatal Hyperparathyroidism With a Heterozygous Calcium-Sensing Receptor (CASR) R185Q Mutation: Clinical Benefit From Cinacalcet. *J Clin Endocrinol Metab* (2011) 96(4):707–12. doi: 10.1210/jc.2010-1306
14. Marx SJ, Attie MF, Spiegel AM, Levine MA, Lasker RD, Fox M. An Association Between Neonatal Severe Primary Hyperparathyreoidism and Familial Hypocalciuric Hypercalcemia in Three Kindreds. *N Engl J Med* (1982) 306(5):257–64. doi: 10.1056/NEJM198202043060502
15. Brown EM. Clinical Lessons From the Calcium-Sensing Receptor. *Nat Clin Pract Endocrinol Metab* (2007) 3(2):122–33. doi: 10.1038/ncpendmet0388
16. Obermannova B, Banghova K, Sumník Z, Dvorakova HM, Betka J, Fencl F, et al. Unusually Severe Phenotype of Neonatal Primary Hyperparathyroidism Due to a Heterozygous Inactivating Mutation in the CASR Gene. *Eur J Pediatr* (2009) 168(5):569–73. doi: 10.1007/s00431-008-0794-y
17. Pollak MR, Brown EM, Chou YHW, Hebert SC, Marx SJ, Steinmann B, et al. Mutations in the Human Ca2+-Sensing Receptor Gene Cause Familial Hypocalciuric Hypercalcemia and Neonatal Severe Hyperparathyroidism. *Cell* (1993) 75(7):1297–303. doi: 10.1016/0092-8674(93)90617-Y
18. Pearce SHS, Trump D, Wooding C, Besser GM, Chew SL, Grant DB, et al. Calcium-Sensing Receptor Mutations in Familial Benign Hypercalcemia and Neonatal Hyperparathyroidism. *J Clin Invest* (1995) 96(6):2683–92. doi: 10.1172/JCI118335
19. Heath H, Odelberg S, Jackson CE, Teh BT, Hayward N, Larsson C, et al. Clustered Inactivating Mutations and Benign Polymorphisms of the Calcium Receptor Gene in Familial Benign Hypocalciuric Hypercalcemia Suggest Receptor Functional Domains. *J Clin Endocrinol Metab* (1996) 81(4):1312–7. doi: 10.1210/jcem.81.4.8636323
20. Fox L, Sadowsky J, Pringle KP, Kidd A, Murdoch J, Cole DEC, et al. Neonatal Hyperparathyroidism and Pamidronate Therapy in an Extremely Premature Infant. *Pediatrics* (2007) 120(5):e1350-4. doi: 10.1542/peds.2006-3209
21. Zajickova K, Vrbikova J, Canaff L, Pawelek PD, Goltzman D, Hendy GN. Identification and Functional Characterization of a Novel Mutation in the Calcium-Sensing Receptor Gene in Familial Hypocalciuric Hypercalcemia: Modulation of Clinical Severity by Vitamin D Status. *J Clin Endocrinol Metab* (2007) 92(7):2616–23. doi: 10.1210/jc.2007-0123
22. Bai M, Quinn S, Trivedi S, Kifor O, Pearce SHS, Pollak MR, et al. Expression and Characterization of Inactivating and Activating Mutations in the Human Ca2+(o)-Sensing Receptor. *J Biol Chem* (1996) 271(32):19537–45. doi: 10.1074/jbc.271.32.19537
23. Bai M, Pearce SHS, Kifor O, Trivedi S, Stauffer UG, Thakker RV, et al. *In Vivo* and *In Vitro* Characterization of Neonatal Hyperparathyroidism Resulting From a De Novo, Heterozygous Mutation in the Ca2+-Sensing Receptor Gene: Normal Maternal Calcium Homeostasis as a Cause of Secondary Hyperparathyroidism in Familial Benign Hyp. *J Clin Invest* (1997) 99(1):88–96. doi: 10.1172/JCI119137
24. Forman TE, Niemi AK, Prahalad P, Shi RZ, Nally LM. Cinacalcet Therapy in an Infant With an R185Q Calcium-Sensing Receptor Mutation Causing Hyperparathyroidism: A Case Report and Review of the Literature. *J Pediatr Endocrinol Metab* (2019) 32(3):305–10. doi: 10.1515/jpem-2018-0307
25. Glaudo M, Letz S, Quinkler M, Bogner U, Elbelt U, Strasburger CJ, et al. Heterozygous Inactivating CaSR Mutations Causing Neonatal Hyperparathyroidism: Function, Inheritance and Phenotype. *Eur J Endocrinol* (2016) 175(5):421–31. doi: 10.1530/EJE-16-0223
26. Murthy A, Murthy NPN, Ashawesh K, Kulambil Padinjakara RN, Anwar A. Familial Hypocalciuric Hypercalcaemia and Pregnancy Outcome. *Endocr Abstr* (2009) 19:P16.
27. Waller S, Kurzawinski T, Spitz L, Thakker R, Cranston T, Pearce S, et al. Neonatal Severe Hyperparathyroidism: Genotype/phenotype Correlation and the Use of Pamidronate as Rescue Therapy. *Eur J Pediatr* (2004) 163(10):589–94. doi: 10.1007/s00431-004-1491-0
28. Tonyushkina KN, O'Connor S, Dunbar NS. A Novel CaSR Mutation Presenting as a Severe Case of Neonatal Familial Hypocalciuric Hypercalcemia. *Int J Pediatr Endocrinol* (2012) 2012(1):1–7. doi: 10.1186/1687-9856-2012-13
29. Harris SS, Joseph A. Neonatal Hyperparathyroidism: The Natural Course in the Absence of Surgical Intervention. *Pediatrics* (1989) 83(1):53–6.
30. Schwarz P, Larsen NE, Lønborg Friis IM, Lillquist K, Brown EM, Gammeltoft S. Familial Hypocalciuric Hypercalcemia and Neonatal Severe Hyperparathyroidism

Associated With Mutations in the Human Ca2+-Sensing Receptor Gene in Three Danish Families. *Scand J Clin Lab Invest* (2000) 60(3):221–8. doi: 10.1080/00365510750044875
31. Ryan BA, Kovacs CS. Maternal and Fetal Vitamin D and Their Roles in Mineral Homeostasis and Fetal Bone Development. *J Endocrinol Invest* (2021) 44(4):643–59. doi: 10.1007/s40618-020-01387-2
32. Rauch F, Schoenau E. Skeletal Development in Premature Infants: A Review of Bone Physiology Beyond Nutritional Aspects. *Arch Dis Child: Fetal Neonatal Ed* (2002) 86(2):82–6. doi: 10.1136/fn.86.2.F82
33. Dershem R, Gorvin CM, Metpally RPR, Krishnamurthy S, Smelser DT, Hannan FM, et al. Familial Hypocalciuric Hypercalcemia Type 1 and Autosomal-Dominant Hypocalcemia Type 1: Prevalence in a Large Healthcare Population. *Am J Hum Genet* (2020) 106(6):734–47. doi: 10.1016/j.ajhg.2020.04.006
34. Yeh MW, Ituarte PHG, Zhou HC, Nishimoto S, Liu I-LA, Harari A, et al. Incidence and Prevalence of Primary Hyperparathyroidism in a Racially Mixed Population. *J Clin Endocrinol Metab* (2013) 98(3):1122–9. doi: 10.1210/jc.2012-4022
35. Wilkinson H, James J. Self Limiting Neonatal Primary Hyperparathyroidism Associated With Familial Hypocalciuric Hypercalcaemia. *Arch Dis Child* (1993) 69(3 SPEC NO):319–21. doi: 10.1136/adc.69.3_Spec_No.319
36. Wüthrich RP, Martin D, Bilezikian JP. The Role of Calcimimetics in the Treatment of Hyperparathyroidism. *Eur J Clin Invest* (2007) 37(12):915–22. doi: 10.1111/j.1365-2362.2007.01874.x
37. Timmers HJLM, Karperien M, Hamdy NAT, De Boer H, Hermus ARMM. Normalization of Serum Calcium by Cinacalcet in a Patient With Hypercalcaemia Due to a De Novo Inactivating Mutation of the Calcium-Sensing Receptor. *J Internal Med* (2006) 260(2):177–82. doi: 10.1111/j.1365-2796.2006.01684.x
38. Festen-Spanjer B, Haring CM, Koster JB, Mudde AH. Correction of Hypercalcaemia by Cinacalcet in Familial Hypocalciuric Hypercalcaemia. *Clin Endocrinol* (2007) 68:324–5. doi: 10.1111/j.1365-2265.2007.03027.x
39. Mayr B, Schnabel D, Do Rr HGN, Schöfl C. Gain and Loss of Function Mutations of the Calcium-Sensing Receptor and Associated Proteins: Current Treatment Concepts. *Eur J Endocrinol* (2016) 174(5):R189–208. doi: 10.1530/EJE-15-1028

Conflict of Interest: The authors declare that the research was conducted in the absence of any commercial or financial relationships that could be construed as a potential conflict of interest.

Publisher's Note: All claims expressed in this article are solely those of the authors and do not necessarily represent those of their affiliated organizations, or those of the publisher, the editors and the reviewers. Any product that may be evaluated in this article, or claim that may be made by its manufacturer, is not guaranteed or endorsed by the publisher.

frontiers in Endocrinology

ORIGINAL RESEARCH
published: 02 November 2021
doi: 10.3389/fendo.2021.746838

Development of the Diabetic Kidney Disease Mouse Model Culturing Embryos in α-Minimum Essential Medium *In Vitro*, and Feeding Barley Diet Attenuated the Pathology

Shiori Ishiyama[1], *Mayu Kimura*[1], *Takao Nakagawa*[2], *Yuka Fujimoto*[3], *Kohei Uchimura*[4], *Satoshi Kishigami*[1,5] *and Kazuki Mochizuki*[1,5]*

[1] Department of Integrated Applied Life Science, Integrated Graduate School of Medicine, Engineering, and Agricultural Sciences, University of Yamanashi, Kofu, Japan, [2] Kiwa Laboratory Animals Co., Ltd., Kiminocho, Japan, [3] Advanced Biotechnology Center, University of Yamanashi, Kofu, Japan, [4] Division of Nephrology, Department of Internal Medicine, Interdisciplinary Graduate School of Medicine and Engineering, University of Yamanashi, Kofu, Japan, [5] Faculty of Life and Environmental Sciences, University of Yamanashi, Kofu, Japan

OPEN ACCESS

Edited by:
Hiroaki Itoh,
Hamamatsu University School of Medicine, Japan

Reviewed by:
Shuntaro Ikeda,
Kyoto University, Japan
Hirotaka Hamada,
University of Toronto, Canada

***Correspondence:**
Kazuki Mochizuki
mochizukik@yamanashi.ac.jp

Specialty section:
This article was submitted to Experimental Endocrinology, a section of the journal Frontiers in Endocrinology

Received: 24 July 2021
Accepted: 07 October 2021
Published: 02 November 2021

Citation:
Ishiyama S, Kimura M, Nakagawa T, Fujimoto Y, Uchimura K, Kishigami S and Mochizuki K (2021) Development of the Diabetic Kidney Disease Mouse Model Culturing Embryos in α-Minimum Essential Medium In Vitro, and Feeding Barley Diet Attenuated the Pathology. Front. Endocrinol. 12:746838. doi: 10.3389/fendo.2021.746838

Diabetic kidney disease (DKD) is a critical complication associated with diabetes; however, there are only a few animal models that can be used to explore its pathogenesis. In the present study, we established a mouse model of DKD using a technique based on the Developmental Origins of Health and Disease theory, i.e., by manipulating the embryonic environment, and investigated whether a dietary intervention could ameliorate the model's pathology. Two-cell embryos were cultured *in vitro* in α-minimum essential medium (MEM; MEM mice) or in standard potassium simplex-optimized medium (KSOM) as controls (KSOM mice) for 48 h, and the embryos were reintroduced into the mothers. The MEM and KSOM mice born were fed a high-fat, high-sugar diet for 58 days after they were 8 weeks old. Subsequently, half of the MEM mice and all KSOM mice were fed a diet containing rice powder (control diet), and the remaining MEM mice were fed a diet containing barley powder (barley diet) for 10 weeks. Glomerulosclerosis and pancreatic exhaustion were observed in MEM mice, but not in control KSOM mice. Renal arteriolar changes, including intimal thickening and increase in the rate of hyalinosis, were more pronounced in MEM mice fed a control diet than in KSOM mice. Immunostaining showed the higher expression of transforming growth factor beta (TGFB) in the proximal/distal renal tubules of MEM mice fed a control diet than in those of KSOM mice. Pathologies, such as glomerulosclerosis, renal arteriolar changes, and higher TGFB expression, were ameliorated by barley diet intake in MEM mice. These findings suggested that the MEM mouse is an effective DKD animal model that shows glomerulosclerosis and renal arteriolar changes, and barley intake can improve these pathologies in MEM mice.

Keywords: diabetic kidney disease (DKD), MEM mice, DOHaD (developmental origins of health and disease), barley, glomerulosclerosis, transforming growth factor beta (TGF- β)

INTRODUCTION

Type 2 diabetes mellitus (T2DM) is a major cause of chronic kidney disease (1, 2), commonly known as diabetic kidney disease (DKD). DKD generally develops and progresses with renal glomerular hyperfiltration, microalbuminuria, apparent albuminuria, and low glomerular filtration rate (GFR), and patients eventually require dialysis (3). A serial, cross-sectional Japanese T2DM cohort study reported that the number of patients with DKD with an estimated glomerular filtration rate (eGFR) < 60 mL/min/1.73 m^2 increased from 12.1% in 1996 to 24.0% in 2004 (4). Therefore, the mechanistic exploration of DKD development and therapy are necessary for DKD prevention.

Glomerular and tubular disorders, induced by mesangial matrix expansion, are considered to be the main features of DKD. Hyperglycemia is known to promote the proliferation of mesangial cells, which leads to the excess production of extracellular matrix (ECM) and induces glomerulosclerosis (5, 6). In addition, hyperglycemia induces the migration of pericytes from the peritubular capillaries to the interstitial space, thereby causing arteriolosclerosis (7). Furthermore, the migration of peritubular pericytes accelerates tubular interstitial changes by enhancing the transition of pericytes into myofibroblasts. DKD can be classified into four categories based on the type of hierarchical glomerular lesions, and tuberous sclerosis is the most characteristic lesion in DKD, with extensive interstitial and vascular lesions formed in DKD of each category (8). Glomerular cell dysfunction impairs glomerular filtration and microvascular permeability, which reduces the levels of body wastes (such as nephrotoxins) in the urine, and also reduces microalbuminuria or albuminuria. However, dietary or drug therapies to prevent or ameliorate DKD are not well developed.

The lack of animal models with disease development similar to that occurring in patients with DKD has delayed research and development of DKD therapies. Several T2DM animal models, such as mutant T2DM models and spontaneous T2DM models, as well as conventional models, exhibit DKD. Compared with age-matched non-diabetic *db*/*m* control mice, obese diabetic *db*/*db* mice carrying the mutant leptin (an anorexigenic hormone) receptor exhibited six times higher urinary albumin levels and lower GFRs at 28 weeks of age and greater mesangial matrix expansion after 16 weeks of age (9–11). *db*/*db* mice with unilateral renal artery stenosis developed severe mesangial sclerosis, progressive interstitial fibrosis, tubular atrophy, and interstitial inflammation, but not mesangial matrix expansion, a major characteristic of DKD (12). Compared with lean control rats, the T2DM model Zucker rat, which carries a mutant leptin receptor and develops obesity at younger ages, exhibited 200-fold higher urinary albumin levels at 16 weeks and 1000 times higher hyperfiltration (non-decreased 50% eGFR) at 26 weeks. These phenotypes can be considered severely pathological compared with those of patients with DKD (13). OLETF rats, which are spontaneous T2DM model rats with a lack of cholecystokinin 1 receptor gene, exhibited diffuse glomerular sclerosis and tuberous sclerosis, along with basement membrane thickening, mesangial proliferation, and fibrin cap formation (14). However, compared with control OLETF rats, OLETF rats fed a 40% (w/w) high-protein diet from 5 to 30 weeks of age showed a progression in nephropathy at 30 weeks, even though they exhibited relatively lower blood glucose levels in the oral glucose tolerance test (OGTT) than 26-week-old control OLETF rats (15). Therefore, diabetes cannot be considered the main cause of kidney dysfunction in the OLETF model. In addition, because T2DM and DKD development in OLETF rats takes longer (20 or more weeks of age) than that in *db*/*db* mice (18 weeks of age), and the developmental stages vary widely among different experimental groups, the OLETF rat model is not suitable for studies on DKD (11, 15). Therefore, the animal models mentioned above do not replicate the manifestations of DKD observed in patients, such as middle albuminuria, glomerular hypertrophy, and mesangial matrix expansion (16).

Recent studies have suggested that environmental factors during developmental stages can induce metabolic diseases, including T2DM and DKD. This is stated as the Developmental Origins of Health and Disease (DOHaD) theory. A retrospective cohort study in Ukraine reported that the odds ratio of T2DM diagnosis at age 40 years or older was higher in individuals born in areas affected with severe-to-extreme famine than in individuals born during famine but in unaffected areas (17). Furthermore, it was reported that the body weight as per gestational age shows positive correlation with total kidney volume at 0, 3, and 18 months after birth. Additionally, premature (< 37 weeks of gestation) children had smaller kidneys compared to mature children (37 to 42 weeks of gestation) (18). In a retrospective case-control study of infants born at ≤ 34 weeks of gestation, compared with appropriate for gestational age premature infants, small for gestational age premature infants had higher serum creatinine on postnatal days 1 and 3 and a lower urinary output (in mL/kg/h) (19). These findings suggest that undernutrition during the gestational period is a risk factor for the development of T2DM and renal insufficiency in adulthood, and SGA offspring are predisposed to these conditions. Recently, we established a T2DM mouse model using techniques based on the DOHaD theory, such as manipulation of the embryonic environment and subsequent administration of high-fat, high-sugar diets. Specifically, we established a mouse model using two-cell-stage embryos

Abbreviations: αMEM, α minimum essential medium; ART, assisted reproductive technology; DKD, diabetic kidney disease; DOHaD, Developmental Origins of Health and Disease; ECM, extracellular matrix; EGCg, epigallocatechin gallate; eGFR, estimated glomerular filtration rate; eNOS, endothelial nitric oxide synthase; EVG, Elastica van Gieson; GFR, glomerular filtration rate; GK rat, Goto-Kakizaki rat; HE, hematoxylin-eosin stain; ICR, Institute of Cancer Research; IVF, *in vitro* fertilization; KC, mice developed from embryos cultured in KSOM and subsequently fed a rice-based diet; KSOM, potassium simplex-optimized medium; MDA, malondialdehyde; MEM, minimum essential medium; MB, mice developed from embryos cultured in MEM and fed a barley-based diet; MR, mice developed from embryos cultured in MEM and fed a rice-based diet; MT, Masson's trichrome; NADKD, normoalbuminuric diabetic kidney disease; NADPH, nicotinamide adenine dinucleotide phosphate; OD, outer diameter; OGTT, oral glucose tolerance test; PAS, Periodic acid-Schiff; SEM, standard error of the mean; TGFB, transforming growth factor beta; T2DM, type 2 diabetes mellitus; 8-hydroxydeoxyguanosine, 8-OHdG.

cultured in α-minimal essential medium (αMEM), followed by embryo transfer into the mother (MEM mice). After birth, the mice were fed a high-fat, high-sugar diet after weaning, and hence, were remarkably hyperglycemic and moderately overweight, similar to patients with T2DM, particularly Asian patients (20). MEM mice also developed non-alcoholic hepatic steatosis with hepatic fibrosis (21), which is frequently observed in patients with T2DM. The factors influencing T2DM development in MEM mice, such as the environmental conditions during the fetal and postnatal periods, is similar to those in patients with T2DM. In addition, the intake of barley, a food abundant in the soluble dietary fiber β-glucan, reduced postprandial hyperglycemia (22) and repressed hepatic fibrosis in MEM mice. However, it is unclear whether MEM mice develop DKD, and whether dietary factors, including barley, attenuate DKD in MEM mice.

In this exploratory animal study, we investigated whether T2DM MEM mice develop DKD, and whether barley intake after birth alleviates the pathology.

MATERIALS AND METHODS

Animals

We have previously demonstrated that mice developed from embryos cultured *in vitro* in α-MEM (MEM mice) exhibit T2DM with postprandial hyperglycemia and non-alcoholic steatohepatitis, in contrast to mice developed from embryos cultured *in vitro* in potassium simplex optimized medium (KSOM) (23). Barley intake for 10 weeks ameliorated non-alcoholic steatohepatitis in MEM mice (21). In this study, we used the same mice (MEM mice and KSOM mice) to explore whether MEM mice develop DKD and to investigate the effects of barley intake on renal pathology. Briefly, 2-cell embryos were obtained from the uteri of Institute of Cancer Research (ICR) pregnant mice aged 8 weeks, and subsequently, the 2-cell embryos were cultured in either α-MEM (135-15175, Wako Pure Chemical Industries, Ltd., Osaka, Japan) or KSOM (ARK Resource, Kumamoto, Japan) control medium (Table S1) for 48 h (morula stage) at 37 °C in a 5% CO_2 incubator. Subsequently, to develop MEM or KSOM mice, the morulae were transplanted in another pregnant mouse (aged 8 weeks) and pregnant mothers, and the mothers with suckling pups were fed the laboratory chow diet (MF, Oriental Yeast Co., Ltd., Tokyo, Japan) until weaning (21 days) at Kiwa Laboratory Animal Co., Ltd. (Wakayama, Japan). After weaning, the pups were fed the laboratory chow diet until they were of 8 weeks, and subsequently, they were fed a high-fat, high-sugar (Western-style) diet (**Supplementary Table S2**) for 58 days. At age 19–25 weeks, MEM/ICR (n = 24) and KSOM/ICR male mice (n = 8) were moved to the University of Yamanashi, where they were provided water and food *ad libitum*, placed in cages (two per cage), and maintained under controlled conditions (temperature 23 ± 2°C; humidity 50% ± 10%; 12 h light/12 h dark cycle). MEM mice were then randomly allocated to two groups of similar age and body mass. Thus, three groups were formed: MEM mice fed a rice-based diet (Niigata Flour Milling Co., Ltd., Niigata, Japan; n = 12; MR group), MEM mice fed a diet containing barley powder (Hakubaku Co., Ltd., Yamanashi, Japan; n = 12; MB group), and KSOM control mice (n = 8) fed a rice-based diet (KC group). One animal in the MB group died during the OGTT and, therefore, its data was not included in the experimental data (21, 23). The diet composition provided by Oriental Yeast Co., Ltd. is provided in **Supplementary Table S2**. We did not calculate the sample sizes or perform the study under blinded conditions because this was an exploratory study. The β-glucan content in the barley diet was 1.06 g/100 g barley (average; n = 2), as determined at Hakubaku Co., Ltd. This animal study was approved by the Ethics Committee of the University of Yamanashi (approval number A30-24) and was performed according to the institutional animal experiment guidelines. The mice were decapitated, and samples were collected from one mouse at a time in the order of MR, MB, and KC to ensure that each group had similar mean dissection times (9:00 am–3:00 pm) (21, 23). Kidney tissue samples were collected and weighed, and the right kidney tissues were snap-frozen in liquid nitrogen and stored at −80°C until use for qRT-PCR and western blotting.

Histological Staining of the Pancreas and Kidney Sections

The pancreas and left kidney were divided into three equal parts, and the middle sections were immediately fixed with 4% paraformaldehyde and incubated overnight in phosphate-buffered saline, with the solution switched to 70% ethanol prior to processing for paraffin embedding, as described previously (21). Each tissue section was embedded in paraffin by New Histo. Science Laboratory Co., Ltd. (Tokyo, Japan). The pancreas sections were stained with hematoxylin-eosin (HE) stain and Masson's trichrome (MT) stain for quantifying the islets of Langerhans and pancreatic β cells and estimating fibrosis. The kidney sections were subjected to Periodic Acid-Schiff (PAS) and Elastica van Gieson (EVG) staining at KAC Co., Ltd. (Shiga, Japan) for quantification of mesangial expansion, glomerulosclerosis, and renal artery injury. Immunostaining for insulin (rabbit monoclonal antibody, 1:1,000; #3014, Cell Signaling Technology) and TGFB (transforming growth factor beta; rabbit polyclonal antibody, 1:1,000; #3711, Cell Signaling Technology) was performed at KAC Co., Ltd. Subsequently, the islets of Langerhans of the pancreas, and the glomerulus, tubule, and renal artery were examined under a light microscope (CX41LF, Olympus Corp., Tokyo, Japan). The islets of Langerhans were observed using HE staining. The fibrotic and insulin-positive areas as well as the pancreatic β cells were analyzed from the digital images (five images per a mouse). Glomerular expansion was assessed using the fractional average diameter based on ten glomeruli per a mouse, and glomerular fibrosis was defined based on the mesangial matrix area (PAS-positive area) per unit diameter, based on observations in ten glomeruli per mouse. The nodular lesion ratios were quantified by counting the pathological, altered glomeruli per total glomeruli in each specimen. Intimal thickening of the renal artery was determined as a percentage of the outer diameter

(OD) (%OD), as described previously (24). In brief, %OD = 100 (T+S)/2OD, where (T+S)/2 is the average of the two-sided intimal thickness. Arteriolar intimal hyalinosis was observed, as reported in previous studies (24, 25), and the hyalinization ratio was quantified in terms of hyalinization vessel counts per total vessel counts in each specimen. The TGFB-positive area was measured in the glomeruli, proximal tubule, and distal tubule, as described previously (26) (one image was randomly selected per a mouse, n = 8–12 images in each experimental group). All digital images were analyzed using the ImageJ software (Image Processing and Analysis in Java, NIH, Bethesda, MD, USA), as recommended (27).

Preparation of Kidney Homogenates and Biochemical Analysis

Approximately 100 mg of each frozen kidney sample was homogenized in 1 mL of RIPA buffer (1% NP-40, 0.1% sodium dodecyl sulfate, 20 mM Tris-HCl [pH 8.0], 5 mM EDTA, 150 mM NaCl, 1 mM Na_3VO_4, 0.1 mM Na_2MoO_4, and 10 mM NaF) containing protease inhibitor cocktail tablets (cOmplete™, Roche Diagnostics K.K., Risch-Rotkreuz, Switzerland), as described previously (21, 23). Five hundred microliters of the homogenates were dispensed and used to measure the levels of malondialdehyde (MDA), 8-hydroxydeoxyguanosine (8-OHdG), and other oxidative markers, in the kidney, as well as for western blotting. Blood glucose and insulin concentrations were measured as described previously (21, 23). Renal and urinary 8-OHdG levels were measured using a highly sensitive ELISA kit for 8-OHdG (Japan Institute for the Control of Aging NIKKEN SEIL CO, Ltd., Shizuoka, Japan), and the renal MDA concentration was measured using a NWLSS™ Malondialdehyde Assay (Northwest Life Science Specialties, LLC, Vancouver, WA, USA). The phosphorous content in the collected plasma samples was measured using a phospha-C Test Wako kit (FUJIFILM Wako Pure Chemical Corporation, Osaka, Japan). All tests were performed according to the manufacturer's instructions.

Statistics Analysis

The results are expressed as mean ± standard error of the mean (SEM). In this study, there were two explanatory variables, such as the difference in culture medium (MEM and KSOM) for *in vitro* embryos and diet differences from the adult stage (control diet and barley-based diet). Therefore, we used Student's *t*-test to compare each explanatory variable between the MEM and KSOM groups or between the control and barley-based diet groups. A P value < 0.05 was considered to be statistically significant. All values were analyzed using Excel Statistics 2010 (Social Survey Research Information Co., Ltd., Tokyo, Japan).

RESULTS

Characteristics and Biochemical Parameters of MEM Mice

As described previously (21, 23), the body weight, non-fasting blood glucose concentrations, and insulin concentrations in MR mice were not higher than those in KC or MB mice. However, food intake was higher in MR mice than in KC mice, and the weight of the pancreas per unit body weight was lower in MB mice than in MR mice. In this study, we measured the weights of the pancreas and kidneys; MDA and 8-OHdG concentrations in the kidney and urine; and plasma phosphorus concentrations in mice. The weights of the kidney and pancreatic tissues did not differ between MR and KC mice or between MR and MB mice. The renal concentration of MDA, an oxidative stress marker, was lower in MB mice than in MR mice, but did not differ between MR and KC mice. The concentrations of 8-OHdG, an indicator of oxidative stress, in the kidney and urine, did not differ between MR and KC mice or between MR and MB mice. MR mice showed higher plasma phosphorus concentrations than KC mice, whereas MB mice showed lower plasma phosphorus concentrations than MR mice (P = 0.055) (**Table 1**). The urinary albumin was not detected (data not shown).

Pancreatic Exhaustion in MEM Mice Under Diabetic Conditions

The islets of Langerhans were assessed by HE-staining, and the areas of fibrosis, and insulin positivity and pancreatic β cells in each islet of Langerhans was assessed by MT staining and immunostaining for insulin, respectively (**Figures 1A–I**). The fibrotic areas were larger in MR mice than in KC mice and smaller in MB mice than in MR mice (**Figure 1J**). The insulin-positive area was smaller in MR mice than in KC mice, whereas it was larger in MB mice than in MR mice (**Figure 1K**). The islet size did not differ between MR mice and KC mice or MR mice and MB mice (**Figure 1L**). All images of HE, MT and Insulin staining of the pancreas of each group (**Supplementary Figures S1–S3**).

Increased Number of Glomerular Lesions in Diabetic MEM Mice

To ascertain whether the pathological characteristics and changes in the glomeruli of MEM mice were owing to the diabetic conditions, we performed PAS-staining (**Figures 2A–C**). The nodular lesion ratio, which is frequently measured in diabetic glomerular pathology, was higher in MR mice than in KC mice, whereas it was lower in MB mice than in MR mice (**Figure 2D**). The glomerular size, a measure of glomerular expansion, was greater in MR mice than in KC mice (**Figure 2E**) and lesser in MB mice than in MR mice. The glomerular fibrotic area, a measure of the mesangial matrix area, was larger in MR mice than in KC mice, but did not differ between MR mice and MB mice (**Figure 2F**). All images of PAS in the glomerulus of each group (**Supplementary Figures S4–S6**).

Renal Arterial Changes in Diabetic MEM Mice

To assess renal artery injury, we examined the intimal thickness and hyalinosis in the renal artery using EVG staining and PAS staining, respectively (**Figures 3A–F**). Intimal thickening, calculated as %OD, was higher in MR mice than in KC mice (**Figure 3G**), whereas it was lower in MB mice than in MR mice. The hyalinization ratio was higher in MR mice than in KC mice

TABLE 1 | Metabolic variables of KSOM control mice and MEM mice after 10 weeks of control or barley diet feeding.

	KC	MR	MB
Age (weeks)	28 ± 0.0	30 ± 0.6*	30 ± 0.7
Body weight (g)	70 ± 3.5	81 ± 4.2	84 ± 3.8
Blood glucose (mg/dL)	191 ± 7	334 ± 73	290 ± 71
Blood insulin (mg/dL)	3.3 ± 1.2	2.3 ± 0.6	1.1 ± 0.1
Kidney weight/body weight (g/g)	0.013 ± 0.001	0.014 ± 0.002	0.013 ± 0.002
Pancreas weight/body weight (g/g)	0.008 ± 0.000	0.009 ± 0.001	0.007 ± 0.001#
Plasma phosphorus (mg/dL)	7.19 ± 0.23	8.15 ± 0.32*	7.32 ± 0.24
Renal MDA/protein (μM)	6.1 ± 0.2	6.7 ± 0.7	5.4 ± 0.5#
Renal 8-OHdG (ng/mL)	0.87 ± 0.04	1.26 ± 0.18	1.07 ± 0.04
Urinary 8-OHdG (ng/mL)	0.03 ± 0.02	0.10 ± 0.03	0.17 ± 0.10
Food consumption (g/day)	4.74 ± 0.04	7.22 ± 0.46*	8.56 ± 1.08

*8-OHdG, 8-hydroxydeoxyguanosine; MB, minimum essential medium (MEM) mice on a barley diet; MDA, malondialdehyde; MR, MEM mice on a rice diet; KC, potassium simplex optimized medium control mice on a rice diet. Data are expressed as means ± SEM for 8-12 mice. Statistical analyses were performed by Student's t-test. *P < 0.05 compared with the KC group; #P < 0.05 compared with the MR group.*

and lower in MB mice than in MR mice (**Figure 3H**). All images of PAS and EVG staining of the kidney of each group (**Supplementary Figures S4–S6**).

Localization of Renal TGFB Protein

We performed immunostaining to evaluate renal TGFB protein distribution, including that in the glomerulus and distal and proximal tubules (**Figures 4A–F**). The areas showing TGFB expression in the proximal and distal tubules were larger in MR mice than in KC or MB mice (**Figures 4H, I**). However, the differences in the glomerular TGFB expression levels were not significant between MR and KC mice or MB mice (P=0.16, P=0.21, respectively) (**Figure 4G**). All images of TGFB staining in the glomerulus and proximal/distal tuble of the kidney of each group (**Supplementary Figure S7–S9**). The TGFB protein level in total kidney did not differ between MR and KC mice or between MR and MB mice. (**Supplementary Figure S10**). There was no differences of the mRNA expression levels of inflammation cytokines between KC and MR, and between MR and MB in the kidney (**Supplementary Figure S11**).

DISCUSSION

In the present study, we provided first evidence that MEM mice developed from two-cell-stage embryos cultured *in vitro* in αMEM exhibited pancreatic exhaustion and glomerulosclerosis, in contrast to control mice developed from embryos cultured in normal KSOM. Furthermore, the administration of dietary barley for 10 weeks after the mice reached an adult stage ameliorated these pathologies.

We observed a higher incidence of typical DKD pathology—nodular lesions and glomerular hypertrophy—in MEM mice that were fed a rice-based diet than in control KSOM mice. In this study, we did not observe microalbuminuria in MEM mice (data not shown), and the plasma phosphorus concentration did not differ between MEM mice fed a rice-based diet and control KSOM mice. The appearance of renal efferent arteriosclerosis in patients with T2DM is frequently associated with microalbuminuria, a marker of early-stage DKD. Thus, MEM mice at the stage evaluated in this study can be considered an animal model of DKD with similar pathology to patients with an earlier stage of DKD, although it remains unclear whether the continuous feeding of a high-fat, high-sugar diet to MEM mice causes DKD progression. Recent clinical studies on DKD suggest that the assessment of DKD development based on urine microalbumin levels is limited because progressive kidney dysfunction (eGFR < 60 mL/min/1.73 m^2) is frequently observed in patients with T2DM with normoalbuminuria. The symptom is referred to as normoalbuminuric DKD (NADKD) or nonalbuminuric diabetic nephropathy (28, 29). There are no reports establishing NADKD animal models with severe renal damage similar to that observed in patients with NADKD. Further works should be examined whether animal models including our MEM mice models reflect human T2DM/DKD pathology by measuring biomarkers in human such as GFR or proteinuria. Additionally, only a few reports have shown that the symptoms in gene mutation-inducible or reagen-inducible DKD animals improve in response to dietary interventions. One study reported that the administration of epigallocatechin gallate (EGCg), a type of green tea extract, to *db/db* mice for 8 weeks reduced the mesangial matrix index by 34%, leading to glomerular dysfunction, in contrast to that in *db/db* mice that did not receive EGCg (30). In the present study, the administration of a barley diet for 10 weeks in adult MEM mice reduced the glomerular and nodular lesions as well as the renal arteriolar lesions. Furthermore, barley intake for only 10 weeks reduced the glomerular lesion ratio by 50%, intimal thickening by 15%, and hyalinosis by 27%. Taken together, MEM mice may be considered NADKD animal models with a similar pathology to patients with DKD, with nodular sclerosis in the glomeruli, and the DKD pathology can be attenuated by dietary interventions.

In this study, we found that the renal arteriolar hyalinosis rate and intimal thickening of the renal arteriola, both of which indicate renal efferent arteriosclerosis (31), were higher in MEM mice fed a rice-based diet than in control KSOM mice. Renal vascular lesions in DKD are linked to renal efferent arteriosclerosis, in which there is an increase of ECM in the interior of renal vascular vessels, which is related to hypertension. Hypertension is one of the strongest risk factors for renal arteriolosclerosis. The elevation of blood pressure

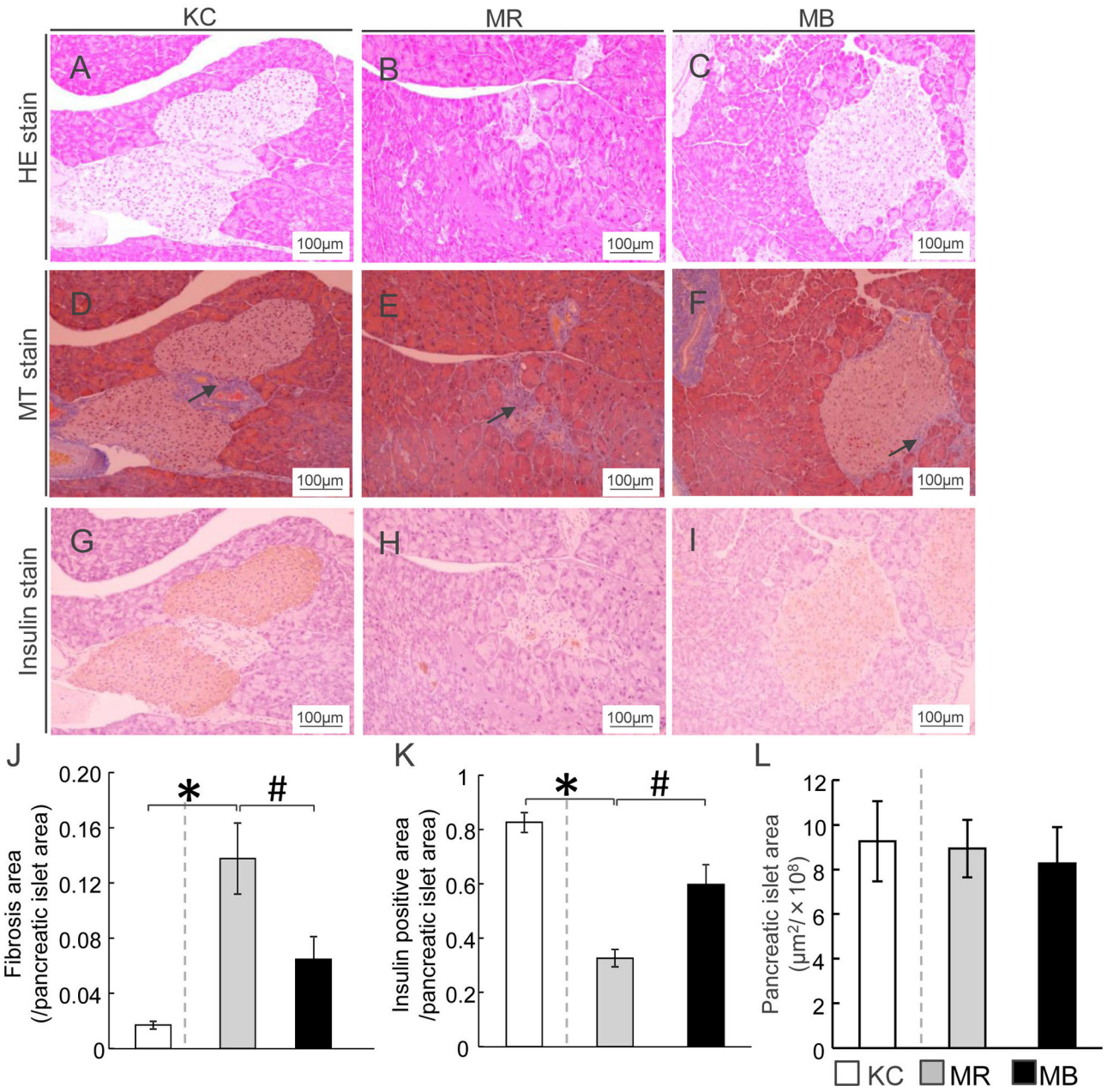

FIGURE 1 | β-Cell area in mice after 10 weeks of experimental diet intake. **(A–C)** Representative histological hematoxylin-eosin staining of pancreatic sections from mice from each of the three experimental groups. **(D–F)** Fibrotic areas in the pancreas within the islets were stained blue after Masson's trichrome staining (arrows). **(G–I)** Insulin-positive areas within the islets are stained brown (scale bar, 100 μm). Ratio of areas with fibrosis **(J)** and insulin-positive cells **(K)** in the pancreatic islets and area of pancreatic islets **(L)**. MB, minimum essential medium (MEM) mice on a barley diet; MR, MEM mice on a rice diet; KC, potassium simplex optimized medium control mice on a rice diet. Data are expressed as the mean ± SEM for 8–12 animals. Data were analyzed using Student's *t*-test. $^{*}P < 0.05$ compared with the KC group; $^{\#}P < 0.05$ compared with the MR group.

induces endothelial collapse and subsequent endothelial cell proliferation for the repair of the renal arteriola, which leads to the development of renal efferent arteriosclerosis (32). Reportedly, greater renal arteriolar hyaline degeneration as well as mesangial matrix proliferation and glomerular fibrosis were observed in patients with NADKD with exacerbated eGFR (<60 mL/min/1.73 m^2) than in patients with normal eGFR NADKD, but there was no difference in the systolic/diastolic blood pressure between patients with NADKD with normal/exacerbated eGFR (33). In representative conventional T2DM models, such as *ob/ob* mice and *db/db* mice, renal efferent arteriosclerosis as well as glomerular lesions were observed in

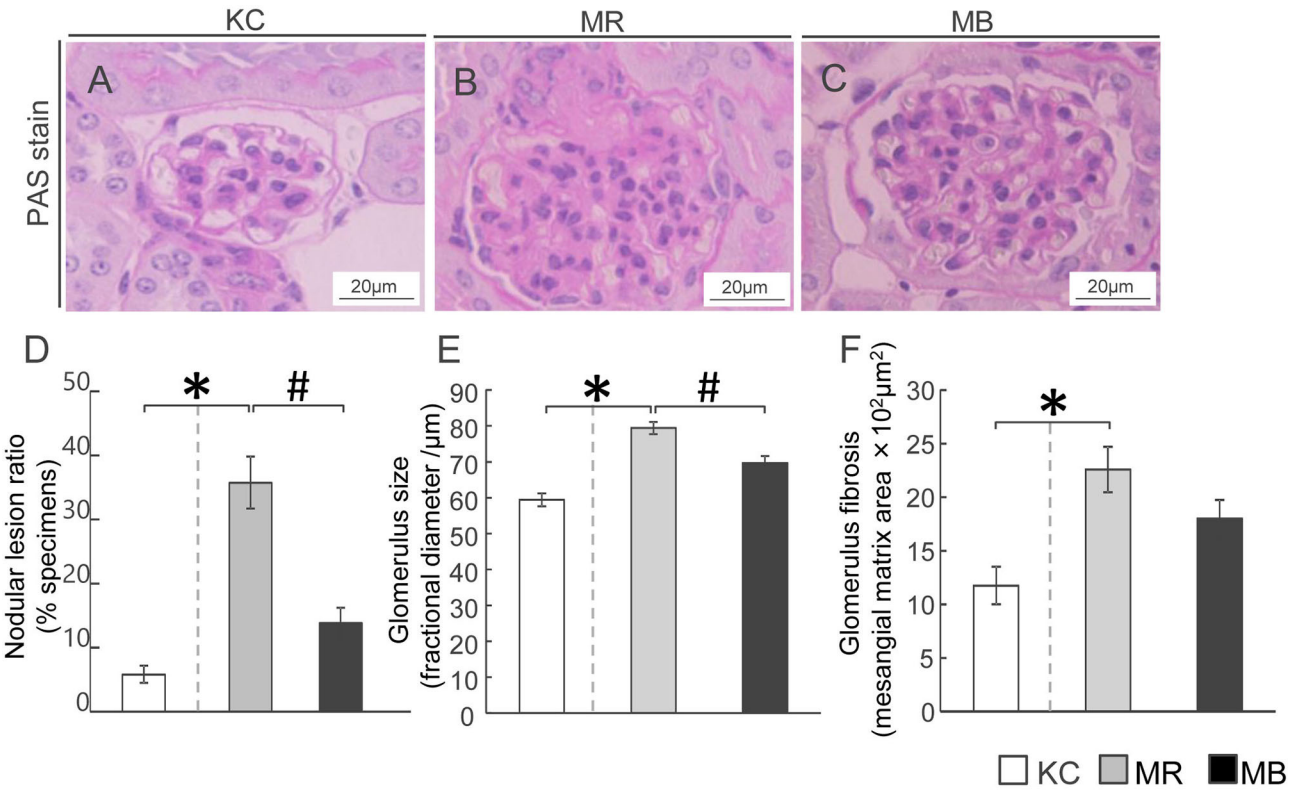

FIGURE 2 | Histopathology showing fibrosis and pathogenesis in the kidneys of mice after 10 weeks of experimental diet intake. **(A–C)** Glomerular fibrosis observed using Periodic acid–Schiff staining (scale bar, 20 μm) in mice from the three groups. **(D–F)** Quantification of the nodular lesion ratio **(D)**, glomerular size **(E)**, and fibrotic area **(F)**. MB, minimum essential medium (MEM) mice on a barley diet; MR, MEM mice on a rice diet; KC, potassium simplex optimized medium control mice on a rice diet. Data are expressed as the mean ± SEM for 8–12 animals. Data were analyzed using Student's *t*-test. $^{*}P < 0.05$ compared with the KC group; $^{\#}P < 0.05$ compared with the MR group.

endothelial nitric oxide synthase (eNOS)-deficient *db/db* mice (34) and -*ob/ob* mice of the BTBR strain (35). eNOS expression in the endothelium is associated with the reduction of blood pressure *via* the relaxation of blood vessels (36). These results indicate that hypertension with diabetes is associated with the development of renal efferent arteriosclerosis. Therefore, renal efferent arteriosclerosis in MEM mice may be caused by hypertension, and the improvement of renal efferent arteriosclerosis in MEM mice by barley intake may require the reduction of hypertension. However, in this study, we did not measure the blood pressure of MEM mice. Reportedly, rat offspring that underwent protein restriction (9% casein) during the fetal period showed reduced nephron number (37). In a human cohort study, participants with a low birth weight had a higher incidence of hypertension at 36 years of age compared to participants with normal birth weight (38), and participants born to mothers who experienced severe famine during early gestation had a higher incidence of hypertension and kidney disease at 58 years of age compared with those born to mothers who did not experience famine during gestation (39). It remains unclear how renal efferent arteriosclerosis is ameliorated by barley intake. A placebo-controlled randomized trial called Study TO Prevent Non-Insulin-Dependent Diabetes Mellitus (STOP-NIDDM) reported that treatment with acarbose, an α-glucosidase inhibitor, in mildly impaired glucose tolerance reduced not only the risk of T2DM progression (36%) (40) but also a develop risk of hypertension (34%) and cardiovascular disease (49%) (41). In addition, treatment with the α-glucosidase inhibitor miglitol (42) and barley (23) lowered the expression of inflammatory cytokines, such as interleukin 1 beta and tumor necrosis factor alpha, and integrins, such as CD11s in peripheral leukocytes of rodents with diabetes. Further investigation is needed to confirm the association between renal arteriolosclerosis and hypertension by blood pressure measurement in MEM mice.

In this study, we found that the number of insulin-positive β cells was lower and the number of fibrotic-areas was higher in the pancreas of MEM mice fed a rice-based diet than in KSOM control mice. Further, the reduction in the number of insulin-positive β cells and expansion of fibrotic areas in the pancreas of MEM mice was ameliorated by barley intake for 10 weeks in the adult stage. Therefore, pancreatic exhaustion in MEM mice was suppressed by barley administration for 10 weeks. A previous study on a T2DM animal model–the Goto-Kakizaki (GK) rat–

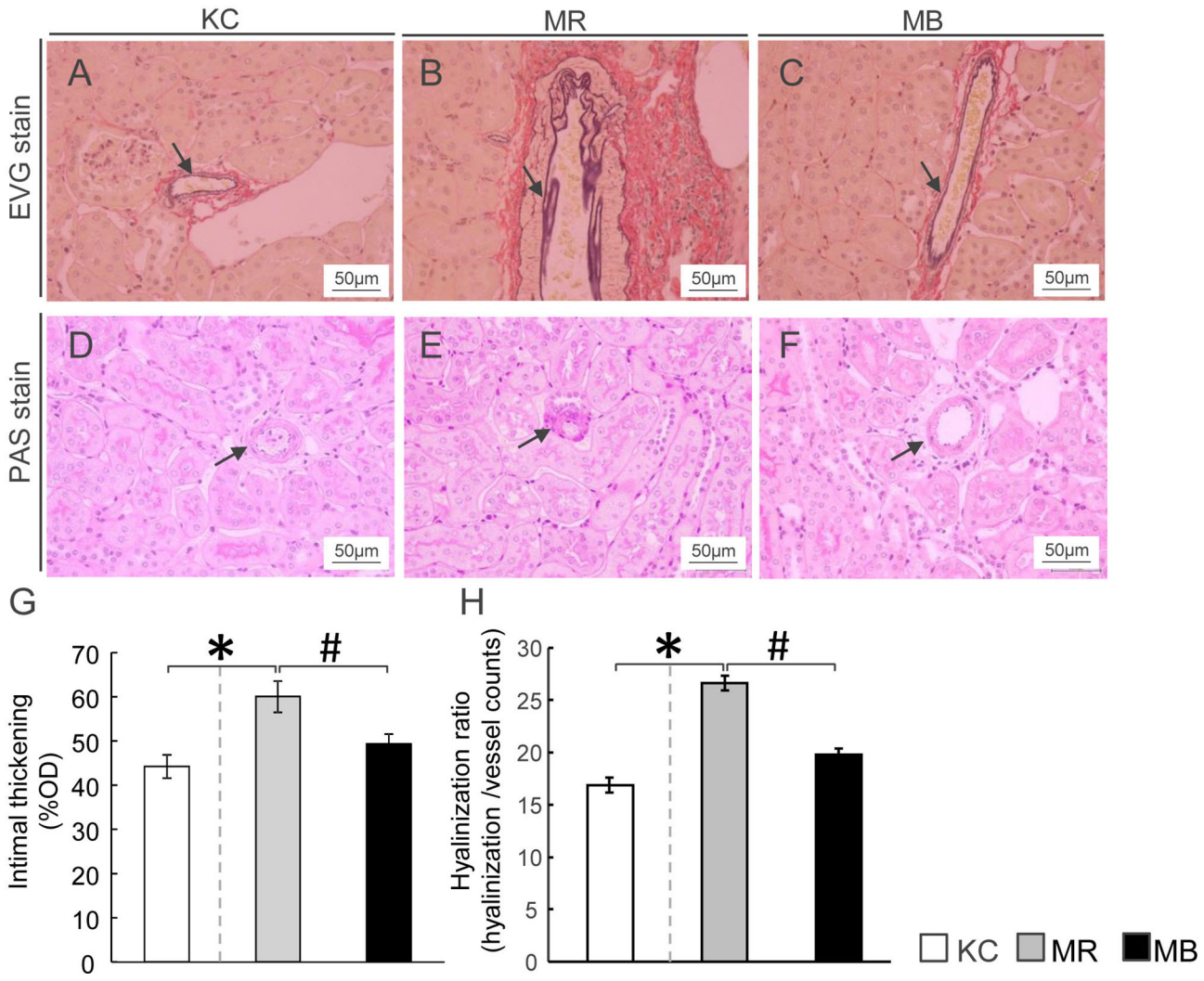

FIGURE 3 | Histopathology showing renal arteriolar intimal thickening and hyalinosis in the kidneys of mice after 10 weeks of experimental diet intake. **(A–C)** Glomerular fibrosis observed using Elastica van Gieson staining (arrow) (scale bar, 50 μm) in mice from the three groups. **(D–F)** Renal arteriolar hyalinosis observed using Periodic acid–Schiff staining (arrow) (scale bar, 50 μm) in mice from the three groups. **(G, H)** Quantification of arteriosclerosis ratio (%OD) by fibro-intimal thickening/vascular media **(G)** and hyalinization of the intrarenal vasculature **(H)**. OD, outer diameter; MB, minimum essential medium (MEM) mice on a barley diet; MR, MEM mice on a rice diet; KC, potassium simplex optimized medium control mice on a rice diet. Data are expressed as the mean ± SEM for 8–12 animals. Data were analyzed using Student's *t*-test. $^{*}P < 0.05$ compared with the KC group; $^{\#}P < 0.05$ compared with the MR group.

demonstrated that 8-week treatment with miglitol, which is an α-glucosidase inhibitor, suppressed postprandial hyperglycemia, in contrast to that in non-treated GK control rats, but it did not improve the insulin secretion capacity and pancreatic exhaustion (43). Another study reported that the miglitol treatment of OLETF rats improved pancreatic exhaustion, but improvement was observed only after treatment for more than 1 year (65 weeks) (44). Additionally, dietary supplementation with acarbose, an α-glucosidase inhibitor, in *db/db* mice for 4 weeks moderately improved the insulin secretion capacity compared with that in *db/db* mice that did not receive the supplement. However, considerably high doses of acarbose (such as 9 g/kg/day) were needed, whereas patients with T2DM are administered doses of 150–300 mg/day (45). Therefore, the MEM mouse is an effective T2DM model that can be used to assess dietary factors and/or drugs to improve T2DM and DKD. However, it should be confirmed whether the T2DM and DKD pathologies in MEM mice are in fact improved by other dietary factors and drugs. Of note, the body weight did not differ significantly between MEM mice fed a rice-based diet and KSOM control mice, whereas food intake was greater in MEM mice fed a rice-based diet than in KSOM control mice. MEM mice show characteristic hyperglycemia with a slightly higher weight and reduced capacity of insulin secretion from the pancreas in spite of overeating, similar to lean Asian patients with T2DM, as shown in a previous study (20). In future studies, it should be

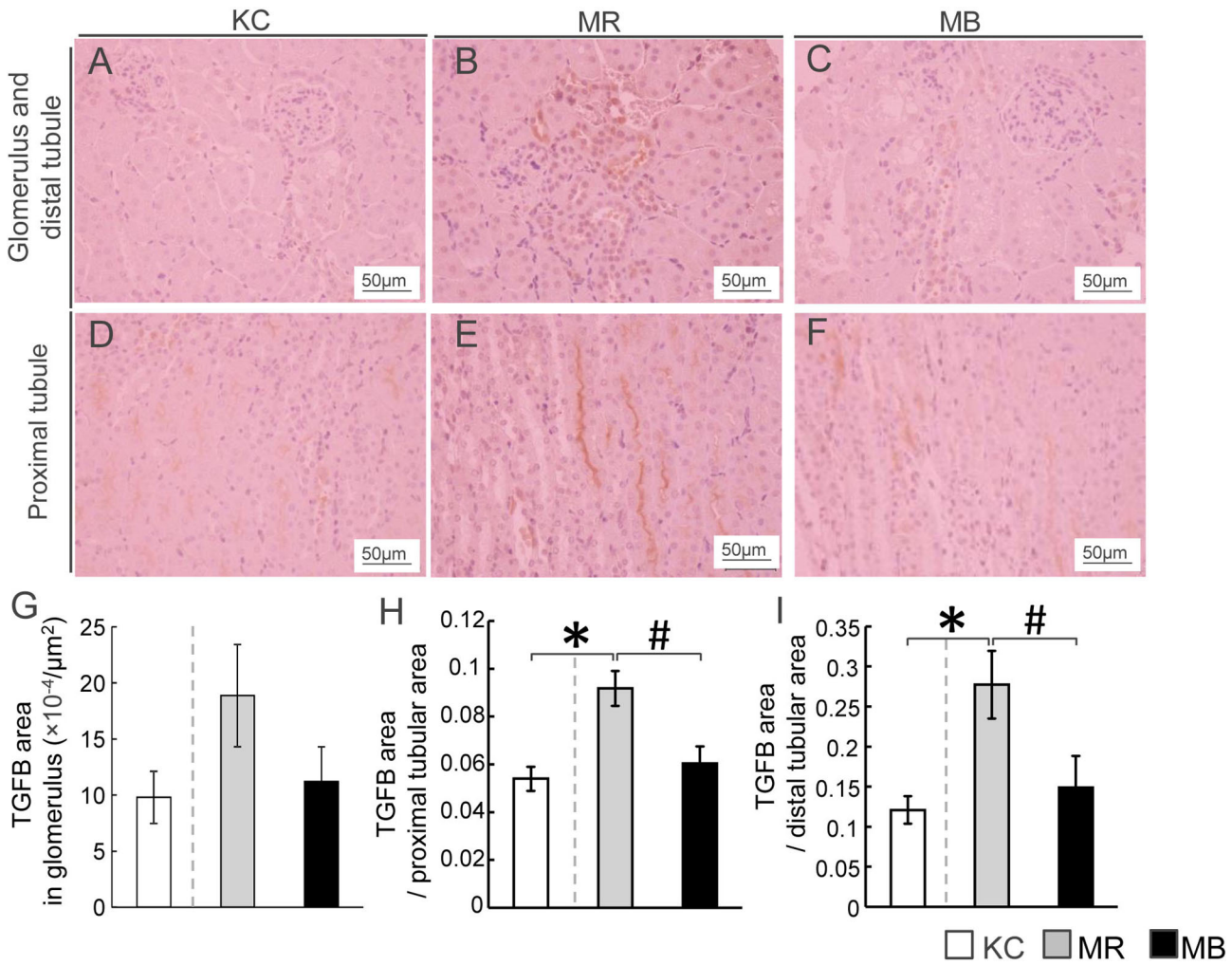

FIGURE 4 | Histopathological evaluation by immunostaining for transforming growth factor beta (TGFB) and quantification of TGFB in the mice kidney tissues after 10 weeks of experimental diet intake. **(A–F)** Representative histological TGFB staining of sections of the glomerulus, distal tubule **(A–C)**, and proximal tubule **(D–F)** in mice from each of the three experimental groups (TGFB-positive areas are stained orange; scale bar, 50 μm). Quantification of the TGFB-positive area in the glomerulus **(G)**, proximal renal tubules **(H)**, and distal renal tubules **(I)**. MB, minimum essential medium (MEM) mice on a barley diet; MR, MEM mice on a rice diet; KC, potassium simplex optimized medium control mice on a rice diet. Data are expressed as the mean ± SEM for 8–12 animals. Data were analyzed using Student's *t*-test. $^{*}P < 0.05$ compared with the KC group; $^{\#}P < 0.05$ compared with the MR group.

investigated whether the capacity of insulin secretion is lower from a prior to development of T2DM/DKD in MEM mice. In addition, it should be examined whether MEM mice can develop T2DM/DKD even when pair-feeding is performed for equal consumption between MEM and KSOM mice.

In the present study, we demonstrated that barley intake improved DKD pathologies, including tuberous sclerosis and renal arteriolar changes, in MEM mice. It was previously reported that barley intake decreased the blood glucose levels 30 min after the meal in healthy participants, suggesting that barley intake can decrease the postprandial blood glucose concentration (46). We previously performed OGTT to assess the glucose tolerance of MEM mice, but the assay could not assess the postprandial blood glucose levels after barley intake in diurnal variation (23). Therefore, the improvement in DKD pathology in MEM mice after barley intake could be attributed to the reduction of postprandial hyperglycemia by barley. Another potential contributor is the prebiotic effect of β-glucan, which is an abundant soluble dietary fiber present in barley. Indeed, it was reported that the daily oral administration of β-glucan (80% purity) at 1 g/kg body weight/day in specific pathogen-free mice fed a 12-week high-fat (60% kcal) diet altered the intestinal bacterial flora in present in feces, although the particular role of the bacterial flora is not fully understood (47). Barley intake for 8 weeks increased the proliferation of probiotic *Lactobacillus* strains, such as *Prevotella*, *Lactobacillus*, and the fiber-degrader S24-7 (*Candidatus Homeothermaceae*) in obese *db/db* mice compared to that in lean *db/m* control or obese *db/db*

mice fed a control diet (48). Further studies are needed to examine whether the intestinal bacterial flora altered by barley intake can improve DKD in MEM mice.

The components of the αMEM responsible for the development of T2DM/DKD pathologies in MEM mice remain unknown, even though the components, such as non-essential amino acids and vitamins, differ between KSOM and αMEM (**Supplementary Table S1**). In human clinical practice, αMEM is not used in the *in vitro* culture of embryos in *in vitro* fertilization (IVF), and media with relatively simple ingredients, similar to KSOM, are used. A study demonstrated that in spite of the same body-mass index, at puberty, children born *via* IVF had higher fasting blood glucose levels, systolic and diastolic blood pressure (49), and peripheral fat mass (50) than children born by spontaneous delivery. In addition, it was reported that children born *via* IVF have a higher risk of low birth weight (<2,500 g) and cardiovascular hospitalization incidence until 18 years compared with children born *via* spontaneous delivery (51) This shows that *in vitro* embryo culture in the early embryo stage may affect health risks, such as that for T2DM/DKD, after birth, and the optimal medium for IVF is still under investigation in human clinical practice. Further studies are needed to identify the components of αMEM that influence the T2DM/DKD pathology in MEM mice to optimize the culture media for assisted reproductive technology (ART) with a low health hazard risk and to determine the mechanism underlying αMEM exposure-induced DKD pathogenesis at the two-cell embryo stage. In addition, the IVF medium used in human clinical practice should be optimized by evaluating T2DM and DKD development in mice that have developed from embryos subjected to *in vitro* culture in the medium. However, the conditions in the mice models are different from those in human disease; therefore, further studies are needed to examine whether the different methods used in ART induce metabolic disorders in mice and humans.

Of note, the glomerular distribution of TGFB protein, a strong risk factor for the development of glomerulosclerosis by mesangial matrix expansion (52), did not differ between MEM mice fed a rice-based diet and KSOM control mice. It has also been reported that *db/db* mice, which exhibit severe non-fasting hyperglycemia (34.8 ± 6.3 mM (mean ± SEM) at 25 weeks of age) (53), expressed TGFB and showed mesangial matrix expansion in the glomerulus. Therefore, MEM mice developed early-stage and non-fulminant DKD. Interestingly, we found that TGFB distribution in the proximal/distal renal tubules was higher in MEM mice fed a rice-based diet than in KSOM control mice. In addition, after MEM mice reached an adult stage, barley intake suppressed TGFB expression in the renal tubules. Kidney sections have been studied to show that TGFB expression is relatively higher in the renal tubules than in the glomerulus in patients with T2DM (54). The kidney contains diverse cell types (including the cells in the glomerulus and proximal/distal tubules) with varied functions. TGFB is reportedly expressed in renal tubules as well as in the glomerulus during the development of nephropathy (55); however, the roles of TGFB in renal tubular dysfunction remain unclear. The results of the present study suggest that a higher TGFB expression in the renal tubules of MEM mice may indicate renal tubular dysfunction. Further studies are required to identify the stage of DKD in MEM mice, to measure TGFB expression in the tubules or glomeruli of MEM mice and patients with DKD, and to determine the roles of TGFB in renal tubular dysfunction. In addition, with the progression of DKD in T2DM, MEM mice from the pre-DKD stage to late-DKD stage should be assessed to confirm whether MEM mice models show pathologies similar to those observed in human T2DM/DKD.

In conclusion, T2DM MEM mice formed from two-cell stage embryos cultured *in vitro* in α-MEM developed DKD, and barley intake after birth ameliorated the DKD pathology in these mice.

DATA AVAILABILITY STATEMENT

The datasets presented in this study can be found in online repositories. The names of the repository/repositories and accession number(s) can be found in the article/**Supplementary Material**.

ETHICS STATEMENT

The animal study was reviewed and approved by the Ethics Committee of the University of Yamanashi (approval number A30-24). Written informed consent was obtained from the owners for the participation of their animals in this study.

AUTHOR CONTRIBUTIONS

SK and KM conceptualized and developed the MEM mice, experiments, and analytical approaches. SI, MK, and TN conducted the experiments. MK and TN contributed to MEM mice development and sample preparation. SI performed histological analyses, biochemical determination, mRNA analysis, western blotting, and statistical analyses. KU contributed assessment of kidney histological analyses and the discussion. SI and KM wrote the paper with contributions from all authors. YF, KU, SK, and KM performed the critical review of the manuscript.

FUNDING

This work was supported by the Mishima Kaiun Memorial Foundation, a Grant-in-Aid for Scientific Research from the Ministry of Education, Culture, Sports, Science, and Technology of Japan [20H04103], the Adaptable and Seamless Technology Transfer Program through target-driven R&D (A-STEP) of the Japan Science and Technology Agency (JST), and the Council of Japan Barley Foods Promotion.

ACKNOWLEDGMENTS

We would like to thank Editage (www.editage.com) for English language editing. We also thank Hakubaku Co., Ltd for donating barley powder.

SUPPLEMENTARY MATERIAL

The Supplementary Material for this article can be found online at: https://www.frontiersin.org/articles/10.3389/fendo.2021.746838/full#supplementary-material

REFERENCES

1. Afkarian M, Zelnick LR, Hall YN, Heagerty PJ, Tuttle K, Weiss NS, et al. Clinical Manifestations of Kidney Disease Among US Adults With Diabetes, 1988-2014. *JAMA* (2016) 316:602–10. doi: 10.1001/jama.2016.10924
2. Koye DN, Shaw JE, Reid CM, Atkins RC, Reutens AT, Magliano DJ. Incidence of Chronic Kidney Disease Among People With Diabetes: A Systematic Review of Observational Studies. *Diabetes Med* (2017) 34:887–901. doi: 10.1111/dme.13324
3. Adler AI, Stevens RJ, Manley SE, Bilous RW, Cull CA, Holman RR, et al. Development and Progression of Nephropathy in Type 2 Diabetes: The United Kingdom Prospective Diabetes Study (UKPDS 64). *Kidney Int* (2003) 63:225–32. doi: 10.1046/j.1523-1755.2003.00712.x
4. Kume S, Araki SI, Ugi S, Morino K, Koya D, Nishio Y, et al. Secular Changes in Clinical Manifestations of Kidney Disease Among Japanese Adults With Type 2 Diabetes From 1996 to 2014. *J Diabetes Investig* (2019) 10:1032–40. doi: 10.1111/jdi.12977
5. Kimmelstiel P, Wilson C. Intercapillary Lesions in the Glomeruli of the Kidney. *Am J Pathol* (1936) 12:83–98.87.
6. Yoshida F, Isobe K, Matsuo S. *In Vivo* Effects of Hyperglycemia on the Outcome of Acute Mesangial Injury in Rats. *J Lab Clin Med* (1995) 125:46–55.
7. Humphreys BD. Targeting Pericyte Differentiation as a Strategy to Modulate Kidney Fibrosis in Diabetic Nephropathy. *Semin Nephrol* (2012) 32:463–70. doi: 10.1016/j.semnephrol.2012.07.009
8. Ferland-McCollough D, Slater S, Richard J, Reni C, Mangialardi G. Pericytes, an Overlooked Player in Vascular Pathobiology. *Pharmacol Ther* (2017) 171:30–42. doi: 10.1016/j.pharmthera.2016.11.008
9. Sharma K, McCue P, Dunn SR. Diabetic Kidney Disease in the Db/Db Mouse. *Am J Physiol Renal Physiol* (2003) 284:F1138–1144. doi: 10.1152/ajprenal.00315.2002
10. Lee SM, Graham A. Early Immunopathologic Events in Experimental Diabetic Nephropathy: A Study in Db/Db Mice. *Exp Mol Pathol* (1980) 33:323–32. doi: 10.1016/0014-4800(80)90030-1
11. Bivona BJ, Park S, Harrison-Bernard LM. Glomerular Filtration Rate Determinations in Conscious Type II Diabetic Mice. *Am J Physiol Renal Physiol* (2011) 300:F618–625. doi: 10.1152/ajprenal.00421.2010
12. Hartono SP, Knudsen BE, Lerman LO, Textor SC, Grande JP. Combined Effect of Hyperfiltration and Renin Angiotensin System Activation on Development of Chronic Kidney Disease in Diabetic Db/Db Mice. *BMC Nephrol* (2014) 15:58. doi: 10.1186/1471-2369-15-58
13. Hempe J, Elvert R, Schmidts HL, Kramer W, Herling AW. Appropriateness of the Zucker Diabetic Fatty Rat as a Model for Diabetic Microvascular Late Complications. *Lab Anim* (2012) 46:32–9. doi: 10.1258/la.2011.010165
14. Kawano K, Hirashima T, Mori S, Natori T. OLETF (Otsuka Long-Evans Tokushima Fatty) Rat: A New NIDDM Rat Strain. *Diabetes Res Clin Pract* (1994) 24(Suppl):S317–320. doi: 10.1016/0168-8227(94)90269-0
15. Kawano K, Mori S, Hirashima T, Man ZW, Natori T. Examination of the Pathogenesis of Diabetic Nephropathy in OLETF Rats. *J Vet Med Sci* (1999) 61:1219–28. doi: 10.1292/jvms.61.1219
16. Soler MJ, Riera M, Batlle D. New Experimental Models of Diabetic Nephropathy in Mice Models of Type 2 Diabetes: Efforts to Replicate Human Nephropathy. *Exp Diabetes Res* (2012) 2012:616313. doi: 10.1155/2012/616313
17. Lumey LH, Khalangot MD, Vaiserman AM. Association Between Type 2 Diabetes and Prenatal Exposure to the Ukraine Famine of 1932-33: A Retrospective Cohort Study. *Lancet Diabetes Endocrinol* (2015) 3:787–94. doi: 10.1016/S2213-8587(15)00279-X
18. Schmidt IM, Chellakooty M, Boisen KA, Damgaard IN, Mau Kai C, Olgaard K, et al. Impaired Kidney Growth in Low-Birth-Weight Children: Distinct Effects of Maturity and Weight for Gestational Age. *Kidney Int* (2005) 68:731–40. doi: 10.1111/j.1523-1755.2005.00451.x
19. Aly H, Davies J, El-Dib M, Massaro A. Renal Function Is Impaired in Small for Gestational Age Premature Infants. *J Matern Fetal Neonatal Med* (2013) 26:388–91. doi: 10.3109/14767058.2012.733767
20. University of Yamanashi, Kishigami S, Mochizuki K, Wakayama T. The Method for Producing Diabetic Animal Model and the Diabetic Animal Model., P2020–31551A. 2020-03-05. (Japanese).
21. Ishiyama S, Kimura M, Umihira N, Matsumoto S, Takahashi A, Nakagawa T, et al. Consumption of Barley Ameliorates the Diabetic Steatohepatitis and Reduces the High Transforming Growth Factor Beta Expression in Mice Grown in Alpha-Minimum Essential Medium *In Vitro* as Embryos. *Biochem Biophys Rep* (2021) 27:101029. doi: 10.1016/j.bbrep.2021.101029
22. Chillo S, Ranawana DV, Pratt M, Henry CJ. Glycemic Response and Glycemic Index of Semolina Spaghetti Enriched With Barley Beta-Glucan. *Nutrition* (2011) 27:653–8. doi: 10.1016/j.nut.2010.07.003
23. Ishiyama S, Kimura M, Umihira N, Matsumoto S, Takahashi A, Nakagawa T, et al. Mice Derived From *In Vitro* alphaMEM-Cultured Preimplantation Embryos Exhibit Postprandial Hyperglycemia and Higher Inflammatory Gene Expression in Peripheral Leukocytes. *Biosci Biotechnol Biochem* (2021) 85:1215–26. doi: 10.1093/bbb/zbab023
24. Tracy RE, Ishii T. What is 'Nephrosclerosis'? Lessons From the US, Japan, and Mexico. *Nephrol Dial Transplant* (2000) 15:1357–66. doi: 10.1093/ndt/15.9.1357
25. Salvatore SP, Cha EK, Rosoff JS, Seshan SV. Nonneoplastic Renal Cortical Scarring at Tumor Nephrectomy Predicts Decline in Kidney Function. *Arch Pathol Lab Med* (2013) 137:531–40. doi: 10.5858/arpa.2012-0070-OA
26. Hong SW, Isono M, Chen S, Iglesias-De La Cruz MC, Han DC, Ziyadeh FN. Increased Glomerular and Tubular Expression of Transforming Growth Factor-Beta1, Its Type II Receptor, and Activation of the Smad Signaling Pathway in the Db/Db Mouse. *Am J Pathol* (2001) 158:1653–63. doi: 10.1016/S0002-9440(10)64121-1
27. Rangan GK, Tesch GH. Quantification of Renal Pathology by Image Analysis. *Nephrol (Carlton)* (2007) 12:553–8. doi: 10.1111/j.1440-1797.2007.00855.x
28. Chen C, Wang C, Hu C, Han Y, Zhao L, Zhu X, et al. Normoalbuminuric Diabetic Kidney Disease. *Front Med* (2017) 11:310–8. doi: 10.1007/s11684-017-0542-7
29. Tsalamandris C, Allen TJ, Gilbert RE, Sinha A, Panagiotopoulos S, Cooper ME, et al. Progressive Decline in Renal Function in Diabetic Patients With and Without Albuminuria. *Diabetes* (1994) 43:649–55. doi: 10.2337/diab.43.5.649
30. Yang XH, Pan Y, Zhan XL, Zhang BL, Guo LL, Jin HM, et al. Epigallocatechin-3-Gallate Attenuates Renal Damage by Suppressing Oxidative Stress in Diabetic Db/Db Mice. *Oxid Med Cell Longev* (2016) 2016:2968462. doi: 10.1155/2016/2968462
31. Tervaert TW, Mooyaart AL, Amann K, Cohen AH, Cook HT, Drachenberg CB, et al. Pathologic Classification of Diabetic Nephropathy. *J Am Soc Nephrol* (2010) 21:556–63. doi: 10.1681/ASN.2010010010
32. Satirapoj B, Adler SG. Comprehensive Approach to Diabetic Nephropathy. *Kidney Res Clin Pract* (2014) 33:121–31. doi: 10.1016/j.krcp.2014.08.001
33. Shimizu M, Furuichi K, Toyama T, Kitajima S, Hara A, Kitagawa K, et al. Long-Term Outcomes of Japanese Type 2 Diabetic Patients With Biopsy-Proven Diabetic Nephropathy. *Diabetes Care* (2013) 36:3655–62. doi: 10.2337/dc13-0298
34. Zhao HJ, Wang S, Cheng H, Zhang MZ, Takahashi T, Fogo AB, et al. Endothelial Nitric Oxide Synthase Deficiency Produces Accelerated Nephropathy in Diabetic Mice. *J Am Soc Nephrol* (2006) 17:2664–9. doi: 10.1681/ASN.2006070798
35. Hudkins KL, Pichaiwong W, Wietecha T, Kowalewska J, Banas MC, Spencer MW, et al. BTBR Ob/Ob Mutant Mice Model Progressive Diabetic

Nephropathy. *J Am Soc Nephrol* (2010) 21:1533–42. doi: 10.1681/ASN.2009121290
36. Forstermann U, Sessa WC. Nitric Oxide Synthases: Regulation and Function. *Eur Heart J* (2012) 33:829–37, 837a-837d. doi: 10.1093/eurheartj/ehr304
37. Boubred F, Daniel L, Buffat C, Tsimaratos M, Oliver C, Pégorier ML, et al. The Magnitude of Nephron Number Reduction Mediates Intrauterine Growth-Restriction-Induced Long Term Chronic Renal Disease in the Rat. A Comparative Study in Two Experimental Models. *J Transl Med* (2016) 14:331. doi: 10.1186/s12967-016-1086-3
38. Barker DJ, Osmond C. Low Birth Weight and Hypertension. *BMJ* (1988) 297:134–5. doi: 10.1136/bmj.297.6641.134-b
39. Painter RC, de Rooij SR, Bossuyt PM, Phillips DI, Osmond C, Barker DJ, et al. Blood Pressure Response to Psychological Stressors in Adults After Prenatal Exposure to the Dutch Famine. *J Hypertens* (2006) 24:1771–8. doi: 10.1097/01.hjh.0000242401.45591.e7
40. Chiasson JL, Josse RG, Gomis R, Hanefeld M, Karasik A, Laakso M, et al. Acarbose for Prevention of Type 2 Diabetes Mellitus: The STOP-NIDDM Randomised Trial. *Lancet* (2002) 359:2072–7. doi: 10.1016/S0140-6736(02)08905-5
41. Chiasson JL, Josse RG, Gomis R, Hanefeld M, Karasik A, Laakso M, et al. Acarbose Treatment and the Risk of Cardiovascular Disease and Hypertension in Patients With Impaired Glucose Tolerance: The STOP-NIDDM Trial. *JAMA* (2003) 290:486–94. doi: 10.1001/jama.290.4.486
42. Fukaya N, Mochizuki K, Shimada M, Goda T. The Alpha-Glucosidase Inhibitor Miglitol Decreases Glucose Fluctuations and Gene Expression of Inflammatory Cytokines Induced by Hyperglycemia in Peripheral Leukocytes. *Nutrition* (2009) 25:657–67. doi: 10.1016/j.nut.2008.11.015
43. Goda T, Suruga K, Komori A, Kuranuki S, Mochizuki K, Makita Y, et al. Effects of Miglitol, an Alpha-Glucosidase Inhibitor, on Glycaemic Status and Histopathological Changes in Islets in Non-Obese, Non-Insulin-Dependent Diabetic Goto-Kakizaki Rats. *Br J Nutr* (2007) 98:702–10. doi: 10.1017/S0007114507742678
44. Fukaya N, Mochizuki K, Tanaka Y, Kumazawa T, Jiuxin Z, Fuchigami M, et al. The Alpha-Glucosidase Inhibitor Miglitol Delays the Development of Diabetes and Dysfunctional Insulin Secretion in Pancreatic Beta-Cells in OLETF Rats. *Eur J Pharmacol* (2009) 624:51–7. doi: 10.1016/j.ejphar.2009.09.048
45. Zhou D, Chen L, Mou X. Acarbose Ameliorates Spontaneous Type2 Diabetes in Db/Db Mice by Inhibiting PDX1 Methylation. *Mol Med Rep* (2021) 23:72. doi: 10.3892/mmr.2020.11710
46. Matsuoka T, Tsuchida A, Yamaji A, Kurosawa C, Shinohara M, Takayama I, et al. Consumption of a Meal Containing Refined Barley Flour Bread Is Associated With a Lower Postprandial Blood Glucose Concentration After a Second Meal Compared With One Containing Refined Wheat Flour Bread in Healthy Japanese: A Randomized Control Trial. *Nutrition* (2020) 72:110637. doi: 10.1016/j.nut.2019.110637
47. Ke X, Walker A, Haange SB, Lagkouvardos I, Liu Y, Kopplin PS, et al. Synbiotic-Driven Improvement of Metabolic Disturbances is Associated With Changes in the Gut Microbiome in Diet-Induced Obese Mice. *Mol Metab* (2019) 22:96–109. doi: 10.1016/j.molmet.2019.01.012
48. Garcia-Mazcorro JF, Mills DA, Murphy K, Noratto G. Effect of Barley Supplementation on the Fecal Microbiota, Caecal Biochemistry, and Key Biomarkers of Obesity and Inflammation in Obese Db/Db Mice. *Eur J Nutr* (2018) 57:2513–28. doi: 10.1007/s00394-017-1523-y
49. Ceelen M, van Weissenbruch MM, Vermeiden JP, van Leeuwen FE, Delemarre-van de Waal HA. Cardiometabolic Differences in Children Born After *In Vitro* Fertilization: Follow-Up Study. *J Clin Endocrinol Metab* (2008) 93:1682–8. doi: 10.1210/jc.2007-2432
50. Ceelen M, van Weissenbruch MM, Roos JC, Vermeiden JP, van Leeuwen FE, et al. Body Composition in Children and Adolescents Born After *In Vitro* Fertilization or Spontaneous Conception. *J Clin Endocrinol Metab* (2007) 92:3417–23. doi: 10.1210/jc.2006-2896
51. Shiloh SR, Sheiner E, Wainstock T, Walfisch A, Segal I, Landau D, et al. Long-Term Cardiovascular Morbidity in Children Born Following Fertility Treatment. *J Pediatr* (2019) 204:84–88.e82. doi: 10.1016/j.jpeds.2018.08.070
52. Meng XM, Nikolic-Paterson DJ, Lan HY. TGF-Beta: The Master Regulator of Fibrosis. *Nat Rev Nephrol* (2016) 12:325–38. doi: 10.1038/nrneph.2016.48
53. Koya D, Haneda M, Nakagawa H, Isshiki K, Sato H, Maeda S, et al. Amelioration of Accelerated Diabetic Mesangial Expansion by Treatment With a PKC Beta Inhibitor in Diabetic Db/Db Mice, a Rodent Model for Type 2 Diabetes. *FASEB J* (2000) 14:439–47. doi: 10.1096/fasebj.14.3.439
54. Miyata KN, Zhao XP, Chang SY, Liao MC, Lo CS, Chenier I, et al. Increased Urinary Excretion of Hedgehog Interacting Protein (Uhhip) in Early Diabetic Kidney Disease. *Transl Res* (2020) 217:1–10. doi: 10.1016/j.trsl.2019.11.001
55. Sierra-Mondragon E, Molina-Jijon E, Namorado-Tonix C, Rodriguez-Munoz R, Pedraza-Chaverri J, Reyes JL. All-Trans Retinoic Acid Ameliorates Inflammatory Response Mediated by TLR4/NF-kappaB During Initiation of Diabetic Nephropathy. *J Nutr Biochem* (2018) 60:47–60. doi: 10.1016/j.jnutbio.2018.06.002

Conflict of Interest: Author TN was employed by company Kiwa Laboratory Animals Co., Ltd.

The remaining authors declare that the research was conducted in the absence of any commercial or financial relationships that could be construed as a potential conflict of interest.

Publisher's Note: All claims expressed in this article are solely those of the authors and do not necessarily represent those of their affiliated organizations, or those of the publisher, the editors and the reviewers. Any product that may be evaluated in this article, or claim that may be made by its manufacturer, is not guaranteed or endorsed by the publisher.

frontiers in Endocrinology

ORIGINAL RESEARCH
published: 09 December 2021
doi: 10.3389/fendo.2021.771193

Associations of Longitudinal Fetal Growth Patterns With Cardiometabolic Factors at Birth

Jia-Shuan Huang[1,2†], Qiao-Zhu Chen[3†], Si-Yu Zheng[1,2], Rema Ramakrishnan[4], Ji-Yuan Zeng[1,2], Can-Peng Zhuo[1,2], Yu-Mian Lai[3], Ya-Shu Kuang[1], Jin-Hua Lu[1,5], Jian-Rong He[1,5,6] and Xiu Qiu[1,5*]*

[1] Division of Birth Cohort Study, Guangzhou Women and Children's Medical Center, Guangzhou Medical University, Guangzhou, China, [2] Paediatrics School, Guangzhou Medical University, Guangzhou, China, [3] Department of Obstetrics and Gynecology, Guangzhou Women and Children's Medical Center, Guangzhou Medical University, Guangzhou, China, [4] National Perinatal Epidemiology Unit, Nuffield Department of Population Health, University of Oxford, Oxford, United Kingdom, [5] Department of Women and Child Health Care and Provincial Key Clinical Specialty of Woman and Child Health, Guangzhou, China, [6] Nuffield Department of Women's and Reproductive Health, University of Oxford, Oxford, United Kingdom

OPEN ACCESS

Edited by:
Tomoko Aoyama,
University of Auckland, New Zealand

Reviewed by:
Satoru Ikenoue,
Keio University, Japan
Yasuko Fujisawa,
Hamamatsu University School of Medicine, Japan

***Correspondence:**
Xiu Qiu
xiu.qiu@bigcs.org
Jian-Rong He
jianrong.he@bigcs.org

[†]These authors share first authorship

Specialty section:
This article was submitted to Pediatric Endocrinology, a section of the journal Frontiers in Endocrinology

Received: 06 September 2021
Accepted: 16 November 2021
Published: 09 December 2021

Citation:
Huang J-S, Chen Q-Z, Zheng S-Y, Ramakrishnan R, Zeng J-Y, Zhuo C-P, Lai Y-M, Kuang Y-S, Lu J-H, He J-R and Qiu X (2021) Associations of Longitudinal Fetal Growth Patterns With Cardiometabolic Factors at Birth. Front. Endocrinol. 12:771193. doi: 10.3389/fendo.2021.771193

Background: Birth weight is associated with cardiometabolic factors at birth. However, it is unclear when these associations occur in fetal life. We aimed to investigate the associations between fetal growth in different gestational periods and cord blood cardiometabolic factors.

Methods: We included 1,458 newborns from the Born in Guangzhou Cohort Study, China. *Z*-scores of fetal size parameters [weight, abdominal circumference (AC), and femur length (FL)] at 22 weeks and growth at 22–27, 28–36, and ≥37 weeks were calculated from multilevel linear spline models. Multiple linear regression was used to examine the associations between fetal growth variables and *z*-scores of cord blood cardiometabolic factors.

Results: Fetal weight at each period was positively associated with insulin levels, with stronger association at 28–36 weeks (β, 0.31; 95% CI, 0.23 to 0.39) and ≥37 weeks (β, 0.15; 95% CI, 0.10 to 0.20) compared with earlier gestational periods. Fetal weight at 28–36 (β, –0.32; 95% CI, –0.39 to –0.24) and ≥37 weeks (β, –0.26; 95% CI, –0.31 to –0.21) was negatively associated with triglyceride levels, whereas weight at 28–36 weeks was positively associated with HDL levels (β, 0.12; 95% CI, 0.04 to 0.20). Similar results were observed for AC. Fetal FL at 22 and 22–27 weeks was associated with increased levels of insulin, glucose, and HDL.

Conclusions: Fetal growth at different gestational periods was associated with cardiometabolic factors at birth, suggesting that an interplay between fetal growth and cardiometabolic factors might exist early in pregnancy.

Keywords: fetal growth, cord blood, birth cohort, insulin, glucose, lipid

INTRODUCTION

Fetal life is the period that an individual is most susceptible to environmental influences due to high plasticity of cells and organs (1, 2). Disturbed intrauterine development can have long-term health implications. According to the developmental origins of health and disease hypothesis, both fetal undernutrition and overnutrition may cause permanent changes to glucose–insulin and lipid metabolism and lead to cardiometabolic diseases in childhood and adulthood such as obesity, cardiovascular diseases, hyperlipidemia, and type 2 diabetes mellitus (1, 2).

Cardiometabolic markers in cord blood reflect the intrauterine metabolic environment and conditions of the fetus and may be an indicator of long-term changes in metabolic functions after birth. Previous studies (3–5), including ours (6), have shown that birth weight is associated with cardiometabolic markers in cord blood, such as insulin, glucose, and lipids. For example, birth weight *z*-score was positively related to cord blood insulin levels (6). In addition, compared with appropriate-for-gestational-age (AGA) infants, small-for-gestational-age (SGA) infants tend to have higher cord blood triglycerides (TG) and lower insulin, high-density lipoprotein cholesterol (HDL), total cholesterol, and low-density lipoprotein cholesterol (LDL) levels (7, 8). In contrast, large-for-gestational-age (LGA) infants have higher cord blood insulin level (9). All these studies have used birth weight as a proxy of fetal growth. However, birth weight is a summary indicator and does not reflect the longitudinal pattern of fetal growth. It is unclear when the association between fetal growth and cardiometabolic markers appears during prenatal period. Also, different fetal biometric parameters represent different dimensions of fetal growth. For instance, abdominal circumference (AC) is considered an indicator of body fat storage and is most predictive of birth weight, whereas femur length (FL) reflects fetal skeletal growth (10). These measures may have different implications for metabolic changes in the fetus. However, no study has examined the associations of different fetal biometric parameters and cardiometabolic markers in cord blood.

In the present study, we investigated the relationship between fetal growth measures (fetal weight, AC, and FL) at different gestational periods and cord blood cardiometabolic factors. The findings of our study may provide insights into the critical period for fetal programming of cardiometabolic health in childhood and adulthood.

METHODS

Study Population

This study was part of the Born in Guangzhou Cohort Study—BIGCS, a prospective study led by Guangzhou Women and Children's Medical Center (GWCMC) that aimed to investigate the influence of environmental, genetic, and social factors on the health of pregnant women and the next generation. The protocol and cohort profile of BIGCS have been previously published (11). Briefly, BIGCS pregnant women are invited to participate when they undergo the first routine prenatal check-ups at GWCMC if they are less than 20 weeks of gestation, planned to give birth at GWCMC, and intended to stay in Guangzhou for ≥3 years after delivery. These women and their children are followed up at multiple time points to collect epidemiological and clinical information and biospecimens. BIGCS has been approved by the Ethics Committee of GWCMC. Written consent has been obtained from all participants.

The eligibility criteria for the current analysis include 1) availability of cord blood samples, 2) availability of maternal fasting blood samples at 14–27 weeks of gestation and data on 2-h 75-g oral glucose tolerance test (OGTT) of the mother, 3) no severe disease before pregnancy (e.g., type 1 or type 2 diabetes, hypertension, kidney diseases), and (4) availability of data on maternal demographic characteristics. This analysis included 1,744 mother–child pairs who were randomly selected from those eligible. Mother–child pairs with no fetal ultrasound growth data (n = 212) or covariates (n = 74) were excluded. This study finally included 1,458 pairs of mothers and children.

Fetal Growth Assessment

Data on fetal biometric measures, including biparietal diameter, head circumference, AC, and FL, were obtained through ultrasound scanning and extracted from the hospital electronic system. Fetal weight was estimated (EFW) using the INTERGROWTH-21st formula based on AC and FL (12). On average, each pregnant woman had three (range, 1–7) ultrasound examinations for fetal growth. An ultrasound examination is routinely performed in the first trimester to confirm gestational age based on crown–rump length. For pregnant women who do not attend antenatal care in the first trimester, gestational age is assessed in early second trimester based on fetal biometrics, including bilateral parietal diameter, head circumference, AC, FL, or cerebellar diameter (13, 14). Well-trained and licensed ultrasonographers in GWCMC conducted these ultrasound measurements. As our previous study shows (15), the mean error of EFW estimation ([EFW – birth weight]/birth weight × 100%) is low (about 4%), and the correlation between two consecutive measurements of fetal biometric parameters performed within a week was high (r > 0.95). These results indicate good quality of the ultrasound data.

Based on our previous study (15) and other studies (16–18), a multilevel linear spline model was used to evaluate the patterns of fetal growth in different gestational periods. Briefly, a fractional polynomial model was first used to determine the best-fitting curve for fetal size (including EFW and birth weight) by gestational age for the whole sample. Two knots (i.e., 28 and 37 weeks) were then selected to divide the entire gestation period into three intervals: "mid-pregnancy" (22–27 weeks), "early-third trimester" (28–36 weeks), and "late-third trimester" (≥37 weeks). We then fitted multilevel linear spline models to estimate fetal growth during each period. The resulting random effects from the models denote individual deviations from average size in early pregnancy (i.e., 22 weeks) and the average growth velocities in the three gestational intervals, which were

converted into sex-specific *z*-scores before further analyses. More information on the modeling process can be found in our previous report (15). The same modeling approach was applied to generate AC and FL *z*-scores based on ultrasound measurements. Fetuses were also classified into "slow," "normal," and "fast" growth if they had a *z*-score ≤−1.28 (i.e., 10th percentile), −1.28 to 1.28, and >1.28 (i.e., 90th percentile), respectively. These cutoff values are equivalent to those for SGA, AGA, and LGA at birth which are commonly used in clinical practice.

Measurement of Cardiometabolic Markers in Cord Blood

Trained midwives collected venous umbilical cord blood using tubes with EDTA anticoagulants. The blood was centrifuged within 24 h. Plasma samples were obtained and stored at −80°C until analysis. A third-party medical laboratory assessed the levels of cardiometabolic factors in cord blood, including insulin, glucose, total cholesterol, HDL, LDL, and TG. Specifically, insulin levels (μIU/ml) were measured using the Roche Immunology Analyzer (cobas 8000 e602, Roche, Basel, Switzerland), and glucose (mmol/L), total cholesterol (mmol/L), HDL (mmol/L), LDL (mmol/L), and TG (mmol/L) were measured using the Roche Chemistry Analyzer (cobas 8000 c702, Roche, Basel, Switzerland). All tests had low (<2%) intraday and interday coefficients of variation. Glucose levels from 77 samples were below the lower limit (i.e., 0.11 mmol/L) of the linear detection range and were therefore excluded from further analysis.

Covariates

We collected information on maternal age, height, pre-pregnancy weight, parity, education level, monthly income, and active/passive smoking during pregnancy using a self-reported questionnaire at recruitment (around 16 weeks of gestation). Height and pre-pregnancy weight were used to calculate pre-pregnancy body mass index (BMI = weight [kg]/height $[m]^2$), which was then categorized into underweight (BMI < 18.5 kg/m^2), normal weight (BMI 18.5–23.9), and overweight/obesity (BMI ≥ 24) based on the Chinese standard (19). In addition, we obtained information on pregnancy complications [hypertensive disorder in pregnancy and gestational diabetes mellitus (GDM)] from the medical records after delivery. Hypertensive disorder in pregnancy was identified using medical record data based on the International Classification of Diseases, Tenth Revision (ICD-10) (O13–O16). The diagnosis of GDM was made using the International Association of Diabetes and Pregnancy Study Group criteria (20).

Statistical Analysis

The levels of cord blood cardiometabolic factors (insulin, glucose, total cholesterol, triglyceride, HDL, and LDL) were log-transformed to address non-normality of their distributions. Since different units and scales were used for different cardiometabolic factors, we then converted the log-transformed variables to *z*-scores (using internal means and standard deviations) for ease of comparison of results.

We used multiple linear regression model to examine the association between fetal growth variables (*z*-scores and growth categories for weight, AC, and FL) at each period and the levels of each cord blood cardiometabolic factor, and the regression coefficient (β) and 95% CI were calculated. Covariates included in these models were maternal age, education level, monthly income, parity, pre-pregnancy BMI, active/passive smoking during pregnancy, hypertensive disorder in pregnancy, and GDM. In the models for fetal growth velocity in the early-third and late-third trimesters, we further adjusted for growth variables in previous periods. However, fetal size in early pregnancy was not included for adjustment because it was highly correlated to growth velocity in mid-pregnancy. In the models of fetal growth categories, the group of "normal" growth was used as a referent and compared with the groups of "slow" and "fast" growth. We first included fetal weight, AC, and FL separately in the models.

We conducted exploratory stratified analyses to investigate whether the associations between fetal growth *z*-scores and cord blood cardiometabolic factor levels differed by maternal characteristics such as pre-pregnancy BMI (underweight vs. normal weight and overweight/obesity), parity (nulliparous vs. multiparous), and GDM (yes vs. no), which have been shown to affect fetal growth or fetal metabolic status. Multiplicative interaction term was included in the multiple linear regression model to assess whether the interaction between fetal growth *z*-scores and these maternal and neonatal characteristics exists. In addition, we conducted sensitivity analysis for the associations between continuous fetal growth variables and cardiometabolic factors, by excluding preterm infants and women with hypertensive disorder in pregnancy.

All data were analyzed by SPSS 21.0, and the statistical significance was set as a two-tailed P <0.05.

RESULTS

Participant characteristics are presented in **Table 1**. The mean age of the participants was 29.5 years. Most of them (80%) were nulliparous. About one in four were underweight before pregnancy, whereas around one in 10 were overweight or obese. About 12% of these women had GDM, 3% had hypertensive disorders in pregnancy, and 29.3% were exposed to active or passive smoking during pregnancy. The mean birth weight of their infants was 3,203 g.

Fetal Weight Growth and Cord Blood Cardiometabolic Factors

Fetal weight *z*-scores at each gestational period were positively associated with cord blood insulin levels, with stronger associations observed in early- (β, 0.31; 95% CI, 0.23–0.39) and late-third trimesters (β, 0.15; 95% CI, 0.10 to 0.20) (**Figure 1**, upper section). Besides this, fetal weight *z*-scores in early- (β, −0.32; 95% CI, −0.39 to −0.24) and late-third (β, −0.26; 95% CI, −0.31 to −0.21) trimesters, but not early and mid-pregnancy, were negatively associated with cord blood TG levels. Fetal weight *z*-score in

TABLE 1 | Characteristics of the study population.

Variables	All *n* = 1458	Boys *n* = 782	Girls *n* = 676
Maternal characteristics			
Age (years), mean (SD)	29.5 (3.3)	29.5 (3.4)	29.5 (3.2)
Educational level (%)			
Middle school or below	89 (6.1)	44 (5.6)	45 (6.7)
Vocational or technical college	296 (20.3)	164 (21.0)	132 (19.5)
Undergraduate	844 (57.9)	455 (58.2)	389 (57.5)
Postgraduate	229 (15.7)	119 (15.2)	110 (16.3)
Monthly income (Yuan) (%)			
≤1,500	101 (6.9)	56 (7.2)	45 (6.7)
1,501–4,500	333 (22.8)	172 (22.0)	161 (23.8)
4,501–9,000	661 (45.3)	352 (45.0)	309 (45.7)
≥9,001	363 (24.9)	202 (25.8)	161 (23.8)
Pre-pregnancy BMI (kg/m^2), mean (SD)	20.6 (2.7)	20.5 (2.7)	20.6 (2.7)
Underweight (%)	337 (23.1)	182 (23.3)	155 (22.9)
Normal weight (%)	968 (66.4)	519 (66.4)	449 (66.4)
Overweight/obesity (%)	153 (10.5)	81 (10.4)	72 (10.7)
Nulliparous (%)	1,167 (80.0)	625 (79.9)	542 (80.2)
Diabetes during pregnancy (%)	179 (12.3)	93 (11.9)	86 (12.7)
Hypertensive disorder in pregnancy (%)	44 (3.0)	20 (2.6)	24 (3.6)
Active/passive smoking (%)	427 (29.3)	224 (28.6)	203 (30.0)
Child's characteristics			
Gestational age (weeks), median (25th–75th percentile)	39.0 (38.0–40.0)	39.0 (38.0–40.0)	39.0 (38.0–40.0)
Birth weight (grams), mean (SD)	3,203 (403)	3,238 (406)	3,162 (396)
Cord blood metabolic factors levels			
Insulin median (25th–75th), μIU/ml	7.42 (4.35–12.51)	7.00 (4.00–11.72)	8.07 (4.86–13.50)
Glucose median (25th–75th), mmol/L	4.96 (3.47–6.15)	5.10 (3.56–6.21)	4.79 (3.36–6.06)
Cholesterol median (25th–75th), mmol/L	1.68 (1.43–1.68)	1.61 (1.38–1.92)	1.72 (1.50–2.01)
Triglyceride median (25th–75th), mmol/L	0.33 (0.27–0.41)	0.34 (0.27–0.41)	0.33 (0.27–0.41)
LDL median (25th–75th), mmol/L	0.58 (0.44–0.73)	0.56 (0.42–0.71)	0.59 (0.46–0.75)
HDL median (25th–75th), mmol/L	0.87 (0.72–1.05)	0.84 (0.72–1.02)	0.91 (0.75–1.09)

SD, standard deviation.

early-third trimester was also positively associated with HDL levels (β, 0.12; 95% CI, 0.04 to 0.20). No evident association was observed between fetal weight *z*-scores and glucose, total cholesterol, and LDL (**Figure 1**, upper section).

Results for fetal weight categories (slow, normal, or fast) were consistent with overall findings for fetal weight *z*-scores. Compared with normal-growth fetuses, slow-growth fetuses had lower levels of cord blood insulin in early- and late-third trimester, whereas fast-growth fetuses had higher insulin levels in early and late trimesters (**Figure 1**, middle and lower sections). In addition, slow-growth fetuses had higher levels of TG in early- and late-third trimester and lower levels of HDL at birth, whereas fast-growth fetuses had lower levels of TG in each gestational period.

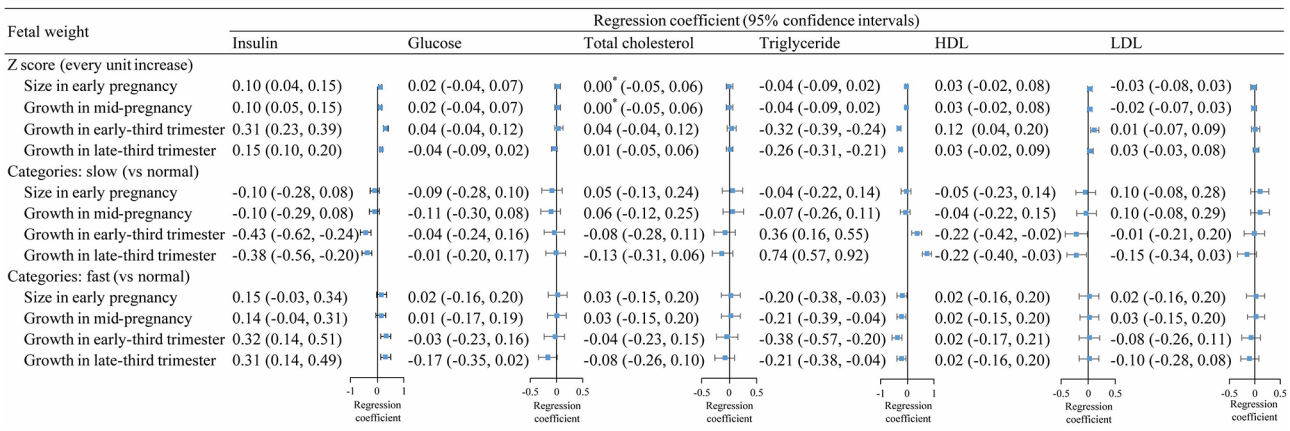

FIGURE 1 | Associations between fetal weight growth in different periods and cord blood metabolic factors. *, >0 and <0.001.

Fetal AC Growth and Cord Blood Cardiometabolic Factors

The patterns of associations between fetal AC *z*-scores and cardiometabolic factors were similar to those for fetal weight growth, although the magnitude of the associations appeared to be smaller (**Figure 2**). The associations for fetal AC categories (slow, normal, or fast) were also similar to the overall results for fetal weight growth. However, the associations between AC categories in late-third trimester and insulin and TG were close to null, whereas the associations for fetal weight categories remained statistically significant.

Fetal FL Growth and Cord Blood Cardiometabolic Factors

Fetal FL *z*-scores in early and mid-pregnancy were associated with increased levels of cord blood insulin, glucose, and HDL (**Figure 3**, upper section). In line with these results, fetuses with slow FL growth in early and mid-pregnancy had lower levels of glucose and HDL at birth, while fetuses with fast FL growth had higher cord blood insulin and HDL levels (**Figure 3**, middle and lower sections). There was insufficient evidence for an association between FL continuous *z*-scores and cord blood TG levels. However, we found that babies with slow FL growth in early- and late-third trimesters had higher TG compared with those with normal FL growth.

Stratified Analysis

Stratified analysis by GDM revealed negative associations of fetal weight and AC *z*-scores before 37 weeks of gestation with cord blood TG being stronger among women without diabetes than those with diabetes ($P_{interaction}$, <0.05) (**Supplementary Tables 1**, **2**). No significant interaction was observed between FL and maternal diabetes status on cardiometabolic factors levels (**Supplementary Table 3**).

There was no evident interaction between fetal growth variables and maternal pre-pregnancy BMI (**Supplementary**

Abdominal circumference	Regression coefficient (95% confidence intervals)					
	Insulin	Glucose	Total cholesterol	Triglyceride	HDL	LDL
Z score (every unit increase)						
Size in early pregnancy	0.10 (0.04, 0.15)	0.02 (-0.03, 0.08)	0.00* (-0.06, 0.05)	-0.04 (-0.09, 0.02)	0.03 (-0.02, 0.08)	-0.04 (-0.09, 0.01)
Growth in mid-pregnancy	0.11 (0.06, 0.16)	0.03 (-0.03, 0.08)	0.00* (-0.05, 0.05)	-0.04 (-0.09, 0.01)	0.03 (-0.02, 0.09)	-0.03 (-0.08, 0.02)
Growth in early-third trimester	0.20 (0.14, 0.25)	0.03 (-0.03, 0.09)	0.04 (-0.02, 0.10)	-0.14 (-0.19, -0.08)	0.08 (0.03, 0.14)	0.02 (-0.04, 0.07)
Growth in late-third trimester	0.06 (0.00, 0.11)	-0.02(-0.07, 0.04)	-0.01 (-0.07, 0.04)	-0.08 (-0.14, -0.03)	0.00* (-0.05, 0.06)	-0.01 (-0.07, 0.04)
Categories: slow (vs normal)						
Size in early pregnancy	-0.12 (-0.29, 0.05)	-0.07 (-0.25, 0.11)	-0.01 (-0.18, 0.16)	-0.02 (-0.19, 0.15)	-0.08 (-0.25, 0.09)	0.07 (-0.10, 0.24)
Growth in mid-pregnancy	-0.13 (-0.30, 0.04)	-0.06 (-0.23, 0.12)	-0.02 (-0.19, 0.15)	0.01 (-0.16, 0.18)	-0.12 (-0.29, 0.05)	0.09 (-0.07, 0.26)
Growth in early-third trimester	-0.46 (-0.64, -0.28)	-0.06 (-0.25, 0.12)	-0.10 (-0.28, 0.08)	0.22 (0.04, 0.39)	-0.16 (-0.34, 0.02)	-0.08 (-0.26, 0.10)
Growth in late-third trimester	-0.18 (-0.37, 0.01)	0.08 (-0.11, 0.28)	-0.16 (-0.35, 0.03)	0.34 (0.15, 0.52)	-0.23 (-0.42, -0.04)	-0.07 (-0.26, 0.12)
Categories: fast (vs normal)						
Size in early pregnancy	0.14 (-0.03, 0.31)	-0.03 (-0.21, 0.15)	-0.13 (-0.30, 0.04)	-0.31 (-0.49, -0.14)	-0.06 (-0.23, 0.12)	-0.13 (-0.30, 0.05)
Growth in mid-pregnancy	0.19 (0.01, 0.37)	0.02 (-0.16, 0.21)	-0.07 (-0.25, 0.11)	-0.26 (-0.44, -0.08)	-0.04 (-0.22, 0.14)	-0.06 (-0.24, 0.12)
Growth in early-third trimester	0.26 (0.07, 0.44)	-0.02 (-0.21, 0.17)	-0.01 (-0.19, 0.18)	-0.25 (-0.44, -0.07)	0.02 (-0.16, 0.21)	-0.04 (-0.22, 0.15)
Growth in late-third trimester	0.06 (-0.12, 0.25)	-0.10 (-0.29, 0.10)	-0.14 (-0.33, 0.04)	0.02 (-0.16, 0.20)	-0.03 (-0.22, 0.15)	-0.22 (-0.41, -0.04)

FIGURE 2 | Association between fetal abdominal circumference growth in different periods and cord blood metabolic factors. *, >0 and <0.001.

Femur length	Regression coefficient (95% confidence intervals)					
	Insulin	Glucose	Total cholesterol	Triglyceride	HDL	LDL
Z score (every unit increase)						
Size in early pregnancy	0.06 (0.01, 0.11)	0.09 (0.04, 0.14)	0.03 (-0.02, 0.08)	-0.02 (-0.07, 0.03)	0.09 (0.04, 0.14)	-0.03 (-0.08, 0.02)
Growth in mid-pregnancy	0.06 (0.01, 0.11)	0.09 (0.03, 0.14)	0.03 (-0.02, 0.09)	-0.02 (-0.07, 0.03)	0.09 (0.04, 0.14)	-0.03 (-0.08, 0.02)
Growth in early-third trimester	0.05 (-0.01, 0.10)	-0.01 (-0.07, 0.05)	0.05 (-0.01, 0.11)	-0.05 (-0.11, 0.01)	0.06 (0.00, 0.11)	0.04 (-0.02, 0.10)
Growth in late-third trimester	0.02 (-0.04, 0.08)	-0.01 (-0.07, 0.05)	-0.02 (-0.08, 0.04)	-0.01 (-0.07, 0.05)	-0.03 (-0.09, 0.03)	0.01 (-0.05, 0.07)
Categories: slow (vs normal)						
Size in early pregnancy	-0.07 (-0.25, 0.11)	-0.25 (-0.43, -0.07)	-0.13 (-0.30, 0.05)	0.02 (-0.15, 0.20)	-0.32 (-0.50, -0.15)	0.08 (-0.10, 0.26)
Growth in mid-pregnancy	-0.12 (-0.29, 0.06)	-0.28 (-0.47, -0.10)	-0.03 (-0.21, 0.15)	0.00* (-0.18, 0.18)	-0.24 (-0.42, -0.06)	0.17 (-0.01, 0.35)
Growth in early-third trimester	-0.02 (-0.20, 0.16)	-0.14 (-0.32, 0.05)	0.04 (-0.15, 0.22)	0.21 (0.03, 0.40)	-0.09 (-0.27, 0.10)	0.07 (-0.11, 0.26)
Growth in late-third trimester	-0.13 (-0.33, 0.06)	0.22 (0.02, 0.42)	-0.04 (-0.23, 0.16)	0.30 (0.10, 0.49)	-0.02 (-0.21, 0.18)	-0.13 (-0.33, 0.06)
Categories: fast (vs normal)						
Size in early pregnancy	0.15 (-0.03, 0.32)	0.10 (-0.08, 0.28)	0.11 (-0.06, 0.29)	0.03 (-0.14, 0.21)	0.17 (0.00, 0.35)	0.01 (-0.17, 0.18)
Growth in mid-pregnancy	0.15 (-0.03, 0.33)	0.12 (-0.06, 0.30)	0.14 (-0.04, 0.32)	-0.01 (-0.18, 0.17)	0.18 (0.01, 0.36)	0.03 (-0.15, 0.21)
Growth in early-third trimester	0.03 (-0.15, 0.21)	-0.02 (-0.21, 0.16)	0.10 (-0.08, 0.28)	-0.01 (-0.19, 0.17)	0.06 (-0.12, 0.24)	0.13 (-0.05, 0.32)
Growth in late-third trimester	0.02 (-0.19, 0.22)	0.10 (-0.11, 0.31)	-0.13 (-0.33, 0.08)	0.16 (-0.04, 0.36)	-0.12 (-0.33, 0.08)	-0.12 (-0.33, 0.08)

FIGURE 3 | Association between fetal femur length growth in different periods and cord blood metabolic factors. *, >0 and <0.001.

Tables 4–6) and parity (**Supplementary Tables 7–9**) for any of the cardiometabolic factors.

Sensitivity Analyses

In sensitivity analyses, the results were similar to the overall analysis when we excluded women with hypertensive disorder in pregnancy (n = 44) (**Supplementary Table 10**) or when we excluded preterm infants (n = 61) (**Supplementary Table 11**).

DISCUSSION

Main Findings

We found that fetal weight at each period was positively associated with cord blood insulin, with stronger associations observed in early- and late-third trimesters than early and mid-pregnancy. Fetal weight in early- and late-third trimesters was also negatively associated with TG and positively associated with HDL. Associations for fetal AC were similar to those for fetal weight. These results suggest that the third trimester could be the important period for fetal insulin and lipid metabolism. On the other hand, fetal FL in the early and mid-pregnancy was positively associated with cord blood insulin, glucose, and HDL, indicating that the first half of pregnancy might be a crucial stage for the interplay between fetal skeletal growth and these metabolic factors. To our knowledge, this is the first study to investigate the associations between fetal growth in different gestational periods and cord blood cardiometabolic factors.

Interpretation of the Results

Our observation that fetal weight and AC were positively associated with cord blood insulin is consistent with previous studies. Ong et al. found that cord blood insulin was positively associated with neonatal birth weight (21). Similarly, SGA neonates had hypoinsulinemia in cord blood at birth compared with AGA neonates (22), whereas insulin levels in LGA infants were significantly higher (21, 23). In addition, a previous study found gestational weight gain rates during the first and second trimesters, but not the third trimester, to be positively associated with cord blood insulin levels (24). In line with this study, we observed that fetal weight at early and mid-pregnancy was associated with insulin levels at birth; however, in contrast to this previous study (24), we found that fetal weight in the third trimester was also associated with cord blood insulin. Discrepancies in the results between the two studies might be related to the difference in exposure definition (e.g., self-reported gestational weight gain vs. ultrasound-based fetal growth), and thus, the results might be not directly comparable.

Our study revealed the association of fetal weight and AC with cord blood insulin to be stronger in late pregnancy than in early pregnancy. Insulin is an important hormone to promote fetal growth. It can not only stimulate fetal insulin sensitive cells to promote tissue utilization of glucose but also promote the storage of glycogen and fat, thereby promoting the growth of the fetus (25). Since fetal growth is fastest in late pregnancy (26), we speculate that fetuses in late pregnancy might be more sensitive to the growth-promoting effect of insulin than fetuses in early pregnancy. On the other hand, fetal growth may affect the levels of circulating insulin. It has been shown that fetal growth restriction can affect the maturation of fetal islet β cells, lead to the inhibition of fetal islet β-cell proliferation, reduce insulin secretion, hinder the activation of amino acid transport system, inhibit protein and fat synthesis, promote lipolysis, and inhibit fetal growth and development (27). These responses enable the fetus to adapt to the adverse intrauterine environment and redistribute nutrients, which ensures the growth and development of the main organs (e.g., brain) of the fetus but results in decreased fetal growth rate (28).

In addition, we found that in the second and third trimesters of pregnancy, fetal weight and AC were negatively associated with cord blood TG. This finding is consistent with previous studies which found that fetuses with intrauterine growth restriction had higher cord blood TG compared with normal-growth fetus (29, 30). Another study showed that AC was negatively associated with cord blood TG levels among growth-restricted fetuses (31). We also found that fetal weight and AC in late pregnancy were positively correlated with cord blood HDL. Interestingly, it has been shown that AC at birth was negatively associated with blood lipid levels in adulthood (32). Taken together, these findings suggest that abnormal fetal growth in late pregnancy might be critical for long-term lipid profile. A possible explanation for these findings is that decelerated fetal growth (especially for AC) may represent insufficient growth of the liver, which could result in dysregulation of lipid metabolism (32). However, the mechanisms for this association need to be studied in future studies.

The relationships between fetal FL or birth length and cord blood cardiometabolic factors have been rarely investigated previously. In the present study, we observed that femur growth in early and mid-pregnancy was positively associated with cord blood insulin and glucose. Fetal insulin, in addition to being a growth hormone, is also an osteogenic hormone, which can stimulate fetal bone mineralization and cartilage synthesis (33) and regulate fetal bone growth (34). Similarly, glucose is essential for fetal osteogenesis and cartilage formation. In the skeletal system, glucose is an important energy source for the development, growth, and maintenance of bone and articular cartilage (35). Therefore, insulin and glucose are two important nutrients for fetal FL growth in the early stage of pregnancy. We also found fetal FL in early and mid-pregnancy to be positively associated with cord blood HDL. The biological explanation for this association warrants further investigation.

In stratified analysis, we found that GDM modified the associations between fetal growth (weight and AC) and cord blood TG. For example, for pregnant women with diabetes, fetal weight growth before 28 weeks of gestation was positively associated with cord blood TG. By contrast, among women

without diabetes, fetal weight growth in the same period was negatively associated with TG. This divergence of association was less pronounced after 28 weeks of gestation. We speculate that it could be related to the metabolic dysfunction induced by GDM. Fetal hyperinsulinemia, resulting from maternal GDM, can promote the synthesis of fat and leads to fetal overgrowth. This effect might be attenuated after 28 weeks when the dietary interventions are usually given to GDM patients for optimal glycemic control to improve pregnancy outcomes (36).

Implications

In this study, we found a positive association between fetal weight and the levels of insulin and high-density lipoprotein in cord blood metabolic factors in all gestational periods, especially during the third trimester. Specifically, slow-growth fetuses in the third trimester had an adverse lipid profile (i.e., high TG and low HDL) at birth, whereas fast-growth fetuses in the third trimester had higher insulin insensitivity (reflected by higher cord blood insulin level). Since adverse cardiometabolic profile at birth may be related to long-term cardiometabolic diseases, efforts should be made to ensure an optimal fetal growth during late pregnancy to improve the short- and long-term cardiometabolic health. However, future studies are still needed to validate our findings.

Strengths and Limitations

Based on a series of ultrasound measurements, we were able to assess longitudinal fetal growth patterns and their associations with cord blood cardiometabolic factors, which have not been reported previously. The prospective cohort design of the current study could reduce the recall bias for data collection. Compared with previous studies on birth weight and cord blood cardiometabolic factors (4, 9, 37), our study had relatively larger sample size and thus increased statistical power. A limitation of our study was that we could only measure metabolic factors in umbilical cord blood at birth. Information about the fetal metabolic status before birth would be useful, which allows the assessment for the dynamic changes of fetal metabolic status. However, it is impractical to collect cord blood samples before birth for normal pregnancies. Another limitation is that only a limited number of cardiometabolic factors were measured and data on adipokines (e.g., leptin and adiponectin), which may also play a role in fetal growth, were unavailable.

CONCLUSIONS

This study shows that fetal growth in different gestational periods was associated with cord blood cardiometabolic factors. These associations were more pronounced for fetal weight and AC growth after 28 weeks than those before 28 weeks, whereas associations for FL growth appeared to stronger before 28 weeks. Our findings suggest that fetal growth and cardiometabolic factors might interplay since early pregnancy. Further studies are needed to elucidate the mechanisms underlying these associations.

DATA AVAILABILITY STATEMENT

The original contributions presented in the study are included in the article/**Supplementary Material**. Further inquiries can be directed to the corresponding authors.

ETHICS STATEMENT

The studies involving human participants were reviewed and approved by the Ethics Committee of Guangzhou Women and Children's Medical Center. The patients/participants provided their written informed consent to participate in this study.

AUTHOR CONTRIBUTIONS

J-RH and XQ conceptualized and designed the study, contributed to the data analysis, interpreted the data, and reviewed and revised the manuscript. J-SH, Q-ZC, S-YZ, J-YZ, and C-PZ analyzed and interpreted the data and draft and revised the manuscript. RR contributed to the data analysis and reviewed and revised the manuscript. Y-ML, Y-SK, and J-HL contributed to the data collection and reviewed and revised the manuscript. All authors approved the final manuscript as submitted and agree to be accountable for all aspects of the work.

FUNDING

The present study was supported by the grants from Ministry of Science and Technology of People's Republic of China (2019YFC0121905) and National Natural Science Foundation of China (grant number, 81703244 and 81673181).

ACKNOWLEDGMENTS

The authors are grateful to the pregnant women who participated in the BIGCS, to the management team, all obstetric care providers who assisted in the implementation of the study, and to all members of the BIGCS Study Group. We thank Ms. Yuting Yang for helping us with the English language editing on the first draft of the manuscript.

SUPPLEMENTARY MATERIAL

The Supplementary Material for this article can be found online at: https://www.frontiersin.org/articles/10.3389/fendo.2021.771193/full#supplementary-material

REFERENCES

1. Perng W, Oken E, Dabelea D. Developmental Overnutrition and Obesity and Type 2 Diabetes in Offspring. *Diabetologia* (2019) 62:1779–88. doi: 10.1007/s00125-019-4914-1
2. Hoffman DJ, Reynolds RM, Hardy DB. Developmental Origins of Health and Disease: Current Knowledge and Potential Mechanisms. *Nutr Rev* (2017) 75:951–70. doi: 10.1093/nutrit/nux053
3. Xu M, Liu B, Wu MF, Chen HT, Cianflone K, Wang ZL. Relationships Among Acylation-Stimulating Protein, Insulin Resistance, Lipometabolism, and Fetal Growth in Gestational Diabetes Mellitus Women. *J Obstet Gynaecol* (2015) 35:341–5. doi: 10.3109/01443615.2014.960376
4. Terrazzan AC, Procianoy RS, Silveira RC. Neonatal Cord Blood Adiponectin and Insulin Levels in Very Low Birth Weight Preterm and Healthy Full-Term Infants. *J Maternal-Fetal Neonatal Med* (2014) 27:616–20. doi: 10.3109/14767058.2013.823939
5. Simón-Muela I, Näf S, Ballesteros M, Vendrell J, Ceperuelo-Mallafre V, de la Flor M, et al. Gender Determines the Actions of Adiponectin Multimers on Fetal Growth and Adiposity. *Am J Obstet Gynecol* (2013) 208:481.e1–7. doi: 10.1016/j.ajog.2013.02.045
6. Wang J, Shen S, Price MJ, Lu J, Sumilo D, Kuang Y, et al. Glucose, Insulin, and Lipids in Cord Blood of Neonates and Their Association With Birthweight: Differential Metabolic Risk of Large for Gestational Age and Small for Gestational Age Babies. *J Pediatr* (2020) 220:64–+. doi: 10.1016/j.jpeds.2020.01.013
7. Katragadda T, Mahabala RS, Shetty S, Baliga S. Comparison of Cord Blood Lipid Profile in Preterm Small for Gestational Age and Appropriate for Gestational Age Newborns. *J Clin Diagn Res: JCDR* (2017) 11:SC05–7. doi: 10.7860/jcdr/2017/24247.9197
8. Bansal N, Cruickshank JK, McElduff P, Durrington PN. Cord Blood Lipoproteins and Prenatal Influences. *Curr Opin Lipidol* (2005) 16:400–8. doi: 10.1097/01.mol.0000174154.61307.16
9. Hou RL, Jin WY, Chen XY, Jin Y, Wang XM, Shao J, et al. Cord Blood C-Peptide, Insulin, HbA1c, and Lipids Levels in Small- and Large-for-Gestational-Age Newborns. *Med Sci Monit* (2014) 20:2097–105. doi: 10.12659/msm.890929
10. Degani S. Fetal Biometry: Clinical, Pathological, and Technical Considerations. *Obstet Gynecol Surv* (2001) 56:159–67. doi: 10.1097/00006254-200103000-00023
11. Qiu X, Lu J-H, He J-R, Lam K-b, Shen S-Y, Guo Y, et al. The Born in Guangzhou Cohort Study (BIGCS). *Eur J Epidemiol* (2017) 32:337–46. doi: 10.1007/s10654-017-0239-x
12. Stirnemann J, Villar J, Salomon LJ, Ohuma E, Ruyan P, Altman DG, et al. International Estimated Fetal Weight Standards of the INTERGROWTH-21st Project. *Ultrasound Obstet Gynecol* (2017) 49:478–86. doi: 10.1002/uog.17347
13. C.U.S.D. ASSOCIATION. Prenatal Ultrasound Guidelines (2012). *Chin J OF Med Ultrasound(Electronic Version)* (2012) 9:574–80. doi: 10.3877/cma.j.issn.1672-6448.2012.07.002
14. American College of Obstetricians and Gynecologists' Committee on Obstetric Practice. Committee Opinion No 700: Methods for Estimating the Due Date. *Obstet Gynecol* (2017) 129:e150–4. doi: 10.1097/aog.0000000000002046
15. He JR, Ramakrishnan R, Wei XL, Lu JH, Lu MS, Xiao WQ, et al. Fetal Growth at Different Gestational Periods and Risk of Impaired Childhood Growth, Low Childhood Weight and Obesity: A Prospective Birth Cohort Study. *Bjog* (2021) 128:1615–24. doi: 10.1111/1471-0528.16698
16. Norris T, Johnson W, Petherick E, Cameron N, Oddie S, Johnson S, et al. Investigating the Relationship Between Fetal Growth and Academic Attainment: Secondary Analysis of the Born in Bradford (BiB) Cohort. *Int J Epidemiol* (2018) 47:1475–84. doi: 10.1093/ije/dyy157
17. Howe LD, Tilling K, Matijasevich A, Petherick ES, Santos AC, Fairley L, et al. Linear Spline Multilevel Models for Summarising Childhood Growth Trajectories: A Guide to Their Application Using Examples From Five Birth Cohorts. *Stat Methods Med Res* (2016) 25:1854–74. doi: 10.1177/0962280213503925
18. Lampl M, Kusanovic JP, Erez O, Espinoza J, Gotsch F, Goncalves L, et al. Early Rapid Growth, Early Birth: Accelerated Fetal Growth and Spontaneous Late Preterm Birth. *Am J Hum Biol* (2009) 21:141–50. doi: 10.1002/ajhb.20840
19. Chen C, Lu FC. The Guidelines for Prevention and Control of Overweight and Obesity in Chinese Adults. *BioMed Environ Sci* (2004) 17 (Suppl):1–36.
20. Zhu W-w, Yang H-x. Diagnosis Gestational Diabetes Mellitus in China. *Diabetes Care* (2013) 36:E76–6. doi: 10.2337/dc12-2624
21. Ong K, Kratzsch J, Kiess W, Costello M, Scott C, Dunger D. Size at Birth and Cord Blood Levels of Insulin, Insulin-Like Growth Factor I (IGF-I), IGF-II, IGF-Binding Protein-1 (IGFBP-1), IGFBP-3, and the Soluble IGF-II/mannose-6-Phosphate Receptor in Term Human Infants. The ALSPAC Study Team. Avon Longitudinal Study of Pregnancy and Childhood. *J Clin Endocrinol Metab* (2000) 85:4266–9. doi: 10.1210/jc.85.11.4266
22. Okdemir D, Hatipoglu N, Kurtoglu S, Siraz UG, Akar HH, Muhtaroglu S, et al. The Role of Irisin, Insulin and Leptin in Maternal and Fetal Interaction. *J Clin Res Pediatr Endocrinol* (2018) 10:307–15. doi: 10.4274/jcrpe.0096
23. Dornhorst A, Nicholls JS, Ali K, Andres C, Adamson DL, Kelly LF, et al. Fetal Proinsulin and Birth Weight. *Diabetic Med* (1994) 11:177–81. doi: 10.1111/j.1464-5491.1994.tb02016.x
24. Rifas-Shiman SL, Fleisch A, Hivert MF, Mantzoros C, Gillman MW, Oken E. First and Second Trimester Gestational Weight Gains are Most Strongly Associated With Cord Blood Levels of Hormones at Delivery Important for Glycemic Control and Somatic Growth. *Metabolism* (2017) 69:112–9. doi: 10.1016/j.metabol.2017.01.019
25. Fowden AL, Hill DJ. Intra-Uterine Programming of the Endocrine Pancreas. *Br Med Bull* (2001) 60:123–42. doi: 10.1093/bmb/60.1.123
26. Grantz KL, Kim S, Grobman WA, Newman R, Owen J, Skupski D, et al. Fetal Growth Velocity: The NICHD Fetal Growth Studies. *Am J Obstet Gynecol* (2018) 219:285.e1–285.e36. doi: 10.1016/j.ajog.2018.05.016
27. Gatford KL, Simmons RA. Prenatal Programming of Insulin Secretion in Intrauterine Growth Restriction. *Clin Obstet Gynecol* (2013) 56:520–8. doi: 10.1097/GRF.0b013e31829e5b29
28. Saltiel AR, Kahn CR. Insulin Signalling and the Regulation of Glucose and Lipid Metabolism. *Nature* (2001) 414:799–806. doi: 10.1038/414799a
29. Milenkovic S, Jankovic B, Mirkovic L, Jovandaric MZ, Milenkovic D, Otasevic B. Lipids and Adipokines in Cord Blood and at 72h in Discordant Dichorionic Twins. *Fetal Pediatr Pathol* (2017) 36:106–22. doi: 10.1080/15513815.2016.1242675
30. Kelishadi R, Badiee Z, Adeli K. Cord Blood Lipid Profile and Associated Factors: Baseline Data of a Birth Cohort Study. *Paediatric Perinatal Epidemiol* (2007) 21:518–24. doi: 10.1111/j.1365-3016.2007.00870.x
31. Roberts A, Nava S, Bocconi L, Salmona S, Nicolini U. Liver Function Tests and Glucose and Lipid Metabolism in Growth-Restricted Fetuses. *Obstet Gynecol* (1999) 94:290–4. doi: 10.1016/s0029-7844(99)00235-5
32. Barker DJ, Martyn CN, Osmond C, Hales CN, Fall CH. Growth *In Utero* and Serum Cholesterol Concentrations in Adult Life. *BMJ (Clin Res ed.)* (1993) 307:1524–7. doi: 10.1136/bmj.307.6918.1524
33. Canalis EM, Dietrich JW, Maina DM, Raisz LG. Hormonal Control of Bone Collagen Synthesis In Vitro. *Effects Insulin Glucagon Endocrinol* (1977) 100:668–74. doi: 10.1210/endo-100-3-668
34. Fowden AL. The Role of Insulin in Prenatal Growth. *J Dev Physiol* (1989) 12:173–82.
35. Mobasheri A. Glucose: An Energy Currency and Structural Precursor in Articular Cartilage and Bone With Emerging Roles as an Extracellular Signaling Molecule and Metabolic Regulator. *Front Endocrinol* (2012) 3:153. doi: 10.3389/fendo.2012.00153
36. Landon MB, Spong CY, Thom E, Carpenter MW, Ramin SM, Casey B, et al. Randomized Trial of Treatment for Mild Gestational Diabetes. *N Engl J Med* (2009) 361:1339–48. doi: 10.1056/NEJMoa0902430
37. Cianfarani S, Maiorana A, Geremia C, Scire G, Spadoni GL, Germani D. Blood Glucose Concentrations are Reduced in Children Born Small for Gestational Age (SGA), and Thyroid-Stimulating Hormone Levels are Increased in SGA With Blunted Postnatal Catch-Up Growth. *J Clin Endocrinol Metab* (2003) 88:2699–705. doi: 10.1210/jc.2002-021882

Conflict of Interest: The authors declare that the research was conducted in the absence of any commercial or financial relationships that could be construed as a potential conflict of interest.

this article, or claim that may be made by its manufacturer, is not guaranteed or endorsed by the publisher.

frontiers in Endocrinology

ORIGINAL RESEARCH
published: 25 January 2022
doi: 10.3389/fendo.2021.805722

Fibroblast Growth Factor 19 in Gestational Diabetes Mellitus and Fetal Growth

Meng-Nan Yang[1,2†], Rong Huang[2†], Xin Liu[1†], Ya-Jie Xu[1†], Wen-Juan Wang[1†], Hua He[1†], Guang-Hui Zhang[3], Tao Zheng[4], Fang Fang[1], Jian-Gao Fan[5], Fei Li[1], Jun Zhang[1], Jiong Li[1,6], Fengxiu Ouyang[1] and Zhong-Cheng Luo[1,2*] for the Shanghai Birth Cohort*

[1] Ministry of Education-Shanghai Key Laboratory of Children's Environmental Health, Early Life Health Institute, and Department of Pediatrics, Xinhua Hospital, Shanghai Jiao-Tong University School of Medicine, Shanghai, China, [2] Department of Obstetrics and Gynecology, Lunenfeld-Tanenbaum Research Institute, Prosserman Centre for Population Health Research, Mount Sinai Hospital, Institute of Health Policy, Management and Evaluation, Dalla Lana School of Public Health, Faculty of Medicine, University of Toronto, Toronto, ON, Canada, [3] Department of Clinical Assay Laboratory, Xinhua Hospital, Shanghai Jiao-Tong University School of Medicine, Shanghai, China, [4] Department of Obstetrics and Gynecology, Xinhua Hospital, Shanghai Jiao-Tong University School of Medicine, Shanghai, China, [5] Center for Fatty Liver, Shanghai Key Lab of Pediatric Gastroenterology and Nutrition, Department of Gastroenterology, Xinhua Hospital, Shanghai Jiao Tong University School of Medicine, Shanghai, China, [6] Department of Clinical Medicine-Department of Clinical Epidemiology, Aarhus University Hospital, Aarhus, Denmark

OPEN ACCESS

Edited by:
Takahiro Nemoto, Nippon Medical School, Japan

Reviewed by:
Yoshifumi Saisho, Keio University School of Medicine, Japan
R. G. Ahmed, Beni-Suef University, Egypt

***Correspondence:**
Zhong-Cheng Luo
zcluo@lunenfeld.ca
Fengxiu Ouyang
ouyangfengxiu@xinhuamed.com.cn

†These authors have contributed equally to this work

Specialty section:
This article was submitted to Pediatric Endocrinology, a section of the journal Frontiers in Endocrinology

Received: *30 October 2021*
Accepted: *27 December 2021*
Published: *25 January 2022*

Citation:
Yang M-N, Huang R, Liu X, Xu Y-J, Wang W-J, He H, Zhang G-H, Zheng T, Fang F, Fan J-G, Li F, Zhang J, Li J, Ouyang F and Luo Z-C (2022) Fibroblast Growth Factor 19 in Gestational Diabetes Mellitus and Fetal Growth. Front. Endocrinol. 12:805722. doi: 10.3389/fendo.2021.805722

Fibroblast growth factor 19 (FGF19) has been implicated in glucose homeostasis. Gestational diabetes mellitus (GDM) enhances fetal insulin secretion and fetal growth. Girls weigh less and are more insulin resistant than boys at birth. We sought to assess whether FGF19 is associated with GDM and fetal growth and explore potential sex dimorphic associations. This was a nested case-control study in the Shanghai Birth Cohort, including 153 pairs of newborns of GDM versus euglycemic mothers matched by infant's sex and gestational age at birth. Cord plasma FGF19, insulin, C-peptide, proinsulin, IGF-I and IGF-II concentrations were measured. Cord plasma FGF19 concentrations were similar in GDM versus euglycemic pregnancies (mean ± SD: 43.5 ± 28.2 versus 44.5 ± 30.2 pg/mL, P=0.38). FGF19 was not correlated with IGF-I or IGF-II. FGF19 concentrations were positively correlated with birth weight (r=0.23, P=0.01) and length (r=0.21, P=0.02) z scores, C-peptide (r=0.27, P=0.002) and proinsulin (r=0.27, P=0.002) concentrations in females. Each SD increment in cord plasma FGF19 was associated with a 0.25 (0.07-0.43) increase in birth weight z score in females. In contrast, FGF19 was not correlated with birth weight or length in males. These sex dimorphic associations remained after adjusting for maternal and neonatal characteristics. The study is the first to demonstrate that GDM does not matter for cord blood FGF19 concentrations. The female specific positive correlation between FGF19 and birth weight is suggestive of a sex-dimorphic role of FGF19 in fetal growth. The observations call for more studies to validate the novel findings and elucidate the underlying mechanisms.

Keywords: fibroblast growth factor 19 (FGF19), gestational diabetes (GD), fetal growth, insulin, C-peptide

INTRODUCTION

Fibroblast growth factor 19 (FGF19) is mainly secreted from the enterocytes in the distal part of the small intestine (1), and is expressed in fetal brain, cartilage, skin and retina (2, 3). FGF19 has been implicated in the regulation of glucose and lipid metabolism (4–6). FGF19 may regulate glucose homeostasis *via* enhancement of glycogen synthesis, glucose catabolism and suppression of gluconeogenesis (5, 7, 8). Decreased circulating FGF19 levels have been reported in obese, insulin resistant and type 2 diabetes patients (9–11). Animal studies suggest that FGF19 may be negatively correlated with adiposity and positively correlated with insulin sensitivity (12–16), and may even reverse diabetes (17, 18).

Gestational diabetes mellitus (GDM) (*de novo* glucose intolerance in pregnancy) is a common cause of enhanced fetal insulin secretion and overgrowth (19), and has been associated with reduced maternal circulating FGF19 levels (20) and placental FGF19 expression (21), and reduced fetal insulin sensitivity (22). We thus hypothesize that GDM may affect fetal FGF19 levels. However, there have been no studies on whether GDM may affect FGF19 concentrations in fetuses or newborns. FGF19 may induce glycogen and protein synthesis in the liver (7, 23) and skeletal muscle mass (24). However, data are scarce concerning whether FGF19 may affect fetal growth in humans. We are aware of only one small study (n=44) which did not detect any association (25). Girls weigh less and are more insulin resistant than boys at birth (26). It is unknown whether any association between FGF19 and fetal growth may differ by sex. Considering theses research data gaps, we sought to examine whether cord blood FGF19 is associated with GDM and fetal growth and explore potential sex-dimorphic associations. The primary research questions are whether GDM affects cord blood FGF19 concentrations, and whether there are differential correlations between FGF19 and fetal growth in males and females.

METHODS

Study Design, Subjects and Specimens

We conducted a nested matched (1:1) case-control study in the Shanghai Birth Cohort (SBC) (27). The SBC is a large, carefully phenotyped birth cohort with linked biospecimen bank for studies on perinatal determinants of infant growth, development and health. Women at preconception or early pregnancy care clinics were recruited from six university-affiliated tertiary obstetric care hospitals in Shanghai between 2013 and 2016, including a total of 4127 pregnancies. The women were followed up at the first, second and third trimesters of pregnancy and delivery. Data and specimens were collected at each study visit. All collected blood samples were kept on ice, stored temporarily in a 4°C refrigerator and centrifuged within 2 hours after the specimen collection. The separated serum and EDTA plasma samples were stored in multiple aliquots at -80°C until assays. The study was approved by the research ethics committees of Xinhua Hospital (the coordination center, reference number M2013-010) and all participating hospitals. Written informed consent was obtained from all study participants.

GDM was diagnosed according to the International Association of Diabetes and Pregnancy Study Groups (IADPSG) criteria (28) - if any one of the blood glucose values was at or above the following thresholds in the 75 g oral glucose tolerance test (OGTT) at 24-28 weeks of gestation: fasting 5.1 mmol/L, 1-hour 10.0 mmol/L and 2-hour 8.5 mmol/L.

As part of the SBC, a nested case control study was designed to study the impacts of GDM on metabolic health biomarkers in the newborns (29). Briefly, cases were the newborns of GDM mothers (n=153), and controls were the newborns of euglycemic mothers (n=153) in the SBC. Cases and controls were matched (1:1) by infant's sex (the same) and gestational age at birth (within 1 week). The present study reported FGF19 in association with GDM and fetal growth.

Birth weight z scores were calculated using the 2015 Chinese sex- and gestational age-specific birth weight standards (30). Birth length z scores were calculated according to sex- and gestational age-specific means and SDs of all singleton infants in the SBC.

Biochemical Assays

Cord plasma FGF19 was measured by an enzyme-linked immunosorbent assay (ELISA) kit (R&D system, Minnesota, USA), and the absorbance was determined using a microplate spectrophotometer (Beckman CX7, USA). Serum insulin and insulin-like growth factor I (IGF-I) concentrations were detected by chemiluminescent assays (ADVIA Centaur and Immulite 2000, Siemens, Germany). Plasma IGF-II was measured by an ELISA kit from R&D systems (Minnesota, USA). Plasma C-peptide and proinsulin were measured by ELISA kits from Mercodia system (Uppsala, Sweden). Plasma total and high-molecular-weight (HMW) adiponectin were measured by an ELISA kit from ALPCO (Salem, NH, USA). Plasma leptin was measured by an ELISA kit from Invitrogen (Carlsbad, CA, USA). The detection limits were 1.17 pg/mL for FGF19, 3.5 pmol/L for insulin, 25 ng/mL for IGF-I, 1.88 pg/mL for IGF-II, 25 pmol/L for C-peptide, and 1.7 pmol/L for proinsulin, 0.034 ng/mL for HMW and total adiponectin, and 3.5 pg/mL for leptin, respectively. Intra-assay and inter-assay coefficients of variation were in the ranges of 6.4-11.6% for FGF19, 2.0-6.5% for insulin and IGF-I, 5.0-8.6% for proinsulin, 0.4-13.5% for C-peptide, 2.4-9.3% for IGF-II, and 6.9%-10.4% for leptin, HMW and total adiponectin, respectively. In all biomarker assays, the laboratory technicians were blinded to the clinical status (GDM or not) of study subjects.

Statistical Analysis

Data are presented as mean ± SD (standard deviation) or median (interquartile range) for continuous variables, and frequency

Abbreviations: FGF19, fibroblast growth factor 19; GDM, gestational diabetes mellitus; OGTT, oral glucose tolerance test; SBC, Shanghai Birth Cohort; IADPSG, International Association of Diabetes and Pregnancy Study Groups; IGF-I, insulin-like growth factor I; IGF-II, insulin-like growth factor II; CI, confidence interval; SD, standard deviation.

(percentage) for categorical variables. Log-transformed biomarker data were used in t-tests, correlation and regression analyses. Pearson partial correlation was used to evaluate the correlations with biomarkers adjusting for gestational age at cord blood sampling/delivery. Differences in correlations in male and female infants were examined by Fisher's z test. Generalized linear models were applied to assess the associations of cord blood FGF19 with GDM, fetal growth and fetal growth factors adjusting for maternal and neonatal characteristics. The co-variables included maternal age, ethnicity, parity, education (university: yes/no), pre-pregnancy BMI (kg/m^2), smoking or alcohol use in pregnancy (yes/no), gestational hypertension, family history of diabetes, family history of hypertension, mode of delivery (caesarean section/vaginal), infant's sex and gestational age (weeks) at birth. We estimated the changes in birth weight and length z scores per SD increment in FGF19. Mediation analyses were conducted to assess whether fetal growth factors may mediate any associations between FGF19 and fetal growth (birth weight or length) using the product ("Baron and Kenney") method (31). Data management and analyses were performed in SAS version 9.4 (SAS Institute, Cary, NC). Two-tailed P<0.05 was considered statistically significant in evaluating the primary research question on whether cord plasma FGF19 concentrations differ between GDM and controls, or whether there are differential correlations between FGF19 and fetal growth (birth weight z score as the primary indicator) in males and females.

RESULTS

Maternal and Neonatal Characteristics

Characteristics of study subjects in this nested study in the Shanghai birth cohort have been described recently (29). Briefly, women with GDM had higher pre-pregnancy BMI than euglycemic women (Mean: 23.6 versus 21.6 kg/m^2) and were more likely to have gestational hypertension (5.2% versus 0.6%) and tended to be more likely to have a family history of diabetes (16.5% versus 9.5%) than women with a euglycemic pregnancy. There were no significant differences in other maternal characteristics including maternal age, education, parity, alcohol use or smoking during pregnancy. The newborns of GDM mothers were more likely to be delivered by caesarean section than the newborns of euglycemic mothers (54.3% versus 33.1%). Mean gestational age at delivery was about 39 weeks in both GDM and euglycemic pregnancies (39.1 and 39.3 weeks). There were 142 (46.6%) caesarean section deliveries (97 elective caesarean sections), and 13 (4.3%) preterm births (<37 weeks in gestational age, all between 34-36 weeks).

Cord Blood FGF19 and Fetal Growth Factors

Adjusting for maternal and neonatal characteristics including pre-pregnancy BMI, family history of hypertension, parity, cesarean section and gestational age at delivery (other covariates did not affect the comparisons, all P>0.2), cord plasma FGF19 (43.5 ± 28.2 versus 44.5 ± 30.2 pg/mL, P=0.38), proinsulin (22.3 ± 17.9 versus 19.3 ± 16.8 pmol/L, P=0.91) and C-peptide (264.3 ± 185.7 versus 269.3 ± 155.3 pmol/L, P=0.29) concentrations were similar in GDM and euglycemic pregnancies (**Table 1**).

Descriptive data on cord plasma insulin, IGF-I, IGF-II, leptin, total and HMW adiponectin were reported elsewhere (29, 32). Briefly, cord plasma IGF-I (76.6 ± 27.8 versus 68.1 ± 25.1 ng/mL, P=0.008) and IGF-II (195.3 ± 32.5 versus 187.5 ± 30.8 ng/mL, P=0.04) concentrations were significantly higher in GDM versus euglycemic pregnancies, while insulin concentrations were not significantly different (29). Cord plasma HMW adiponectin concentrations were lower in GDM versus euglycemic pregnancies, while leptin and total adiponectin concentrations were not significantly different (32).

Determinants of Cord Blood FGF19

Cord plasma FGF19 concentrations were similar in male versus female newborns (43.9 ± 29.4 versus 44.2 ± 29.1 pg/mL, P=0.46), and were higher in preterm versus term births (64.6 ± 33.4 versus 43.2 ± 28.8 pg/mL, P=0.009) and in caesarean section versus vaginal deliveries (47.1 ± 28.7 versus 41.4 ± 29.5 pg/mL, P=0.09). Compared with vaginal deliveries, FGF19 concentrations were higher in elective caesarean sections (49.9 ± 30.3 pg/mL, P=0.03), but similar in emergency caesarean sections (40.9 ± 24.2 pg/mL, P=0.92). Other maternal and neonatal factors were not associated with cord plasma FGF19 concentrations (all P>0.05).

TABLE 1 | Cord plasma FGF19, proinsulin and C-peptide concentrations in the newborns of GDM versus euglycemic (control) mothers (matched by infant sex and gestational age) in the Shanghai Birth Cohort.

	GDM (n=153)	Control (n=153)	Crude P*	Adjusted P*
FGF19	43.5±28.2	44.5±30.2	0.88	0.38
(pg/mL)	35.2 (25.5, 53.8)	36.0 (24.1, 52.5)		
Proinsulin	22.3±17.9	19.3±16.8	0.66	0.91
(pmol/L)	16.5 (11. 5, 27.2)	15.6 (11.3, 21.4)		
C-Peptide	264.3±185.7	269.3±155.3	0.09	0.29
(pmol/L)	230.0 (141.0, 344.0)	243.4 (162.6, 339.2)		

Data presented are mean±SD and median (inter-quartile range).

GDM, Gestational diabetes mellitus; FGF19, Fibroblast growth factor 19.

**Crude P values were from paired t-tests. Adjusted P values were from generalized linear models in the comparisons of log-transformed biomarker data between the two groups adjusted for maternal (pre-pregnancy BMI, family history of hypertension, parity) and neonatal (cesarean section, gestational age) characteristics; other factors (all P>0.2) were excluded since they were similar and did not affect the comparisons. All comparisons were based on log-transformed data for biomarkers.*

FGF19 in Correlations With Fetal Growth and Fetal Growth Factors

There were significant interactions (all P<0.05) between FGF19 and infant sex in relation to fetal growth (birth weight or length z score), C-peptide and proinsulin. Therefore, we present the correlation coefficients stratified by infant's sex. Gestational age was negatively correlated with cord plasma FGF19 (r=-0.17, P=0.003). Adjusting for gestational age at delivery/blood sampling, cord plasma FGF19 concentrations were positively correlated with birth weight (r=0.23, P=0.01) and birth length (r=0.21, P=0.02) z scores, C-peptide (r=0.27, P=0.002) and proinsulin (r=0.27, P=0.002) concentrations in female newborns (**Table 2** and **Figure 1**). The positive correlation between cord plasma FGF19 and birth weight in females remained if further adjusting for cord plasma C-peptide (r=0.21, P=0.01). In contrast, cord plasma FGF19 was not correlated with birth weight or length but was negatively correlated with C-peptide (r=-0.23, P=0.003) in male newborns. The correlations between FGF19 and proinsulin or C-peptide are in opposite directions in females and males (tests for differences in correlation coefficients, all P<0.05). Cord plasma FGF19 was not correlated with IGF-I, IGF-II, leptin, HMW or total adiponectin in both sexes. All these correlations were not significantly different in GDM and controls (**Table 3**).

Adjusted Associations Between FGF19 and Fetal Growth

Adjusting for maternal and neonatal characteristics in female newborns, each SD increment in cord plasma FGF19 was associated with a 0.25 [95% confidence interval (CI): 0.07, 0.43] increase in birth weight (P=0.01), a 0.20 (0.01, 0.40) increase in birth length (P=0.047), a 0.18 (0.09, 0.27) increase in cord blood insulin (P<0.001), a 0.32 (0.17, 0.47) increase in C-peptide (P<0.001), and a 0.44 (0.24, 0.64) increase in proinsulin (P<0.001), respectively (**Table 4**, standardized regression coefficients; all continuous variables in z scores in the regression analyses). In contrast, in male newborns, cord plasma FGF19 was not associated with birth weight, length, insulin or proinsulin, while each SD increment in FGF19 was associated with a 0.19 (0.02, 0.37) decrease in C-peptide (P=0.03) (opposite to the association in female newborns).

Mediation Analyses

Mediation analyses showed that cord blood proinsulin could partly explain the association between FGF19 and fetal growth in female newborns (**Table 5**). Proinsulin could account for 34.8% of the effect size of FGF19 for birth weight (P=0.037), and 55.1% of the effect size for birth length (P=0.016), respectively. There were no significant mediation effects for other fetal growth factors (insulin, C-peptide, IGF-I or IGF-II) in the associations of FGF19 with birth weight and length.

DISCUSSION

Main Findings

We observed that GDM was not associated with cord blood FGF19. FGF19 was positively correlated with fetal growth (birth weight or length) in females only, suggesting a sex-dimorphic role of FGF19 in fetal growth.

Data Interpretation and Comparisons With Findings in Previous Studies

Decreased circulating FGF19 levels have been reported in women with GDM (20), and in subjects with type 2 diabetes (33). Circulating FGF19 levels appear to be unrelated to age or sex in adults (34, 35). We are unaware of any reports on whether there are altered cord blood FGF19 concentrations in GDM. We observed similar cord plasma FGF19 concentrations in GDM and euglycemic pregnancies, and in male and female newborns, suggesting no impact of GDM or fetal sex on fetal FGF19 levels.

A previous study did not detect any association between caesarean section on cord blood FGF19, probably due to small sample size (11 caesarean, 33 vaginal deliveries) and low power (25). In contrast, our much larger study (142 caesarean, 163 vaginal deliveries) demonstrated higher cord blood FGF19

TABLE 2 | Cord blood FGF19 in correlations with birth weight, birth length, fetal growth factors, leptin and adiponectin in males and females.

	Males		Females		
	r	P	r	P	P*
Birth weight	-0.01	0.90	0.23	**0.01**	**0.039**
Birth length	-0.04	0.66	0.21	**0.02**	**0.045**
IGF-I	0.01	0.90	0.02	0.79	0.91
IGF-II	0.07	0.37	0.05	0.54	0.89
Proinsulin	-0.13	0.10	0.27	**0.002**	**<0.001**
Insulin	0.02	0.83	0.15	0.09	0.26
C-peptide	-0.23	**0.003**	0.27	**0.002**	**<0.001**
Leptin	-0.14	0.08	0.11	0.22	0.12
Adiponectin, HMW	-0.01	0.87	-0.002	0.98	0.91
Adiponectin, Total	0.05	0.49	0.04	0.64	0.88

Data presented are Pearson partial correlation coefficients adjusting for gestational age at delivery/cord blood sampling. Data were in z scores for birth weight and length, and were log-transformed for biomarkers in the correlation analyses.

FGF19, Fibroblast growth factor 19; IGF-I, insulin-like growth factor-I; IGF-II, insulin-like growth factor-II; HMW, high molecular weight.

**P values in z tests for differences in correlation coefficients in males and females.*

P values in bold: P < 0.05.

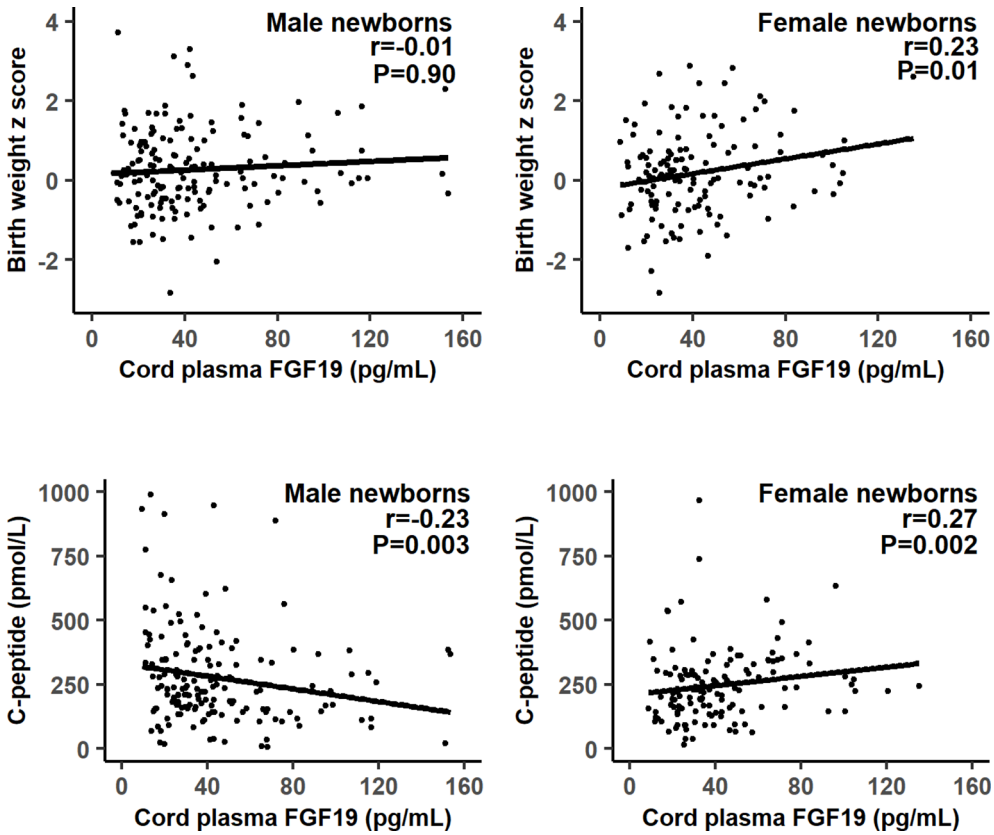

FIGURE 1 | Scatter plots illustrating the differential correlations between cord plasma fibroblast growth factor 19 (FGF19) and fetal growth (birth weight z score) or C-peptide in males and females.

concentrations even in elective caesarean deliveries (n=92). Gestational age has been negatively correlated with neonatal blood FGF19 concentration (36). This is consistent with our observed negative correlation between gestational age and cord blood FGF19 concentration. FGF19 appears to be secreted at higher levels at earlier gestational ages.

A small study (n=44) (25) did not find any difference in cord FGF19 concentrations between birth weight small- vs. appropriate-

TABLE 3 | Cord blood FGF19 in correlations with birth weight, birth length and fetal growth factors, leptin and adiponectin in the newborns of GDM and euglycemic (control) mothers.

	GDM		Control		
	r	P	r	P	P*
Birth weight	0.13	0.12	0.07	0.43	0.57
Birth length	0.18	**0.035**	-0.02	0.86	0.11
IGF-I	0.13	0.13	-0.07	0.41	0.10
IGF-II	0.15	0.07	-0.02	0.82	0.15
Proinsulin	0.10	0.23	-0.03	0.67	0.25
Insulin	0.11	0.20	0.03	0.70	0.52
C-peptide	-0.0004	1.00	-0.08	0.33	0.49
Leptin	0.04	0.63	-0.11	0.17	0.09
Adiponectin, HMW	-0.07	0.42	0.06	0.45	0.41
Adiponectin, Total	0.03	0.75	0.08	0.35	0.92

Data presented are Pearson partial correlation coefficients adjusting for gestational age at delivery/cord blood sampling. Data were in z scores for birth weight and length, and were log-transformed for biomarkers in the correlation analyses.

FGF19, Fibroblast growth factor 19; IGF-I, insulin-like growth factor-I; IGF-II, insulin-like growth factor-II; HMW, high molecular weight.

**P values in comparisons of correlation coefficients in GDM and control infants.*

P values in bold: P < 0.05.

TABLE 4 | The adjusted associations of cord blood FGF19 with birth weight, birth length, insulin, proinsulin, C-peptide, IGF-I and IGF-II, leptin and adiponectin in males and females.

Data in z score	Males β (95% CI)	P	Females β (95% CI)	P
Birth weight	-0.07 (-0.25, 0.10)	0.40	0.25 (0.07, 0.43)	**0.008**
Birth length	-0.06 (-0.24, 0.13)	0.54	0.20 (0.01, 0.40)	**0.047**
Insulin	0.16 (-0.04, 0.37)	0.12	0.18 (0.09, 0.27)	**<0.001**
Proinsulin	-0.11 (-0.25, 0.04)	0.15	0.44 (0.24, 0.64)	**<0.001**
C-peptide	-0.19 (-0.37, -0.02)	**0.03**	0.32 (0.17, 0.47)	**<0.001**
IGF-I	-0.10 (-0.26, 0.06)	0.21	0.06 (-0.13, 0.26)	0.50
IGF-II	0.08 (-0.08, 0.23)	0.34	0.07 (-0.12, 0.27)	0.46
Leptin	-0.06 (-0.20, 0.08)	0.40	0.08 (-0.12, 0.27)	0.45
Adiponectin, HMW	0.01 (-0.15, 0.16)	0.93	-0.07 (-0.25, 0.11)	0.45
Adiponectin, Total	-0.02 (-0.19, 0.14)	0.78	-0.03 (-0.19, 0.14)	0.75

Data (β) presented are the standardized changes in birth weight, birth length or each fetal growth factor per SD increment in FGF19 from generalized linear models adjusting for maternal (pre-pregnancy BMI, family history of hypertension, parity) and neonatal (cesarean section, gestational age) characteristics; other maternal and neonatal factors were excluded since they did not affect the comparisons (all P>0.2). Standardized z score data were used for all continuous variables in the regression analyses. The SDs for calculating the z scores in cord blood biomarkers were 29.2 pg/mL for FGF19, 55.2 pmol/L for insulin, 17.4 pmol/L for proinsulin, 170.7 pmol/L for C-peptide, 26.8 ng/mL for IGF-I, and 31.8 ng/mL for IGF-II, 7.2 ng/mL for leptin, 7.8 (μg/mL) for HMW adiponectin and 15.4 (μg/mL) for total adiponectin, respectively.

There were significant interactions between FGF19 and sex in relation to birth weight (P=0.019), birth length (P=0.055), proinsulin (P < 0.0001) and C-peptide (P < 0.0001).

P values in bold: P < 0.05.

for-gestational-age infants (no sex specific data). In contrast, we observed that cord blood FGF19 was positively correlated with birth weight and length in females only, suggesting that FGF19 may have a sex-dimorphic role in fetal growth. The observation adds to the growing evidence that there may be sex-specific impacts of certain early life factors (32). Females are more insulin resistant than males at birth (26, 37). Sex difference in fetal growth may emerge *via* sex specific intrauterine endocrine or metabolic factors (38). FGF19 may play a role in skeletal muscle growth and protein synthesis (7, 23, 24). We speculate that FGF19 may promote fetal growth in females under an unknown female fetus-specific endocrine environment.

Our data provide some weak evidence suggesting that insulin may mediate the association between FGF19 and fetal growth in females. Mediation analyses showed that cord blood proinsulin - a precursor to insulin, a surrogate indicator of insulin secretion, partly mediated the positive association between FGF19 and birth weight or length in female newborns, but no mediation effects were observed for insulin, C-peptide, IGF-I or IGF-II. A study in diabetic patients reported that serum FGF19 was positively associated with insulin (11). We did not detect any association between cord blood FGF19 and insulin. However, insulin levels may only reflect short-term glucose exposure levels. We did observe that cord plasma FGF19 was positively correlated with proinsulin and C-peptide which are indicators of chronic glucose exposure levels.

Interestingly, opposite to the positive correlations between cord plasma FGF19 and C-peptide or proinsulin in females, negative correlations were observed in males. We are unaware of any reports on the correlations between FGF19 and insulin or its secretion related C-peptide and proinsulin in newborns. Our data are suggestive of a sex dimorphic association between FGF19 and chronic insulin secretion levels during fetal life. The positive correlation between FGF19 and C-peptide is consistent with the positive correlation between FGF19 and fetal growth in females. However, the negative correlation between FGF19 and C-peptide is incongruent with the absence of a negative correlation between FGF19 and fetal growth in males, suggesting the need for caution in data interpretation. More studies are warranted to confirm this finding.

Circulating FGF19 and insulin concentrations are positively correlated in patients with type 2 diabetes (11), suggesting that FGF19 may participate in insulin-dependent glucose regulation. Individuals with isolated impaired fasting glucose have decreased serum FGF19 levels, suggesting that FGF19 may play a role in basal

TABLE 5 | Mediation analyses in the associations of cord blood FGF19 with fetal growth (birth weight, birth length) in female newborns (n=140).

	Birth weight z score	P	Birth length z score	P
FGF19 (total effect)	0.25 (0.07, 0.43)	**0.008**	0.20 (0.01, 0.40)	**0.047**
*Mediation by				
Insulin	0.01 (-0.05, 0.08)	0.71	0.006 (-0.07, 0.08)	0.88
Proinsulin	0.09 (0.006, 0.17)	**0.037**	0.11 (0.02, 0.20)	**0.016**
C-peptide	-0.02 (-0.09, 0.05)	0.61	-0.02 (-0.10, 0.06)	0.65
IGF-I	0.02 (-0.05, 0.10)	0.51	0.01 (-0.02, 0.04)	0.55
IGF-II	0.02 (-0.03, 0.07)	0.47	0.01 (-0.02, 0.05)	0.49

Data (β) presented are the changes in fetal growth (birth weight or birth length) per SD increment in each cord blood biomarker from generalized linear models. Standardized z score data were used for all continuous predictor variables in the regression models. The SDs for calculating the z scores in cord blood biomarkers were 29.2 pg/mL for FGF19, 55.2 pmol/L for insulin, 17.4 pmol/L for proinsulin, 170.7 pmol/L for C-peptide, 26.8 ng/mL for IGF-I, and 31.8 ng/mL for IGF-II, respectively.

**The mediation effects presented are the change (95% CI) in the outcome (birth weight or length z score) per SD increment in cord blood insulin, proinsulin, C-peptide, IGF-I or IGF-II (evaluated separately) that could account for the effect of cord blood FGF19 on fetal growth (birth weight or length). The mediation effects were estimated by the product (Baron and Kenney) method.*

P values in bold: P < 0.05.

insulin secretion (33). These findings are consistent with the observed positive correlation between cord plasma FGF19 and C-peptide in female newborns. Unexpectedly, we observed a negative correlation between cord blood FGF19 and C-peptide in males. Further studies are warranted to verify whether this may be a true or chance finding.

Strengths, Limitations and Future Research Directions

The main strengths include the large birth cohort, timely collection and processing of cord blood specimens, and high-quality biochemical assays (low inter-assay and intra-assay coefficients of variation). The main limitation is the observational nature of the study; causality cannot be ascertained. We had no data on inflammatory biomarkers. Future studies may explore whether fetal FGF19 levels are correlated with inflammatory biomarkers. The study was limited to Chinese subjects. More studies in other ethnic groups are required to understand the generalizability of the study findings.

In conclusion, our study data indicate that GDM may not affect cord blood FGF19 levels, and that there may be a sex-dimorphic role of FGF19 in fetal growth. The observations call for more studies to validate the novel findings and elucidate the underlying mechanisms.

DATA AVAILABILITY STATEMENT

The datasets presented in this article are not readily available because access to the deidentified participant research data must be approved by the research ethics board on a case-by-case basis, please contact the corresponding authors (zcluo@lunenfeld.ca; ouyangfengxiu@xinhuamed.com.cn) for assistance in data access request.

ETHICS STATEMENT

The studies involving human participants were reviewed and approved by Xinhua Hospital, Shanghai Jiao-Tong University School of Medicine, reference number M2013-010. The patients/participants provided their written informed consent to participate in this study.

AUTHOR CONTRIBUTIONS

Z-CL, G-HZ, J-GF, FL, JL, JZ, and FO conceived the study. M-NY, RH, YJ-X, XL, W-JW, HH, FF, G-HZ, TZ, FL, JZ, JL, FO, and Z-CL contributed to the acquisition of research data. M-NY and RH conducted the literature review, data analysis, and drafted the manuscript. All authors contributed to revising the article critically for important intellectual content and approved the final version for publication.

FUNDING

Supported by research grants from the Ministry of Science and Technology of China (2019YFA0802501, 2017YFE0124700), the Shanghai Municipal Health Commission (2020CXJQ01), the Shanghai Municipal Science and Technology Commission (19410713500, 21410713500), the National Natural Science Foundation of China (82073570, 81961128023, 81903323, 81761128035 and 81930095), the National Human Genetic Resources Sharing Service Platform (2005DKA21300), and the Canadian Institutes of Health Research (158616). The funders have no role in all aspects of the study, including study design, data collection and analysis, the preparation of the manuscript and the decision for publication.

ACKNOWLEDGMENTS

We gratefully acknowledged all research staff who had contributed to patient recruitment and data collection in the Shanghai Birth Cohort. Z-CL is the guarantor of this work taking full responsibility for the work as a whole including the study design, access to data, and the decision to submit and publish the manuscript.

REFERENCES

1. Holt J, Luo G, Billin A, Bisi J, McNeill Y, Kozarsky K, et al. Definition of a Novel Growth Factor-Dependent Signalcascade for the Suppression of Bile Acid Biosynthesis. *Genes Dev* (2003) 17(13):1581–91. doi: 10.1101/gad.1083503
2. Nishimura T, Utsunomiya Y, Hoshikawa M, Ohuchi H, Itoh N. Structure and Expression of a Novel Human FGF, FGF-19, Expressed in the Fetal Brain. *Biochim Biophys Acta* (1999) 1444(1):148–51. doi: 10.1016/s0167-4781(98)00255-3
3. Xie M, Holcomb I, Deuel B, Dowd P, Huang A, Vagts A, et al. FGF-19, a Novel Fibroblast Growth Factor With Unique Specificity for FGFR4. *Cytokine* (1999) 11(10):729–35. doi: 10.1006/cyto.1999.0485
4. Dolegowska K, Marchelek-Mysliwiec M, Nowosiad-Magda M, Slawinski M, Dolegowska B. FGF19 Subfamily Members: FGF19 and FGF21. *J Physiol Biochem* (2019) 75(2):229–40. doi: 10.1007/s13105-019-00675-7
5. Somm E, Jornayvaz F. Fibroblast Growth Factor 15/19: From Basic Functions to Therapeutic Perspectives. *Endocr Rev* (2018) 39(6):960–89. doi: 10.1210/er.2018-00134
6. Itoh N. Hormone-Like (Endocrine) Fgfs: Their Evolutionary History and Roles in Development, Metabolism, and Disease. *Cell Tissue Res* (2010) 342(1):1–11. doi: 10.1007/s00441-010-1024-2
7. Kir S, Beddow S, Samuel V, Miller P, Previs S, Suino-Powell K, et al. FGF19 as a Postprandial, Insulin-Independent Activator of Hepatic Protein and Glycogen Synthesis. *Sci (New York NY)* (2011) 331(6024):1621–4. doi: 10.1126/science.1198363
8. Zhang F, Yu L, Lin X, Cheng P, He L, Li X, et al. Minireview: Roles of Fibroblast Growth Factors 19 and 21 in Metabolic Regulation and Chronic Diseases. *Mol Endocrinol* (2015) 29(10):1400–13. doi: 10.1210/me.2015-1155
9. Mráz M, Lacinová Z, Kaválková P, Haluzíková D, Trachta P, Drápalová J, et al. Serum Concentrations of Fibroblast Growth Factor 19 in Patients With Obesity and Type 2 Diabetes Mellitus: The Influence of Acute

Hyperinsulinemia, Very-Low Calorie Diet and PPAR-α Agonist Treatment. *Physiol Res* (2011) 60(4):627–36. doi: 10.33549/physiolres.932099
10. Gallego-Escuredo J, Gómez-Ambrosi J, Catalan V, Domingo P, Giralt M, Frühbeck G, et al. Opposite Alterations in FGF21 and FGF19 Levels and Disturbed Expression of the Receptor Machinery for Endocrine FGFs in Obese Patients. *Int J Obes (Lond)* (2015) 39(1):121–9. doi: 10.1038/ijo.2014.76
11. Tang M, Su J, Xu T, Wang X, Zhang D, Wang X. Serum Fibroblast Growth Factor 19 and Endogenous Islet Beta Cell Function in Type 2 Diabetic Patients. *Diabetol Metab Syndr* (2019) 11:79. doi: 10.1186/s13098-019-0475-1
12. Ge H, Zhang J, Gong Y, Gupte J, Ye J, Weiszmann J, et al. Fibroblast Growth Factor Receptor 4 (FGFR4) Deficiency Improves Insulin Resistance and Glucose Metabolism Under Diet-Induced Obesity Conditions. *J Biol Chem* (2014) 289(44):30470–80. doi: 10.1074/jbc.M114.592022
13. Tomlinson E, Fu L, John L, Hultgren B, Huang X, Renz M, et al. Transgenic Mice Expressing Human Fibroblast Growth Factor-19 Display Increased Metabolic Rate and Decreased Adiposity. *Endocrinology* (2002) 143 (5):1741–7. doi: 10.1210/endo.143.5.8850
14. Adams A, Coskun T, Rovira A, Schneider M, Raches D, Micanovic R, et al. Fundamentals of FGF19 & FGF21 Action *In Vitro* and *In Vivo*. *PloS One* (2012) 7(5):e38438. doi: 10.1371/journal.pone.0038438
15. Hansen A, Vienberg S, Lykkegaard K, Zhao X, Tingqing G, Han D, et al. Db/Dbdifferential Receptor Selectivity of the FGF15/FGF19 Orthologues Determines Distinct Metabolic Activities in Mice. *Biochem J* (2018) 475 (18):2985–96. doi: 10.1042/bcj20180555
16. Zhao S, Wang D, Li Z, Xu S, Chen H, Ding W, et al. FGF15/FGF19 Alleviates Insulin Resistance and Upregulates Placental IRS1/GLUT Expression in Pregnant Mice Fed a High-Fat Diet. *Placenta* (2021) 112:81–8. doi: 10.1016/j.placenta.2021.07.286
17. Fu L, John L, Adams S, Yu X, Tomlinson E, Renz M, et al. Fibroblast Growth Factor 19 Increases Metabolic Rate and Reverses Dietary and Leptin-Deficient Diabetes. *Endocrinology* (2004) 145(6):2594–603. doi: 10.1210/en.2003-1671
18. Morton G, Matsen M, Bracy D, Meek T, Nguyen H, Stefanovski D, et al. FGF19 Action in the Brain Induces Insulin-Independent Glucose Lowering. *J Clin Invest* (2013) 123(11):4799–808. doi: 10.1172/jci70710
19. Kc K, Shakya S, Zhang H. Gestational Diabetes Mellitus and Macrosomia: A Literature Review. *Ann Nutr Metab* (2015) 66:14–20. doi: 10.1159/000371628
20. Wang D, Zhu W, Li J, An C, Wang Z. Serum Concentrations of Fibroblast Growth Factors 19 and 21 in Women With Gestational Diabetes Mellitus: Association With Insulin Resistance, Adiponectin, and Polycystic Ovary Syndrome History. *PloS One* (2013) 8(11):e81190. doi: 10.1371/journal.pone.0081190
21. Wang D, Xu S, Ding W, Zhu C, Deng S, Qiu X, et al. Decreased Placental and Muscular Expression of the Fibroblast Growth Factor 19 in Gestational Diabetes Mellitus. *J Diabetes Investig* (2019) 10(1):171–81. doi: 10.1111/jdi.12859
22. Luo ZC, Delvin E, Fraser W, Audibert F, Deal C, Julien P, et al. Maternal Glucose Tolerance in Pregnancy Affects Fetal Insulin Sensitivity. *Diabetes Care* (2010) 33(9):2055–61. doi: 10.2337/dc10-0819
23. Kir S, Kliewer S, Mangelsdorf D. Roles of FGF19 in Liver Metabolism. *Cold Spring Harb Symp Quant Biol* (2011) 76:139–44. doi: 10.1101/sqb.2011.76.010710
24. Benoit B, Meugnier E, Castelli M, Chanon S, Vieille-Marchiset A, Durand C, et al. Fibroblast Growth Factor 19 Regulates Skeletal Muscle Mass and Ameliorates Muscle Wasting in Mice. *Nat Med* (2017) 23(8):990–6. doi: 10.1038/nm.4363
25. Sánchez-Infantes D, Gallego-Escuredo J, Díaz M, Aragonés G, Sebastiani G, López-Bermejo A, et al. Circulating FGF19 and FGF21 Surge in Early Infancy From Infra- to Supra-Adult Concentrations. *Int J Obes (Lond)* (2015) 39 (5):742–6. doi: 10.1038/ijo.2015.2
26. Shields B, Knight B, Hopper H, Hill A, Powell R, Hattersley A, et al. Measurement of Cord Insulin and Insulin-Related Peptides Suggests That Girls Are More Insulin Resistant Than Boys at Birth. *Diabetes Care* (2007) 30 (10):2661–6. doi: 10.2337/dc06-1501
27. Zhang J, Tian Y, Wang W, Ouyang F, Xu J, Yu X, et al. Cohort Profile: The Shanghai Birth Cohort. *Int J Epidemiol* (2019) 48(1):21–21g. doi: 10.1093/ije/dyy277
28. Metzger B, Gabbe S, Persson B, Buchanan T, Catalano P, Damm P, et al. International Association of Diabetes and Pregnancy Study Groups Recommendations on the Diagnosis and Classification of Hyperglycemia in Pregnancy. *Diabetes Care* (2010) 33(3):676–82. doi: 10.2337/dc09-1848
29. Wang W, Zhang L, Zheng T, Zhang G, Du K, Yang M, et al. Fetuin-A and Fetal Growth in Gestational Diabetes Mellitus. *BMJ Open Diabetes Res Care* (2020) 8(1):e000864. doi: 10.1136/bmjdrc-2019-000864
30. Zhu L, Zhang R, Zhang S, Shi W, Yan W, Wang X, et al. Chinese Neonatal Birth Weight Curve for Different Gestational Age. *Zhonghua Er Ke Za Zhi* (2015) 53(2):97–103. doi: 10.3760/cma.j.issn.0578-1310.2015.02.007
31. VanderWeele T. Mediation Analysis: A Practitioner's Guide. *Annu Rev Public Health* (2016) 37:17–32. doi: 10.1146/annurev-publhealth-032315-021402
32. Yang M, Chiu H, Wang W, Fang F, Zhang G, Zhu H, et al. Sex Dimorphism in the Associations of Gestational Diabetes With Cord Blood Adiponectin and Retinol-Binding Protein 4. *BMJ Open Diabetes Res Care* (2020) 8(1):e001310. doi: 10.1136/bmjdrc-2020-001310
33. Fang Q, Li H, Song Q, Yang W, Hou X, Ma X, et al. Serum Fibroblast Growth Factor 19 Levels Are Decreased in Chinese Subjects With Impaired Fasting Glucose and Inversely Associated With Fasting Plasma Glucose Levels. *Diabetes Care* (2013) 36(9):2810–4. doi: 10.2337/dc12-1766
34. Glman C, Angelin B, Rudling M. Pronounced Variation in Bile Acid Synthesis in Humans is Related to Gender, Hypertriglyceridaemia and Circulating Levels of Fibroblast Growth Factor 19. *J Intern Med* (2011) 270(6):580–8. doi: 10.1111/j.1365-2796.2011.02466.x
35. Stejskal D, Karpísek M, Hanulová Z, Stejskal P. Fibroblast Growth Factor-19: Development, Analytical Characterization and Clinical Evaluation of a New ELISA Test. *Scand J Clin Lab Invest* (2008) 68(6):501–7. doi: 10.1080/00365510701854967
36. Memon N, Griffin I, Lee C, Herdt A, Weinberger B, Hegyi T, et al. Developmental Regulation of the Gut-Liver (FGF19-CYP7A1) Axis in Neonates. *J Matern Fetal Neonatal Med* (2020) 33(6):987–92. doi: 10.1080/14767058.2018.1513483
37. Mittendorfer B. Insulin Resistance: Sex Matters. *Curr Opin Clin Nutr Metab Care* (2005) 8(4):367–72. doi: 10.1097/01.mco.0000172574.64019.98
38. Alur P. Sex Differences in Nutrition, Growth, and Metabolism in Preterm Infants. *Front Pediatr* (2019) 7:22. doi: 10.3389/fped.2019.00022

Conflict of Interest: The authors declare that the research was conducted in the absence of any commercial or financial relationships that could be construed as a potential conflict of interest.

frontiers in Endocrinology

ORIGINAL RESEARCH
published: 01 February 2022
doi: 10.3389/fendo.2021.797680

Maternal Nutrition During Gestation Alters Histochemical Properties, and mRNA and microRNA Expression in Adipose Tissue of Wagyu Fetuses

*Yi Zhang[1,2], Konosuke Otomaru[3], Kazunaga Oshima[4], Yuji Goto[4], Ichiro Oshima[1], Susumu Muroya[5], Mitsue Sano[6], Sanggun Roh[7] and Takafumi Gotoh[1,2]**

[1] Faculty of Agriculture, Kagoshima University, Kagoshima, Japan, [2] Kuju Agricultural Research Center, Kyushu University, Taketa, Japan, [3] Joint Faculty of Veterinary Medicine, Kagoshima University, Kagoshima, Japan, [4] Western Region Agricultural Research Center, National Agriculture and Food Research Organization (NARO), Oda, Japan, [5] Institute of Livestock and Grassland Science, National Agriculture and Food Research Organization (NARO), Tsukuba, Japan, [6] Department of Nutrition, School of Human Cultures, The University of Shiga Prefecture, Hikone, Japan, [7] Graduate School of Agricultural Science, Tohoku University, Sendai, Japan

OPEN ACCESS

Edited by:
Takahiro Nemoto,
Nippon Medical School, Japan

Reviewed by:
Elke Albrecht,
Leibniz Institute for Farm Animal Biology (FBN), Germany
Stephen Brent Smith,
Texas A&M University, United States

***Correspondence:**
Takafumi Gotoh
gotoh@agri.kagoshima-u.ac.jp

Specialty section:
This article was submitted to Experimental Endocrinology, a section of the journal Frontiers in Endocrinology

Received: 19 October 2021
Accepted: 15 December 2021
Published: 01 February 2022

Citation:
Zhang Y, Otomaru K, Oshima K, Goto Y, Oshima I, Muroya S, Sano M, Roh S and Gotoh T (2022) Maternal Nutrition During Gestation Alters Histochemical Properties, and mRNA and microRNA Expression in Adipose Tissue of Wagyu Fetuses. Front. Endocrinol. 12:797680. doi: 10.3389/fendo.2021.797680

We hypothesized that maternal low or high nutrition would give unique effects to morphological and molecular dynamics in adipose tissue of fetus of fatty breed Wagyu (Japanese Black) cattle which produce highly marbled beef. This study aimed to determine the effects of maternal energy intake in Wagyu cows, during gestation on fetal adipose tissue development, histochemical properties, and gene and microRNA (miRNA) expression. Cows were allocated to one of two nutritional energy groups: 120% (HIGH) or 60% nutritional requirements of (LOW). Fetuses (n = 6 per treatment) were removed from pregnant cows by cesarean section at fetal age 260 ± 8 days and euthanized. Subcutaneous adipose tissue (SAT), thoracic cavity visceral adipose tissue (TVAT), and perirenal adipose tissue (PAT) were collected for analysis. In histochemical analysis, in SAT and PAT, HIGH fetuses had greater diameter of adipocytes than LOW fetuses ($P<0.05$). Only in SAT, LOW fetuses had more Leptin (LEP) mRNA and tended to have more Peroxisome Proliferator-Activated Receptor gamma (PPARG) CCAAT-enhancer-binding proteins alpha (CEBPA) and Glucose transporter (GLUT) 4 mRNA ($P<0.10$). In all SAT, TVAT, and PAT, LOW fetuses had higher levels of the brown adipose tissue (BAT) biomarkers Uncoupling Protein (UCP) 1 and PPARG coactivator (PGC) 1α mRNA than HIGH fetuses ($P<0.08$). Meanwhile, in the other adipose tissue, LOW fetuses had lower PPARG, CEBPA, and Zinc Finger Protein (ZFP) 423 (in TVAT and PAT), FASN (in TVAT), LEP and GLUT4 mRNA (in PAT; $P<0.10$). In particular, in TVAT and PAT, LOW fetuses exhibited lower expression of WAT biomarkers (PPARG and ZFP423). Differential expression of various miRNAs related to adipogenesis between the LOW and HIGH

fetuses was detected in an adipose tissue-specific manner (P<0.10). Based on adipose tissue-specific effects of maternal nutrition, these findings suggested that poor maternal nutrition in Wagyu cattle increased BAT development in SAT, TVAT and PAT, while elevated maternal nutrition stimulated fetal SAT development compared with that of TVAT and PAT.

Keywords: maternal nutrition, Wagyu fetus, adipose tissue, gene expression, histochemical property

INTRODUCTION

Through its major contribution as a source of protein in people's diets, beef plays an important role in human health. To improve meat quality-related factors such as juiciness and flavor, intramuscular adipose tissue is crucial (1, 2). However, adipose tissue in carcasses, that is, SAT, renal adipose tissue, and intermuscular adipose tissue, is basically useless or wasted adipose tissue from the perspective of human consumption. Actually, we partly use Wagyu adipose tissue as a material for processed beef in Japan, however a huge amount of wasted adipose tissue is still abandoned. Wagyu (Japanese Black) cattle have not only a greater percentage of intramuscular fat but also a greater mass of carcass adipose tissue than European cattle (3). Although Wagyu is a unique animal model regarding obesity and intramuscular fat accumulation, we would like to shift the focus on its development from increasing intramuscular fat to instead reducing wasted adipose tissue. However, the molecular mechanism behind the accumulation of such adipose tissue in cattle is unknown.

Adipose tissue is scattered throughout the body but comprises 5% to 35% of cattle body mass, depending on age, genotype, and nutrition (4). In terms of the anatomically distinct sites where adipose tissue develops, there are three major sites of accumulation, visceral, subcutaneous, and intermuscular, which are further subdivided into smaller depots defined by anatomical location. The formation of discernible adipocytes begins mid-gestation in beef cattle (4–6). Prior and Laster (7) confirmed that the maternal period during mid- to late gestation in cattle is crucial for adipose tissue development. Additionally, during fetal muscle development, a small portion of the progenitor cells differentiate into adipocytes, which also form intramuscular fat and marbling in the offspring (8). Some studies have demonstrated that the manipulation of maternal nutrition, including over- and undernutrition during gestation, impacts on adipose tissue development and the expression of adipogenesis marker genes in fetuses (4, 9, 10). This suggests that maternal nutrition during gestation plays an important role in adipose tissue development in fetuses.

There are two types of adipose tissue in mammals, white adipose tissue (WAT) and brown adipose tissue (BAT), which have markedly different morphological roles and biological functions (11). In newborns, BAT is essential for ensuring effective adaptation to the extrauterine environment, and the growth of both WAT and BAT during gestation is largely dependent on the supply of nutrients from mother to fetus (12). There are differences of depots place between rodents (interscapular), large mammals and human (around the central organs and supraclavicular region; 12). Change in maternal nutrition at defined stages of gestation would ultimately have long-term adverse effects on the offspring by modifying normal profiles of adipose development. For example, suboptimal maternal nutrition during early to mid-gestation was reported to result in excess macrophage accumulation and the onset of insulin resistance in an adipose tissue depot-specific manner in offspring (12).

At the molecular level, many important factors involved in adipogenesis have been found (PPARG, CEBPA, Stearoyl-CoA desaturase (SCD), Fatty acid synthase (FASN), Fatty acid binding protein (FABP) 4, LEP, TNFα, and ZFP423) (13–17), and in recent years factors involved in the development of brown adipocytes (Uncoupling protein (UCP) 1, PR/SET domain (PRDM) 16, and PGC1α have also been identified (18). Factors related to adipocyte development and metabolism (IGF1, IGF2 GLUT4, INSR, IRS1 PI3K, AKT1, AKT2, and mTOR1) have been considered (19–22). Furthermore, as another factors affecting these genes expression, miRNAs (miRNA-15b, 16 b, 19b, 27b, 33a, 101, 130a, 148a, 152, 196a, 204, 296-3p, and 378) have been noticed (23–33). It has been still unclear how maternal nutrition affects these factors in fetal adipose tissues of Wagyu cattle and its differences among different adipose depots.

We also previously demonstrated that Wagyu cows fed diets with reduced [60% of nutritional requirement: Japan Feeding Standard for Beef Cattle (34;JSFBC)] and slightly greater than required nutritional content (120% of nutritional requirement: JSFBC) from pre-conception to gestational day 260 produced fetuses with phenotypic differences, including fetuses from the latter group having greater adipose tissue mass (2.12-fold), muscle mass (1.42-fold), bone mass (1.24-fold), and fetal body weight (1.39-fold; 35). Several ruminant groups were used to examine the impacts of under- and overnutrition on fetal development; few phenotypic differences in fetuses were identified, although there were differences in gene expression in muscle (36–40). Fetuses with different phenotypes were obtained by different maternal nutrition during gestation (35), these differences might alter the metabolic rate of the whole fetus and change adipose tissue metabolism. We hypothesized that inadequate maternal energy status would alter fetal adipose tissue development in an adipose tissue depot-specific manner in Wagyu fetuses. The objective of this study was thus to determine the consequences of higher or lower maternal energy status throughout gestation on Wagyu fetuses as follows: 1) on the morphology of adipocytes in SAT, and PAT;

and 2) on the expression of genes and miRNAs related to growth, adipogenesis, and glucose metabolism in SAT, TVAT, and PAT.

MATERIALS AND METHODS

Animals, Diets, and Experimental Design

The animal study was reviewed and approved by Kagoshima University Animal Care and Use Committee (A18007). Written informed consent was obtained from the owners of the animals for their participation in this study. The experimental details were previously reported elsewhere (35). Briefly, multiparous Wagyu cows (n = 32) were obtained from Kagoshima University Iriki farm (n = 12) and Western Region Agricultural Research Center (n = 20). The cows were randomly assigned to two dietary treatment groups matched for body mass: diets formulated to meet either 60% (LOW) or 120% (HIGH) of their Japan Feeding Standard for Beef Cattle (34)-predicted energy requirements using formula feed. All cows were housed in a drylot, and diets were individually provided twice daily for 2 months prior to and throughout gestation using stanchions that locked each cow in until all feed had been consumed.

The total mixed ration consisted of whole-crop silage, composed of rice plants, dried timothy grass, rye straw, brown rice, beer lees, sugar cane pellets, tofu lees, soy sauce cake, sugar cane bagasse, rice bran, corn steep liquor, condensed sweet potato distillers' solubles, rice trienol, calcium, and water. The final crude nutrient composition of mixed feed, on a dry-matter basis, was 56.1% NDF, 36.0% ADF, 11.1% ash, 8.00% crude protein, 0.60% calcium, and 0.30% phosphate. The metabolizable energy provided by the feed was 8.56 MJ/kg dry matter.

All cows were synchronized using a controlled internal drug release device (Easybreed, InterAg Co. Ltd., Hamilton, New Zealand). All cows were inseminated with frozen male-sorted semen from the same sire (Yurikatsuyasu, Kedaka line) to produce half-brothers and to minimize other influencing effects except for nutritional status. After breeding, six cows from each group became pregnant.

Slaughter and Sample Collection

Maternal body weight was measured every month from the start of the study until cows were transported to Kagoshima University Veterinary Teaching Hospital on day 260 ± 8.3 of gestation. Fetuses were obtained by cesarean section and euthanized. The fetal body weight, and weights of carcass muscle, carcass bone, and adipose tissue depots including SAT, TVAT, and PAT were measured as described by Zhang et al. (35).

Sample Processing

SAT was collected from total adipose tissue between skin and the outermost parts of skeletal muscle from the right carcass to measure the weight. SAT samples for histochemical and molecular analysis were taken from adipose tissue located around between forelimb and body trunk. TVAT was collected from the thoracic and visceral cavity of the right-side carcass, and PAT was taken from adipose tissue covering the left kidney. The fetal adipose tissue was dissected free of other connective tissue and these samples for histological analysis were immediately covered with Tissue Tek (tissue freezing medium; Sakura Fine Technical, Tokyo, Japan), rinsed in ice-cold saline, snap-frozen in liquid nitrogen, and stored at −80°C until use.

Histochemical and Immunohistochemical Analyses

A 1-cm^3 core of adipose tissue from SAT, TVAT and PAT, immediately covered with tissue freezing medium (Tissue Tek; Sakaura Fine Technical, Tokyo, Japan), snap-frozen in liquid nitrogen, and stored at −80°C until analysis. Adipose tissue samples were sectioned at 10-μm thickness using a cryostat microtome CM3050 S (Leica, Bensheim, Germany). These sections were fixed by 10% formaldehyde and stained by using Harris Modified Hematoxylin (Fisher Scientific, Fair Lawn, NJ, USA) and Eosin Y (EMD Chemicals, Gibbstown, NJ, USA).

Rabbit polyclonal antibody to human Ucp1 (ab10983) was obtained from Abcam (Cambridge, MA, UK) to examine immunolocalization in the SAT, TVAT, and PAT. According to the manufacturer, this antibody was predicted to recognize bovine Ucp1 (41). Endogenous peroxidase was blocked using BLOXALL™ Endogenous Peroxidase and Alkaline Phosphatase Blocking Solution (Vector Laboratories, Inc., Burlingame, CA, USA) for 10 min at room temperature. The sections were washed with PBS and treated using VECTASTAIN ABC Kit, Peroxidase (Rabbit IgG) (Vector Laboratories, Inc.). In accordance with the manufacturer's instructions, normal goat serum blocking solution was applied for 20 min at room temperature. After washing with PBS, the sections were incubated with the anti-Ucp1 antibody (diluted 1:400) overnight at 4°C. The sections were then washed with PBS and incubated with a biotinylated goat anti-rabbit secondary antibody for 30 min at room temperature. After washing with PBS, the sections were incubated with peroxidase-conjugated streptavidin for 30 min at room temperature. After washing with PBS, the DAB substrate kit (Nichirei Biosciences, Tokyo, Japan) was applied to the sections for 5 min at room temperature, followed by counterstaining with hematoxylin. The sections were then dehydrated and mounted. The experiments were repeated at least three times and the positive staining was reproducibly detected. The sections were captured with an BZ-X800 ALL-IN-ONE fluorescence microscope (Keyence, Tokyo, Japan) under the same microscope objective (30×), and five randomly chosen fields were taken per section for a total of 20 images per animal. Images were randomly selected for analysis, the diameter of adipocytes based on the average of maximum dimension of the long axis and that of the axis perpendicular to the long axis was calculated for at least 50 cells per field area, and at least 250 adipocytes were measured per animal *via* image analysis using CELL image analysis software (Keyence, Tokyo, Japan) and the cross-sectional area (CSA) of adipocyte was calculated by using the average of the diameter.

Total RNA Extraction and Real-Time qPCR

Total RNA from each adipose tissue was extracted from less than 100 mg of tissue using miniRNeasy Lipid Tissue Kit (Qiagen,

Germantown, MD, USA), in accordance with the manufacturer's instructions. Total RNA samples were quantified using a spectrophotometer (ND-1000; NanoDrop, Wilmington, DE, USA). The purity of RNA (A_{260}/A_{280}) for all samples was above 1.9 and the RNA was stored at −80°C until cDNA synthesis. Total RNA (500 ng) from each individual calf and tissue was reverse-transcribed with the High-Capacity cDNA Reverse Transcription Kit (Life Technologies Inc., Carlsbad, CA, USA), in accordance with the manufacturer's instructions. The RT products (cDNA) were stored at −30°C for relative quantification by PCR.

The primers were designed using Primer Express 3.0 with a minimum amplicon size of 80 bp (when possible, amplicons of 100–200 bp were chosen), and aligned against publicly available databases using BLASTN (Basic Local Alignment Sequence Tool for Nucleic Acid) at the website of the National Center for Biotechnology Information (NCBI; Bethesda, MD, USA; **Table 1**). Before qPCR, primers were tested in a 20 µl PCR reaction using the same protocol as described for qPCR except for the final dissociation protocol. For primer testing, we used a universal reference cDNA (RNA mixture from four different bovine tissues) to ensure identification of the desired genes. A total of 5 µl of the PCR product was run in a 2% agarose gel stained with ethidium bromide (2 µl). The remaining 15 µl was cleaned using the QIAquick PCR Purification Kit (Qiagen). Only those primers that did not present as a primer-dimer, had a single band at the expected size in the gel, and had the right amplification product (verified by sequencing) were used for qPCR. The accuracy of each primer pair was also evaluated by the presence of a unique peak during the dissociation step at the end of quantitative PCR (qPCR).

Real-time PCR analysis was performed in triplicate using 100 ng of cDNA in 96-well fast plates using the SYBR Fast Master Mix ABI Prism (D-Mark Biosciences, Toronto, Canada) and the Step-One Plus Real-time PCR system (Life Technologies Inc.). A blank sample and a minus RT were added to control for nonspecific amplification. Relative standard curves, made from a serial dilution of pooled cDNA from the tissue of interest and ranging from 20 to 0.02 ng, were used to determine the relative quantity of each sample. The amplification efficiency for each gene was determined using serial dilution of tissue-specific cDNA and was found to be 100 ± 10% for all genes. The resulting qPCR amplicons were also sequenced to confirm their identity. For each tissue, two to four endogenous controls were tested and the best individual or combination of endogenous control was chosen using NormFinder. Therefore, Ribosomal protein L32 (RPL32) and Ribosomal protein S18 (RPS18) were used as endogenous controls (**Table 1**) to correct for RNA extraction and reverse-transcription efficiency in the adipose tissues (SAT, TVAF, and PAT, respectively). The endogenous controls were also tested for any treatment effect and were found to be stable among samples within each tissue type, confirming their usefulness as suitable endogenous controls. Sequence-specific products were identified by generating a melting curve in which the Cycle Threshold (CT) value represented the cycle number at which a fluorescent signal was statistically greater than the background. The relative mRNA expression was quantified using the $2^{-\Delta\Delta Ct}$ method and thereby the fold change was calculated (**Supplementary Tables**).

Quantitative RT-PCR Analysis for MicroRNA

Total RNA from each adipose tissue was extracted from less than 100 mg of adipose tissue using the miRNeasy Kit (Qiagen, Germantown, MD, USA), in accordance with the manufacturer's instructions. Following that, all total RNA samples were quantified using a spectrophotometer (ND-1000; NanoDrop, Wilmington, DE, USA). The purity of RNA (A_{260}/A_{280}) for all samples was above 1.9, and total RNA from each individual calf and tissue was reverse-transcribed with Mir-X miRNA First-Strand Synthesis Kit (Takara Bio USA, Inc.), in accordance with the manufacturer's instructions. Briefly, cDNAs were reverse-transcribed from 100 ng of total RNA using 2× mRQ buffer and mRQ enzyme miRNA assay. This was performed in a thermal cycler, in which the tube was incubated for 1 h at 37°C, followed by termination at 85°C for 5 min to inactivate the enzymes. After that, 90 µl of ddH_2O was added to bring the total volume to 100 µl. Next, the reverse-transcription product was amplified with TB Green qRT-PCR miRNA assay, in accordance with the manufacturer's instructions, while fluorescence signal was detected with a Plus-one Real-time PCR System Detector® (Applied Biosystems). U6 snRNA was selected as reference miRNA in this study due to its stable expression among all animals and treatments. In the current study, the expression of miRNAs (miR-15b, 16b, 19b, 27b, 33a, 101, 130a, 148a, 152, 196a, 204, 296-3p, and 378) was analyzed (**Table 2**). The relative quantification of miRNA (or miR) was performed using the $2^{-\Delta\Delta CT}$ method (**Supplementary Tables**).

Statistical Analysis

Data were analyzed as a randomized complete block design with cow as the experimental unit. The fixed effect was maternal treatment and the random effect included maternal farm of origin. Data were analyzed using SAS (Version 9.2, SAS Institute, Inc. Carey, NC, USA) and treatment means were compared using the PDIFF option. Expression differences of mRNA and microRNA between three kinds of adipose tissue depots (SAT, TVAT, and PAT) were determined using Dunnett's modified Tukey-Kramer pairwise multiple comparison test (DTK). Differences were considered significant at $p < 0.05$ and trends were considered at $0.05 < p < 0.10$.

RESULTS

Phenotypic Data

The fetuses obtained in this experiment at slaughter (day 260 ± 8.3) showed marked differences between the LOW and HIGH groups, as reported by Zhang et al. (35; **Table 3**). The body, carcass muscle, carcass adipose tissue, and carcass bone weights of LOW fetuses were lower than those of HIGH

TABLE 1 | Primer sequences for gene expression measured by real-time PCR.

	Gene		Sequence 5'–3'	GenBank Accesion	Product Size (bp)
Peroxisome proliferator-activated receptor gamma	*PPARG*	Fwd	ACCACCGTTGACTTCTCCAG	NM_181024.2	137
		Rev	ACAGGCTCCACTTTGATTGC		
CCAAT/enhancer-binding protein alpha	*CEBPA*	Fwd	GCTGACCAGTGACAATGACC	NM_176784.2	109
		Rev	CTTGACCAGGGAGCTCTCG		
Stearoyl-CoA desaturase (delta-9-desaturase)	*SCD*	Fwd	CGACCTAAGAGCCGAGAAGC	NM_173959.4	195
		Rev	GCAGCACTATTCACCAGCCAG		
Fatty acid synthase	*FASN*	Fwd	CTACCAAGCCAGGCAGGTC	NM_001012669.1	226
		Rev	GCCATTGTACTTGGGCTTGT		
Fatty acid binding protein 4	*FABP4*	Fwd	ACAGGAAAGTCAAGAGCATCGT	NM_174314	235
		Rev	TGGACAACGTATCCAGCAGA		
Leptin	*LEP*	Fwd	TGACATCTCACACACGCAGTC	XM_010804453.3	114
		Rev	ATCGCCAATGTCTGGTCCAT		
Tumor Necrosis Factor α	*TNFα*	Fwd	AAGCATGATCCGGGATGTGG	NM_173966.3/ XM_027524120.1	180
		Rev	GACTGCTCTTCCCTCTGGGG		
Uncoupling protein 1	*UCP1*	Fwd	AAACAGAAGGGCCAGTGAAA	NM_001166528.1	220
		Rev	TGCAGTCTGACCTTGACCAC		
PR/SET Domain 16	*PRDM16*	Fwd	CCTTCCCGGGTCCTTACCTA	XM_015475185.2	152
		Rev	CAGGTGGGCAGGTGTGATAG		
PPARG coactivator 1 α	*PGC1α*	Fwd	TGCAGTACACATCAGCCTCA	NM_177945.3	95
		Rev	TGCCAGGAGTTTGGTTGTGAT		
Zinc finger protein 423	*ZFP423*	Fwd	CGCTCGGTGAAAGTTGAAGA	NM_001101893.1	216
		Rev	CTGACAGTGATCGCAGGTGT		
Insulin-like growth factor 1	*IGF1*	Fwd	GATGCTCTCCAGTTCGTGTG	NM_001077828	141
		Rev	CTCCAGCCTCCTCAGATCAC		
Insulin-like growth factor 1 receptor	*IGF1R*	Fwd	CAAAGGCAATCTGCTCATCA	NM_001244612	139
		Rev	CAGGAAGGACAAGGAGACCA		
Insulin-like growth factor 2 receptor	*IGF2*	Fwd	CCAGCGATTAGAAGTGAGCC	NM_174087.3	95
		Rev	AGACCTAGTGGGGCGGTC		
Insulin-like growth factor 2 receptor	*IGF2R*	Fwd	GCAATGCTAAGCTTTCGTATTACG	NM_174352	188
		Rev	GGTGTACCACCGGAAGTTGTATG		
Insulin receptor	*INSR*	Fwd	CCTATGCCCTGGTGTCACTT	XM_002688832	114
		Rev	GCTGCCTTAGGTTCTGGTTG		
Insulin receptor substrate 1	*IRS1*	Fwd	TGGACATCACAGCAGAATGAAGA	XM_003585773.5	287
		Rev	CATGTGGCCAGCTAAGTCCT		
Phosphoinositide-3-kinase	*PI3K(R2)*	Fwd	AACCGAGAGATCGACAAGCG	NM_174576.2	99
		Rev	TTCTGAGTGAGCCACACAAGG		
Protein kinase B	*AKT1*	Fwd	TGAAGACTTTCTGCGGGACC	NM_173986.2	141
		Rev	CCTGGTTGTAGAAGGGCAGG		
AKT serine/threonine kinase 2	*AKT2*	Fwd	ACGAGGAAGGAGTAAAGCGA	NM_001206146.1	148
		Rev	AGCCAGCCTTCTTTGATGACA		
Mechanistic target of rapamycin kinase	*mTOR1*	Fwd	CCTTGGCACAACAGTGCATC	XM_002694043.6	285
		Rev	AGGTCCTCATGTCCTCGTGA		
Glucose transporter 4	*GLUT4*	Fwd	GCTTCCAACAGATCGGCTCTG	NM_174604.1	174
		Rev	CCAGCCAGGTCTCATTGTAGC		
Reference genes	*RPS18*	Fwd	TTCCAGCACATCTTGCGAGT	NM_001033614.2	178
		Rev	TCACACGTTCCACCTCATCC		
	RPL 32	Fwd	GCCATCTCTGACTCGGCATC	NM_001034783.2	169
		Rev	TTGAATCTTCTGCGCACCCT		

fetuses ($p < 0.05$). Regarding the specific adipose depots, the weights of SAT (3.03-fold), TVAT (1.47-fold), and PAT (1.45-fold) were greater in HIGH fetuses than in LOW fetuses, as shown in **Table 3** (35).

Adipose Tissue Morphology

The frequency of adipocytes CSA in SAT showed similar patterns between LOW and HIGH fetuses, however, the relative frequency of 201-400 μm^2 adipocyte CSA was somewhat higher in LOW fetuses (**Figure 1**, S-1). The frequency of adipocyte CSA in TVAT showed higher frequency of 801-1000 μm^2 adipocyte CSA in LOW fetuses and, on the other hand, there were two peaks of relative frequencies (601-800 μm^2 and 1201-1400 μm^2) in HIGH fetuses (**Figure 1**, T-1). The frequency of adipocyte CSA in PAT showed the highest at 801-1000 μm^2 in LOW fetuses, and meanwhile at 1001-1200 μm^2in HIGH fetuses (**Figure 1**, P-1). In SAT ($p < 0.01$) and PAT ($p < 0.05$), the average adipocyte diameter was greater in HIGH fetuses than in LOW ones (**Figure 1**, S-2, P-2). Consistent with these results, the adipocyte number/unit area of SAT ($p < 0.05$) and PAT ($p < 0.01$) was greater in LOW fetuses than in HIGH ones (**Figure 1**, S-3, P-3). There were no differences in adipocyte diameter and adipocyte number/unit area in TVAT between the treatment groups (**Figure 1**, T-1, 2 and 3).

TABLE 2 | Primer sequences for miRNA expression measured by real-time PCR.

Representative miRNA	Accession	Mature Sequence	Forward Primer 5'–3'	Length
bta-miR-15b	MIMAT0003792	20 - uagcagcacaucaugguuuaca - 41	TAGCAGCACATCATGGTTTACA	22
bta-miR-16b	MIMAT0003525	17 - uagcagcacguaaauauuggc - 37	TAGCAGCACGTAAATATTGGC	21
bta-miR-19b	MIMAT0004337	54 - ugugcaaauccaugcaaaacuga - 76	TGTGCAAATCCATGCAAAACTGA	23
bta-miR-27b	MIMAT0003546	61 - uucacaguggcuaaguucugc - 81	TTCACAGTGGCTAAGTTCTGC	21
bta-miR-33a	MIMAT0009294	6 - gugcauuguaguugcauugca - 26	GTGCATTGTAGTTGCATTGCA	21
bta-miR-101	MIMAT0003520	49 - uacaguacugugauaacugaa - 69	GCGCTACAGTACTGTGATAACTGAA	25
bta-miR-130a	MIMAT0009223	55 - cagugcaauguuaaaagggcau - 76	CAGTGCAATGTTAAAAGGGCAT	22
bta-miR-148a	MIMAT0003522	44 - ucagugcacuacagaacuuugu - 65	TCAGTGCACTACAGAACTTTGT	22
bta-miR-152	MIMAT0009238	53 - ucagugcaugacagaacuuggg - 74	TCAGTGCATGACAGAACTTGGG	22
bta-miR-196a	MIMAT0009255	16 - uagguaguuucauguuguuggg - 37	TAGGTAGTTTCATGTTGTTGGG	22
bta-miR-204	MIMAT0004338	23 - uucccuuugucauccuaugccu - 44	TTCCCTTTGTCATCCTATGCCT	22
bta-miR-296-3p	MIMAT0009273	47 - gaggguuggggcggaggcuuucc - 68	GAGGGTTGGGCGGAGGCTTTCC	22
bta-miR-378	MIMAT0009305	43 - acuggacuuggagucagaaggc - 64	ACTGGACTTGGAGTCAGAAGGC	22
U6-F		ctcgcttcggcagcaca	AACGCTTCACGAATTTGCGT	20

**bta, Bos taurus; miR, microRNA.*

TABLE 3 | Effects of LOW or HIGH maternal nutrition of Wagyu cows during the entirety of gestation on the fetal BW and fat weight.

Item	Weight (g)		*p*-value	HIGH/LOW[5]	Ratio [3](%)		*p*-value
	LOW[1]	HIGH[2]			LOW	HIGH	
Animals, No.	6	6			6	6	
Fetal BW, g	23390.0	32653.0	0.0018	1.396			
fat weight[4], g	333.0	708.0	0.0004	2.126	5.4	8.1	0.023
TVAT[6]	25.5	37.6	0.018	1.475	0.5	0.5	0.937
SAT	41.5	125.8	0.006	3.032	0.8	1.6	0.032
PAT[7]	82.2	119.2	0.006	1.450	0.4	0.4	0.769
other fat	183.8	425.4					

*Data are mean ± standard error. [1,2]Wagyu cows were fed diets providing a low (60%; LOW) or high nutrition level (120%: HIGH), according to the JFSBC (34) nutritional requirements. [3]Ratio of mass relative to the calculated fetal half-carcass (right side) mass. [4]Mass calculated for the right half of the carcass with right-side perirenal adipose tissue. [5]Fold difference between the high-nutrition group and the low-nutrition group for variables with p<0.10. [6]The weights of adipose tissue of the thoracic or peritoneal cavity on the right side of the carcass. [7]The adipose tissue surrounding the right and left kidneys. *These data are from Zhang et al. (35).*

mRNA Expression

In SAT, LOW fetuses had a higher level of LEP ($p = 0.045$) and tended to have higher PPARG ($p = 0.078$), CEBPA ($p = 0.098$), UCP1 ($p = 0.072$), PGC1 ($p = 0.053$), IGF2 ($p = 0.098$), AKT2 ($p = 0.087$), and GlUT4 ($p = 0.092$) mRNA levels than HIGH fetuses (**Figures 2A, B**).

In TVAT, LOW fetuses had higher PGC1α ($p = 0.045$) and lower ZFP423 ($p = 0.042$) mRNA levels, and tended to have a higher UCP1 ($p = 0.067$) mRNA level than HIGH fetuses (**Figure 2A**). Meanwhile, LOW fetuses had lower PPARG($p = 0.059$), CEBPA ($p = 0.053$), FASN ($p = 0.086$), IGF2 ($p = 0.069$), and IRS1 ($p = 0.071$) mRNA levels than HIGH fetuses (**Figure 2A, B**).

In PAT, LOW fetuses had a higher UCP1 ($p = 0.046$) mRNA level and tended to have a higher PGC1α ($p = 0.073$) mRNA level than HIGH fetuses. Conversely, LOW fetuses had lower PPARG ($p = 0.066$), CEBPA ($p = 0.052$), LEP ($p = 0.068$), TNFα ($p = 0.079$), ZFP423 ($p = 0.078$), and GLUT4 ($p = 0.054$) mRNA levels than HIGH fetuses (**Figure 2A, B**).

The expression of PPARG (both LOW and HIGH), CEBPA (both LOW and HIGH), IGF2 (both LOW and HIGH), and AKT2 (HIGH) mRNAs was greater in SAT than in TVAT and PAT ($p < 0.05$) with no significant difference in the TVAT and PAT (**Figure 3**). The expression of SCD (LOW) and IGF2R (LOW) mRNAs was greatest in SAT and least in PAT ($p < 0.05$). The expression of LEP(LOW), TNFα (HIGH), and PI3K (LOW) mRNAs was greater in SAT and TVAT relative to PAT ($p < 0.05$) without significant difference in the SAT and the TVAT. The expression of UCP1 (LOW) mRNA was greatest in PAT and least in TVAT ($p < 0.05$). The expression of UCP1 (HIGH), PRDM16 (LOW), PGC1 (both LOW and HIGH), ZFP423 (HIGH), IGF1 (HIGH), IGF2R (HIGH), PI3K (HIGH), mTOR1 (HIGH), and GLUT4 (HIGH) mRNAs was greater in SAT and PAT than in TVAT ($p < 0.05$), whereas in the SAT and the PAT, they showed no significant difference. Conversely, the expression of IGF1 (LOW) and IGF1R (LOW) m RNAs was greater in TVAT than in SAT and PAT ($p < 0.05$) without significant difference in the SAT and the PAT. The expression of IGF1R (HIGH) mRNA was greater in PAT than in SAT and TVAT ($p < 0.05$) without significant difference in the SAT and the TVAT. No significant difference was observed between SAT, TVAT and PAT in the expression of other genes in the nutritional treatment groups not shown so far (**Figure 3**).

Immunohistochemistry

Immunohistochemical analysis of SAT, TVAT, and PAT revealed UCP1-positive staining as a marker of brown adipocytes in both LOW and HIGH fetuses (**Figure 4**).

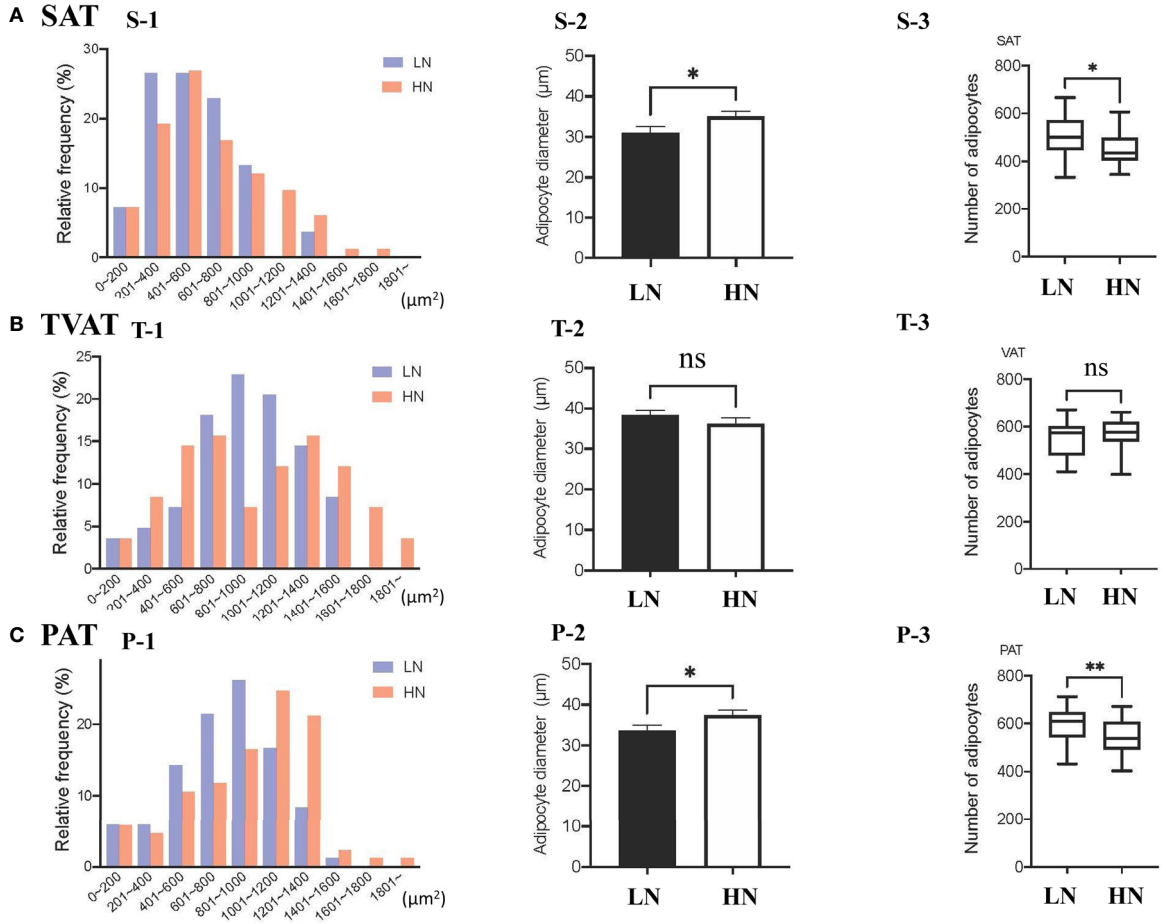

FIGURE 1 | **(A)** Relative frequency distribution of SAT CSA (S-1), diameter (S-2), and number of adipocytes within the same area (S-3) in subcutaneous adipose tissue (SAT) between LOW and HIGH fetuses. **(B)** Relative frequency distribution of TVAT CSA (T-1), diameter (T-2), and number of adipocytes in the same area (T-3) in thoracic cavity visceral adipose tissue (TVAT) between LOW and HIGH fetuses. **(C)** Relative frequency distribution of PAT CSA (P-1), diameter (P-2), and number of adipocytes within the same area (P-3) in perirenal adipose tissue (PAT) between LOW and HIGH fetuses. Fetuses: 260 ± 8.3 days of fetal age. LOW: n=6. HIGH: n=6. Values are means with standard errors. Significant differences between fetal groups are denoted by $^{*}p < 0.05$ and $^{**}p < 0.01$.

miRNA Expression

In SAT, Low fetuses had a higher level of miR-15b ($p = 0.021$) and tended to have higher levels of miR-33a ($p = 0.057$) and miR-196a ($p = 0.054$; **Figure 5**). Conversely, LOW fetuses had a lower level of miR-378 ($p = 0.042$) and tended to have a lower level of miR-152 ($p = 0.088$).

In TVAT, LOW fetuses had a higher level of miR-15b ($p = 0.011$). Meanwhile, LOW fetuses had lower levels of miR-33a ($p = 0.014$), miR-204 ($p = 0.022$), and miR-378 ($p = 0.009$) and tended to have a lower level of miR-101 ($p = 0.059$; **Figure 5A**).

In PAT, LOW fetuses had higher levels of miR-196a ($p = 0.018$) and miR-378 ($p = 0.047$) than HIGH fetuses. Similarly, LOW fetuses tended to have a higher level of miR-101 ($p = 0.072$). Conversely, LOW fetuses had lower levels of miR-16b ($p = 0.013$) and miR-27b ($p = 0.034$) than HIGH fetuses. Simultaneously, LOW fetuses tended to have lower levels of miR-33a ($p = 0.064$), miR-204 ($p = 0.053$), and miR-296-3p ($p = 0.069$; **Figure 5A**).

The expression of miR-33a (LOW) and 130a (LOW) was greater in SAT than in TVAT and PAT ($p < 0.05$) with no significant difference in the TVAT and the PAT (**Figure 5B**). The expression of miR-15b (LOW) and 196a (LOW) was greatest in SAT and least in TVAT ($p < 0.05$). The expression of miR-15b (HIGH), 16b (LOW), 101 (LOW), and 296-3p (HIGH) was greater in SAT and PAT relative to TVAT ($p < 0.05$) without significant difference in the SAT and the PAT. The expression of miR-16b (HIGH), 152 (HIGH), and 378 (LOW) was greater in PAT than in SAT and TVAT ($p < 0.05$) with no significant difference in the SAT and the TVAT. The expression of miR-196a (HIGH) was greatest in TVAT and least in SAT ($p < 0.05$). No significant difference was observed between SAT, TVAT and PAT in the expression of other miRNAs in the nutritional treatment groups not shown so far (**Figure 5B**).

DISCUSSION

The function of adipose tissue changes with development. In the newborn, BAT is needed to ensure an effective response to the

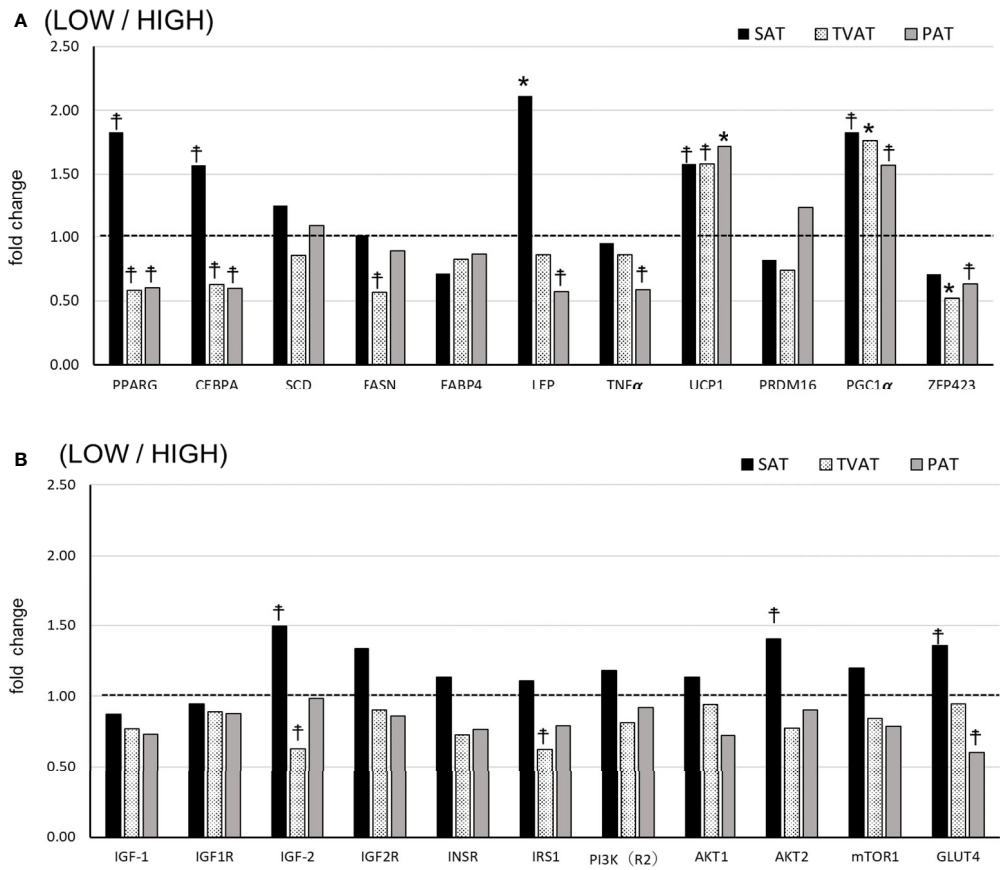

FIGURE 2 | Comparison of fold change of mRNA abundance in subcutaneous (SAT), thoracic cavity visceral (TVAT), and perirenal adipose tissues (PAT) between LOW and HIGH fetuses in Wagyu cattle. **(A)** Adipogenesis including brown adipose tissues (LOW/HIGH), **(B)** growth factors, and glucose metabolism (LOW/HIGH). The horizontal dotted line (at the value "1") showed the relative mRNA expression of the HIGH fetuses. The foldchange was calculated as the relative expression based on the mean of the target gene Ct value of LOW and HIGH fetuses. Fetuses: 260 ± 8.3 days of fetal age. LOW: n=6. HIGH: n=6. *Significant difference and †trend ($p < 0.05$ and $p < 0.1$, respectively) between LOW and HIGH fetuses.

extrauterine environment. Overall adipose tissue mass increases during late gestation, with a mixture of white and brown adipocytes. After that, during postnatal life, some, but not all, adipose depots are replaced by white adipocytes. The changes in maternal nutrition at the mid and the late gestation modify adipose tissue development profiles (12, 42). The gene expression change occurs in an adipose tissue depot-specific manner in offspring born to mothers fed lower nutrition from early to mid-gestation in cattle (43). Maternal low nutrition decreased the expression of Adipocyte Protein (AP) 2 and GLUT4 mRNAs and increased the expression of Cluster of Differentiation (CD) 36 mRNAs in PAT, but not in SAT of offspring in crossbred Angus cattle (43). However, the detailed differential-responses and its relationships of mass and molecular dynamics between SAT, TVAT and PAT in fetuses of different maternal nutrition have not been examined well in cattle. In this study, we demonstrated that lower or higher maternal nutrition during gestation could alter adipose tissue mass, adipocyte size, and gene expression in an adipose-tissue-specific manner in fetuses of Wagyu cattle. In all adipose tissue of LOW fetuses, gene expression analysis indicated enhanced BAT development. In addition, gene expression related to WAT differed between SAT and the other adipose tissues (TVAT and PAT), suggesting the different susceptibility of adipose tissue to maternal nutrition.

There is a need to develop an efficient feeding system because the cost of feeding cattle is increasing. Although the body adipose tissue of beef cattle is not only for energy storage but also an endocrine organ affecting metabolism (44) as well as meat quality and quantity (3), in the beef industry carcass adipose tissue is practically and economically wasted, apart from intramuscular adipose tissue (45). Regulating the development of adipose tissue in cattle could lead to the development of an efficient feeding system. In cows, not only growth but also reproduction and maintenance of body functions require adequate nutrition. Animals use energy and nutrients obtained from feed in various ways. Ferrell and Jenkins (46) reported that, in mature beef cows, maintenance requirements represent approximately 70% to 75% of the total annual energy requirements. In this study, we established two nutritional groups allocated 60% and 120% of nutritional requirements during gestation and identified

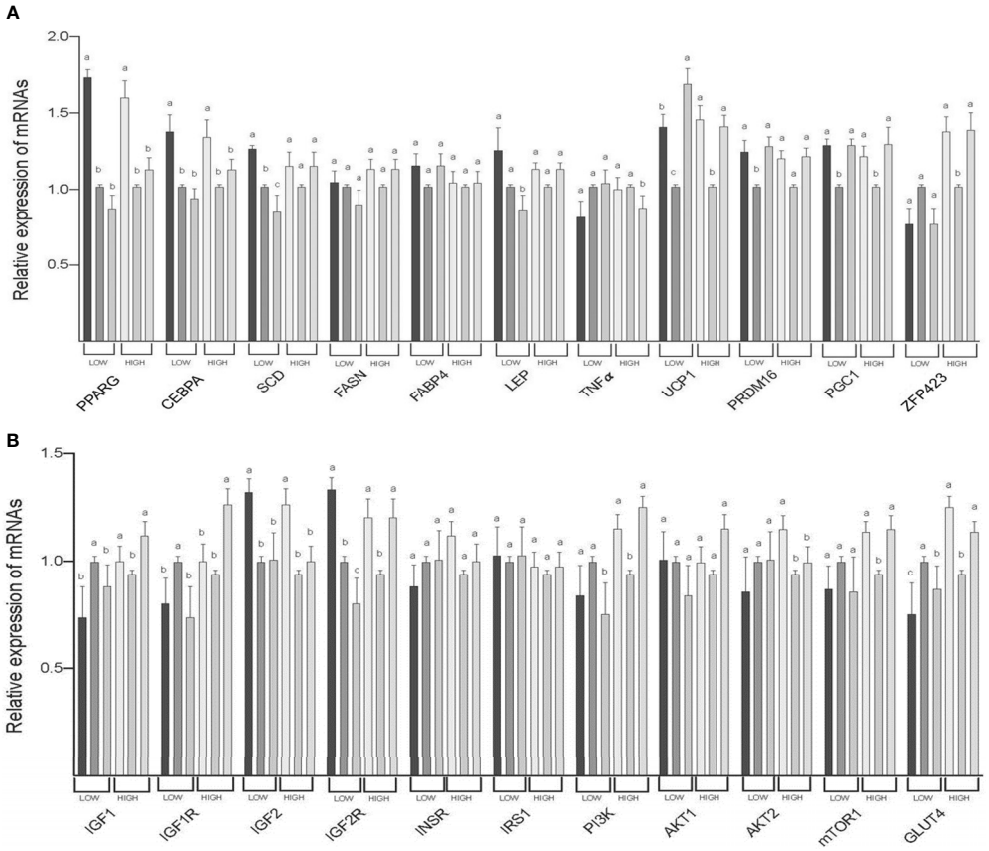

FIGURE 3 | Comparison of mRNA abundance among subcutaneous (SAT), thoracic cavity visceral (TVAT), and perirenal adipose tissues (PAT) in the LOW and the HIGH fetuses in Wagyu cattle. **(A)** Adipogenesis including brown adipose tissues (LOW/HIGH), **(A)** growth factors, and glucose metabolism (LOW/HIGH). Fetuses: 260 ± 8.3 days of fetal age. LOW: n=6. HIGH: n=6. ^{a,b,c}Significant difference ($p < 0.05$) among SAT, TVAT, and PAT in the LOW and the HIGH fetuses.

clear phenotypic differences in fetuses between them (35). Chronic restriction of maternal nutrition has been indicated to reduce basal metabolic rate (47, 48) and to impact fetal development (42, 49). In this study, differences in the development of adipocytes of SAT, TVAT, and PAT between LOW and HIGH fetuses were shown, that namely, adipose tissue mass increased in HIGH fetuses. The expression of UCP1 and PGC1α mRNA increased or tended to increase in SAT, TVAT, and PAT of LOW fetuses and only in SAT of LOW fetuses had more LEP mRNA and tended to have more PPARG, CEBPA, and GLUT4 mRNA. Thus Maternal nutrition would thus strongly affect the accumulation of adipocytes and the activation of their gene expression in the fetus.

As an endocrine organ, adipose tissue is not only involved in energy storage but also acts as a complex, important, and metabolically active part of the body (44). Adipose tissue is scattered throughout the whole body, but makes up 5% to 35% of cattle body mass, which is dependent on age, genotype, and nutrition (4). In adipose tissue, there are three major depot locations, visceral, subcutaneous, and intermuscular depots, which can be further subdivided into smaller depots defined by anatomical location (perirenal and omental) (4). In Wagyu cattle, with growth and fattening, subcutaneous and visceral adipose tissue exhibits particular development that differs from the findings in European breeds such as Holstein, German Angus, and Belgian Blue cattle (3). In mammals including cattle, adipose tissue has been classified into two distinct types: one is white adipose tissue, which has a major function in energy storage; and the other is brown adipose tissue, which is specialized for energy expenditure (4). In recent time, beige adipose tissue, which is a mixture of brown and white adipocyte, was identified. Beige adipocyte is transdifferentiated from WAT and has many similar morphological and functional properties with brown adipocyte (50).

In cattle, the perirenal adipose tissue starts to appear in fetuses from around day 80 of gestation, followed by visceral, subcutaneous, and intermuscular adipose tissue from day 180 of gestation onward, whereas intramuscular adipocytes in fetus muscles starts to develop from mid- and late-gestation (6, 8), and discernible intramuscular adipocytes filled with lipid develop after birth in earnest (4). Considering the results obtained in this study, given the specific functions and different distributions of individual adipose tissue depots, nutritional interventions during gestation could impact on fetal adipose tissue development in

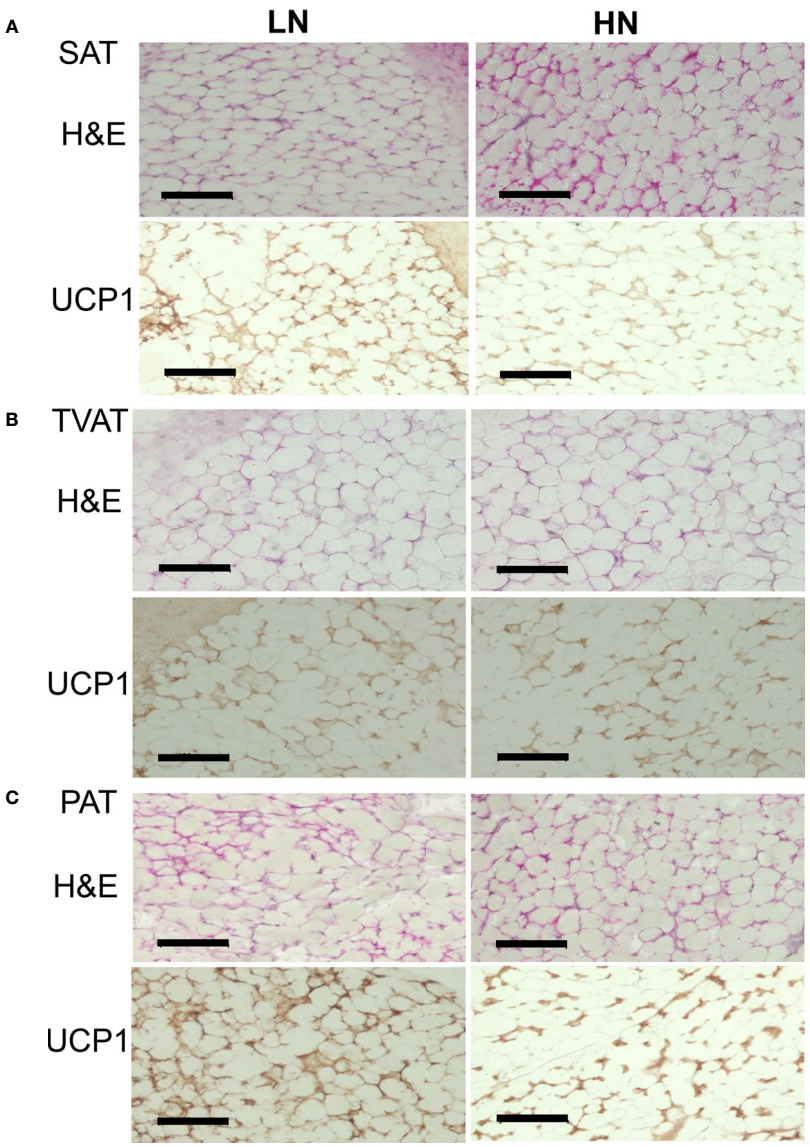

FIGURE 4 | Representative images of H&E staining and immunohistochemical staining of UCP1 in LOW and HIGH fetuses. UCP1: uncoupling protein 1. SAT: subcutaneous adipose tissue (**A**, SAT). TVAT: thoracic cavity visceral adipose tissue (**B**, TVAT). PAT: perirenal adipose tissue (**C**, PAT) in Wagyu fetuses. Fetuses: 260 ± 8.3 days of fetal age. LOW: n=6. HIGH: n=6. Black scale bar represents 100 μm. Magnification: 30×.

diverse ways. However, few studies focusing on ruminants have evaluated the effects of suboptimal maternal nutrition on the development of fetal adipose tissue. Jennings et al. (51) found that maternal high (146% nutrition requirement) and low (72% nutrition requirement) nutrition during mid-gestation did not affect the expression of genes related to adipogenesis in subcutaneous adipose tissue of Angus crossbred fetuses at d 180. These results suggest that fetal growth characteristics are not affected by the level of maternal nutritional manipulation imposed in the study during mid-gestation. While, Long et al. (43) fattened the offspring exposed to 55% maternal nutrition during early gestation, indicated no differences in distribution of subcutaneous and perirenal adipose tissue compared with the control offspring, but the expression of AP2, CD36, and GLUT4 in the perirenal adipose tissue was suppressed in low nutrition group. Regardless of the animal species, the effects of maternal nutrition on fetal development are supposed to be affected by the timing of treatment during gestation (49, 52), although here we manipulated maternal nutrition during the entirety of gestation.

In this study, the adipocyte diameters of SAT and PAT were greater in HIGH fetuses, while there were no differences in adipocyte diameter in TVAT between LOW and HIGH fetuses. This suggested that specific adipose tissue depots showed different responses to suboptimal maternal nutrition during

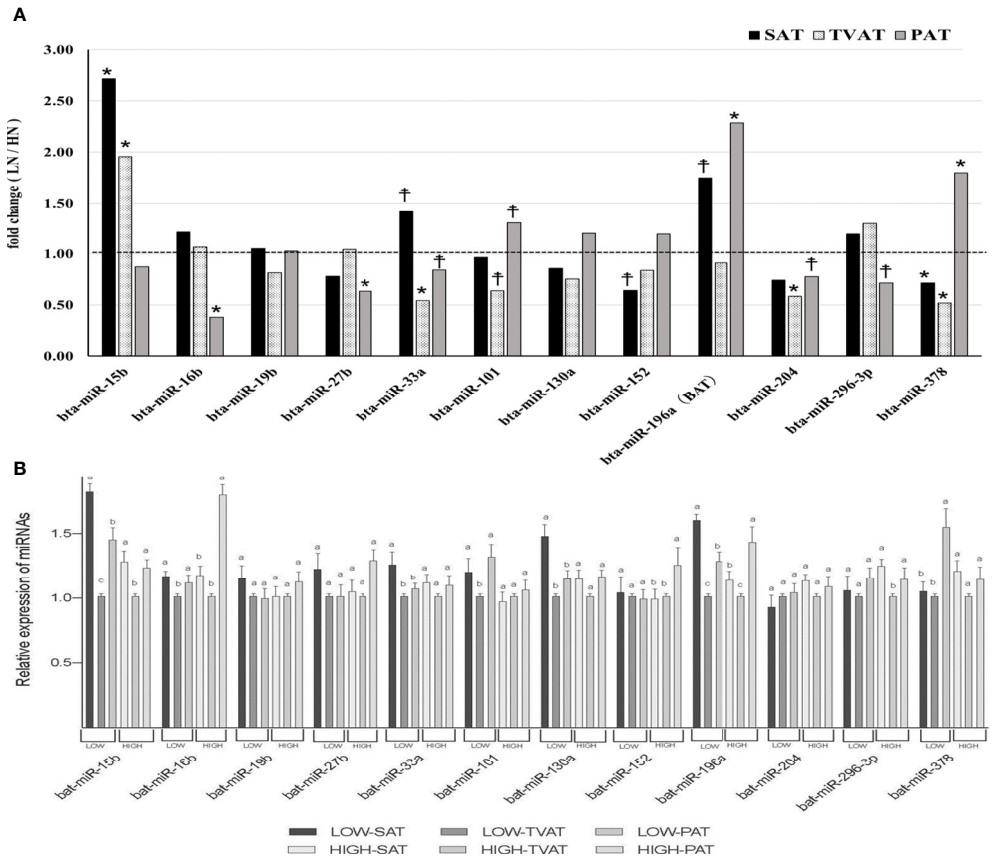

FIGURE 5 | Comparison of miRNAs in adipose tissues. **(A)** Comparison of fold change (**LOW/HIGH**) of miRNA abundance in subcutaneous (SAT), thoracic cavity visceral (TVAT), and perirenal adipose tissues (PAT) between LOW and HIGH fetuses in Wagyu cattle. The horizontal dotted line (at the value "1") showed the relative miRNA expression of the HIGH fetuses. The foldchange was calculated as the relative expression based on the mean of the target gene Ct value of LOW and HIGH fetuses. **(B)** Comparison of mRNA abundance between SAT, TVAT, and PAT in the LOW and the HIGH fetuses in Wagyu cattle. Fetus age: Fetuses: 260 ± 8.3 days of fetal age. LOW: n=6. HIGH: n=6. *Significant difference and †trend ($p < 0.05$ and $p < 0.1$, respectively) between LOW and HIGH fetuses. ^{a,b,c} Significant difference ($p < 0.05$) between SAT, TVAT, and PAT in the LOW and the HIGH fetuses.

pregnancy. Moreover, it was also suggested that the adipocytes of SAT and PAT were more sensitive to nutritional deficiencies. In calves born from dams fed a restricted level of protein, the mass weight of perirenal adipose tissue, adipocyte size, and lipogenic activities were reported to be similar to those in control calves at birth (53).

We estimated the number of adipocytes (**Figure 6**) based on the adipocyte diameter and mass of adipose tissue in SAT, TVAT, and PAT (35). In this simulation, we used 0.92 g/cm^3 as the adipose tissue density (54) and assumed that the adipocytes were spherical for this calculation. The results showed that the numbers of adipocytes in SAT (2.3-fold), TVAT (1.6-fold) were greater in HIGH fetuses than in LOW ones ($p < 0.01$; **Figure 6**). This suggests that maternal nutrition would alter the number of adipocytes in adipose tissue, with SAT and TVAT being particularly sensitive to this. However, the number of adipocytes could be increased after birth by proliferation (55).

In the immunohistochemical observation on UCP1-positive status, SAT, TVAT, and PAT seemed to show greater numbers of brown adipocytes in LOW fetuses than in HIGH fetuses. These findings are supported by the higher UCP1 mRNA expression in SAT, TVAT, and PAT (**Figure 4**). This suggested that maternal overnutrition could suppress brown adipocyte development during gestation. Similar to this result, when the dams consumed a suboptimal amount of nutrients during the final month of gestation, birth weight and adipose tissue mass were reduced, but this is highly likely to reflect a reduction in adipose tissue stores rather than a reduction in the amount of brown adipose tissue in mammals (12). Intriguingly, the reduced amount of adipose tissue present in newborns has a greater capacity to maintain UCP1 as a BAT biomarker, which could be indicative of a protective mechanism against subsequent exposure to some environment with temperature change or an obesogenic environment in human (12). Furthermore, enhanced maternal nutrition from mid- to late gestation could accelerate the activity of glucocorticoids and a series of inflammatory responses in newborns when key inflammatory genes were upregulated (56). However, maternal overfeeding (150% of control) during mid- to late gestation did not affect the weight of

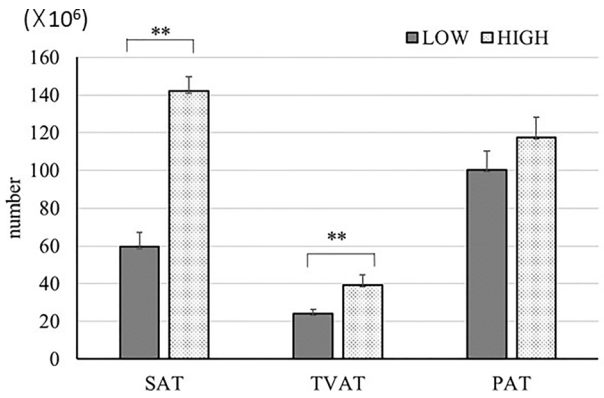

FIGURE 6 | Estimation of adipocyte number in SAT, TVAT, and PAT of LOW and HIGH fetuses. Values were calculated based on the values from adipocyte diameter analysis (**Figure 1**) and data of each adipose tissue mass. Adipose tissue density: 0.92 g/cm^3 (54). Fetuses: 260 ± 8.3 days of fetal age. LOW: n=6. HIGH: n=6. Values are means with standard errors. Significant differences between fetal groups are denoted by $^{**}p < 0.01$.

perirenal BAT or the adipocyte diameter of fetuses, but increased some adipogenic factor, PPARG, and in lipoprotein lipase, adiponectin, and LEP mRNA expression in PAT (57).

In the adipogenesis, PPARG, CEBPA, SCD, FASN, FABP 4, ZFP423, and LEP have the crucial role (13–17). The changes in the expression of various mRNAs in this study suggested that the adipogenesis of Wagyu fetuses could be susceptible to change due to maternal nutritional status during gestation in a manner dependent on each particular adipose tissue depot. The formation and composition of adipose tissue in cattle are derived from a complex process. They are controlled by multiple parameters including genetic factors, nutritional status, feeding system, species, and sex in cattle (58). In this study, the pattern of gene expression in SAT differed from those in TVAT and PAT. Regarding SAT, HIGH fetuses had 3-fold greater mass than LOW fetuses, while for TVAT and PAT, HIGH fetuses had only 1.4-fold greater mass (35). In addition, SAT from LOW fetuses had greater expression of PPARG, CEBPA, and LEP mRNA, which might suggest that they were trying to develop WAT because the formation of WAT was delayed due to maternal lower nutrition compared with that from HIGH fetuses. Moreover, only in SAT, LOW fetuses tended to have higher levels of IGF2, AK2, and GLUT4 mRNA. Thus, in SAT, depending on the maternal nutritional level, LOW fetuses showed different patterns of mRNA expression related to genes involved in growth and glucose metabolism compared with the findings for TVAT and PAT. Enhanced LEP mRNA expression indicates elevated insulin sensitivity (59), while enhanced GLUT4 expression indicates elevated glucose intake (60). In addition, increased expression of PPARG and CEBPA mRNA in SAT indicates that adipocyte differentiation is activated (61, 62).

Conversely, in TVAT and PAT, LOW fetuses tended to have lower expression of PPARG and CEBPA mRNA and, in PAT, also tended to have lower expression of LEP mRNA, showing the opposite tendency to SAT. SAT is a layer of subcutaneous fat is located between the dermis and the underlying fascia on the outer muscle. SAT is not only serving as a reserve source of energy for the body, but also SAT helps to physically insulate the body from cold (63) and radiates heat in the case of containing BAT in a part of SAT. Moreover, in all of SAT, TVAT, and PAT, LOW fetuses had higher levels of UCP1 and PGC1α mRNA, indicating that brown adipocyte formation was activated in LOW fetuses. Heat-producing adipocytes, brown adipocytes, drive heat production through the close coordination of substrate supply with the mitochondrial oxidative machinery and effectors that control the rate of substrate oxidation (64, 65). Brown adipocyte as a heat production effector specifically expresses UCP1, which is the best characterized marker of BAT (66). With regard to adipose tissue mass, LOW fetuses had only half the carcass mass of HIGH fetuses (35), resulting in the heat-producing ability also being lower. Landis et al. (67) reported the expression of UCP mRNA in the tail-head subcutaneous adipose tissue of cross-bred fetuses though the gene expression level was low. These dynamics of gene expression suggested that, in LOW fetuses, brown adipocytes are activated more for thermogenesis to increase the potential for survival.

In this study, in PAT, LOW fetuses tended to have a lower level of GLUT4 mRNA. Undernutrition during late pregnancy in sheep was reported to reduce the expression of GLUT4 protein in renal adipose tissue and simultaneously generate glucose resistance in offspring at 1 year of age (68). However, the renal and omental adipose tissue mass levels of nutrient restricted group during late gestation were increased compared with those of control group (68). Further research is needed to investigate whether LOW fetuses exhibit an increase in mass later in life. In PAT, lower maternal nutrition increased the levels of PPARG and UCP1 mRNAs in fetuses compared with higher maternal nutrition and a positive correlation between the levels of PPARG and UCP1 mRNAs was reported in sheep (69). These findings were not consistent with our results showing decreased abundance of PPARG mRNA and increased abundance of UCP1 mRNA in LOW fetuses.

Wagyu (Japanese Black) cattle is a unique breed with a high capacity to produce marbled meat. In Wagyu, not only did intramuscular adipose tissue increase 12-fold (2.18% to 26.77%) but also SAT increased 14-fold (3.11% to 44.26%)

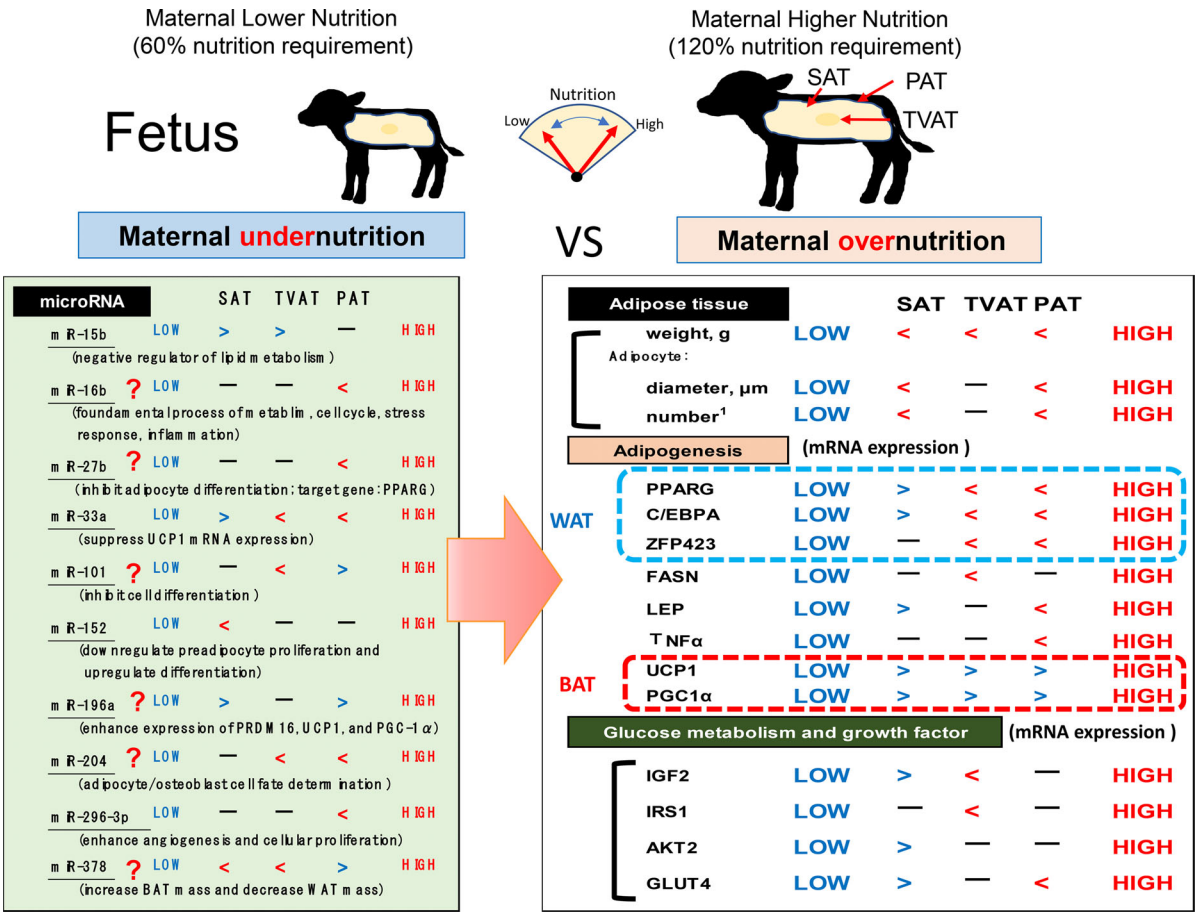

FIGURE 7 | Hypothetical scheme of the influences of maternal under- or overnutrition on the associations between fetal SAT, TVAT, and PAT development in weight, histochemical properties, gene expression (related to adipogenesis, growth factors, and glucose metabolism), and miR expression. Inequality sign is based on $p < 0.10$.

during fattening (8 to 26 months of age), which contrasts with the finding for PAT (5.25-fold: 4.58% to 24.07%; 3). Conceivably, this ability could be revealed during the fetal development period, and this potential is likely to be influenced by maternal nutrition during gestation. In this study, the sensitivity of fetal SAT to maternal nutrition was quite high.

Notably, studies in mice have shown that ZFP423 is a transcription factor responsible for the adipogenic commitment of progenitor cells (70). The expression of ZFP423 commits progenitor cells to the adipogenic lineage and ensures their differentiation into pre-adipocytes, subsequently inducing PPARG expression, which results in their terminal differentiation (15). The importance of ZFP423 in bovine adipogenesis was further confirmed (16). Shao et al. (71) reported that Fetal development of subcutaneous white adipose tissue is dependent on ZFP423. In this study, in TVAT and PAT, LOW fetuses had a lower expression level of ZFP423 mRNA than HIGH fetuses ($p<0.10$). On the other hand, it was suggested that LOW fetuses activated white adipose tissue formation in SAT because of increased ZFP423 expression.

The brown adipocytes originate primarily from cells in the dermomyotome expressing engrailed 1 (En1), myogenic factor 5 (Myf5), and paired-box protein 7 (Pax7), which can also give rise to muscle cells during the fetal period (72, 73). Thus, the fate of myogenesis during fetal development might be associated with brown adipocytes, which could in turn be affected by maternal nutrition. Although in mouse, Yang et al. (74) previously observed that maternal overnutrition increased the white adipogenesis of progenitors in highly nourished fetuses, while high maternal nutrition during lactation also impaired the thermogenic function of BAT in offspring (75). Therefore, accompanied by lower levels of UCP1, PRDM16, and PGC1α mRNAs in HIGH fetuses, it is suggested that the manipulation of maternal nutrition, especially long-term maternal overnutrition, might adversely affect brown adipose tissue mass and its function in adipose depots of the fetus.

MicroRNAs have been shown to be important for various biological processes including adipose tissue development. This time we have chosen miRNAs which powerfully affect gene expression related adipogenesis. It has been demonstrated that microRNAs play a critical role in regulating differentiation and function in both WAT and BAT (76, 77). In this study, similar to the results of mRNA expression, differential expression of

miRNAs was observed among adipocytes of SAT, TVAT, and PAT (**Figure 5A**). These findings suggested that the manipulation of maternal nutrition throughout gestation could change the miRNA expression dynamics and differentially regulate the development of each adipocyte depot.

miR-15b expression increased in SAT and TVAT of LOW fetuses, but not in PAT. miR-15b has been found to regulate lipid metabolism negatively in adipocytes (regulating DLK1 as a target gene; 25). Increased miR-15b expression in SAT and TVAT of LOW fetuses might reduce lipid metabolism and lead to decreases in lipid content in adipocytes and adipocyte differentiation by reducing the amount of DLK1 (25).

A number of key transcription factors including PPARG and CEBPA/B are known to regulate adipocyte terminal differentiation and lipid metabolism (78), while miRNAs have been demonstrated to regulate adipocyte differentiation through both direct and indirect targeting of these critical transcription factors, as well as their downstream targets (77). PPARG is considered the master regulator of adipocyte differentiation and is a direct target of miR-27a/b (79) and miR-130 (80). Although PPARG mRNA exhibited different expression in adipose tissue among SAT, TVAT, and PAT, miR-27b decreased the expression only in PAT and miRNA-130a did not show any differences in expression in each adipose tissue depot. This suggested that maternal nutrition could affect adipose tissue development, but not through these miRNAs in fetuses. Meanwhile, the inhibition of miR-27b in glucocorticoid-treated mice was found to increase energy expenditure, reduce body weight, and improve the regulation of glucose homeostasis (31). These effects are likely mediated through the targeting of PRDM16, although numerous other factors are involved in promoting BAT function, including PPARA and PPARG coactivator 1-beta (PGC-1β), which have also been identified as targets of miR-27 (81).

Interestingly, miR-196a plays an essential role in BAT progenitor cells and induces the "browning" of WAT, with enhanced expression of BAT genes, inducing PRDM16, UCP1, and PGC-1α (18: rodent). Moreover, miR-196a promotes "browning" by directly binding and suppressing Homeobox C8 (HoxC8), a determinant of white adipogenesis (82: vertebrate; 28: mouse). Because the development of BAT in TVAT of LOW fetuses is promoted with no change of miR-196a expression between LOW and HIGH fetuses, it was suggested that miR-196a was not responsible for promoting BAT development.

miR-378 has been characterized as another positive regulator of BAT (26). In transgenic mice, miR-378 is associated with increased BAT mass and decreased WAT mass, which might be caused by BAT expansion and increased energy expenditure (26). miR-378 was shown to be increased in PAT of LOW fetuses, while UCP1 and PGC-1α mRNA expression was also increased in PAT. It appears that malnutrition could promote BAT development in PAT of LOW fetuses. However, the expression of miR-378 in SAT and TVAT indicated the opposite trend to that in PAT, so it seems that the biological function of miR-378 in PAT differs from those in SAT and TVAT, which is altered by maternal nutrition.

miR-204 showed a lower level in TVAT and PAT of LOW fetuses, but not in SAT. Indeed, miR- has been found to target runt-related transcription factor 2 (RUNX2), which is considered the master regulator of osteoblast differentiation and is one of the main sites of miRNA-mediated adipocyte/osteoblast cell fate determination, resulting in impaired osteogenesis and improved adipogenesis (24). It is suggested that malnutrition during gestation might influence adipose development through downregulating miR-204.

miR-16b regulates metabolism, cell cycle, and inflammatory stress response (83, 84). miR-33a suppresses UCP1 mRNA expression by regulating target genes in BAT (32). In SAT, LOW fetuses retained higher UCP1 mRNA expression although miR-33a expression was higher than that in HIGH fetuses. Meanwhile, there was reasonable interaction between TVAT and PAT, indicating decreased miR-33a and enhanced UCP1 mRNA expression. miR-101 inhibits cell differentiation and induces apoptosis (33). There were different expression patterns of miR-101 expression between TVAT and PAT. miR-152 was previously reported to downregulate preadipocyte proliferation and upregulate differentiation in an *in vitro* experiment using 3T3-L1 (29). Only in SAT, LOW fetuses had a lower abundance of miR-152. This suggests that adipocyte differentiation might be activated more in SAT. miR296-3p enhances angiogenesis and cellular proliferation and conversely downregulates apoptosis (27). Only in PAT, decreased expression of miR-296-3p was observed in LOW fetuses, suggesting that angiogenesis and cellular proliferation might be activated in PAT. However, more recently, updated information regarding these miRNAs has been reported (85). We have to carefully examine the related information and verify the relationship between the obtained data and adipose tissue development in bovine fetuses.

Finally, when comparing the differences in gene expression between adipose tissue depots, 10 genes showed a similar relationship between LOW and HIGH fetuses (**Figure 3**). However, other genes showed different patterns of gene expression between LOW and HIGH fetuses. In particular, the expression of PPARG, CEBPA, and IGF2 mRNA was higher in SAT than in TVAT and PAT in both LOW and HIGH fetuses, and it was speculated that WAT formation and development were enhanced in SAT. On the other hand, UCP1 as a marker of Brown adipose tissue has higher expression in PAT than TVAT, suggesting that PAT has more Brown adipocytes. In general, it was suggested that the molecule dynamics in SAT and PAT were more activated compared with the TVAT. When comparing the differences in miRNA expression between the adipose tissue depots, no differences of half miRNAs expression were observed between SAT, TVAT, and PAT, and the related pattern was different between the LOW and HIGH fetuses (**Figure 5B**). There seems to be many cases of higher miRNA expression in the SAT and PAT than in TVAT. However, further studies are needed regarding these reasons.

CONCLUSION

The present study revealed that maternal nutrition during gestation affected the development of adipose tissue by changing not only mass but also mRNA and miRNA

expression in an adipose depot-specific manner in fetuses of fatty breed, Wagyu cattle (**Figure 7**). These findings suggest that low maternal nutrition would lead to the development of BAT in fetal adipose tissues and this BAT activation in LOW fetuses might be a priority and delayed WAT formation due to lower nutrition. Intriguingly, more significant differences in mRNA expression were observed in SAT and PAT than in TVAT. Moreover, in SAT and PAT, HIGH fetuses had a greater diameter of adipocytes than LOW fetuses. Meanwhile, the findings also suggested that lower maternal nutrition during gestation could suppress the WAT development in TVAT and PAT, but would accelerate that in SAT. The sensitivity of fetuses to low maternal nutrition in SAT would differ from that in TVAT and PAT. Various miRNAs showed significant differences between the LOW and HIGH fetuses in an adipose tissue-specific manner.

DATA AVAILABILITY STATEMENT

The data sets presented in this study can be found in online repositories. The names of the repository/repositories and accession number(s) can be found in the article/**Supplementary Material**.

ETHICS STATEMENT

The animal study was reviewed and approved by Kagoshima University Animal Care and Use Committee (A18007).

AUTHOR CONTRIBUTIONS

YZ: Conceptualization, methodology, software, writing—original draft preparation. KoO: Surgery management, animal care, data curation/investigation/validation. KaO: Reproduction management, animal care, data curation investigation validation. YG: Reproduction management, animal care, data curation/investigation/validation. IO: Reproduction management, data curation/investigation/validation. SM: Data curation/investigation/validation. MS: Data curation/investigation/validation. SR: Physiological data curation, methodology writing—review and editing. TG: Supervision, conceptualization, funding acquisition, writing—review and editing. All authors contributed to the article and approved the submitted version.

FUNDING

This study received funding from Leave a Nest Co., Ltd., the Canon Foundation (R15-0089), Japan Racing Association and Kakenhi (No. 26310312 and19KT0013) from the Japan Society for the Promotion of Science. The authors declare that the funders had no role in study design, data collection and analysis, decision to publish, or preparation of the manuscript.

ACKNOWLEDGMENTS

The authors wish to thank Aoi Kinoshita, Rena Saneshima, Yukiko Nagao, Yasuko Okamura, and Makoto Futohashi for their technical assistance with the sampling. The authors also thank Edanz (https://jp.edanz.com/ac) for editing the English text of a draft of this manuscript.

SUPPLEMENTARY MATERIAL

The Supplementary Material for this article can be found online at: https://www.frontiersin.org/articles/10.3389/fendo.2021.797680/full#supplementary-material

REFERENCES

1. Hornstein I, Wasserman A. Sensory Characteristics of Meat. Part 2-Chemistry of Meat Flavor. In: JF Price, BS Schweigert, editors. *The Science of Meat and Meta Products, 3rd ed.* Westport, CT: Food and Nutrition Press (1987). p. 329–47.
2. Wheeler TL, Cundiff LV, Koch M. Effect of Marbling Degree on Beef Palatability in Bos Taurus and Bos Indicus Cattle. *J Anim Sci* (1994) 72:3145–51. doi: 10.2527/1994.72123145x
3. Gotoh T, Albrecht E, Teuscher F, Kawabata K, Sakashita K, Iwamoto H, et al. Differences in Muscle and Fat Accretion in Japanese Black and European Cattle. *Meat Sci* (2009) 82:300–8. doi: 10.1016/j.meatsci.2009.01.026
4. Bonnet M, Cassar-Malek I, Chilliard Y, Picard B. Ontogenesis of Muscle and Adipose Tissues and Their Interactions in Ruminants and Other Species. *Animal* (2010) 4:1093–109. doi: 10.1017/S1751731110000601
5. Fève B. Adipogenesis: Cellular and Molecular Aspects. *Best Pract Res Clin Endocrinol Metab* (2005) 19:483–99. doi: 10.1016/j.beem.2005.07.007
6. Du M, Tong J, Zhao J, Underwood KR, Zhu M, Ford SP, et al. Fetal Programming of Skeletal Muscle Development in Ruminant Animals. *J Anim Sci* (2010) 88(13 Suppl):E51–60. doi: 10.2527/jas.2009-2311
7. Prior RL, Laster DB. Development of the Bovine Fetus. *J Anim Sci* (1979) 48:1546–53. doi: 10.2527/jas1979.4861546x
8. Albrecht E, Kuzinski J, Komolka K, Gotoh T, Maak S. Localization and Abundance of Early Markers of Fat Cell Differentiation in the Skeletal Muscle of Cattle During Growth Are DLK1-positive Cells the Origin of Marbling Flecks? *Meat Science* (2015) 100:237–45. doi: 10.1016/j.meatsci.2014.10.012
9. Ford SP, Hess BW, Schwope MM, Nijland MJ, Gilbert JS, Vonnahme KA, et al. Maternal Undernutrition During Early to Mid-Gestation in the Ewe Results in Altered Growth, Adiposity, and Glucose Tolerance in Male Offspring. *J Anim Sci* (2007) 85:1285–94. doi: 10.2527/jas.2005-624
10. Funston RN, Larson DM, Vonnahme KA. Effects of Maternal Nutrition on Conceptus Growth and Offspring Performance: Implications for Beef Cattle Production. *J Anim Sci* (2010) 88:E205–15. doi: 10.2527/jas.2009-2351
11. Rodríguez A, Ezquerro S, Méndez-Giménez L, Becerril S, Frühbeck G. Revisiting the Adipocyte: A Model for Integration of Cytokine Signaling in the Regulation of Energy Metabolism. *Am J Physiol Endocrinol Metab* (2015) 309:E691–714. doi: 10.1152/ajpendo.00297.2015
12. Symonds ME, Pope M, Sharkey D, Budge H. Adipose Tissue and Fetal Programming. *Diabetologia* (2012) 55:1597–606. doi: 10.1007/s00125-012-2505-5
13. Hotamisligil GS, Shargill NS, Spiegelman BM. Adipose Expression of Tumor Necrosis Factor-Alpha: Direct Role in Obesity-Linked Insulin Resistance. *Science* (1993) 259:87–91. doi: 10.1126/science.7678183
14. Zhang J, Fu M, Cui T, Xiong C, Xu K, Zhong W, et al. Selective Disruption of Pparγ2 Impairs the Development of Adipose Tissue and Insulin Sensitivity. *Proc Natl Acad Sci* (2004) 101:10703–8. doi: 10.1073/pnas.0403652101

15. Gupta RK, Mepani RJ, Kleiner S, Lo JC, Khandekar MJ, Cohen P, et al. Zfp423 Expression Identifies Committed Preadipocytes and Localizes to Adipose Endothelial and Perivascular Cells. *Cell Metab* (2012) 15:230–9. doi: 10.1016/j.cmet.2012.01.010
16. Huang Y, Zhao JX, Yan X, Zhu MJ, Long NM, McCormick RJ, et al. Maternal Obesity Enhances Collagen Accumulation and Cross-Linking in Skeletal Muscle of Ovine Offspring. *PloS One* (2012) 7:e31691. doi: 10.1371/journal.pone.0031691
17. De Jager N, Hudson NJ, Reverter A, Barnard R, Café LM, Greenwood PL, et al. Gene Expression Phenotypes for Lipid Metabolism and Intramuscular Fat in Skeletal Muscle of Cattle. *J Anim Sci* (2013) 91:1112–28. doi: 10.2527/jas.2012-5409
18. Mori M, Nakagami H, Rodriguez-Araujo G, Nimura K, Kaneda Y. Essential Role for miR-196a in Brown Adipogenesis of White Fat Progenitor Cells. *PloS Biol* (2012) 10:e1001314. doi: 10.1371/journal.pbio.1001314
19. Menghini R, Marchetti V, Cardellini M, Hribal ML, Mauriello A, Lauro D, et al. Phosphorylation of GATA2 by Akt Increases Adipose Tissue Differentiation and Reduces Adipose Tissue-Related Inflammation: A Novel Pathway Linking Obesity to Atherosclerosis. *Circulation* (2005) 111:1946–53. doi: 10.1161/01.CIR.0000161814.02942.B2
20. Khan AH, Pessin JE. Insulin Regulation of Glucose Uptake: A Complex Interplay of Intracellular Signaling Pathways. *Diabetologia* (2002) 45:1475–83. doi: 10.1007/s00125-002-0974-7
21. Fernyhough ME, Okine E, Hausman G, Vierck JL, Dodson MV. PPARgamma and GLUT-4 Expression as Developmental Regulators/Markers for Preadipocyte Differentiation Into an Adipocyte. *Domest Anim Endocrinol* (2007) 33:367–78. doi: 10.1016/j.domaniend.2007.05.001
22. Lee P, Jung SM, Guertin DA. The Complex Roles of mTOR in Adipocytes and Beyond. *Trends Endocrinol Metab* (2017) 28:319–39. doi: 10.1016/j.tem.2017.01.004
23. McGregor RA, Choi MS. microRNAs in the Regulation of Adipogenesis and Obesity. *Curr Mol Med* (2011) 11:304–16. doi: 10.2174/156652411795677990
24. Huang J, Zhao L, Xing L, Chen D. MicroRNA-204 Regulates Runx2 Protein Expression and Mesenchymal Progenitor Cell Differentiation. *Stem Cells* (2010) 28:357–64. doi: 10.1002/stem.288
25. Andersen DC, Jensen CH, Schneider M, Nossent AY, Eskildsen T, Hansen JL, et al. MicroRNA-15a Fine-Tunes the Level of Delta-Like 1 Homolog (DLK1) in Proliferating 3T3-L1 Preadipocytes. *Exp Cell Res* (2010) 316:1681–91. doi: 10.1016/j.yexcr.2010.04.002
26. Pan D, Mao C, Quattrochi B, Friedline RH, Zhu L, Jung DY, et al. MicroRNA-378 Controls Classical Brown Fat Expansion to Counteract Obesity. *Nat Commun* (2014) 5:4725. doi: 10.1038/ncomms5725
27. Li H, Ouyang XP, Jiang T, Zheng XL, He PP, Zhao GJ. MicroRNA-296: A Promising Target in the Pathogenesis of Atherosclerosis? *Mol Med* (2018) 24:12. doi: 10.1186/s10020-018-0012-y
28. Schulz TJ, Huang TL, Tran TT, Zhang H, Townsend KL, Shadrach JL, et al. Identification of Inducible Brown Adipocyte Progenitors Residing in Skeletal Muscle and White Fat. *Proc Natl Acad Sci USA* (2011) 108:143–8. doi: 10.1073/pnas.1010929108
29. Fan Y, Gan M, Tan Y, Chen L, Shen L, Niu L, et al. Mir-152 Regulates 3t3-L1 Preadipocyte Proliferation and Differentiation. *Molecules* (2019) 24:3379. doi: 10.3390/molecules24183379
30. Shi C, Zhang M, Tong M, Yang L, Pang L, Chen L, et al. miR-148a is Associated With Obesity and Modulates Adipocyte Differentiation of Mesenchymal Stem Cells Through Wnt Signaling. *Sci Rep* (2015) 22:9930. doi: 10.1038/srep09930
31. Kong X, Yu J, Bi J, Qi H, Di W, Wu L, et al. Glucocorticoids Transcriptionally Regulate miR-27b Expression Promoting Body Fat Accumulation *via* Suppressing the Browning of White Adipose Tissue. *Diabetes* (2015) 64:393–404. doi: 10.2337/db14-0395
32. Afonso MS, Verma N, Solingen CV, Cyr Y, Sharma M, Perie L, et al. MicroRNA-33 Inhibits Adaptive Thermogenesis and Adipose Tissue Beiging. *Arteriosclerosis Thrombosis Vasc Biol* (2021) 41:1360–73. doi: 10.1161/ATVBAHA.120.315798
33. Guan H, Dai Z, Ma Y, Wang Z, Liu X, Wang X. MicroRNA-101 Inhibits Cell Proliferation and Induces Apoptosis by Targeting EYA1 in Breast Cancer. *Int J Mol Med* (2016) 37:1643–51. doi: 10.3892/ijmm.2016.2557
34. National Agriculture and Food Research Organization (NARO). *Japanese Feeding Standard for Beef Cattle (JFSBC)*. Tokyo: Japan Livestock Industry Association, corporation (2008).
35. Zhang Y, Otomaru K, Oshima K, Goto Y, Oshima I, Muroya S, et al. Effects of Low and High Levels of Maternal Nutrition Consumed for the Entirety of Gestation on the Development of Muscle, Adipose Tissue, Bone, and the Organs of Wagyu Cattle Fetuses. *Anim Sci J* (2021) 92:e13600. doi: 10.1111/asj.13600
36. Zhu MJ, Han B, Tong J, Ma C, Kimzey JM, Underwood KR, et al. AMP-Activated Protein Kinase Signaling Pathways are Down Regulated and Skeletal Muscle Development Impaired in Fetuses of Obese, Over-Nourished Sheep. *J Physiol* (2008) 586:2651–64. doi: 10.1113/jphysiol.2007.149633
37. Tong JF, Yan X, Zhu MJ, Ford SP, Nathanielsz PW, Du M. Maternal Obesity Downregulates Myogenesis and Beta-Catenin Signaling in Fetal Skeletal Muscle. *Am J Physiol Endocrinol Metab* (2009) 296:E917–24. doi: 10.1152/ajpendo.90924.2008
38. Paradis F, Wood KM, Swanson KC, Miller SP, McBride BW, Fitzsimmons C. Maternal Nutrient Restriction in Mid-to-Late Gestation Influences Fetal mRNA Expression in Muscle Tissues in Beef Cattle. *BMC Genomics* (2017) 18:632. doi: 10.1186/s12864-017-4051-5
39. Martin DM, Jones AK, Pillai SM, Hoffman ML, McFadden KK, Zinn SA, et al. Maternal Restricted- and Over-Feeding During Gestation Result in Distinct Lipid and Amino Metabolite Profiles I the Longissimus Muscle of the Offspring. *Front Physiol* (2019) 10:515. doi: 10.3389/fphys.2019.00515
40. Gauvin MC, Pillai MS, Reed SA, Stevens JR, Hoffman ML, Jones AK, et al. Poor Maternal Nutrition During Gestation in Sheep Alters Prenatal Muscle Growth and Development in Offspring. *J Anim Sci* (2020) 98:skz388. doi: 10.1093/jas/skz388
41. Asano H, Yamada T, Hashimoto O, Umemoto T, Sato R, Ohwatari S, et al. Diet-Induced Changes in Ucp1 Expression in Bovine Adipose Tissues. *Gen Comp Endocrinol* (2013) 184:87–92. doi: 10.1016/j.ygcen.2013.01.006
42. Du M, Wang B, Fu X, Yang Q, Zhu MJ. Fetal Programming in Meat Production. *Meat Sci* (2015) 109:40–7. doi: 10.1016/j.meatsci.2015.04.010
43. Long NM, Prado-Cooper MJ, Krehbiel CR, DeSilva U, Wettemann RP. Effects of Nutrient Restriction of Bovine Dams During Early Gestation on Postnatal Growth, Carcass and Organ Characteristics, and Gene Expression in Adipose Tissue and Muscle. *J Anim Sci* (2010) 88:3251–61. doi: 10.2527/jas.2009-2512
44. Kershaw EE, Flier JS. Adipose Tissue as an Endocrine Organ. *J Clin Endocrinol Metab* (2004) 89:2548–56. doi: 10.1210/jc.2004-0395
45. Albrecht EA, Schering L, Liu Y, Komolka K, Kühn C, Wimmers K, et al. Factors Influencing Bovine Intramuscular Adipose Tissue Development and Cellularity. *J Anim Sci* (2017) 95:2244–54. doi: 10.2527/jam2016-0786
46. Ferrell CL, Jenkins TG. Cow Type and the Nutritional Environment: Nutritional Aspects. *J Anim Sci* (1985) 61:725–41. doi: 10.2527/jas1985.613725x
47. Blaxter KL, Wainman FW, Davidson JL. The Voluntary Intake of Food by Sheep and Cattle in Relation to Their Energy Requirements for Maintenance. *Anim Prod* (1966) 8:75–83. doi: 10.1017/S0003356100037739
48. Labussière E, van Milgen J, de Lange CFM, Noblet J. Maintenance Energy Requirements of Growing Pigs and Calves Are Influenced by Feeding Level. *J Nutr* (2011) 141:1855–61. doi: 10.3945/jn.111.141291
49. Symonds ME, Stephenson T, Gardner DS, Budge H. Long-Term Effects of Nutritional Programming of the Embryo and Fetus: Mechanisms and Critical Windows. *Reprod Fertil Dev* (2007) 19:53–63. doi: 10.1071/rd06130
50. Cheng L, Wang J, Dai H, Duan Y, An Y, Shi L, et al. Brown and Beige Adipose Tissue: A Novel Therapeutic Strategy for Obesity and Type 2 Diabetes Mellitus. *Adipocyte* (2021) 10(1):48–65. doi: 10.1080/21623945.2020.1870060
51. Jennings TD, Gonda MG, Underwood KR, Wertz-Lutz AE, Blair AD. The Influence of Maternal Nutrition on Expression of Genes Responsible for Adipogenesis and Myogenesis in the Bovine Fetus. *Animal* (2016) 10:1697–705. doi: 10.1017/S1751731116000665
52. Redmer DA, Wallace JM, Reynolds LP. Effect of Nutrient Intake During Pregnancy on Fetal and Placental Growth and Vascular Development. *Domest Anim Endocrinol* (2004) 27:199–217. doi: 10.1016/j.domaniend.2004.06.006
53. Martin GS, Carstens GE, Taylor TL, Sweatt CR, Eli AG, Lunt DK, et al. Prepartum Protein Restriction Does Not Alter Norepinephrine-Induced Thermogenesis or Brown Adipose Tissue Function in Newborn Calves. *J Nutr* (1997) 127:1929–37. doi: 10.1093/jn/127.10.1929
54. Farvid MS, Ng TWK, Chan DC, Barrett PHR, Watts GF. Association of Adiponectin and Resistin With Adipose Tissue Compartments, Insulin Resistance and Dyslipidaemia. *Diabetes Obes Metab* (2005) 7:406–13. doi: 10.1111/j.1463-1326.2004.00410.x

55. Robelin J. Cellularity of Bovine Adipose Tissues: Developmental Changes From 15 to 65 Percent Mature Weight. *J Lipid Res* (1981) 22:452–7. doi: 10.1016/S0022-2275(20)34959-2
56. Gnanalingham MG, Mostyn A, Symonds ME, Stephenson T. Ontogeny and Nutritional Programming of Adiposity in Sheep: Potential Role of Glucocorticoid Action and Uncoupling Protein-2. *Am J Physiol Regul Integr Comp Physiol* (2005) 289:R1407–15. doi: 10.1152/ajpregu.00375.2005
57. Muhlhausler BS, Duffield JA, McMillen IC. Increased Maternal Nutrition Stimulates Peroxisome Proliferator Activated Receptor-Gamma, Adiponectin, and Leptin Messenger Ribonucleic Acid Expression in Adipose Tissue Before Birth. *Endocrinology* (2007) 148:878–85. doi: 10.1210/en.2006-1115
58. Ladeira MM, Schoonmaker JP, Gionbelli MP, Dias JCO, Gionbelli TRS, Carvalho JRR, et al. Nutrigenomics and Beef Quality: A Review About Lipogenesis. *Int J Mol Sci* (2016) 17:918. doi: 10.3390/ijms17060918
59. Yau SW, Henry BA, Russo VC, McConell GK, Clarke IJ, Werther GA, et al. Leptin Enhances Insulin Sensitivity by Direct and Sympathetic Nervous System Regulation of Muscle IGFBP-2 Expression: Evidence from Nonrodent Models. *Endocrinology* (2014) 155:2133–43. doi: 10.1210/en.2013-2099
60. Carvalho E, Kotani K, Peroni OD, Kahn BB. Adipose-Specific Overexpression of GLUT4 Reverses Insulin Resistance and Diabetes in Mice Lacking GLUT4 Selectively in Muscle. *Am J Physiol Endocrinol Metab* (2005) 289:E551–61. doi: 10.1152/ajpendo.00116.2005
61. Clarke SL, Robinson CE, Gimble JM. CAAT/enhancer Binding Proteins Directly Modulate Transcription From the Peroxisome Proliferator-Activated Receptor Gamma 2 Promoter. *Biochem Biophys Res Commun* (1997) 240:99–103. doi: 10.1006/bbrc.1997.7627
62. Wu Z, Rosen ED, Brun R, Hauser S, Adelmant G, Troy AE, et al. Cross-Regulation of C/EBP Alpha and PPAR Gamma Controls the Transcriptional Pathway of Adipogenesis and Insulin Sensitivity. *Mol Cell* (1999) 3:151–8. doi: 10.1016/s1097-2765(00)80306-8
63. Lawrence TLJ, Fowler VR, Novakofski JE. Chapter 4. Tissues: Basic Structure and Growth. In: *Growth, Growth of Farm Animals, 3rd Ed*. London, UK: CAB International (2012). p. 139–73.
64. Wang GX, Meyer JG, Cai W, Softic S, Li ME, Verdin E, et al. Regulation of UCP1 and Mitochondrial Metabolism in Brown Adipose Tissue by Reversible Succinylation. *Mol Cell* (2019) 74:844–57. doi: 10.1016/j.molcel.2019.03.021
65. Ikeda K, Maretich P, Kajimura S. The Common and Distinct Features of Brown and Beige Adipocytes. *Trends Endocrinol Metab* (2018) 29:191–200. doi: 10.1016/j.tem.2018.01.001
66. Chouchani ET, Kazak L, Spiegelman BM. New Advances in Adaptive Thermogenesis: UCP1 and Beyond. *Cell Metab* (2019) 29:27–37. doi: 10.1016/j.cmet.2018.11.002
67. Landis MD, Cars tens GE, MPhil EG, Randal RD, Green KK, Slay L, et al. Ontogenic Development of Brown Adipose Tissue in Angus and Brahman Fetal Calves. *J Anim Sci* (2002) 80:591–601. doi: 10.2527/2002.803591x
68. Gardner DS, Tingey K, Van Bon BW, Ozanne SE, Wilson V, Dandrea J, et al. Programming of Glucose-Insulin Metabolism in Adult Sheep After Maternal Undernutrition. *Am J Physiol Regul Integr Comp Physiol* (2005) 289:R947–54. doi: 10.1152/ajpregu.00120.2005
69. Bispham J, Gardner DS, Gnanalingham MG, Stephenson T, Symonds ME, Budge H. Maternal Nutritional Programming of Fetal Adipose Tissue Development: Differential Effects on Messenger Ribonucleic Acid Abundance for Uncoupling Proteins and Peroxisome Proliferator-Activated and Prolactin Receptors. *Endocrinology* (2005) 146:3943–9. doi: 10.1210/en.2005-0246
70. Gupta RK, Arany Z, Seale P, Mepani RJ, Ye L, Conroe HM, et al. Transcriptional Control of Preadipocyte Determination by Zfp423. *Nature* (2010) 464:619–23. doi: 10.1038/nature08816
71. Shao M, Hepler C, Vishvanath L, MacPherson KA, Busbuso NC, Gupta RK. Fetal Development of Subcutaneous White Adipose Tissue is Dependent on Zfp423. *Mol Metab* (2017) 6:111–24. doi: 10.1016/j.molmet.2016.11.009
72. Seale P, Bjork B, Yang W, Kajimura S, Chin S, Kuang S, et al. PRDM16 Controls a Brown Fat/Skeletal Muscle Switch. *Nature* (2008) 454:961–7. doi: 10.1038/nature07182
73. Lepper C, Fan CM. Inducible Lineage Tracing of Pax7-Descendant Cells Reveals Embryonic Origin of Adult Satellite Cells. *Genesis* (2010) 48:424–36. doi: 10.1002/dvg.20630
74. Yang QY, Liang JF, Rogers CJ, Zhao JX, Zhu MJ, Du M. Maternal Obesity Induces Epigenetic Modifications to Facilitate Zfp423 Expression and Enhance Adipogenic Differentiation in Fetal Mice. *Diabetes* (2013) 62:3727–35. doi: 10.2337/db13-0433
75. Liang X, Yang Q, Zhang L, Maricelli JW, Rodgers BD, Zhu MJ, et al. Maternal High-Fat Diet During Lactation Impairs Thermogenic Function of Brown Adipose Tissue in Offspring Mice. *Sci Rep* (2016) 6:34345. doi: 10.1038/srep34345
76. Hilton C, Neville MJ, Karpe F. MicroRNAs in Adipose Tissue: Their Role in Adipogenesis and Obesity. *Int J Obes (Lond)* (2013) 37:325–32. doi: 10.1038/ijo.2012.59
77. Price NL, Fernández-Hernando C. miRNA Regulation of White and Brown Adipose Tissue Differentiation and Function. *Biochim Biophys Acta* (2016) 1861:2104–10. doi: 10.1016/j.bbalip.2016.02.010
78. Spiegelman BM, Puigserver P, Wu Z. Regulation of Adipogenesis and Energy Balance by PPARgamma and PGC-1. *Int J Obes Relat Metab Disord* (2000) 4:S8–10. doi: 10.1038/sj.ijo.0801492
79. Lin Q, Gao Z, Alarcon RM, Ye J, Yun Z. A Role of miR-27 in the Regulation of Adipogenesis. *FEBS J* (2009) 276:2348–58. doi: 10.1111/j.1742-4658.2009.06967.x
80. Lee EK, Lee MJ, Abdelmohsen K, Kim W, Kim MM, Srikantan S, et al. miR-130 Suppresses Adipogenesis by Inhibiting Peroxisome Proliferator-Activated Receptor Gamma Expression. *Mol Cell Biol* (2011) 31:626–38. doi: 10.1128/MCB.00894-10
81. Sun L, Trajkovski M. MiR-27 Orchestrates the Transcriptional Regulation of Brown Adipogenesis. *Metabolism* (2014) 63(2):272–82. doi: 10.1016/j.metabol.2013.10.004
82. Gesta S, Tseng YH, Kahn CR. Developmental Origin of Fat: Tracking Obesity to its Source. *Cell* (2007) 131:242–56. doi: 10.1016/j.cell.2007.10.004
83. Yan X, Zhu MJ, Dodson MV, Du M. Developmental Programming of Fetal Skeletal Muscle and Adipose Tissue Development. *J Genom* (2013) 1:29–38. doi: 10.7150/jgen.3930
84. Burak K, Lamoureux L, Boese A, Majer A, Saba R, Niu Y, et al. MicroRNA-16 Targets mRNA Involved in Neurite Extension and Branching in Hippocampal Neurons During Presymptomatic Prion Disease. *Neurobiol Dis* (2018) 112:1–13. doi: 10.1016/j.nbd.2017.12.011
85. Gebert LFR, MacRae IJ. Regulation of microRNA Function in Animals. *Nat Rev Mol Cell Biol* (2019) 20:21–37. doi: 10.1038/s41580-018-0045-7

Conflict of Interest: The authors declare that the research was conducted in the absence of any commercial or financial relationships that could be construed as a potential conflict of interest.

frontiers in Endocrinology

MINI REVIEW
published: 03 February 2022
doi: 10.3389/fendo.2022.839436

Developmental Origins of Metaflammation; A Bridge to the Future Between the DOHaD Theory and Evolutionary Biology

*Hiroaki Itoh, Megumi Ueda, Misako Suzuki and Yukiko Kohmura-Kobayashi**

Department of Obstetrics and Gynecology, Hamamatsu University School of Medicine, Hamamatsu, Japan

Metabolic syndrome refers to obesity-associated metabolic disorders that increase the risk of type 2 diabetes, coronary diseases, stroke, and other disabilities. Environmental imbalance during the early developmental period affects health and increases susceptibility to non-communicable diseases, including metabolic syndrome, in later life; therefore, the Developmental Origins of Health and Disease (DOHaD) theory was established. According to the DOHaD theory, the hypothesis of the energy-saving 'Thrifty Phenotype' in undernourished fetuses is one of the well-accepted schemes as a risk of developing metabolic syndrome. This phenotype is evolutionarily advantageous for survival of the fittest in a hangry environment after birth, a strong selection pressure, but increases the risk of developing metabolic syndrome under an obesogenic diet according to the 'Mismatch' hypothesis. Increasing evidences support that chronic inflammation pathophysiologically connects obesity to metabolic disorders in metabolic syndrome, leading to the concept of 'Metaflammation'. 'Metaflammation' in humans is proposed to originate from the evolutionary conservation of crosstalk between immune and metabolic pathways; however, few studies have investigated the contribution of evolutionary maladaptation to the pathophysiology of 'Metaflammation'. Therefore, it is promising to investigate 'Metaflammation' from the viewpoint of selective advantages and its 'Mismatch' to an unexpected environment in contemporary lifestyles, in consideration of the principal concept of evolutionarily conserved nutrient sensing and immune signaling systems.

Keywords: developmental origins of health and disease (DOHaD), metabolic syndrome, obesity, pregnancy, adipose tissue

OPEN ACCESS

Edited by:
Cunming Duan,
University of Michigan, United States

Reviewed by:
Hirotaka Hamada,
University of Toronto, Canada

***Correspondence:**
Yukiko Kohmura-Kobayashi
yukki@hama-med.ac.jp

Specialty section:
This article was submitted to Experimental Endocrinology, a section of the journal Frontiers in Endocrinology

Received: *20 December 2021*
Accepted: *10 January 2022*
Published: *03 February 2022*

Citation:
Itoh H, Ueda M, Suzuki M and Kohmura-Kobayashi Y (2022) Developmental Origins of Metaflammation; A Bridge to the Future Between the DOHaD Theory and Evolutionary Biology. Front. Endocrinol. 13:839436. doi: 10.3389/fendo.2022.839436

INTRODUCTION

Metabolic syndrome refers to the co-occurrence of cardiovascular risk factors, including obesity-associated metabolic disorders, such as insulin resistance, atherogenic dyslipidemia, and hypertension, and is now a global public health issue despite being initially reported in Western countries (1). The prevalence of metabolic syndrome was recently reported to be higher in the urban

populations of some developing countries than in Western countries, which has, in turn, increased the prevalence of type 2 diabetes, coronary diseases, stroke, and other disabilities (2).

Numerous epidemiological and animal studies demonstrated that environmental disturbances in the early critical period have an impact on health and increase susceptibility to non-communicable diseases, such as metabolic syndrome, in later life; therefore, the theory of Developmental Origins of Health and Disease (DOHaD) was established (3–6). According to the DOHaD theory, one of the well-accepted proposals for the risk of developing metabolic syndrome is the hypothesis of the energy-saving 'Thrifty Phenotype' in undernourished fetuses, which is evolutionarily advantageous for survival of the fittest in a starved environment after birth, a strong selection pressure, but increases the risk of metabolic syndrome under an obesogenic diet according to the 'Mismatch' hypothesis (7). This concept connects metabolic syndrome to the maladaptation of the evolutionarily acquired plasticity of metabolic regulation against the selection pressure of starvation.

Recent studies reported that chronic inflammation is pathophysiologically associated with obesity and metabolic disorders in metabolic syndrome; therefore, the concept of "Metaflammation" has been established (8, 9). 'Metaflammation' in humans is proposed to originate from the evolutionary conservation of crosstalk between immune and metabolic pathways, for example, based on the composition of the fat body of *Drosophila melanogaster* (9). In the evolutionary history of humans, immune and metabolic crosstalk appeared to be associated, at least partly, with responses and/or adaptation to the selection pressures of infection and/or starvation; however, to the best of our knowledge, few studies have focused on its contribution to the pathophysiology of 'Metaflammation' in metabolic syndrome. On the other hand, according to the DOHaD hypothesis, offspring with the energy-saving 'Thrifty Phenotype' (10) are predisposed to metabolic syndrome under an obesogenic diet according to the 'Mismatch' hypothesis (7).

In this mini review, we introduce the relationship between the 'Thrifty Phenotype' and metabolic syndrome in the DOHaD scheme as well as that between 'Metaflammation' and evolutionarily conserved nutrient sensing and immune signaling systems. We also discuss the importance of investigating 'Metaflammation' from the viewpoint of selective advantages and its 'Mismatch' to unexpected modern environments in consideration of the DOHaD concept, in addition to the principal concept of evolutionarily conserved nutrient sensing and immune signaling systems.

THE 'THRIFTY PHENOTYPE' HYPOTHESIS IN THE DOHaD THEORY; STARVATION AS A SELECTION PRESSURE

Initial evidence to support the concept of DOHaD was the deterioration of health in adulthood of British small babies with low birth weight (11, 12) and Dutch fetuses with undernourishment due to maternal starvation in World War II (13, 14). Rapid infantile growth, presumably indicative of an abundant nutrient supply after birth, particularly with low birth weight, is also causatively associated with obesity and/or metabolic syndrome in later life (15–19). These findings suggest that the continuous trajectory from an undernourished environment during the fetal period to an excessive nutrient supply after birth specifically leads to metabolic disruptions in later life. Hales and Barker proposed the 'Thrifty Phenotype' hypothesis, in which the body size of fetuses is reduced as an adaption to an insufficient energy supply *in utero* through the acquisition of the permanent energy-saving phenotype, resulting in a low birth weight (10, 20, 21). The 'Thrifty Phenotype' in offspring is hypothesized to be advantageous for survival of the fittest in a starved environment because of low energy demands, but increases the risk of diabetes and/or obesity under an obesogenic diet (10, 21) due to reduced insulin sensitivity, a predisposition to authentic and ectopic fat accumulation, and a lower respiratory oxygen quotient, which are risk factors for metabolic syndrome (20–23).

Starvation is one of strongest selection pressures from an evolutionary viewpoint not only in humans, but also in animals (24). The 'Thrifty Phenotype' is acquired phenotypic plasticity that changes offspring into energy-saving individuals in response to the presence or absence of a starved environment after birth as an adaptation to the selection pressure of repeated starvation waves (25). Based on the long evolutionary history of humans with repeating periods of starvation, the recent era of an overwhelming food supply in developed and some rapidly developing countries is an evolutionary exception. Therefore, it is plausible that the developmentally acquired plasticity of the 'Thrifty Phenotype' with energy-saving metabolic regulation mismatches an environment with an excess energy supply, thereby increasing the risk of obesity and diabetes, the so-called state of metabolic syndrome.

Gluckman and Hanson proposed not only the 'Mismatch' hypothesis (7), but also the 'Predictive Adaptive Responses (PARs)' hypothesis (26, 27). In the intrauterine setting, PARs primarily function to improve future fitness to expected conditions after birth, such as starvation, through evolutionarily acquired phenotypic plasticity for adaptation (26). The 'Mismatch' hypothesis indicates maladaptation to the unexpected environment of the new era, which increases susceptibility to non-communicable diseases in adulthood (7). These concepts indicate that the upstream risk of metabolic disorders is connected, at least partly, to the maladaptation of developmentally modified phenotypes by evolutionarily acquired plasticity, particularly in response to the expectation of starvation, a strong selection pressure (27, 28).

EVOLUTIONARY ASPECT OF 'METAFLAMMATION'; EVOLUTIONARY CONSERVATION OF CROSSTALK BETWEEN IMMUNE AND METABOLIC PATHWAYS

The pathogenesis of obesity with various metabolic disorders is based on a close relationship between nutrient excess and the activation of the innate immune system in the majority of organs

involved in energy homeostasis (8, 9, 29–31). Increasing evidence indicates that inflammation occurs with obesity and may play a causative role not only in the development of insulin resistance and disruption of other aspects of energy homeostasis, but also in the augmentation of fat accumulation (9, 29). The characteristics of obesity-associated chronic inflammation differ from other general inflammatory paradigms in that it involves tonic activation of the innate immune system, which has an impact on metabolic homeostasis, generally for a lifetime, and affects multiple organs, such as adipose tissue, the pancreas, liver, muscle, and brain (9, 29). This led to the establishment of the concept of 'Metaflammation' (8, 9).

In addition to starvation, infection is a strong selection pressure in animals (32). The avoidance of these two major selection pressures through adjustments to nutrient and immune conditions has been the most important task for animals to survive for hundreds of millions of years (32, 33). The strong relationship between nutrient sensing and immune signaling is rooted in their common evolutionary origins. For example, the hematopoietic system, adipose tissue, and liver are all organized in one functional unit in the fat body of *D. melanogaster* (8). This developmental heritage is responsible for the highly overlapping biological repertoire of these organs, their effects on metabolic and immune cells, and the close relationship between immune and metabolic response systems, which supports the concept of 'Metaflammation' from an evolutionary viewpoint (8, 9). The fat body of *Drosophila* is capable of sensing both infectious and metabolic disturbances, and studies on *Drosophila* have provided important insights into highly conserved immuno-metabolic pathways in mammals (8, 9).

Accumulated evidence has also highlighted the crucial role of metabolic reprogramming in macrophage activation not only in immuno-metabolic pathways, but also in the pathophysiological concept of 'Metaflammation' (34–36). The infiltration of macrophages and also its associated immune cells into metabolic organs, such as the liver, brain, pancreas, and adipose tissue, is an important factor influencing the maintenance of tissue homeostasis as well as the pathogenesis of metabolic disorders (9). Tissue macrophages function as direct modulators of metabolism, for example, by inducing the polarization of macrophages towards a pro-inflammatory (M1-polarized) phenotype that blocks the effects of insulin (37), to which the contribution of epigenomic alterations (38) and macrophage-secreted products (39) has been demonstrated. It is important to note that many other immune cell types, including dendritic cells, mast cells, eosinophils, and lymphoid cells, may also be involved in metabolic tissue homeostasis and the control of glucose metabolism (9). Therefore, the evolutionary preservation of crosstalk between immune and metabolic pathways is one of the principal concepts of metabolic syndrome.

'METAFLAMMATION' IN THE DOHaD SCHEME

To the best of our knowledge, limited evidence is currently available to support a direct relationship between 'Metaflammation' and the scheme of DOHaD for the pathophysiology of metabolic syndrome. The liver and adipose tissues are representative organs of 'Metaflammation', where infiltration of immune cells as well as fat accumulation is frequently observed in metabolic syndrome (8). We developed mice animal model of fetal undernutrition by maternal energy restriction, the offspring of which showed deterioration of fat deposit in the adipose tissue (40) and liver (41) on a high fat diet. Interestingly, the offspring also showed the significant infiltration of macrophages into the adipose tissue (40) and liver (41) (**Figure 1**); thus, we proposed this as a model of 'Metaflammation' in the DOHaD scheme. We also demonstrated that intrauterine undernutrition induced significant increases in endoplasmic reticulum (ER) stress markers in the fatty liver of adult pups (41), while the oral administration of the ER stress alleviator, tauroursodeoxycholic acid (TUDCA), markedly ameliorated macrophage infiltration and hepatic steatosis only in pups that experienced undernourishment *in utero* (41, 42) (**Figure 1**). Based on these findings, we propose the involvement of ER stress programming in the developmental origins of 'Metaflammation' (**Figure 2**). This speculation is consistent with recent findings showing the critical involvement of ER stress in the co-regulation of chronic inflammation and metabolic disorders (43–45).

Fetal-derived immune cells have been implicated in the development of immune diseases. Mass et al. proposed fetal-derived immune cells as prime transmitters of the long-term consequences of prenatal adversity, namely, inflammatory, degenerative, and metabolic disorders, and, thus, are potential contributors to the DOHaD theory (46). Previous studies suggested the commitment of erythro-myeloid progenitors produced in the extra-embryonic yolk sac to the establishment of long-lasting immunological memory (36, 46–48). Yahara et al. proposed the involvement of erythro-myeloid progenitors in bone regeneration after birth (49). Wu et al. also reported the potential contribution of erythro-myeloid progenitors to homeostasis after birth (50). Nevertheless, the mechanisms by which the memory of tissue-resident macrophages, if actually present, is transferred to mature macrophages remain unclear.

DISCUSSION

The DOHaD theory is partly derived from retrospective epidemiological observations of susceptibilities to metabolic disorders in offspring that experienced maternal starvation during gestation, such as in the Dutch Famine in World War II (13, 51) and the Great Chinese Famine (52, 53). Since the basic structures of all organs are formed and basic cross-talk between organs is constituted during the embryonic and fetal stages, the 'Thrifty Phenotype' hypothesis of acquiring a permanent constitution of low energy consumption in order to adapt to the low nutrient supply *in utero* is plausible (10). The 'Thrifty Phenotype' is a type of evolutionarily acquired plasticity in metabolic regulation for humans to survive against the powerful selection pressure of cyclically repeating periods of starvation. However, the 'Thrifty Phenotype' mismatches an obesogenic diet and is causatively associated with diabetes,

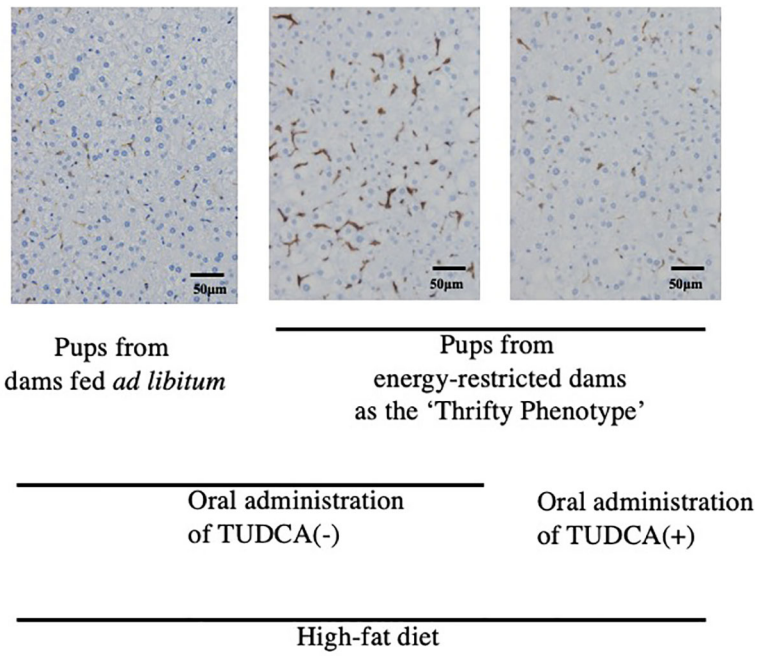

FIGURE 1 | Immunohistochemistry of F4/80-positive hepatic macrophages from 22-week-old pups fed a high-fat diet (Reference 41). Positive staining is brown. TUDCA, Tauroursodeoxycholic acid.

obesity, and associated metabolic disorders in developed and some rapidly developing countries; therefore, the 'Mismatch' hypothesis was proposed (7). The essential concepts of the 'Thrifty Phenotype' and 'Mismatch' hypothesis of the DOHaD theory involve the evolutionary acquisition of plasticity in nutrient sensing against starvation and its maladaptation to an unexpected modern environment (**Figure 2**).

Chronic low-grade inflammation has recently been proposed as a bridge between augmented fat accumulation and metabolic disorders, such as insulin resistance (29); therefore, the concept of 'Metaflammation' is now widely accepted (8, 9). The concept of 'Metaflammation' is also based on evolutionary adaptation against the selection pressures of starvation and infection, i.e. nutrient sensing and immune signaling (8, 9). The fat body of *Drosophila* is capable of sensing both infectious and metabolic disturbances and evolutionarily differentiated into adipose tissue, the liver, and immune cells in mammals; therefore, this mutual functional control mechanism has been preserved between immune cells and the representative organs of adipose tissue and the liver (8, 9). A similar mutual regulatory mechanism with immune cells has also been proposed in other organs, such as the pancreas and brain, in the concept of 'Metaflammation' (9). Therefore, a similar evolutionary trajectory of nutrient sensing and immune signaling underlies the 'Metaflammation' concept (**Figure 2**).

The 'Thrifty Phenotype' is hypothesized to be advantageous for survival of the fittest in a starved environment; however, to the best of our knowledge, there is limited evidence to support the contribution of 'Metaflammation' to survival against infection and/or starvation. The contribution of the potentially long-lasting memory of erythro-myeloid progenitors to the risk of specific diseases in later life, but not to overall survival, has been investigated (36, 46–48). However, we cannot deny the possibility of some unidentified host survival advantage to chronic inflammation or low-grade inflammatory responses incapable of pathogen elimination due to its preservation throughout evolution (**Figure 2**). Although the involvement of crosstalk between immune and metabolic pathways in the acquisition of the 'Thrifty Phenotype' in the DOHaD scheme has not yet been elucidated, the evolutionary conservation of this crosstalk has been suggested to contribute to the maintenance of homeostasis in individual organs and is presumably associated with the significant accumulation of fat deposits concomitant with metabolic disruption in metabolic syndrome (**Figure 2**).

Our mouse model revealed that undernourishment *in utero* significantly enhanced the infiltration of macrophages into adipose tissue (40) and the liver (41) (**Figure 1**) only in mice fed a high-fat diet, and this was concurrent with the deterioration of metabolic disorders. We previously reported that this mouse model of undernourishment *in utero* partly represented the 'Thrifty Phenotype' due to low levels of diet-induced thermogenesis and a predisposition to obesity (54). The findings of these animal studies strongly suggest that a 'Mismatch' to an obesogenic diet in 'Thrifty Phenotype' offspring is causatively associated with a malfunction or imbalance in immunometabolic crosstalk, namely, 'Metaflammation', particularly under an obesogenic diet (**Figure 2**). Therefore, a more detailed understanding of the fundamental pathophysiology of 'Metaflammation' is needed to clarify plasticity in the memory of

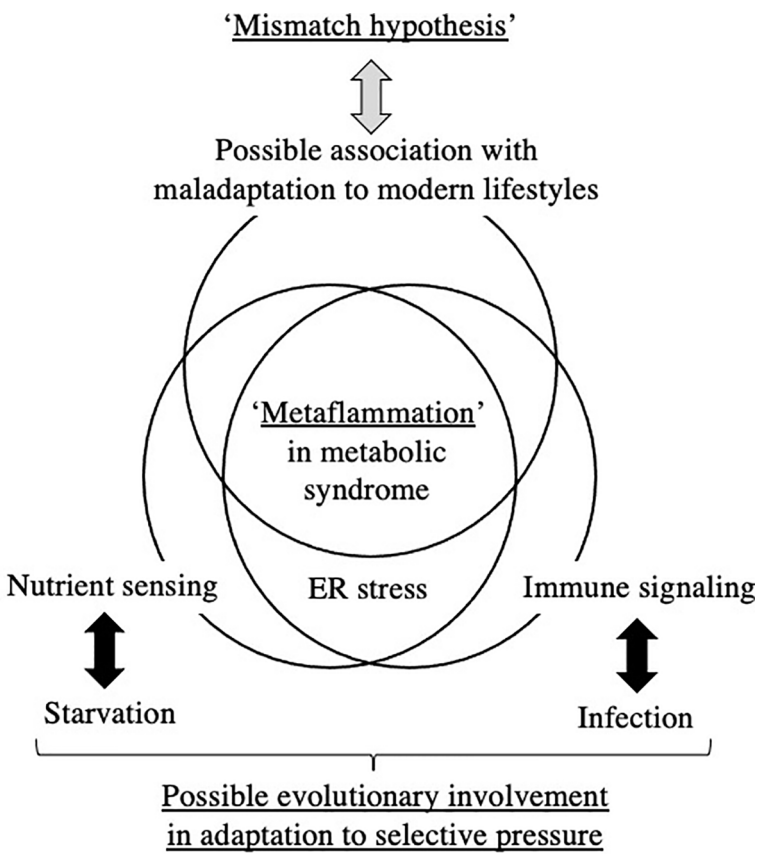

FIGURE 2 | Hypothetical understanding of 'Metaflammation' in metabolic syndrome from the viewpoint of the DOHaD theory and evolutionary biology. ER; endoplasmic reticulum.

tissue-resident immune cells, such as macrophages, from the viewpoint of selective advantages and its mismatch to an unexpected new environment, in addition to the principal concept of evolutionarily conserved nutrient and immune sensing systems.

ER is a major site in cells for protein folding and trafficking and ER malfunctions, such as ER stress, promote the unfolded protein response and activate various stress signaling pathways (43, 45). Previous studies proposed roles for ER stress in the common upstream regulators of immune and metabolic functions in 'Metaflammation' (43, 45). In our mouse model of the 'Thrifty Phenotype', the oral administration of the ER stress alleviator, TUDCA, to pups significantly ameliorated the infiltration of macrophages in the liver only if they experienced undernourishment *in utero* (41) (**Figure 1**). These findings suggest the importance of the regulation of ER stress as a promising research target upstream of developmentally induced 'Metaflammation' (**Figure 2**).

On the other hand, functional 'Trade-off' for adapting to the environmental disruption is also an important concept of the DOHaD theory (6). It is known that the immune function of hibernating animals is suppressed during the hibernation period when a large amount of fat is stored (55), suggesting a possible presence of a kind of 'Trade-off' between fat accumulation and immune activation for the purpose of adapting to the cyclical transitions between hibernation and activity periods. Since coordinate regulation of nutrient and immune functions is a key concept of 'Metaflammation', it might be a clue for understanding the pathogenesis of 'Metaflammation' from DOHaD theory, to investigate a possible 'Trade-off' in 'Metaflammation' between nutrient sensing and immune signaling systems in response to the environmental diversity.

In conclusion, in consideration of the 'Thrifty Phenotype' and 'Mismatch' hypothesis in the DOHaD theory, a promising research target is 'Metaflammation' from the viewpoint of selective advantages and its mismatch to an unexpected modern environment, in addition to the principal concept of evolutionarily conserved nutrient sensing and immune signaling systems.

AUTHOR CONTRIBUTIONS

All authors listed have made a substantial, direct, and intellectual contribution to the work and approved it for publication.

FUNDING

This work was supported by JSPS KAKENHI Grant Numbers JP20H03823, JP20K09666, and JP20K16886, and AMED under Grant Number JP20gm1310009.

ACKNOWLEDGMENTS

The authors thank Mrs. Miuta Sawai, Yumiko Yamamoto, Naoko Kondo, and Kazuko Sugiyama for their secretarial or technical assistance.

REFERENCES

1. Huang PL. A Comprehensive Definition for Metabolic Syndrome. *Dis Model Mech* (2009) 2(5-6):231–7. doi: 10.1242/dmm.001180
2. Eckel RH, Alberti KG, Grundy SM, Zimmet PZ. The Metabolic Syndrome. *Lancet* (2010) 375(9710):181–3. doi: 10.1016/S0140-6736(09)61794-3
3. Gluckman PD, Hanson MA. *Developmental Origins of Health and Disease*. Cambridge: Cambridge University Press (2006).
4. Hanson MA, Gluckman PD. Developmental Origins of Health and Disease - Global Public Health Implications. *Best Pract Res Clin obstetrics Gynaecol* (2014) 29(1):24–31. doi: 10.1016/j.bpobgyn.2014.06.007
5. Itoh H, Kanayama N. *Developmental Origins of Health and Diseases (Dohad); Perspective Toward Preemptive Medicine*. In: Konishi I, editor. Singapore: Springer Nature (2017).
6. Fleming TP, Watkins AJ, Velazquez MA, Mathers JC, Prentice AM, Stephenson J, et al. Origins of Lifetime Health Around the Time of Conception: Causes and Consequences. *Lancet* (2018) 391(10132):1842–52. doi: 10.1016/S0140-6736(18)30312-X
7. Gluckman PD, Hanson MA. *Mismatch Why Our World No Longer Fits Our Bidies*. Oxford: Oxford University Press (2006).
8. Hotamisligil GS. Inflammation and Metabolic Disorders. *Nature* (2006) 444 (7121):860–7. doi: 10.1038/nature05485
9. Hotamisligil GS. Inflammation, Metaflammation and Immunometabolic Disorders. *Nature* (2017) 542(7640):177–85. doi: 10.1038/nature21363
10. Hales CN, Barker DJ. The Thrifty Phenotype Hypothesis. *Br Med Bull* (2001) 60:5–20. doi: 10.1093/bmb/60.1.5
11. Barker DJ. The Origins of the Developmental Origins Theory. *J Intern Med* (2007) 261(5):412–7. doi: 10.1111/j.1365-2796.2007.01809.x
12. Barker DJ, Gluckman PD, Godfrey KM, Harding JE, Owens JA, Robinson JS. Fetal Nutrition and Cardiovascular Disease in Adult Life. *Lancet* (1993) 341 (8850):938–41. doi: 10.1016/0140-6736(93)91224-a
13. Kyle UG, Pichard C. The Dutch Famine of 1944-1945: A Pathophysiological Model of Long-Term Consequences of Wasting Disease. *Curr Opin Clin Nutr Metab Care* (2006) 9(4):388–94. doi: 10.1097/01.mco.0000232898.74415.42
14. Painter RC, Roseboom TJ, Bleker OP. Prenatal Exposure to the Dutch Famine and Disease in Later Life: An Overview. *Reprod Toxicol* (2005) 20(3):345–52. doi: 10.1016/j.reprotox.2005.04.005
15. Eriksson J, Forsen T, Tuomilehto J, Osmond C, Barker D. Size at Birth, Childhood Growth and Obesity in Adult Life. *Int J Obes Relat Metab Disord* (2001) 25(5):735–40. doi: 10.1038/sj.ijo.0801602
16. Ong KK. Size at Birth, Postnatal Growth and Risk of Obesity. *Horm Res* (2006) 65 Suppl 3:65–9. doi: 10.1159/000091508. HRE2006065S03065.
17. Ekelund U, Ong KK, Linne Y, Neovius M, Brage S, Dunger DB, et al. Association of Weight Gain in Infancy and Early Childhood With Metabolic Risk in Young Adults. *J Clin Endocrinol Metab* (2007) 92(1):98–103. doi: 10.1210/jc.2006-1071
18. Singhal A. Long-Term Adverse Effects of Early Growth Acceleration or Catch-Up Growth. *Ann Nutr Metab* (2017) 70(3):236–40. doi: 10.1159/000464302
19. Martin A, Connelly A, Bland RM, Reilly JJ. Health Impact of Catch-Up Growth in Low-Birth Weight Infants: Systematic Review, Evidence Appraisal, and Meta-Analysis. *Matern Child Nutr* (2017) 13(1):10.1111/mcn.12297. doi: 10.1111/mcn.12297
20. Wells JC. Environmental Quality, Developmental Plasticity and the Thrifty Phenotype: A Review of Evolutionary Models. *Evol Bioinform Online* (2007) 3:109–20. doi: 10.1177/117693430700300027
21. Wells JC. The Thrifty Phenotype: An Adaptation in Growth or Metabolism? *Am J Hum Biol* (2011) 23(1):65–75. doi: 10.1002/ajhb.21100
22. Dulloo AG. Regulation of Fat Storage *via* Suppressed Thermogenesis: A Thrifty Phenotype That Predisposes Individuals With Catch-Up Growth to Insulin Resistance and Obesity. *Horm Res* (2006) 65 Suppl 3:90–7. doi: 10.1159/000091512
23. Stocker CJ, Arch JR, Cawthorne MA. Fetal Origins of Insulin Resistance and Obesity. *Proc Nutr Soc* (2005) 64(2):143–51. doi: 10.1079/pns2005417
24. Prentice AM. Starvation in Humans: Evolutionary Background and Contemporary Implications. *Mech Ageing Dev* (2005) 126(9):976–81. doi: 10.1016/j.mad.2005.03.018
25. Higginson AD, McNamara JM, Houston AI. Fatness and Fitness: Exposing the Logic of Evolutionary Explanations for Obesity. *Proc Biol Sci* (2016) 283 (1822):20152443. doi: 10.1098/rspb.2015.2443
26. Gluckman PD, Hanson MA, Spencer HG. Predictive Adaptive Responses and Human Evolution. *Trends Ecol Evol* (2005) 20(10):527–33. doi: 10.1016/j.tree.2005.08.001
27. Gluckman PD, Hanson MA, Low FM. Evolutionary and Developmental Mismatches Are Consequences of Adaptive Developmental Plasticity in Humans and Have Implications for Later Disease Risk. *Philos Trans R Soc Lond B Biol Sci* (2019) 374(1770):20180109. doi: 10.1098/rstb.2018.0109
28. Bateson P, Gluckman P, Hanson M. The Biology of Developmental Plasticity and the Predictive Adaptive Response Hypothesis. *J Physiol* (2014) 592 (11):2357–68. doi: 10.1113/jphysiol.2014.271460
29. Saltiel AR, Olefsky JM. Inflammatory Mechanisms Linking Obesity and Metabolic Disease. *J Clin Invest* (2017) 127(1):1–4. doi: 10.1172/JCI92035
30. Lackey DE, Olefsky JM. Regulation of Metabolism by the Innate Immune System. *Nat Rev Endocrinol* (2016) 12(1):15–28. doi: 10.1038/nrendo.2015.189
31. Lumeng CN, Saltiel AR. Inflammatory Links Between Obesity and Metabolic Disease. *J Clin Invest* (2011) 121(6):2111–7. doi: 10.1172/JCI57132
32. Barreiro LB, Quintana-Murci L. Evolutionary and Population (Epi)Genetics of Immunity to Infection. *Hum Genet* (2020) 139(6-7):723–32. doi: 10.1007/s00439-020-02167-x
33. Soukas AA, Zhou B. Surviving Starvation Simply Without Tfeb. *PloS Biol* (2019) 17(5):e3000285. doi: 10.1371/journal.pbio.3000285
34. Van den Bossche J, O'Neill LA, Menon D. Macrophage Immunometabolism: Where Are We (Going)? *Trends Immunol* (2017) 38(6):395–406. doi: 10.1016/j.it.2017.03.001
35. Lauterbach MA, Wunderlich FT. Macrophage Function in Obesity-Induced Inflammation and Insulin Resistance. *Pflugers Arch* (2017) 469(3-4):385–96. doi: 10.1007/s00424-017-1955-5
36. Christ A, Lauterbach M, Latz E. Western Diet and the Immune System: An Inflammatory Connection. *Immunity* (2019) 51(5):794–811. doi: 10.1016/j.immuni.2019.09.020
37. Lumeng CN, Bodzin JL, Saltiel AR. Obesity Induces a Phenotypic Switch in Adipose Tissue Macrophage Polarization. *J Clin Invest* (2007) 117(1):175–84. doi: 10.1172/JCI29881
38. Fan R, Toubal A, Goni S, Drareni K, Huang Z, Alzaid F, et al. Loss of the Co-Repressor GPS2 Sensitizes Macrophage Activation Upon Metabolic Stress Induced by Obesity and Type 2 Diabetes. *Nat Med* (2016) 22(7):780–91. doi: 10.1038/nm.4114
39. Li P, Liu S, Lu M, Bandyopadhyay G, Oh D, Imamura T, et al. Hematopoietic-Derived Galectin-3 Causes Cellular and Systemic Insulin Resistance. *Cell* (2016) 167(4):973–84.e12. doi: 10.1016/j.cell.2016.10.025
40. Kohmura YK, Kanayama N, Muramatsu K, Tamura N, Yaguchi C, Uchida T, et al. Association Between Body Weight at Weaning and Remodeling in the Subcutaneous Adipose Tissue of Obese Adult Mice With Undernourishment *in Utero*. *Reprod Sci* (2013) 20(7):813–27. doi: 10.1177/1933719112466300
41. Muramatsu-Kato K, Itoh H, Kohmura-Kobayashi Y, Ferdous UJ, Tamura N, Yaguchi C, et al. Undernourishment *in Utero* Primes Hepatic Steatosis in Adult Mice Offspring on an Obesogenic Diet; Involvement of Endoplasmic Reticulum Stress. *Sci Rep* (2015) 5:16867. doi: 10.1038/srep16867

42. Urmi JF, Itoh H, Muramatsu-Kato K, Kohmura-Kobayashi Y, Hariya N, Jain D, et al. Plasticity of Histone Modifications Around Cidea and Cidec Genes With Secondary Bile in the Amelioration of Developmentally-Programmed Hepatic Steatosis. *Sci Rep* (2019) 9(1):17100. doi: 10.1038/s41598-019-52943-7
43. Hotamisligil GS. Endoplasmic Reticulum Stress and the Inflammatory Basis of Metabolic Disease. *Cell* (2010) 140(6):900–17. doi: 10.1016/j.cell.2010.02.034
44. Sikkeland J, Lindstad T, Nenseth HZ, Dezitter X, Qu S, Muhumed RM, et al. Inflammation and ER Stress Differentially Regulate STAMP2 Expression and Localization in Adipocytes. *Metabolism* (2019) 93:75–85. doi: 10.1016/j.metabol.2019.01.014
45. Riaz TA, Junjappa RP, Handigund M, Ferdous J, Kim HR, Chae HJ. Role of Endoplasmic Reticulum Stress Sensor IRE1alpha in Cellular Physiology, Calcium, ROS Signaling, and Metaflammation. *Cells* (2020) 9(5):1160. doi: 10.3390/cells9051160
46. Mass E, Gentek R. Fetal-Derived Immune Cells at the Roots of Lifelong Pathophysiology. *Front Cell Dev Biol* (2021) 9:648313. doi: 10.3389/fcell.2021.648313
47. Chen T, Liu HX, Yan HY, Wu DM, Ping J. Developmental Origins of Inflammatory and Immune Diseases. *Mol Hum Reprod* (2016) 22(8):858–65. doi: 10.1093/molehr/gaw036
48. Azzoni E, Boiers C, Brunelli S, Ronchi AE. Editorial: Fetal/Embryonic Hematopoietic Progenitors and Their Impact on Adult Diseases. *Front Cell Dev Biol* (2021) 9:732649. doi: 10.3389/fcell.2021.732649
49. Yahara Y, Ma X, Gracia L, Alman BA. Monocyte/Macrophage Lineage Cells From Fetal Erythromyeloid Progenitors Orchestrate Bone Remodeling and Repair. *Front Cell Dev Biol* (2021) 9:622035. doi: 10.3389/fcell.2021.622035
50. Wu Y, Hirschi KK. Tissue-Resident Macrophage Development and Function. *Front Cell Dev Biol* (2020) 8:617879. doi: 10.3389/fcell.2020.617879
51. de Rooij SR, Painter RC, Holleman F, Bossuyt PM, Roseboom TJ. The Metabolic Syndrome in Adults Prenatally Exposed to the Dutch Famine. *Am J Clin Nutr* (2007) 86(4):1219–24. doi: 10.1093/ajcn/86.4.1219
52. Zheng X, Wang Y, Ren W, Luo R, Zhang S, Zhang JH, et al. Risk of Metabolic Syndrome in Adults Exposed to the Great Chinese Famine During the Fetal Life and Early Childhood. *Eur J Clin Nutr* (2012) 66(2):231–6. doi: 10.1038/ejcn.2011.161
53. Yan S, Hou W, Wu H, Jiang W, Li Y, Zhang Y, et al. Prenatal Exposure to the Chinese Famine and the Risk of Metabolic Syndrome in Adulthood Across Consecutive Generations. *Eur J Clin Nutr* (2020) 74(8):1229–36. doi: 10.1038/s41430-020-0561-3
54. Yura S, Itoh H, Sagawa N, Yamamoto H, Masuzaki H, Nakao K, et al. Role of Premature Leptin Surge in Obesity Resulting From Intrauterine Undernutrition. *Cell Metab* (2005) 1(6):371–8. doi: 10.1016/j.cmet.2005.05.005
55. Bouma HR, Carey HV, Kroese FG. Hibernation: The Immune System at Rest? *J Leukoc Biol* (2010) 88(4):619–24. doi: 10.1189/jlb.0310174

Conflict of Interest: The authors declare that the research was conducted in the absence of any commercial or financial relationships that could be construed as a potential conflict of interest.

Publisher's Note: All claims expressed in this article are solely those of the authors and do not necessarily represent those of their affiliated organizations, or those of the publisher, the editors and the reviewers. Any product that may be evaluated in this article, or claim that may be made by its manufacturer, is not guaranteed or endorsed by the publisher.

frontiers in Endocrinology

MINI REVIEW
published: 18 February 2022
doi: 10.3389/fendo.2022.852636

Insights Into the Regulation of Offspring Growth by Maternally Derived Ghrelin

Takahiro Sato[1*], *Takanori Ida*[2], *Yuki Shiimura*[1,3,4], *Kazuma Matsui*[1], *Kanae Oishi*[1] *and Masayasu Kojima*[1*]

[1] Division of Molecular Genetics, Institute of Life Science, Kurume University, Kurume, Japan, [2] Division for Identification and Analysis of Bioactive Peptides, Department of Bioactive Peptides, Frontier Science Research Center, University of Miyazaki, Miyazaki, Japan, [3] Department of Cell Biology, Graduate School of Medicine, Kyoto University, Kyoto, Japan, [4] Department of Molecular and Cellular Physiology, Stanford University School of Medicine, Stanford, CA, United States

The regulation of fetal development by bioactive substances such as hormones and neuropeptides derived from the gestational mother is considered to be essential for the development of the fetus. On the other hand, it has been suggested that changes in the physiological state of the pregnant mother due to various factors may alter the secretion of these bioactive substances and induce metabolic changes in the offspring, such as obesity, overeating, and inflammation, thereby affecting postnatal growth and health. However, our knowledge of how gestational maternal bioactive substances modulate offspring physiology remains fragmented and lacks a systematic understanding. In this mini-review, we focus on ghrelin, which regulates growth and energy metabolism, to advance our understanding of the mechanisms by which maternally derived ghrelin regulates the growth and health of the offspring. Understanding the regulation of offspring growth by maternally-derived ghrelin is expected to clarify the fetal onset of metabolic abnormalities and lead to a better understanding of lifelong health in the next generation of offspring.

Keywords: offspring, growth, maternal ghrelin, GHS-R, placenta

OPEN ACCESS

Edited by:
Hiroaki Itoh, Hamamatsu University School of Medicine, Japan

Reviewed by:
Tomoya Nakamachi, University of Toyama, Japan
Ken Fujiwara, Kanagawa University, Japan

***Correspondence:**
Takahiro Sato
satou_takahiro@kurume-u.ac.jp
Masayasu Kojima
kojima_masayasu@kurume-u.ac.jp

Specialty section:
This article was submitted to Experimental Endocrinology, a section of the journal Frontiers in Endocrinology

Received: *11 January 2022*
Accepted: *19 January 2022*
Published: *18 February 2022*

Citation:
Sato T, Ida T, Shiimura Y, Matsui K, Oishi K and Kojima M (2022) Insights Into the Regulation of Offspring Growth by Maternally Derived Ghrelin. Front. Endocrinol. 13:852636. doi: 10.3389/fendo.2022.852636

INTRODUCTION

Ghrelin is a peptide hormone purified from the stomach as an endogenous ligand for the GH secretagogue receptor (GHS-R) (1). The ghrelin receptor GHS-R is highly conserved from fish to humans and is widely expressed in central and peripheral organs such as the brain, pituitary gland, and pancreas (2–7). Therefore, the ghrelin-GHS-R system is involved in the regulation of various physiological functions such as growth hormone (GH) secretion (1), feeding (8), body temperature (9), gastric motility (10), gastric acid secretion (11), insulin and gastrin secretion (12), circulatory systems (13, 14), and stress responses (14). Neonatal rats treated with ghrelin showed faster eye and vaginal opening, indicating that ghrelin is also involved in neonatal development (15). Furthermore, in rodents, it has been shown that ghrelin secreted from the stomach and placenta of pregnant mothers may also act on the fetus (16), suggesting that maternally-derived ghrelin may regulate fetal growth and affect postnatal health. In this mini-review, we will first outline the molecular structure and physiological function of ghrelin to understand the changes in maternal physiological status

and ghrelin secretion. Next, we will advance our understanding of the role of maternal ghrelin in the regulation of offspring growth, particularly in the fetus, and discuss the effects of maternal ghrelin on the maintenance and disruption of offspring health after birth.

BASIC KNOWLEDGE ABOUT GHRELIN AND GHS-R

Molecular Structure and Distribution of Ghrelin

Ghrelin is a peptide hormone discovered in rat and human stomachs as an endogenous ligand for GHS-R (1) (**Figure 1A**). Human ghrelin is a bioactive peptide of 28 amino acid residues with a molecular weight of 3,370.9. The side chain of the third serine residue is esterified with octanoic acid (molecular weight 144), a fatty acid with an 8-carbon chain containing no double bond (1). Ghrelin has been identified in a variety of mammals, birds, reptiles, amphibians, and fish, all of which have the third serine or threonine residue modified by a fatty acid (1, 18–26) (**Figure 1B**). Ghrelin is a potent stimulator of GH secretion both *in vitro* and *in vivo*, hence the name "ghrelin" is based on the Indo-European languages "ghre" for "grow" (1). The name "ghrelin" also includes the meaning "to release" GH (1). On the other hand, ghrelin molecules that are not modified with fatty acids are called desacyl ghrelin and do not have GH release activity (27). Ghrelin is the only peptide hormone in mammals that is acylated and modified by octanoic acid, and this acylation modification is catalyzed by ghrelin O-acyltransferase (GOAT) (28) (**Figure 1A**). When conducting research on ghrelin, it is necessary to consider the characteristic molecular structure of ghrelin and the associated biosynthetic pathway.

Ghrelin is most abundant in the stomach and is also secreted by the duodenum (26, 27, 29–33). Other small amounts of ghrelin production have been found in the hypothalamus, pancreas, kidney, and placenta (5, 34–37) In the stomach, ghrelin is most abundant in the gastric fundus where it is produced in oxyntic glands, and is a closed endocrine cell not in contact with the lumen (29). Ghrelin-producing cells have been called X/A-like cells because they contain many secretory

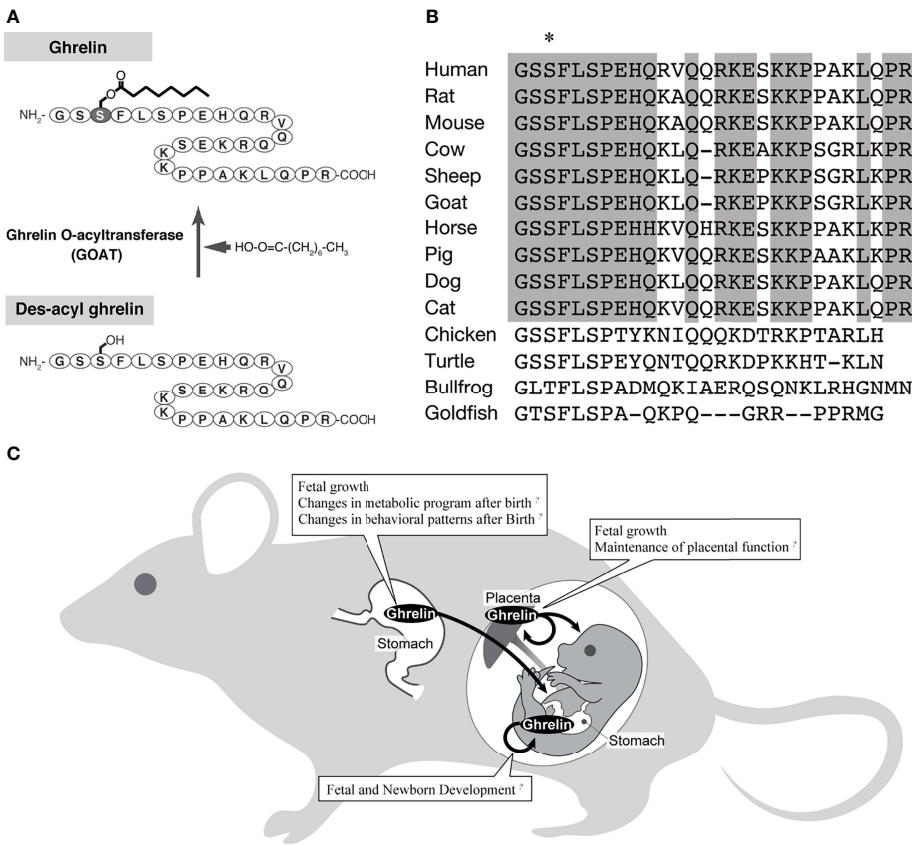

FIGURE 1 | The biochemistry of ghrelin and the action of ghrelin in the fetus. **(A)** Biosynthesis of ghrelin. The active form of ghrelin is produced by the action of a ghrelin-specific fatty acid modifying enzyme (GOAT). **(B)** Comparison of ghrelin sequences, mainly from mammals (modified from Ida et al., 2010) (17). Asterisk indicates amino acid residues with fatty acid modifications. Gray boxes indicate amino acids that are highly conserved among mammals. **(C)** A schematic diagram of the pathway of ghrelin from the mother to the fetus.

granules and resemble A cells that produce glucagon in the pancreas (26, 29, 38). Ghrelin has been reported to be stored in electron-dense secretory granules of nearly uniform size, 120 nm in diameter. Ghrelin cells account for 20-25% of the endocrine cells in the gastric body and are the second most abundant endocrine cells after histamine-producing enterochromaffin-like cells (29).

Molecular Structure and Distribution of GHS-R

The GHS-R gene consists of two exons: the first exon encodes the first through fifth transmembrane regions, and the second exon encodes the sixth through seventh transmembrane regions (39, 40). The ghrelin receptor gene produces two types of mRNAs, type 1a and type 1b. Type 1a receptor binds ghrelin as a seven-transmembrane G protein-coupled receptor (GPCR), whereas type 1b is a five-transmembrane receptor and does not bind ghrelin (40). Recently, several ghrelin receptor structures have been determined, including the active-ghrelin binding form (41–43). The ligand-binding pocket of the ghrelin receptor has a unique architecture, a bifurcated pocket not found in closely related GPCRs, and this structural feature is known to be utilized to recognize the octanoic acid modification of ghrelin. After activation, GHS-R binds to the trimeric Gq protein and promotes Ca^{2+} release from the endoplasmic reticulum *via* activation of phospholipases and production of inositol 3-phosphate (40). This Ca^{2+} pathway is the intracellular signaling system of ghrelin.

GHS-Rs are highly conserved from fish to humans and are widely expressed in central and peripheral organs such as the brain (hypothalamus, cerebral cortex, hippocampus, substantia nigra, brainstem, etc.), pituitary gland, and pancreas (2–7). This broad distribution of GHS-R allows ghrelin to exhibit a wide variety of physiological effects.

Physiological Functions of Ghrelin

Ghrelin has a wide variety of physiological effects that can affect maternal maintenance and fetal growth. In particular, the stimulation of GH release from the pituitary gland and the enhancement of feeding in the hypothalamus are known to be the major physiological effects of the ghrelin/GHS-R axis.

Regulation of Growth Hormone Secretion by Ghrelin

Although many factors regulate the synthesis and secretion of GH in the pituitary gland, GH secretion is essentially regulated by three ligand/ligand-receptor axes the classically known growth hormone-releasing hormone (GHRH)/GHRH receptors of the hypothalamic-pituitary axis, somatostatin (SST)/SST receptors, and ghrelin/GHS-R. In terms of GH secretion, GHRH/GHRH receptors are primarily responsible for GH synthesis and secondary to GH release, ghrelin/GHS-R are primarily responsible for GH release and secondary to GH synthesis, and somatostatin/somatostatin receptors work to inhibit GH release (1, 44). Ghrelin secreted from the stomach stimulates GH secretion by stimulating afferent vagal nerves expressing nearby GHS-Rs (45). Ghrelin secreted from ghrelin neurons in the hypothalamic arcuate nucleus also binds to GHS-Rs expressed on GHRH neurons to release GHRH and induce GH secretion (46).

Hyperphagic Effect of Ghrelin

Another major physiological effect of ghrelin is its ability to promote food intake. When ghrelin is administered centrally or peripherally to rats or mice, it promotes feeding and weight gain (8, 47, 48). However, ghrelin-induced food intake is not associated with GH secretion. In addition, subcutaneous transplantation of a ghrelin-producing cell line into nude mice increases blood ghrelin levels, increasing food intake (49). This cell line maintains the physiological regulation of ghrelin secretion, such that ghrelin secretion is decreased by the addition of glucose or insulin. Therefore, the blood ghrelin level of nude mice transplanted with this cell line is thought to have increased while retaining the physiological ghrelin secretion pattern to some extent.

Orexigenic peptides such as neuropeptide Y (NPY) and agouti-related peptide (AgRP) are present in the hypothalamus. These peptides exhibit an orexigenic effect when administered intraventricularly but not when administered peripherally. The orexigenic effect of ghrelin occurs not only by intracerebroventricular administration but also by intravenous and intraperitoneal administration, indicating that ghrelin is the only peripheral hunger signal (8). The hypothalamus contains an important central nucleus involved in the regulation of food intake, where a large amount of information is integrated to control energy metabolism. The orexigenic effect of ghrelin occurs when ghrelin activates NPY/AgRP neurons expressing GHS-R and promotes the secretion of NPY and AgRP (8). Ghrelin administered intravenously also activates NPY/AgRP neurons to promote feeding (45). The involvement of the vagus nerve, a brain nerve that transmits various information from the gastrointestinal tract to the interneurons and neocortex *via* the brainstem, has been reported as a pathway for the central effects of ghrelin secreted from the stomach (45). According to this report, ghrelin binds to GHS-R, which is produced by vagal afferent neurons and transported to afferent fiber terminals, and inhibits the electrical activity of vagal afferent fibers. In addition, ghrelin information is transmitted to the solitary nucleus of the medulla oblongata, where it changes neurons and stimulates NPY/AgRP neurons in the hypothalamus, thereby promoting feeding. However, since there are some reports on the pathway through the blood-brain barrier (50–52), it is necessary to continue to monitor the progress of research on how ghrelin secreted from the stomach acts on the central nervous system.

Regulation of Energy Metabolism

Ghrelin is also involved in the regulation of energy metabolism. Continuous subcutaneous administration of large amounts of ghrelin increases body weight, and since the respiratory quotient increases at this time, it is thought that this is due to an increase in adipose tissue associated with suppression of body fat utilization (47). In mice, ghrelin maintains the diurnal rhythm of body temperature and induces torpor, an energy-conserving phenomenon in which body temperature is markedly lowered during starvation (9). In humans, plasma ghrelin concentration is inversely correlated with body mass index (BMI), and is reported to be low in obese individuals and high in cases of anorexia nervosa, severe heart failure, and lung cancer with strong cachexia.

This suggests that ghrelin is activated during negative energy balance and maintains homeostasis by stimulating food intake, fat accumulation, and lowering body temperature. Thus, ghrelin regulates energy metabolism through a variety of functions, but it has been reported that there is no correlation between ghrelin levels and gestational weight gain in overweight and normal groups in pregnant humans.

Effects of Ghrelin On the Cardiovascular System

Ghrelin also acts in the regulation of the cardiovascular system. When ghrelin is administered continuously to a rat model of chronic heart failure, improvements in cardiac function are observed, including a decrease in peripheral vascular resistance, an increase in cardiac output, an increase in left ventricular ejection fraction, inhibition of left ventricular remodeling development, and promotion of compensatory cardiac hypertrophy in the non-infarcted area (14). This is thought to be a direct effect of ghrelin and an effect mediated by GH/insulin-like growth factor-1 (IGF-1), which is increased by ghrelin (14). Ghrelin also causes increased blood flow and decreased blood pressure in a GH- and IGF-1-independent manner, which may be due to the vasodilator effect of ghrelin, since GHS-R is also present in blood vessels (53). In addition, a single dose of ghrelin intravenously in healthy subjects has a relatively long-lasting blood pressure (mean arterial pressure) lowering effect of about 10 mmHg, along with an increase in plasma GH concentration, and also increases cardiac index and cardiac output without changing heart rate (13). This indicates that ghrelin alters circulatory dynamics by suppressing the sympathetic nervous system. As mentioned above, plasma GH and ghrelin concentrations are elevated in patients with chronic heart failure associated with cachexia, but they are positively correlated with BMI, plasma tumor necrosis factor-α, and plasma GH concentrations (54), suggesting that ghrelin functions in a compensatory manner in the pathogenesis of cachexia, in which energy metabolism tends toward catabolism. In preeclampsia, a known complication of pregnancy, ghrelin secretion is increased, and serum ghrelin levels have been reported to correlate negatively with blood pressure (55, 56). It has been suggested that this is because ghrelin improves endothelial function by enhancing angiogenesis through the Jagged1/Notch2/VEGF pathway (57).

MATERNAL GHRELIN AND FETAL GROWTH

Various perspectives on the effects of ghrelin on fetal growth have been reported (**Figure 1C**), including ghrelin in the maternal circulating blood acting through the placenta and by placenta-derived ghrelin (**Table 1**). In the rat fetus, ghrelin mRNA has been slightly observed in the stomach from late pregnancy, whereas GHS-R mRNA has been detected at high levels in various peripheral fetal tissues from as early as embryonic day 14, and has also been confirmed by immunohistochemistry (16, 59, 61). Therefore, the regulation of fetal growth by ghrelin is thought to be essentially due to maternally derived ghrelin.

Maternal ghrelin includes ghrelin derived from the placenta and ghrelin derived from the maternal circulating blood (36, 58–60, 62). Placental ghrelin has been found in human and rat placentas, and ghrelin mRNA has been detected both in the first trimester and postpartum in humans (36). Immunohistochemical analysis has also shown that ghrelin is expressed in the human placenta in the first trimester in cytotrophoblasts and rarely in syncytiotrophoblasts (36). In addition, ghrelin was also identified in BeWo cells, a cell line of human choriocarcinoma (36). Ghrelin is also detected by immunohistochemistry in the cytoplasm of labyrinth trophoblast of the rat placenta, but placental ghrelin mRNA from pregnant rats shows a characteristic expression profile in which ghrelin is almost undetectable in early pregnancy, reaches its peak expression on day 16 of pregnancy, and decreases in late pregnancy (36). In other words, ghrelin is present in both human and rat placentas and shows a pregnancy-related time course of expression (36). It has been suggested that the function of placental-derived ghrelin may be to influence postnatal weight gain, but this appears to be limited to cases where the mother's weight is normal (62).

On the other hand, research on ghrelin derived from maternal circulating blood was been conducted early in the discovery of

TABLE 1 | Detection of ghrelin in the placenta.

Animal species	Detection Sites	Detection Periods	Detection Methods	References
Human				
Ghrelin	Cytotrophoblast cells.	First-trimester.	Immunohistochemistry	(36)
Ghrelin mRNA		First trimester and after delivery.	RT-PCR	(36)
Rat				
Ghrelin	The cytoplasm of labyrinth trophoblast.	Day 21 of pregnancy.	Immunohistochemistry	(36)
Ghrelin mRNA		Almost undetectable during early pregnancy, with a sharp peak of expression at day 16 and decreasing in the latest stages of gestation. Embryonic day 17 (E17).	RT-PCR & Northern blot *In situ* hybridization	(36) (58)
Mouse				
Ghrelin	Labyrinthine trophoblast cells	Gestational day 17.5 (GD17.5).	Immunohistochemistry	(59)
Ovine				
Ghrelin	The maternal epithelium, caruncle and trophectoderm.	All gestational time points.	Immunohistochemistry	(60)

ghrelin. It was found that a single injection of ghrelin into the mother increased the concentration of circulating ghrelin in the fetus within 5 minutes after injection, and it was reported that maternal ghrelin was readily transferred to the fetal circulation (16). This study also found that chronic treatment of rat mothers with ghrelin increased birth weight, and that restricting maternal food intake with paired feeding after ghrelin administration stimulated fetal growth, while active maternal immunization decreased fetal weight during pregnancy (16). It has also been reported that maternal ghrelin administration can alter the behavior of the offspring (15). Administration of ghrelin to pregnant mice suppressed exploratory behavior of the pups in an open field test (15). The pups had high plasma levels of basal corticotropin-releasing hormone and did not respond to acute restraint stress (15). It has also been found that repeated maternal restraint stress increases maternal and fetal plasma acyl ghrelin concentrations (15). Thus, it can be seen that increased maternal ghrelin under physiological conditions such as stress is transported to the fetus and alters the endocrine environment of the offspring, affecting their behavior. In addition, female wild-type mice born from ghrelin heterozygous dams exposed to ghrelin deficiency *in utero* have reduced reproductive capacity and smaller litters (63). In addition, implantation of wild-type embryos into the uterus of mice exposed to intrauterine ghrelin deficiency results in a 60% reduction in implantation rate compared to embryos implanted in non-exposed uteri (63). Uterine expression of several genes important for implantation is also altered in the uterus of mice exposed to intrauterine ghrelin deficiency, and abnormalities in endometrial proliferation have been observed (63), leading to the conclusion that exposure to reduced ghrelin in the uterus causes defects in uterine developmental programming and subsequent infertility in wild-type offspring.

Thus, we can see that ghrelin derived from the placenta and maternal circulating blood maintains pregnancy by regulating implantation and fetal growth, and also influences the endocrine environment and behavior of the offspring after birth. However, since studies with ghrelin gene-deficient mice have not found abnormalities in the number of pups or newborn weight (9, 64), it is essential to understand the role of maternally derived ghrelin while clarifying the effects of endogenous and exogenous ghrelin.

FUTURE PERSPECTIVES

As mentioned in the introduction, the regulation of fetal growth by bioactive substances such as hormones and neuropeptides derived from the gestational mother is essential. However, there remains a lack of knowledge on how the modulation of these bioactive substances leads to future health and susceptibility to certain diseases. To accumulate such knowledge, it is necessary to promote research on bioactive substances of gestational maternal origin, whose secretory dynamics have been elucidated, which have also been shown to act reliably on the fetus, and whose involvement in disease has been clarified. In this regard, ghrelin may be one of the most important targets for understanding the fetal onset of metabolic abnormalities.

Although ghrelin has a variety of physiological effects, it is comprehensively a hormone that maintains homeostasis by exerting anabolic effects in hyper-catabolic conditions such as fasting, insulin, and leptin administration. Ghrelin secretion is known to be altered by ingesting factors that may be related to lifestyle, such as a high-fat diet or nicotine (47, 65), and is elevated in hyperemesis gravidarum, a physiological condition unique to pregnant women (66). In addition to these reports, the fact that ghrelin is secreted by or passes through the placenta in pregnant females implies that changes in ghrelin secretion due to maternal preferences, lifestyle, and physiological conditions may affect the health of the offspring in various ways. Furthermore, it has been suggested that the hyperghrelinemia during maternal undernourishment rewires the hypothalamic development of the offspring when fed a high-fat diet, affecting GHS-R signaling and contributing to the hyperphagia and the increase in body weight (67). Although this report does not describe the effects of maternally-derived ghrelin, it shows that maternal malnutrition also affects GHS-R signaling in the offspring, which is an important finding when considering offspring growth.

As the world's population is currently increasing, the elderly population is also expected to increase along with the development of medical science. Therefore, it is necessary to identify high-risk groups at prenatal and developmental stages, and to realize preemptive medicine through early intervention using food components and other means. Ghrelin is a peptide hormone with a characteristic molecular structure, and it is known that octanoic acid, a side chain necessary for the expression of activity, is added simply by oral administration (68). This suggests that ghrelin may be a good target molecule for healthy longevity.

CONCLUSION

There are two main types of maternally-derived ghrelin: ghrelin secreted from the placenta and ghrelin secreted from the stomach and passed through the placenta. The mechanisms by which these ghrelin act during the embryonic period of the offspring are still under investigation, but as described in this mini-review, maternally-derived ghrelin appears to regulate implantation and fetal growth, maintain pregnancy, and even influence the endocrine environment and behavior of the offspring after birth. Therefore, abnormal maternal ghrelin secretion may interfere with the normal growth of the offspring during embryonic and developmental stages, leading to subsequent functional disorders and diseases. In the future, it is hoped that the mechanisms by which maternally-derived ghrelin regulates fetal function will be elucidated at the molecular level, and that this knowledge will be coupled with an understanding of healthy longevity.

AUTHOR CONTRIBUTIONS

TS examined the data and wrote the manuscript. TS, TI, YS, KM, KO, and MK contributed to the discussion and reviewed the manuscript. All authors contributed to the article and approved the submitted version.

FUNDING

This work was funded by a Grant-in-Aid for Scientific Research (C) (No.20K08898, to TS) from JSPS KAKENHI; and grants (to TS) from the Ishibashi Foundation for the Promotion of Science, the Takeda Scientific Foundation, and the Kobayashi Foundation (No. 215) in Japan.

REFERENCES

1. Kojima M, Hosoda H, Date Y, Nakazato M, Matsuo H, Kangawa K. Ghrelin is a Growth-Hormone-Releasing Acylated Peptide From Stomach. *Nature* (1999) 402:656–60. doi: 10.1038/45230
2. Palyha OC, Feighner SD, Tan CP, McKee KK, Hreniuk DL, Gao YD, et al. Ligand Activation Domain of Human Orphan Growth Hormone (GH) Secretagogue Receptor (GHS-R) Conserved From Pufferfish to Humans. *Mol Endocrinol* (2000) 14:160–9. doi: 10.1210/mend.14.1.0412
3. Chan CB, Cheng CHK. Identification and Functional Characterization of Two Alternatively Spliced Growth Hormone Secretagogue Receptor Transcripts From the Pituitary of Black Seabream Acanthopagrus Schlegeli. *Mol Cell Endocrinol* (2004) 214:81–95. doi: 10.1016/j.mce.2003.11.020
4. Tanaka M, Miyazaki T, Yamamoto I, Nakai N, Ohta Y, Tsushima N, et al. Molecular Characterization of Chicken Growth Hormone Secretagogue Receptor Gene. *Gen Comp Endocrinol* (2003) 134:198–202. doi: 10.1016/S0016-6480(03)00247-8
5. Gnanapavan S, Kola B, Bustin SA, Morris DG, McGee P, Fairclough P, et al. The Tissue Distribution of the mRNA of Ghrelin and Subtypes of its Receptor, GHS-R, in Humans. *J Clin Endocrinol Metab* (2002) 87:2988. doi: 10.1210/jcem.87.6.8739
6. Guan XM, Yu H, Palyha OC, McKee KK, Feighner SD, Sirinathsinghji DJS, et al. Distribution of Mrna Encoding the Growth Hormone Secretagogue Receptor in Brain and Peripheral Tissues. *Mol Brain Res* (1997) 48:23–9. doi: 10.1016/S0169-328X(97)00071-5
7. Bennett PA, Thomas GB, Howard AD, Feighner SD, van der Ploeg LHT, Smith RG, et al. Hypothalamic Growth Hormone Secretagogue-Receptor (GHS-R) Expression is Regulated by Growth Hormone in the Rat. *Endocrinology* (1997) 138:4552–7. doi: 10.1210/endo.138.11.5476
8. Nakazato M, Murakami N, Date Y, Kojima M, Matsuo H, Kangawa K, et al. A Role for Ghrelin in the Central Regulation of Feeding. *Nature* (2001) 409:194–8. doi: 10.1038/35051587
9. Sato T, Oishi K, Koga D, Ida T, Sakai Y, Kangawa K, et al. Thermoregulatory Role of Ghrelin in the Induction of Torpor Under a Restricted Feeding Condition. *Sci Rep* (2021) 11:17954. doi: 10.1038/s41598-021-97440-y
10. Masuda Y, Tanaka T, Inomata N, Ohnuma N, Tanaka S, Itoh Z, et al. Ghrelin Stimulates Gastric Acid Secretion and Motility in Rats. *Biochem Biophys Res Commun* (2000) 276:905–8. doi: 10.1006/bbrc.2000.3568
11. Date Y, Nakazato M, Murakami N, Kojima M, Kangawa K, Matsukura S. Ghrelin Acts in the Central Nervous System to Stimulate Gastric Acid Secretion. *Biochem Biophys Res Commun* (2001) 280:904–7. doi: 10.1006/bbrc.2000.4212
12. Heung-Man L, Wang G, Englander EW, Kojima M, Greeley GH. Ghrelin, a New Gastrointestinal Endocrine Peptide That Stimulates Insulin Secretion: Enteric Distribution, Ontogeny, Influence of Endocrine, and Dietary Manipulations. *Endocrinology* (2002) 143:185–90. doi: 10.1210/endo.143.1.8602
13. Nagaya N, Kojima M, Uematsu M, Yamagishi M, Hosoda H, Oya H, et al. Hemodynamic and Hormonal Effects of Human Ghrelin in Healthy Volunteers. *Am J Physiol - Regul Integr Comp Physiol* (2001) 280:R1483–7. doi: 10.1152/ajpregu.2001.280.5.r1483
14. Nagaya N, Uematsu M, Kojima M, Ikeda Y, Yoshihara F, Shimizu W, et al. Chronic Administration of Ghrelin Improves Left Ventricular Dysfunction and Attenuates Development of Cardiac Cachexia in Rats With Heart Failure. *Circulation* (2001) 104:1430–5. doi: 10.1161/hc3601.095575
15. Hayashida T, Nakahara K, Mondal MS, Date Y, Nakazato M, Kojima M, et al. Ghrelin in Neonatal Rats: Distribution in Stomach and its Possible Role. *J Endocrinol* (2002) 173:239–45. doi: 10.1677/joe.0.1730239
16. Nakahara K, Nakagawa M, Baba Y, Sato M, Toshinai K, Date Y, et al. Maternal Ghrelin Plays an Important Role in Rat Fetal Development During Pregnancy. *Endocrinology* (2006) 147:1333–42. doi: 10.1210/en.2005-0708
17. Ida T, Miyazato M, Lin XZ, Kaiya H, Sato T, Nakahara K, et al. Purification and Characterization of Caprine Ghrelin and its Effect on Growth Hormone Release. *J Mol Neurosci* (2010) 42:99–105. doi: 10.1007/s12031-010-9379-0
18. Angeloni SV, Glynn N, Ambrosini G, Garant MJ, Higley JD, Suomi S, et al. Characterization of the Rhesus Monkey Ghrelin Gene and Factors Influencing Ghrelin Gene Expression and Fasting Plasma Levels. *Endocrinology* (2004) 145:2197–205. doi: 10.1210/en.2003-1103
19. Galas L, Chartrel N, Kojima M, Kangawa K, Vaudry H. Immunohistochemical Localization and Biochemical Characterization of Ghrelin in the Brain and Stomach of the Frog Rana Esculenta. *J Comp Neurol* (2002) 450:34–44. doi: 10.1002/cne.10291
20. Kaiya H, Kojima M, Hosoda H, Moriyama S, Takahashi A, Kawauchi H, et al. Peptide Purification, Complementary Deoxyribonucleic Acid (DNA) and Genomic DNA Cloning, and Functional Characterization of Ghrelin in Rainbow Trout. *Endocrinology* (2003) 144:5215–26. doi: 10.1210/en.2003-1085
21. Unniappan S, Lin X, Cervini L, Rivier J, Kaiya H, Kangawa K, et al. Goldfish Ghrelin: Molecular Characterization of the Complementary Deoxyribonucleic Acid, Partial Gene Structure and Evidence for its Stimulatory Role in Food Intake. *Endocrinology* (2002) 143:4143–6. doi: 10.1210/en.2002-220644
22. Kaiya H, Kojima M, Hosoda H, Riley LG, Hirano T, Grau EG, et al. Identification of Tilapia Ghrelin and its Effects on Growth Hormone and Prolactin Release in the Tilapia, Oreochromis Mossambicus. *Comp Biochem Physiol - B Biochem Mol Biol* (2003) 135:421–9. doi: 10.1016/S1096-4959(03)00109-X
23. Kaiya H, Kojima M, Hosoda H, Riley LG, Hirano T, Grau EG, et al. Amidated Fish Ghrelin: Purification, Cdna Cloning in the Japanese Eel and its Biological Activity. *J Endocrinol* (2003) 176:415–23. doi: 10.1677/joe.0.1760415
24. Parhar IS, Sato H, Sakuma Y. Ghrelin Gene in Cichlid Fish is Modulated by Sex and Development. *Biochem Biophys Res Commun* (2003) 305:169–75. doi: 10.1016/S0006-291X(03)00729-0
25. Tanaka M, Hayashida Y, Iguchi T, Nakao N, Nakai N, Nakashima K. Organization of the Mouse Ghrelin Gene and Promoter: Occurrence of a Short Noncoding First Exon. *Endocrinology* (2001) 142:3697–700. doi: 10.1210/endo.142.8.8433
26. Yabuki A, Ojima T, Kojima M, Nishi Y, Mifune H, Matsumoto M, et al. Characterization and Species Differences in Gastric Ghrelin Cells From Mice, Rats and Hamsters. *J Anat* (2004) 205:239–46. doi: 10.1111/j.0021-8782.2004.00331.x
27. Hosoda H, Kojima M, Matsuo H, Kangawa K. Ghrelin and Des-Acyl Ghrelin: Two Major Forms of Rat Ghrelin Peptide in Gastrointestinal Tissue. *Biochem Biophys Res Commun* (2000) 279:909–13. doi: 10.1006/bbrc.2000.4039
28. Yang J, Brown MS, Liang G, Grishin NV, Goldstein JL. Identification of the Acyltransferase That Octanoylates Ghrelin, an Appetite-Stimulating Peptide Hormone. *Cell* (2008) 132:387–96. doi: 10.1016/j.cell.2008.01.017
29. Date Y, Kojima M, Hosoda H, Sawaguchi A, Mondal MS, Suganuma T, et al. Ghrelin, a Novel Growth Hormone-Releasing Acylated Peptide, is Synthesized in a Distinct Endocrine Cell Type in the Gastrointestinal Tracts of Rats and Humans. *Endocrinology* (2000) 141:4255–61. doi: 10.1210/endo.141.11.7757
30. Sakata I, Nakamura K, Yamazaki M, Matsubara M, Hayashi Y, Kangawa K, et al. Ghrelin-Producing Cells Exist as Two Types of Cells, Closed- and Opened-Type Cells, in the Rat Gastrointestinal Tract. *Peptides* (2002) 23:531–6. doi: 10.1016/S0196-9781(01)00633-7
31. Rindi G, Necchi V, Savio A, Torsello A, Zoli M, Locatelli V, et al. Characterisation of Gastric Ghrelin Cells in Man and Other Mammals: Studies in Adult and Fetal Tissues. *Histochem Cell Biol* (2002) 117:511–9. doi: 10.1007/s00418-002-0415-1
32. Tomasetto C, Wendling C, Rio MC, Poitras P. Identification of Cdna Encoding Motilin Related Peptide/Ghrelin Precursor From Dog Fundus. *Peptides* (2001) 22:2055–9. doi: 10.1016/S0196-9781(01)00557-5

33. Ariyasu H, Takaya K, Tagami T, Ogawa Y, Hosoda K, Akamizu T, et al. Stomach is a Major Source of Circulating Ghrelin, and Feeding State Determines Plasma Ghrelin-Like Immunoreactivity Levels in Humans. *J Clin Endocrinol Metab* (2001) 86:4753–8. doi: 10.1210/jcem.86.10.7885
34. Sato T, Fukue Y, Teranishi H, Yoshida Y, Kojima M. Molecular Forms of Hypothalamic Ghrelin and its Regulation by Fasting and 2-Deoxy-D-Glucose Administration. *Endocrinology* (2005) 146:2510–6. doi: 10.1210/en.2005-0174
35. Mori K, Yoshimoto A, Takaya K, Hosoda K, Ariyasu H, Yahata K, et al. Kidney Produces a Novel Acylated Peptide, Ghrelin. *FEBS Lett* (2000) 486:213–6. doi: 10.1016/S0014-5793(00)02308-5
36. Gualillo O, Caminos JE, Blanco M, Garcìa-Caballero T, Kojima M, Kangawa K, et al. Ghrelin, a Novel Placental-Derived Hormone. *Endocrinology* (2001) 142:788–94. doi: 10.1210/endo.142.2.7987
37. Date Y, Nakazato M, Hashiguchi S, Dezaki K, Mondal MS, Hosoda H, et al. Ghrelin is Present in Pancreatic α-Cells of Humans and Rats and Stimulates Insulin Secretion. *Diabetes* (2002) 51:124–9. doi: 10.2337/diabetes.51.1.124
38. Dornonville de la Cour C, Björkqvist M, Sandvik AK, Bakke I, Zhao CM, Chen D. Håkanson R. a-Like Cells in the Rat Stomach Contain Ghrelin and do Not Operate Under Gastrin Control. *Regul Peptides* (2001) 99:141–50. doi: 10.1016/S0167-0115(01)00243-9
39. McKee KK, Palyha OC, Feighner SD, Hreniuk DL, Tan CP, Phillips MS, et al. Molecular Analysis of Rat Pituitary and Hypothalamic Growth Hormone Secretagogue Receptors. *Mol Endocrinol* (1997) 11:415–23. doi: 10.1210/mend.11.4.9908
40. Howard AD, Feighner SD, Cully DF, Arena JP, Liberator PA, Rosenblum CI, et al. A Receptor in Pituitary and Hypothalamus That Functions in Growth Hormone Release. *Science* (1996) 273:974–7. doi: 10.1126/science.273.5277.974
41. Liu H, Sun D, Myasnikov A, Damian M, Baneres JL, Sun J, et al. Structural Basis of Human Ghrelin Receptor Signaling by Ghrelin and the Synthetic Agonist Ibutamoren. *Nat Commun* (2021) 12:6410. doi: 10.1038/s41467-021-26735-5
42. Wang Y, Guo S, Zhuang Y, Yun Y, Xu P, He X, et al. Molecular Recognition of an Acyl-Peptide Hormone and Activation of Ghrelin Receptor. *Nat Commun* (2021) 12:5064. doi: 10.1038/s41467-021-25364-2
43. Shiimura Y, Horita S, Hamamoto A, Asada H, Hirata K, Tanaka M, et al. Structure of an Antagonist-Bound Ghrelin Receptor Reveals Possible Ghrelin Recognition Mode. *Nat Commun* (2020) 11:4160. doi: 10.1038/s41467-020-17554-1
44. Lin-Su K, Wajnrajch MP. Growth Hormone Releasing Hormone (GHRH) and the GHRH Receptor. *Rev Endocrine Metab Disord* (2002) 3:313–23. doi: 10.1023/A:1020949507265
45. Date Y, Murakami N, Toshinai K, Matsukura S, Niijima A, Matsuo H, et al. The Role of the Gastric Afferent Vagal Nerve in Ghrelin-Induced Feeding and Growth Hormone Secretion in Rats. *Gastroenterology* (2002) 123:1120–8. doi: 10.1053/gast.2002.35954
46. Mano-Otagiri A, Nemoto T, Sekino A, Yamauchi N, Shuto Y, Sugihara H, et al. Growth Hormone-Releasing Hormone (GHRH) Neurons in the Arcuate Nucleus (Arc) of the Hypothalamus are Decreased in Transgenic Rats Whose Expression of Ghrelin Receptor is Attenuated: Evidence That Ghrelin Receptor is Involved in the Up-Regulation of GHRH Expression in the Arc. *Endocrinology* (2006) 147:4093–103. doi: 10.1210/en.2005-1619
47. Tschop M, Smiley DL, Heiman ML. Ghrelin Induces Adiposity in Rodents. *Nature* (2000) 407:908–13. doi: 10.1038/35038090
48. Wren AM, Seal LJ, Cohen MA, Brynes AE, Frost GS, Murphy KG, et al. Ghrelin Enhances Appetite and Increases Food Intake in Humans. *J Clin Endocrinol Metab* (2001) 86:5992. doi: 10.1210/jc.86.12.5992
49. Iwakura H, Li Y, Ariyasu H, Hosoda H, Kanamoto N, Bando M, et al. Establishment of a Novel Ghrelin-Producing Cell Line. *Endocrinology* (2010) 151:2940–5. doi: 10.1210/en.2010-0090
50. Banks WA, Tschöp M, Robinson SM, Heiman ML. Extent and Direction of Ghrelin Transport Across the Blood-Brain Barrier is Determined by its Unique Primary Structure. *J Pharmacol Exp Ther* (2002) 302:822–7. doi: 10.1124/jpet.102.034827
51. Uriarte M, de Francesco PN, Fernandez G, Cabral A, Castrogiovanni D, Lalonde T, et al. Evidence Supporting a Role for the Blood-Cerebrospinal Fluid Barrier Transporting Circulating Ghrelin Into the Brain. *Mol Neurobiol* (2019) 56:4120–34. doi: 10.1007/s12035-018-1362-8
52. Rhea EM, Salameh TS, Gray S, Niu J, Banks WA, Tong J. Ghrelin Transport Across the Blood–Brain Barrier can Occur Independently of the Growth Hormone Secretagogue Receptor. *Mol Metab* (2018) 18:88–96. doi: 10.1016/j.molmet.2018.09.007
53. Okumura H, Nagaya N, Enomoto M, Nakagawa E, Oya H, Kangawa K. Vasodilatory Effect of Ghrelin, an Endogenous Peptide From the Stomach. *J Cardiovasc Pharmacol* (2002) 39:779–83. doi: 10.1097/00005344-200206000-00001
54. Shimizu Y, Nagaya N, Isobe T, Imazu M, Okumura H, Hosoda H, et al. Increased Plasma Ghrelin Level in Lung Cancer Cachexia. *Clin Cancer Res* (2003) 9:774–8.
55. Aydin S, Guzel SP, Kumru S, Aydin S, Akin O, Kavak E, et al. Serum Leptin and Ghrelin Concentration of Maternal Serum, Areterial and Venous Cord Blood in Healthy and Preeclamptic Pregnant Women. *J Physiol Biochem* (2008) 64:51–9. doi: 10.1007/bf03168234
56. Erol O, Ellidağ HY, Ayik H, Bülbiil GA, Derbent AU, Kulaksizoğlu S, et al. Increased Serum Ghrelin in Preeclampsia: Is Ghrelin a Friend or a Foe? *Ginekologia Polska* (2016) 87:277–82. doi: 10.17772/gp/57852
57. Wang X, Yang L, Chen Y, Zhang L, Fei H. Ghrelin Promotes Angiogenesis by Activating the Jagged1/Notch2/VEGF Pathway in Preeclampsia. *J Obstetrics Gynaecol Res* (2021) 47:486–94. doi: 10.1111/jog.14555
58. Torsello A, Scibona B, Leo G, Bresciani E, Avallone R, Bulgarelli I, et al. Ontogeny and Tissue-Specific Regulation of Ghrelin Mrna Expression Suggest That Ghrelin is Primarily Involved in the Control of Extraendocrine Functions in the Rat. *Neuroendocrinology* (2003) 77:91–9. doi: 10.1159/000068653
59. Kaur H, Muhlhausler BS, Sim PSL, Page AJ, Li H, Nunez-Salces M, et al. Pregnancy, But Not Dietary Octanoic Acid Supplementation, Stimulates the Ghrelin-Pituitary Growth Hormone Axis in Mice. *J Endocrinol* (2020) 245:327–42. doi: 10.1530/JOE-20-0072
60. Harrison JL, Adam CL, Brown YA, Wallace JM, Aitken RP, Lea RG, et al. An Immunohistochemical Study of the Localization and Developmental Expression of Ghrelin and its Functional Receptor in the Ovine Placenta. *Reprod Biol Endocrinol* (2007) 5:25. doi: 10.1186/1477-7827-5-25
61. Sato M, Nakahara K, Goto S, Kaiya H, Miyazato M, Date Y, et al. Effects of Ghrelin and Des-Acyl Ghrelin on Neurogenesis of the Rat Fetal Spinal Cord. *Biochem Biophys Res Commun* (2006) 350:598–603. doi: 10.1016/j.bbrc.2006.09.088
62. Allbrand M, Åman J, Lodefalk M. Placental Ghrelin and Leptin Expression and Cord Blood Ghrelin, Adiponectin, Leptin, and C-Peptide Levels in Severe Maternal Obesity. *J Maternal-Fetal Neonatal Med* (2018) 31:2839–64. doi: 10.1080/14767058.2017.1358262
63. Martin JR, Lieber SB, McGrath J, Shanabrough M, Horvath TL, Taylor HS. Maternal Ghrelin Deficiency Compromises Reproduction in Female Progeny Through Altered Uterine Developmental Programming. *Endocrinology* (2011) 152:2060–6. doi: 10.1210/en.2010-1485
64. Sun Y, Ahmed S, Smith RG. Deletion of Ghrelin Impairs Neither Growth Nor Appetite. *Mol Cell Biol* (2003) 23:7973–81. doi: 10.1128/mcb.23.22.7973-7981.2003
65. Sato T, Oishi K, Ida T, Kojima M. Suppressive Effect of Ghrelin on Nicotine-Induced Clock Gene Expression in the Mouse Pancreas. *Endocrine J* (2020) 67:73–80. doi: 10.1507/endocrj.EJ19-0169
66. Oruç AS, Mert I, Akturk M, Aslan E, Polat B, Buyukkagnici U, et al. Ghrelin and Motilin Levels in Hyperemesis Gravidarum. *Arch Gynecol Obstetrics* (2013) 287:1087–93. doi: 10.1007/s00404-012-2705-8
67. Sun S, Corbeels K, Desmet L, Segers A, Wang Q, van der Schueren B, et al. Involvement of the GHSR in the Developmental Programming and Metabolic Disturbances Induced by Maternal Undernutrition. *J Nutr Biochem* (2020) 85:108468. doi: 10.1016/j.jnutbio.2020.108468
68. Nishi Y, Hiejima H, Hosoda H, Kaiya H, Mori K, Fukue Y, et al. Ingested Medium-Chain Fatty Acids are Directly Utilized for the Acyl Modification of Ghrelin. *Endocrinology* (2005) 146:2255–65. doi: 10.1210/en.2004-0695

Conflict of Interest: The authors declare that the research was conducted in the absence of any commercial or financial relationships that could be construed as a potential conflict of interest.

this article, or claim that may be made by its manufacturer, is not guaranteed or endorsed by the publisher.

frontiers in Endocrinology

ORIGINAL RESEARCH
published: 24 February 2022
doi: 10.3389/fendo.2022.818064

Comparative Analysis of Gene Expression Profiles in the Adipose Tissue of Obese Adult Mice With Rapid Infantile Growth After Undernourishment *In Utero*

Misako Suzuki[1], *Yukiko Kohmura-Kobayashi*[1]*, *Megumi Ueda*[1], *Naomi Furuta-Isomura*[1], *Masako Matsumoto*[1], *Tomoaki Oda*[1], *Kenta Kawai*[1], *Toshiya Itoh*[1], *Madoka Matsuya*[1], *Megumi Narumi*[1], *Naoaki Tamura*[1], *Toshiyuki Uchida*[1], *Kazuki Mochizuki*[2] *and Hiroaki Itoh*[1]

[1] *Department of Obstetrics and Gynecology, Hamamatsu University School of Medicine, Hamamatsu, Japan,* [2] *Laboratory of Food and Nutritional Sciences, Department of Local Produce and Food Sciences, Faculty of Life and Environmental Sciences, University of Yamanashi, Yamanashi, Japan*

OPEN ACCESS

Edited by:
Cunming Duan,
University of Michigan, United States

Reviewed by:
Takafumi Gotoh,
Kagoshima University, Japan
Susumu Muroya,
Institute of Livestock and Grassland Science (NARO), Japan
Hiroyasu Kamei,
Kanazawa University, Japan

***Correspondence:**
Yukiko Kohmura-Kobayashi
yukki@hama-med.ac.jp

Specialty section:
This article was submitted to Experimental Endocrinology, a section of the journal Frontiers in Endocrinology

Received: *19 November 2021*
Accepted: *31 January 2022*
Published: *24 February 2022*

Citation:
Suzuki M, Kohmura-Kobayashi Y, Ueda M, Furuta-Isomura N, Matsumoto M, Oda T, Kawai K, Itoh T, Matsuya M, Narumi M, Tamura N, Uchida T, Mochizuki K and Itoh H (2022) Comparative Analysis of Gene Expression Profiles in the Adipose Tissue of Obese Adult Mice With Rapid Infantile Growth After Undernourishment In Utero. Front. Endocrinol. 13:818064. doi: 10.3389/fendo.2022.818064

Rapid infantile growth (RG) markedly increases the risk of obesity and metabolic disorders in adulthood, particularly among neonates born small. To elucidate the molecular mechanisms by which RG following undernourishment *in utero* (UN) contributes to the deterioration of adult fat deposition, we developed a UN mouse model using maternal energy restriction, followed by RG achieved by adjustments to 4 pups per litter soon after birth. A high-fat diet (HFD) was fed to weaned pups treated or not (Veh) with tauroursodeoxycholic acid (TU). UN-RG pups showed the deterioration of diet-induced obesity and fat deposition, which was ameliorated by TU. We performed a microarray analysis of epididymal adipose tissue and two gene enrichment analyses (NN-Veh *vs* UN-RD-Veh and UN-RG-Veh *vs* UN-RG-TU). The results obtained identified 4 common gene ontologies (GO) terms of inflammatory pathways. In addition to the inflammatory characteristics of 4 GO terms, the results of heatmap and principal component analyses of the representative genes from 4 GO terms, genes of interest (GOI; *Saa3, Ubd, S100a8, Hpx, Casp1, Agt, Ptgs2*) selected from the 4 GO terms, and immunohistochemistry of macrophages collectively suggested the critical involvement of inflammation in the regulation of fat deposition in the responses to UN and TU. Therefore, the present results support the 'Developmental Origins of Metaflammation', the last word of which was recently proposed by the concept of metabolic disorders induced by low-grade systemic inflammation.

Keywords: obesity, pregnancy, adipose tissue, inflammation, catch-up growth, Developmental Origins of Health and Disease (DOHaD), low birth weight, macrophage

INTRODUCTION

We are in the midst of a worldwide obesity epidemic. The global prevalence of obesity has doubled since 1980 (1) and is now an international public health issue (2). Obesity is frequently associated with impaired glucose tolerance, dyslipidemia, and hypertension, and the combination of these metabolic disorders is associated with atherosclerosis-related diseases. Therefore, the concept of metabolic syndrome has been proposed (3). Increasing evidence has demonstrated that environmental disruptions in the early susceptible period affect health and promote a predisposition to non-communicable diseases (NCDs) in later life, based upon which the concept of the Developmental Origins of Health and Disease (DOHaD) was established (4, 5). Eriksson et al. (2001) identified a high body mass index (BMI) at 7 years old as a risk factor for adult obesity with low-birth weights in 3,659 individuals born at Helsinki University Hospital between 1924 and 1933 (6). Ong et al. conducted systematic reviews and demonstrated that rapid infantile weight gain was consistently associated with an increased risk of obesity later in life (7). Ekelund et al. (2007) showed that rapid infantile weight gain was associated with clustered metabolic disruptions in 128 affected individuals at the age of 17 years (8). Martin et al. (2017) performed a systemic review and found that longer-term health outcomes found catch-up growth were associated with a higher body mass, BMI, or cholesterol in later life; however, catch-up growth following low birth weight may have short-term benefits for individuals with low birth weight (9). Singhal et al. (2017) reported that growth acceleration in healthy infants born at term (either normal or small for gestation) may be associated with an increased long-term risk of obesity and NCDs; however, the benefits of rapid infant weight gain for later neurodevelopment supports its encouragement in infants born preterm (10). These findings led us to the concept that rapid infantile growth (RG) in term newborns, particularly with low-birth weights, is causatively associated with a predisposition to obesity and metabolic syndrome in later life. However, to the best of our knowledge, the underlying molecular mechanisms by which RG in small newborns programs a predisposition to the deterioration of fat deposition have not yet been elucidated. Indeed, risk of NCDs resulted from RG in small newborns applies well to 'Mismatch hypothesis' (11) (12), one of central hypotheses of DOHaD theory. In the present study, we hypothesized the presence of specific pattens in gene expression profiles of the adipose tissue of pups with RG and undernutrition *in utero* (UN).

We established a mouse model of UN using maternal energy restriction, which develops the phenotypes of various NCDs (13–15), and subsequently demonstrated that diet-induced fat deposition in adipose tissue and the liver was significantly greater in UN pups than in normal nutrition (NN) pups (13, 16–18). Oral treatments with the hydrophilic secondary bile acid tauroursodeoxycholic acid (TUDCA), an endoplasmic reticulum (ER) stress alleviator, markedly ameliorated developmentally-induced hepatic steatosis in UN pups, but not in NN pups (17, 18). Therefore, modifications to this animal model of UN are promising for investigating the effects of RG on developmentally-programed fat deposition and its amelioration by TUDCA (TU).

The overall aim of the present study was to examine the characteristics of gene expression profiles associated with the changes in the amount of adult adipose tissue deposition, i.e. deteriorations induced by RG after UN and improvements by TU. The specific objectives of the present study were 1) to develop a mouse model of RG soon after birth by reducing the number of pups per litter to 4 pups (UN-RG) compared to 8 pups per litter for NN, 2) to investigate the effects of TU on UN-RG pups and NN pups fed a high-fat diet (HFD), 3) to perform a microarray analysis followed by a gene enrichment analysis of epididymal fat tissues (NN-Veh *vs* UN-RG-Veh and UN-RG-Veh *vs* UN-RG-TU) in order to identify common gene ontologies (GO) terms, 4) to conduct heatmap and principal component analyses of the common GO identified, 5) to identify genes of interest (GOI) from these GO terms and subject them to quantitative RT-PCR, and 6) to immunohistochemically assess the infiltration of macrophages in epididymal adipose tissue in consideration of the characteristics of the GO terms and GOI identified.

MATERIALS AND METHODS

Mouse Model of UN-RG

The procedures used are shown in **Figures 1A, B**. We modified our previously reported animal model of maternal energy restriction (13, 14, 16–19) such that pups were subjected to RG during the lactation period until weaning (19.5 d) following UN by maternal energy restriction. In brief, pregnant C57Bl/6 NCrSlc mice were purchased at 7.5 days post coitum (dpc) from Japan SLC, Inc. (Hamamatsu, Japan) and housed individually with free access to water under a 12-h light/dark cycle in a specific-pathogen free facility. There was no symptom of infection in dams and pups all through the experiment. Regular chow (formula number D06121301, Research Diets Inc., New Brunswick, NJ) was grinded into a fine powder and placed into a feeding basket (SN-950; Shimano Manufacturing, Co., Ltd., Tokyo, Japan). Dams were divided into two groups at 11.5 dpc. The NN group was fed powdered regular chow *ad libitum* (20 dams). Based on data obtained on the previous day, the daily energy intake of the UN group (20 dams) was restricted to 60% that of NN dams from 11.5 dpc to the day before the delivery of pups (17.5 dpc). In the morning of 18.5 dpc, 2.5 g of powdered standard diet was supplied to UN dams, followed by 3.5 g of extra food in the evening of 18.5 dpc just before the night of parturition to prevent the consumption of pups. NN and UN dams were both fed *ad libitum* after delivery, with powdered chow being changed to sticks 2.5 days after delivery.

The same dams nursed pups. In UN dams, the number of pups was adjusted to 4 per litter at 1.5 days of age (d) for the purpose of inducing RG during the lactation period (UN-RG pups; 60 randomly selected pups)(**Figure 1B**). In NN dams, the number of pups was adjusted to 8 per litter at 1.5 d as the control (NN pups; 60 randomly selected pups)(**Figure 1B**). Male pups

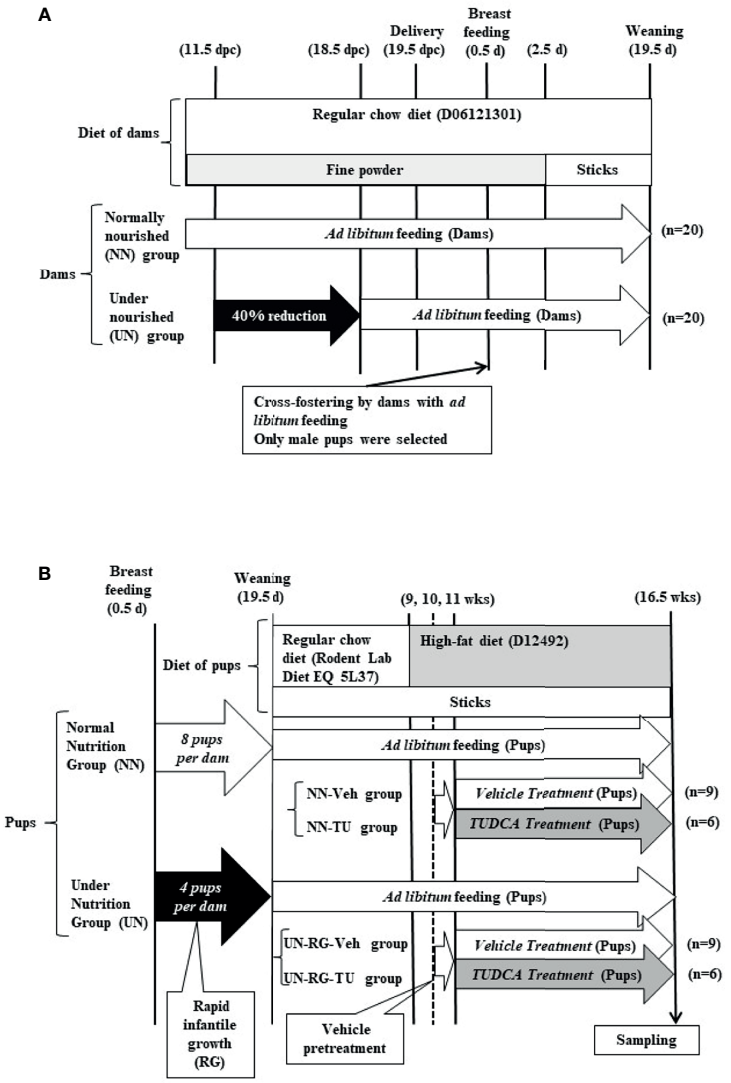

FIGURE 1 | Schematic illustration of experimental procedures in dams **(A)** and pups **(B)**.

were selected, and female pups were only included when matching odd numbers of 4 or 8 per litter. Rodent Lab Diet EQ 5L37 (Japan SLC, Inc., Hamamatsu, Japan) was supplied after weaning. A HFD containing 60% lipids (formula number D12492, Research Diets Inc.) was supplied to all pups from 9 to 16.5 wks. At 9 wks, we randomly selected 15 pups each from NN pups and UN-RG pups (a total of 30 pups). Between 11 and 16.5 wks, TUDCA (Merck Japan Ltd., Tokyo, Japan) (TU) or vehicle distilled water (Veh) was orally administered by gastric lavage at 0.5 g/kg body weight per day as previously described (17, 18), resulting in four groups, i.e. NN-Veh (n=9), NN-TU (n=6), UN-RG-Veh (n=9), and UN-RG-TU (n=6) groups (**Figure 1B**).

All experimental procedures were conducted in accordance with standards of humane animal care and approved by the Animal Research Committee, Hamamatsu University School of Medicine (H20-014).

Tissue Sampling

At 16.5 wks of age, all pups in the independent experimental cohort were decapitated and samples of blood and epididymal adipose tissue were collected. Sampling was systematically performed from 9:00AM to 3:00PM under feeding by a trained technician blinded to the study. To measure adipose tissue weights, we used a GX-600 (A&D Company, Limited, Tokyo, Japan) with a minimum weighing value of 0.001g and standard deviation of 0.001 g. Some samples of adipose tissue were fixed in 10% formaldehyde (0.1 M sodium cacodylate buffer, pH 7.4) and embedded in paraffin for a morphological analysis. Tissue orientation was not taken into consideration when embedding

the tissue. The remaining tissue was snap frozen using liquid nitrogen in blocks and stored at –80°C for mRNA extraction.

Blood Sampling and Measurement

Immediately after the decapitation of pups, blood glucose levels were measured with ACC-CHEK Compact Plus (Roche Diagnostics Japan, Tokyo, Japan) and blood samples were collected into heparin-coated glass tubes and centrifuged at 1200×*g* at 4°C for 15 min. The plasma obtained was aliquoted and stored at –30°C until assayed. Total cholesterol, triglyceride, and HDL cholesterol levels were measured using FUJI DRI-CHEM 3500 (FUJIFILM Holdings Co., Tokyo, Japan).

Microarray Analysis

Aliquots (250 ng) of total RNA obtained from 4 animals per group at 16.5 wks were individually converted to cDNA and labeled with Clariom™ S Assay, mouse (Thermo Fisher Scientific, Inc., cat.# 902930) and GeneChip™WT PLUS Reagent Kit (Thermo Fisher Scientific, Inc., cat.# 902281) according to the manufacturer's instructions. Hybridization, washing, and staining were performed using the Hybridization, Wash, and Stain Kit (Thermo Fisher Scientific, Inc., cat.# 900720), GeneChip™ Hybridization Oven 645 (Thermo Fisher Scientific, Inc.), and GeneChip™ Fluidics Station 450 (Thermo Fisher Scientific, Inc.), according to the manufacturer's protocols. After washing, Array Strips were analyzed using GeneChip™ Scanner 3000 7G (Thermo Fisher Scientific, Inc.). Data were validated using Expression Console™ and Transcriptome Analysis Console™ Software (Thermo Fisher Scientific, Inc.). A cut-off point of ≤-1.3 or ≥1.3 of the linear fold change and P-values was used. We submitted our microarray data, which was approved under the accession number GSE18830 to the GEO repository.

Gene Enrichment, Heatmap, and Principal Component Analyses

A gene enrichment analysis of our list of genes from microarray data was performed to identify which molecular functions and biological processes were overrepresented (20). We used the Metascape online tool (https://metascape.org/gp/index.html#/main/step1) for the enrichment analysis of our gene list. Metascape provides automated meta-analysis tools to understand common and unique pathways within a group of orthogonal target-discovery studies. The terms of individual GO represent biological processes, cellular components, and molecular function categories, as well as Kyoto Encyclopedia of Genes and Genomes pathways, based on the Metascape online tools (21).

Heatmap and principal component analyses of the NN-Veh, UN-RG-Veh, and UN-RG-TU groups were performed using GraphPad Prism 9 (GraphPad Software, San Diego, CA, USA).

Quantitative RT-PCR Analysis of Adipose Tissue

Total RNA was extracted from subcutaneous adipose tissue as previously described (13). Gene expression was evaluated by quantitative RT-PCR using the High Capacity RNA to cDNA Master Mix (catalog number 4390777; Applied Biosystems, Foster city, CA) and SYBR Green PCR Master Mix (catalog number 4309115; Applied Biosystems), according to the manufacturer's recommendations. 18S ribosomal mRNA expression was used as an internal control. The primers used are listed in **Table 1**.

Histological Assessment of Adipose Tissue

Adipose tissue blocks embedded in paraffin were cut into 3-μm-thick sections. A macrophage-specific F4/80 rat monoclonal antibody (MCA497GA, AbD Serotec, Kidlington, UK) was applied to the sections. Detection was performed with a polymer detection kit (ChemMate EnVision™; Dako Japan, Tokyo, Japan) according to the manufacturer's instructions, followed by a reaction with 3,3'-diaminobenzidine and counterstaining with hematoxylin.

Four microscopic fields (0.6 mm^2 × 4) were arbitrarily selected in each section, and the number of positive cells was counted.

Statistical Analysis

Data are expressed as means ± standard deviations. The significance of differences between two mean values was assessed using the Student's *t*-test or the Mann-Whitney U test, where appropriate. GraphPad Prism Version 9 (GraphPad Software, San Diego, CA) was used for statistical calculations. The significance of differences among four mean values was assessed using ANOVA with Tukey's multiple comparison test. A P-value of less than 0.05 was considered to be significant.

TABLE 1 | Forward and revers primers used in quantitative RT-PCR.

	Genebank accession number	Forward	Reverse
Saa3	NM_011315.3	AACTATGATGCTGCCCGGAG	GCTCCATGTCCCGTGAACTT
Ubd	NM_023137.3	TCCGAGTTCGAAGATCCAGC	CTTCCAGCTTCTTTCCGTTGC
S100a8	NM_013650.2	ACTTCGAGGAGTTCCTTGCG	TGCTACTCCTTGTGGCTGTC
Hpx	NM_017371.2	TCCTGGGATCAGCCTTGAGA	ACCTCTGTCCATGTTGCCTG
Casp1	NM_009807.2	ACTGACTGGGACCCTCAAGT	GCAAGACGTGTACGAGTGGT
Agt	NM_007428.4	TTGGCGCTGAAGGATACACA	GATGTATACGCGGTCCCCAG
Ptgs2	NM_011198.4	TGAGTGGGGTGATGAGCAAC	AAGTGGTAACCGCTCAGGTG

RESULTS

Body Weight and Energy Intake Changes in Dams and Pups With or Without UN Followed by RG

Mean body weight from 8.5 to 16.5 d was significantly higher in UN-RG pups than in NN pups (**Figures 2C, D**). Similar growth patterns were observed in UN-RG and NN pups after weaning (**Figure 2C**).

After HFD, body weights were significantly higher in UN-RG-Veh pups than in NN-Veh pups (**Figures 3B, C**). Body weights were significantly lower in UN-RG-TU pups than in UN-RG-Veh pups (**Figures 3B, C**). Similar results were also observed for epididymal adipose tissue weight (UN-RG-TU *vs* UN-RG-Veh) (**Figure 3D**). TU did not alter energy intake per body weight (NN-TU *vs* NN-Veh and UN-RG-TU *vs* UN-RG-Veh) (**Figure 3E**).

Blood lipid profiles and glucose levels are summarized in **Table 2**.

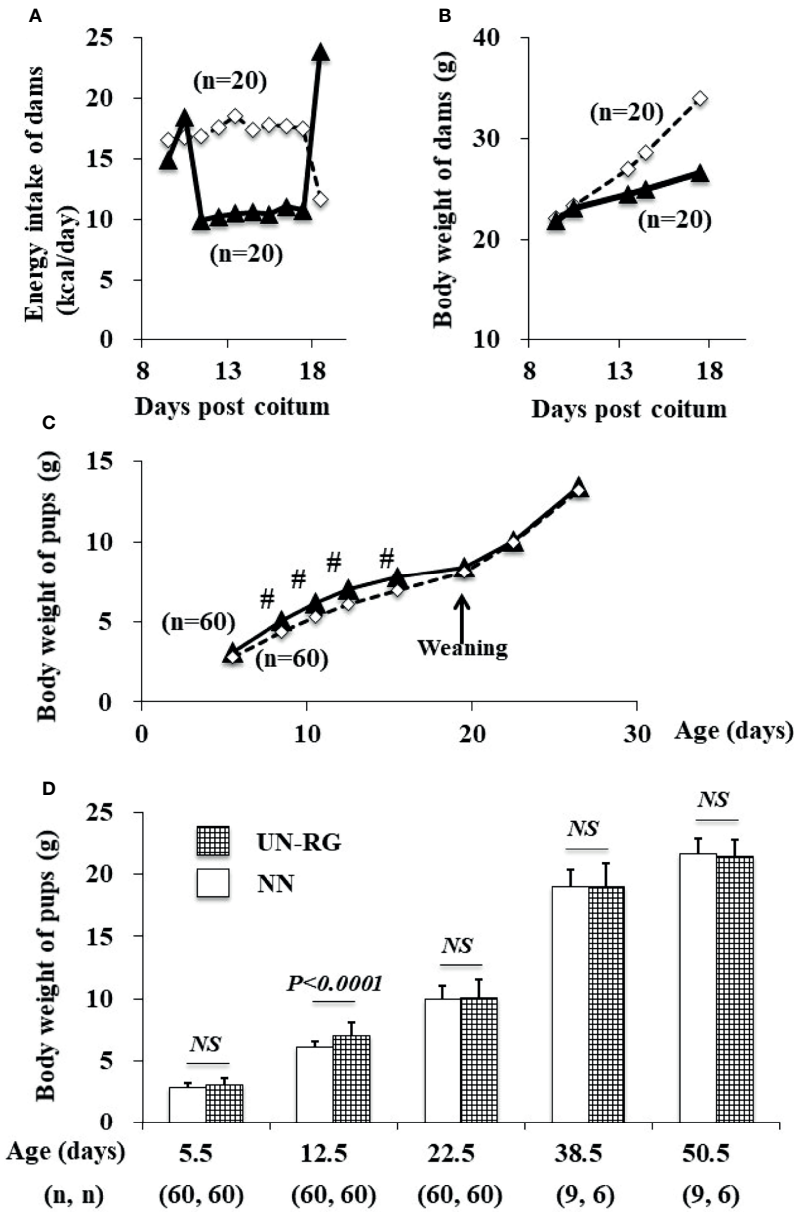

FIGURE 2 | Changes in the energy intake **(A)** and body weight **(B)** of dams during pregnancy and in the body weight of pups **(C, D)** before HFD. White rectangles indicate NN dams **(A, B)** and pups **(C)**. Black triangles indicate UN **(A, B)** dams and UN-RG pups **(C)**. Means of the data were plotted **(A–C)**. #P < 0.01. NS, no statistical significance.

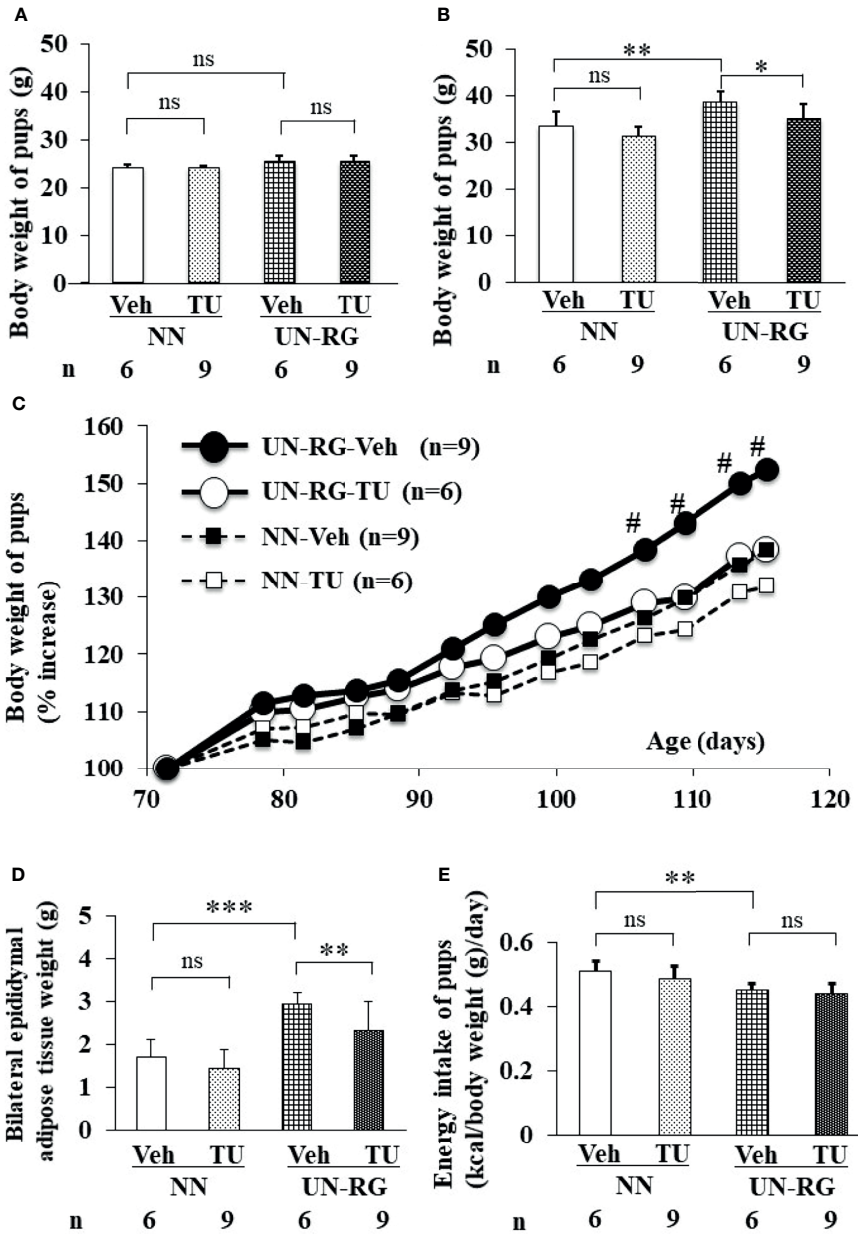

FIGURE 3 | Changes in the body or tissue weight **(A–D)** and energy intake **(E)** of pups before **(A)** and after **(B–E)** HFD. Body weight [**(A)**; 9 wks] [**(B)**; 16.5 wks] [**(C)**; 9-16.5 wks],, epididymal adipose tissue weight [**(D)**; 16.5 wks), and energy intake [**(E)**; 15 wks]. Tissue sampling was performed at 16.5 wks. $^{\#}P < 0.01$ *vs* NN-Veh. *P < 0.05; **P < 0.01; ***P < 0.001. NS, no statistical significance. Means of the data were plotted **(C)**.

Microarray, Gene Enrichment, Heatmap, and Principal Component Analyses of Epididymal Adipose Tissues at 16.5 Wks

Figure 4A shows volcano plots of microarray analyses of gene expression profiles in the epididymal adipose tissues of UN-RG-Veh and NN-Veh pups at 16.5 wks. The results of the gene enrichment analysis and resultant GO terms in ascending order of P-values are shown in **Figure 4B**. **Figure 5A** shows volcano plots of the microarray analysis of gene expression profiles in the epididymal adipose tissues of UN-RG-TU and UN-RG-Veh pups at 16.5 wks. The results of the gene enrichment analysis and resultant GO terms in ascending order of P-values are shown in **Figure 5B**. The representative genes which were not normalized by TU in UN-RG pups were summarized in **Supplementary Table 2**.

The following GO terms were commonly observed in the results of two gene enrichment analyses: 1) Inflammatory response, 2) Response to interferon-γ, 3) Regulation of

TABLE 2 | Body weight, adipose tissue weight, and lipid and glucose levels in blood at 16 wks.

	NN		UN-RG	
	Veh (n = 9)	**TU (n = 6)**	**Veh (n = 9)**	**TU (n = 6)**
Body weight (g)	33.5 ± 3.0	31.3 ± 2.3#	38.6 ± 2.4#	34.6 ± 2.6*
Left epididymal adipose tissue weight (g)	0.9 ± 0.2	0.7 ± 0.2	1.5 ± 0.1#	1.1 ± 0.3*
Serum total cholesterol (mg/dl)	195.8 ± 53.6	149.9 ± 25.9#	248.2 ± 23.4#	187.6 ± 50.1*
Triglycerides (mg/dl)	151.0 ± 40.7	127.9 ± 24.4	130.0 ± 17.4	147.6 ± 25.4
Serum HDL cholesterol (mg/dl)	172.5 ± 50.8	139.3 ± 23.5#	219.0 ± 14.2	159.3 ± 42.8*
Blood glucose (mg/dl)	221.0 ± 10.2	187.7 ± 10.7#	221.3 ± 45.9	183.2 ± 25.1*

*$P < 0.05$ vs UN-RG-Veh. #$P < 0.05$ vs NN- Veh.

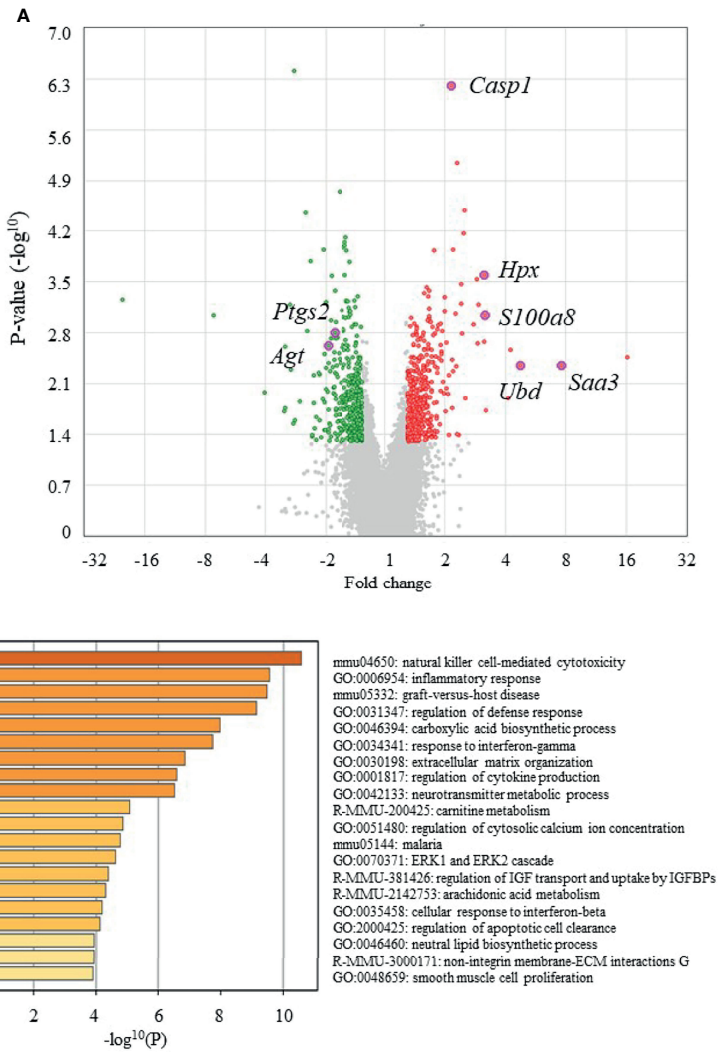

FIGURE 4 | Volcano plots **(A)** and gene ontologies (GO) terms from a gene enrichment analysis **(B)** using microarray data from epididymal adipose tissues of UN-RG-Veh and NN-Veh pups (4 each) at 16.5 wks. The names of 7 GOI (**Table 3**) were plotted in volcano plots **(A)**.

cytokine production, and 4) Cellular response to interferon-β (**Figure 4B**, **5B**), suggesting their principal involvement in the changes observed in fat deposition in epididymal adipose tissue in response to UN-RG and/or TU. We have no clear explanation why these 4 GO terms commonly observed in two gene enrichment analysis and speculate that they may represent the pathways being involved in the plasticity of adipose tissue deposition in pups with UN-RG and TU. Representative

changes in the gene expression profiles of the 4 GO terms are summarized in **Supplementary Table 1**.

Figure 6 shows heatmaps of relative fold increases in the expression of representative genes in the 4 newly identified GO terms in NN-Veh, UN-RG-Veh, and UN-RG-TU pups. The results obtained showed that the expression of genes up-regulated by UN-RG was suppressed by TU and vice versa. However, we were unable to obtain clear patterns for heatmaps by clustering related genes (data not shown); therefore, we simply listed gene names on the vertical axis (**Figures 6A–D**). The principal component analysis revealed similar changes in gene expression patterns between NN and TU in comparison with UN (**Figure 6E**).

Table 3 summarizes 7 genes of interest (GOI) that were observed at least twice in these 4 GO terms and also met the conditions of a ≤−2 or ≥2 linear fold change and P-value <0.05. The quantitative PCR analysis confirmed that UN-RG (*vs* NN-Veh) significantly up-regulated the gene expression of *Saa3*, *Ubd*, *S100a8*, and *Hpx*, significantly down-regulated the gene expression of *Agt*, and did not significantly affect the gene expression of *Casp1* and *Ptgs2* (**Figure 7**). In contrast, TU induced significantly down-regulated the gene expression of *Saa3*, *Ubd*, *S100a8*, and *Hpx*, significantly up-regulated the gene expression of *Agt* and *Ptgs2* and did not significantly affect the gene expression of *Casp1* (UN-RG-Veh *vs* UN-RG-TU) in UN-RG pups (**Figure 7**). In NN pups, TU did not significantly affect the expression of any of the 7 genes examined (NN-Veh *vs* NN-TU) (**Figure 7**).

Macrophage Infiltration in Epididymal Adipose Tissue

Crown-like structures were detected in the epididymal adipose tissue of pups fed the HFD at 16.5 wks of age (**Figure 8A**). Most

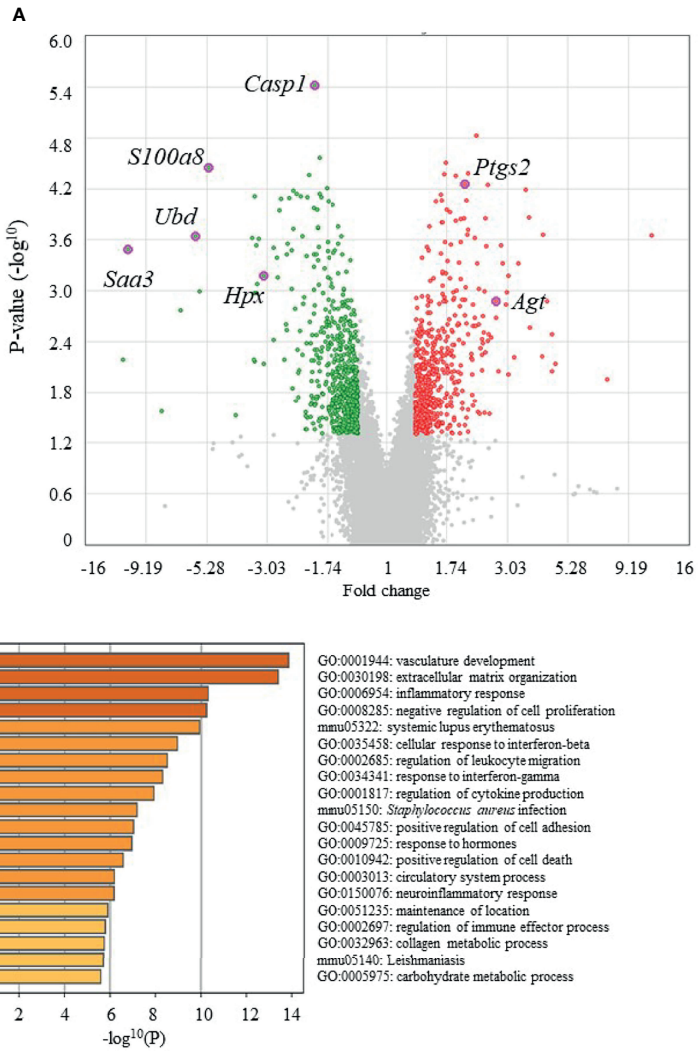

FIGURE 5 | Volcano plots **(A)** and GO terms from a gene enrichment analysis **(B)** using microarray data from epididymal adipose tissues of UN-RG-TU and UN-RG-Veh pups (4 each) at 16.5 wks. The names of 7 GOI (**Table 3**) were plotted in volcano plots **(A)**.

TABLE 3 | List of genes of interests (GOI).

Gene symbol	NN-Veh *vs* UN-RG-Veh		UN-RG-Veh *vs* UN-RG-TU	
	Fold change	P-value	Fold change	P-value
Saa3	7.60	0.0045	-10.88	0.0003
Ubd	4.73	0.0045	-5.86	0.0002
S100a8	3.17	0.0009	-5.19	<0.0001
Hpx	3.14	0.0003	-3.14	0.0007
Casp1	2.15	<0.0001	-1.96	<0.0001
Agt	-1.94	0.0024	2.73	0.0013
Ptgs2	-1.8	0.0016	2.05	<0.0001

These seven genes were observed at least twice in four different gene ontologies (GO), i.e. 1) Inflammatory response, 2) Response to interferon-γ, 3) Regulation of cytokine production, and 4) Cellular response to interferon-β, and also met the conditions of a ≤–2 or ≥2 linear fold change and P-value <0.05. These four GO were commonly observed in two GO enrichment analyses (UN-RG-Veh vs NN-Veh and UN-RG-TU vs UN-RG-Veh) using data from the microarray analysis of epididymal adipose tissue.

of these crown-like structures were immunohistochemically positive for F4/80, corresponding to infiltrated or resident macrophages (**Figure 8A**). The mean number of F4/80-positive cells was significantly higher in UN-RG-Veh pups than in NN-Veh pups (**Figure 8B**). TU induced a significant decrease in the mean number of F4/80-positive cells in UN-RG pups (UN-RG-Veh *vs* UN-RG-TU) (**Figure 8B**).

DISCUSSION

Increasing evidence supports RG being causatively associated with obesity and/or metabolic syndrome in later life, particularly in neonates born small (6–10); however, the benefits of RG for later neurodevelopment supports its encouragement in infants born preterm (10). In the present study, we newly established a mouse model of RG during the lactation period following UN (UN-RG) (**Figures 1**, **2**), by modifying our previous model of UN (13–18). UN-RG pups developed diet-induced obesity (**Figure 3**) as well as metabolic disorders (**Table 2**), mimicking the phenotype of diet-induced obesity and associated metabolic syndrome causatively connected with rapid infantile growth (6–10).

As shown **Figures 2C, D**, mean body weight from 8.5 d to 16.5 d was significantly higher in UN-RG pups than in NN pups, but similar at weaning 18.5 d. Our previous study showed that mean body weight of simple UN pups from fetal period (18.5 dpc) to early infantile period (3.5 d) was significantly lower than in NN pups (13). Therefore, it is noted that the present UN-RG pups experienced drastic changes from relatively small fetal body weight to large neonatal body weight (5.5 d-16.5 d), which we believe is an appropriate animal model of the small human babes who experienced rapid growth after birth and suffered from NCDs in later life, as reported by epidemiological studies (6, 7), corresponding to 'Mismatch' hypothesis in DOHaD theory (11, 12).

In the present study, we focused to design the animal model for mimicking the epidemiological outcomes of infantile rapid growth of small neonate (6, 7) and did not simultaneously carry out only RG pups experiment due mainly to animal facility limitation. However, we developed UN-RG animal model, considering that risk of NCDs resulted from RG in small human newborns applies well to 'Mismatch hypothesis' (11, 12), one of central hypotheses of DOHaD theory. 'Mismatch hypothesis' is based on the concept that small fetuses developmentally adapted to the low energy supply and caused 'Mismatch' to the abundant energy supply after birth, resulted in predisposition to obesity and associated metabolic disorders (11, 12). It is undeniable that the adult phenotype of UN-RG pups might be similar to that of RG pups. It is also unclear if an experience of the UN affected the degree of RG, although it was speculated that main contributor of RG was increased breast feeding in UN-RG pups. Nevertheless, we would like to note that simple RG pups model is a clearly different research target from UN-RG pups, because simple RG pups mimic babies with normal birth weight who experienced rapid infantile growth, which is not directly associated with 'Mismatch hypothesis' (11, 12).

We performed a comprehensive analysis of gene expression profiles in epididymal adipose tissue as a visceral fat pad. We initially investigated the effects of UN-RG on gene expression profiles in epididymal adipose tissue using a microarray analysis (NN-Veh *vs* UN-RG-Veh), displayed the results in volcano plots (**Figure 4A**), and then conducted a gene enrichment analysis, which identified the top 20 GO terms in ascending order of P-values (**Figure 4B**). Since TU significantly attenuated diet-induced obesity (**Figures 3B, C**) and epididymal fat deposition (**Figure 3D**), we examined its effects on gene expression profiles in epididymal adipose tissue using a microarray analysis (UN-RD-Veh *vs* UN-RG-TU). The results obtained were displayed in volcano plots (**Figure 5A**). A subsequent gene enrichment analysis identified the top 20 GO terms in ascending order of P-values (**Figure 5B**).

In 4 inflammatory GO terms, heatmap analysis of the mRNA expression of representative genes showed the genes of increased expression by UN showed a decrease by TU; while the genes of decreased expression by UN showed an increase by TU (**Figures 6A–D**), which suggests their coordinated contribution to the inflammatory changes observed in fat pads in response to UN and TU. However, we were unable to obtain a clear pattern for heatmaps by clustering related genes and, thus, simply listed gene names on the vertical axis (**Figures 6A–D**). We then performed a principal component analysis, which revealed similar changes in gene expression patterns between NN and TU in comparison with UN (**Figure 6E**).

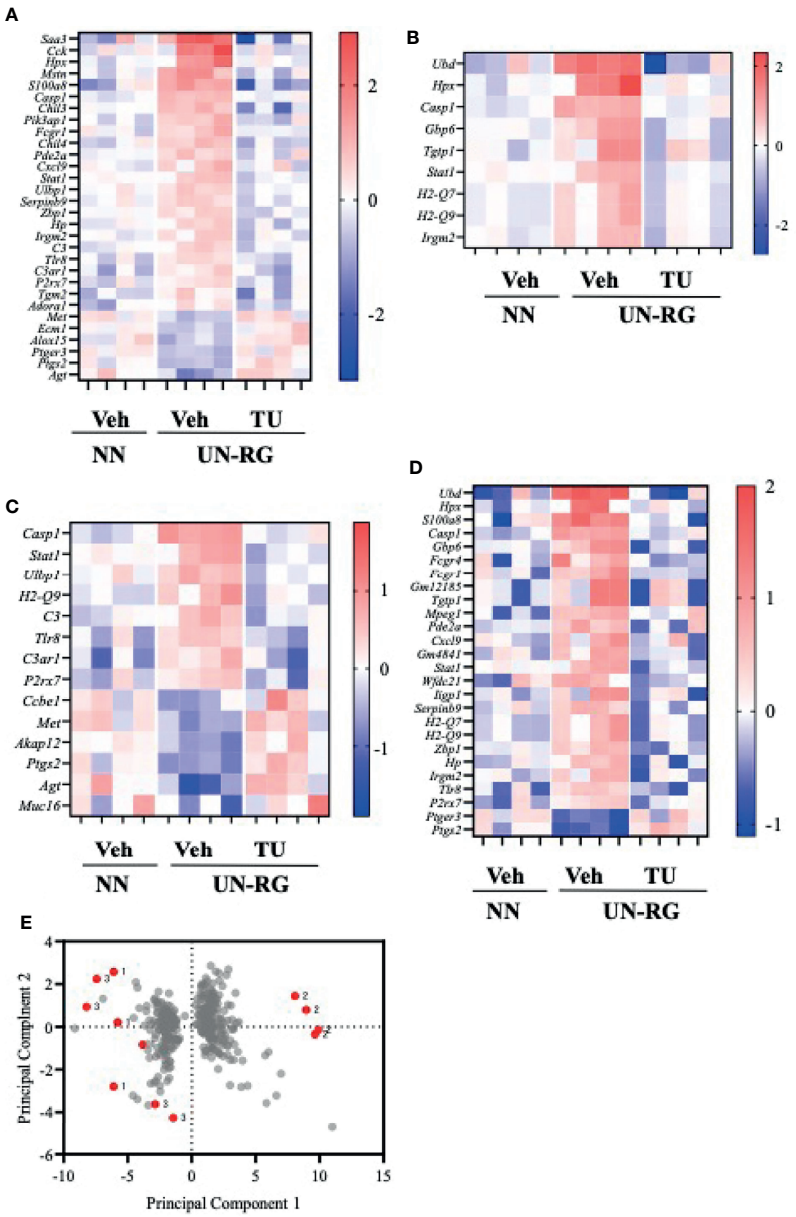

FIGURE 6 | Heatmaps of the mRNA expression of representative genes from 4 GO terms **(A–D)** and a principal component analysis **(E)** of NN-Veh, UN-RG-Veh, and UN-RG-TU pups (mean of 4 pups each). **A**) Inflammatory response, **B**) Response to interferon-γ, **C**) Regulation of cytokine production, and **D**) Cellular response to interferon-β. These 4 GO terms were commonly observed in two gene enrichment analyses, i.e. **Figures 4B** and **5B**. **(E)** A principle component analysis: gray dots indicate principle scores, while red dots show the loading of NN-Veh (1), UN-RG-Veh (2), and UN-RG-TU (3). There was a tendency that NN-Veh (1) and UN-RG-TU (3) showed similar distribution in comparison with the distribution of UN-RG-Veh (2).

We subsequently acknowledged the following 4 GO terms: 1) Inflammatory response, 2) Response to interferon-γ, 3) Regulation of cytokine production, and 4) Cellular response to interferon-β, all of which were commonly detected in the two different GO terms groups (**Figures 4B**, **5B**), for the purpose of identifying potential critical pathways contributing to the plasticity observed in the regulation of fat deposition, which responded not only to UN, but also to TU (**Figures 3B–D**). All 4 GO terms were directly related to inflammatory reactions, suggesting that inflammation is a key phenomenon in the plasticity of the regulation of fat deposition in this animal model. Top GO term of natural killer cell-mediated cytotoxicity (UN-RG-Veh *vs* NN-Veh) also supports a possible involvement of inflammation (**Figure 4B**) (22, 23). It is noted that GO terms of carnitine metabolism and regulation of apoptotic cell clearance, direct pathways of lipid metabolism,

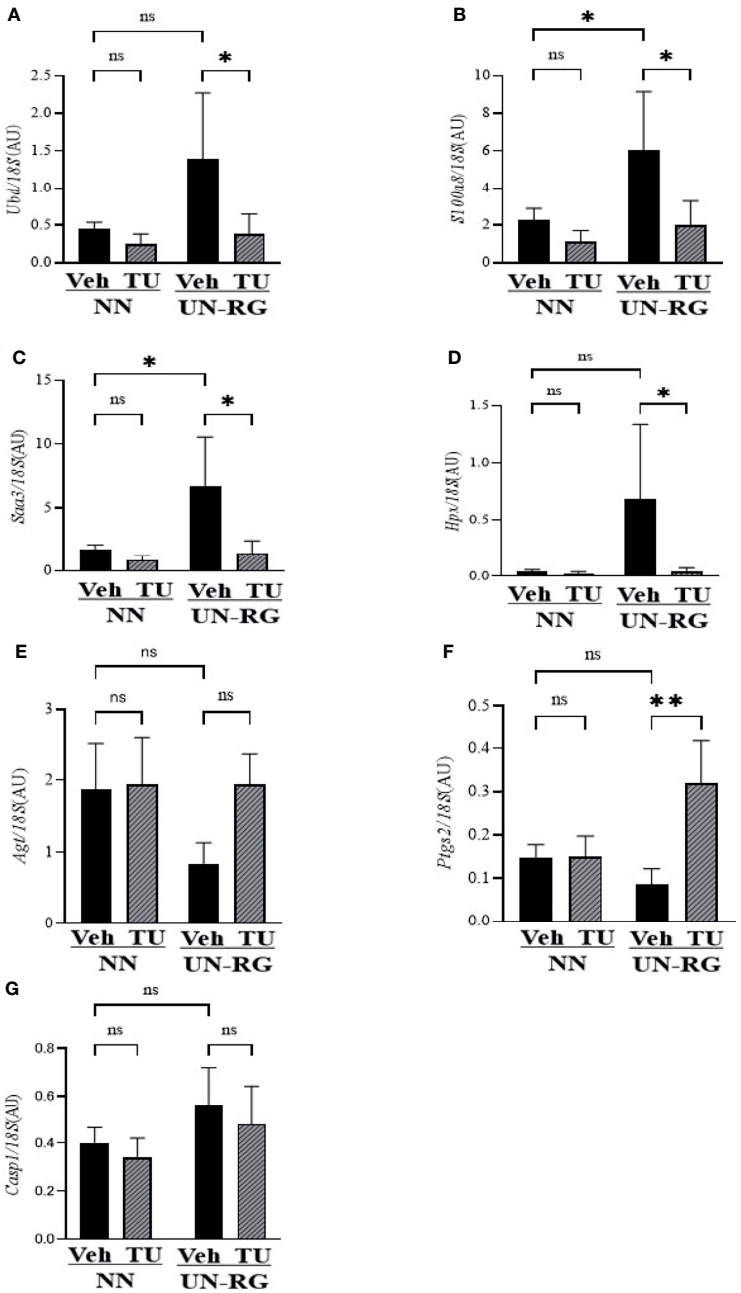

FIGURE 7 | Quantitative RT-PCR analysis of the mRNA expression of seven GOI (**Table 3**) in epididymal adipose tissues of NN-Veh, NN-TU, UN-RG-Veh, and UN-RG-TN pups at 16.5 wks. *P < 0.05; **P < 0.01. ns, no statistically significant.

were demonstrated by comparison between NN-Veh and UN-RG-Veh (**Figure 4B**), but not between UN-RG-Veh and UN-RG-TU (**Figure 5B**). We speculate that UN-RG might induce lipid metabolism as well as inflammation and that TU might affect mainly inflammatory regulation. More investigation is necessary to prove this speculation. TUDCA is an alleviator of ER stress, and it is noted that changes of *Kdelr 3*, ER protein retention receptor 3, gene expression was observed by comparison between NN-Veh and UN-RG-Veh (original microarray data is available by referring GSE18830 of the GEO repository).

Recent studies reported that obesity and its metabolic disruption are closely associated with low-level systemic inflammation, based upon which the concept of 'metaflammation' was proposed (24–27). Hotamisligil et al. (2017) proposed adipose tissue, the liver, pancreas, and brain as representative organs of 'metaflammation'

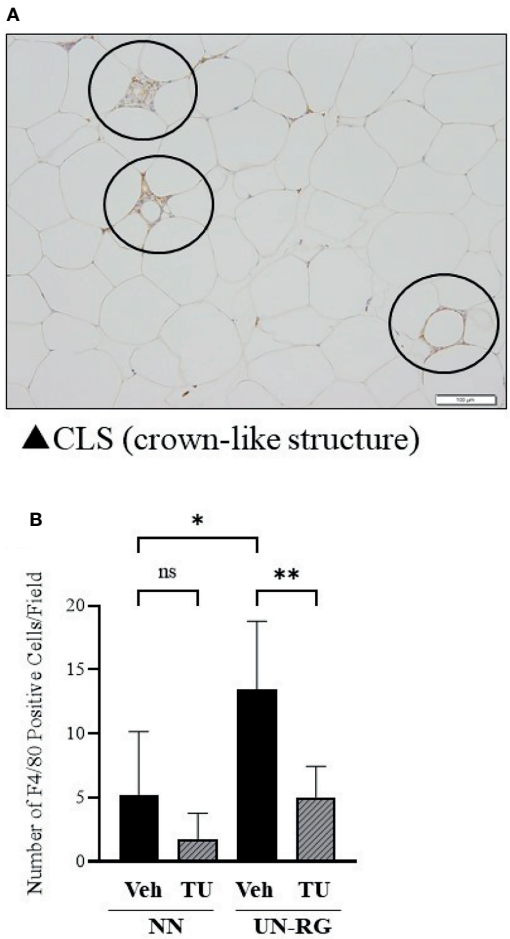

FIGURE 8 | Immunohistochemical detection of macrophages in epididymal adipose tissue. Circles indicate immunostaining for F4/80 in crown-like structures of epididymal adipose tissue from UN-RG-Veh pups at 16.5 wks of age **(A)** and the average number of F4/80-positive cells in the epididymal adipose tissue of NN-Veh, NN-TU, UN-RG-Veh, and UN-RG-TU pups **(B)**. The white bar indicates 100 μm. *P < 0.05, **P < 0.01.

(27). Lauterbach et al. (2017) suggested the principal involvement of tissue-resident macrophages in 'metaflammation' (28). Therefore, we performed an immunohistochemical analysis of macrophages in epididymal adipose tissue (**Figure 8A**) and found that UN-RG induced significant increases in the numbers of macrophages, while TU reversed this effect (**Figure 8B**, **Supplementary Figure 2**). These results support the critical contribution of 'metaflammation' to the adjustment of fat deposition in this animal model. There was a tendency of increase in the gene expression ratio of CD11c/CD163 in epididymal adipose tissue of UN-RG pups at 16.5 wks, but statistically not significant (**Supplementary Figure 1**). It is a future aim of the study to investigate the characteristics of these macrophages.

Previous studies proposed the potentially long-lasting embryonal memory of immune cells, including tissue-resident macrophages. Mass et al. (2021) suggested that fetal-derived immune cells are the prime transmitters of the long-term consequences of prenatal adversities, causing inflammatory, degenerative, and metabolic disorders (29). The potential commitment of erythro-myeloid progenitors produced in the extra-embryonic yolk sac to the ability to establish long-lasting immunological memory has been proposed (29–31); however, the exact mechanisms by which the memory of tissue resident macrophages is transferred to older generation macrophages remain unclear. Troger et al. (2013) demonstrated that the ability of the innate immune system of the growth-restricted fetus to mount an immune response was weakened after birth (32). Gotz et al. (2007) reported that prenatal stress may alter the number and proliferation of lymphocytes as well as the cytotoxicity of natural killer cells in the blood of male adult rat offspring (33). The gene expression profiles obtained in the present study also support the causative relationship of an environmental imbalance during the early critical period with the predisposition of adults to metaflammation; however, we did not detect immune memory in the macrophages of adipose tissue in this animal model.

In the search for the main molecular mechanisms in this animal model, we identified 7 GOI: *Saa3*, *Ubd*, *S100a8*, *Hpx*, *Casp1*, *Agt*, and *Ptgs2*, which were observed at least twice in the 4 GO terms that we selected in the present study, and also meet the conditions of a ≤−2 or ≥2 linear fold change and P-value <0.05 (**Table 3**). Quantitative RT-PCR reconfirmed the changes in their gene expression profiles in response to UN-RG and TU, except for *Casp1* (**Figure 7**). We currently have no clear explanation for the discrepancy regarding *Casp1*. Although limited information is currently available on their contribution to metaflammation in the DOHaD scheme, these genes play the following critical roles in the regulation of general inflammation. *Saa3* (34), *Agt* (35), and *Ptgs2* (36) are all involved in the inflammation of obesity. *Ubd* has been implicated in inflammation in nonalcoholic fatty liver disease (37). *Hpx* functions as an antioxidant and regulates inflammation (38). *Casp1* is an effector of NLRC4 inflammasomes (39) and converts pro-IL-1β and pro-IL-18 into their biologically active forms (40). Regarding the activation of macrophages, *Saa3* has been shown to promote the infiltration of macrophages in adipose tissue (41), while *S100a8* plays a central role in obesity-promoting macrophage-based inflammation (42) and induces the secretion of cytokines from mononuclear cells (43). We would like to speculate possible a series of reactions by these genes in macrophage-based metaflammation, 1) induction of macrophage migration by *Saa3*, 2) induction of the secretion of cytokines from macrophage by *S100a8*, 3) activation of cytokines secreted from macrophage by *Casp1*, and 4) possible connection to insulin sensitivity by *Ubd* nd/or *Hpx*. More intensive studies are needed to clarify the direct involvement of these genes in the developmentally-induced augmentation of macrophage infiltration and metabolic disruption in the adipose tissue of this animal model. Epigenetic changes in these seven GOI are now under investigation by our research group. It is our future aim to investigate the involvement of these GOI in the developmentally-induced regulation of fat deposition and

macrophage infiltration in this animal model. Our previous study showed that gene expression of *MCP-1* and *TNF-α* correlated with subcutaneous adipose tissue weight at 17 wks of simple UN pups, but not in NN pups (16), indirectly suggested a possible association between fat deposit and expression of inflammatory cytokines. We have no clear explanation why these two genes were not identified as GOI in UN-RG pups, because we did not carry out microarray analysis at that time and *MCP-1* and *TNF-α* were selected as representative inflammatory cytokines in UN pups, and also because the present UN-RG pups was designed to represent 'Mismatch hypothesis' in DOHaD theory (11, 12), quite different from simple UN pups at that time.

There are some limitations in the present study. We investigated 4 groups of pups, i.e. the NN-Veh, NN-TU, UN-RG-Veh, and UN-RG-TU groups, but not a NN-RG-Veh or NN-RG-TU group because of the restrictions of our animal facility accommodation. It is noted that Lizarraga-Mollinedo reported that different growth speed in the pups with undernourishment *in utero* showed conflicting levels of gene expression patterns in adipose tissue compared to normally nourished pups by using rat animal model (44). We did not investigate a condition without HFD due to the same animal facility limitation. We did not investigate time course of gene expression profiles. Furthermore, we were unable to obtain clear patterns for heatmaps by clustering related genes and, thus, simply listed gene names on the vertical axis of heatmaps (**Figures 6A-D**). We identified 7 GOI from 4 GO terms based on the results of microarray and gene enrichment analyses; however, we did not demonstrate their direct contribution to the programing of metaflammation in this animal model. We did not measure the plasma levels of inflammatory cytokines due to lack of the serum. Further study is needed to prove the involvement of 7 GOI in the pathophysiology of metaflammation. As for quantitative RT-PCR, 18S ribosomal mRNA expression was used as an internal control; however, we did not assess the effect of RG or TU on its expression. The main contributor of RG was supposed to be breastfeeding in this animal model; however, we could not assess the changes in breastfeeding of dams due to technical limitation. In the preset study, we focused on the assessment of epididymal adipose tissue, as a visceral fat, and did not investigate subcutaneous and retroperitoneal adipose tissues. It is a future aim of the study to investigate the changes in gene expression in subcutaneous and retroperitoneal adipose tissues.

In summary, we newly established a mouse animal model of RG during the lactation period following UN (**Figures 1**, **2**, **Table 2**), the offspring of which developed diet-induced obesity and metabolic disorders, which were significantly improved by TU (**Figure 3**), although we did not assess UN pups without GR. The microarray analysis and subsequent gene enrichment analysis (**Figure 4**, **Figure 5**) identified 4 GO terms of inflammatory pathways, indicating the critical contribution of chronic inflammation to developmentally-programed fat deposition and its amelioration by TU. The results of the heatmap and principal component analyses of the representative genes of the 4 GO terms (**Figure 6**), changes in the gene expression profiles of 7 GOI (**Table 3**, **Figure 7**) selected from 4 GO terms, and immunohistochemistry on macrophages (**Figure 8**) collectively support the proposal of the 'Developmental Origins of Metaflammation'. Future epigenetic and immunological investigations, with a focus on 7 GOI, are needed to further establish this concept.

DATA AVAILABILITY STATEMENT

The datasets presented in this study can be found in online repositories. The names of the repository/repositories and accession number(s) can be found in the article/**Supplementary Material**.

ETHICS STATEMENT

The animal study was reviewed and approved by the Animal Research Committee, Hamamatsu University School of Medicine (H20-014). Written informed consent was obtained from the owners for the participation of their animals in this study.

AUTHOR CONTRIBUTIONS

MS and YK-K performed and analyzed all experiments. MS and HI wrote the manuscript. MU, KM, and HI designed the study. NF-I, TO, and MasM performed histological examinations. MS, TO, KK, TI, and MadM supported data collection and animal experiments, sample preparation, and data analysis. NT, TU, MN, and YK-K supported data collection, discussions, and statistical analyses. MS, TO, KK, and TI supported data analyses and preparation of the manuscript. KM supported the gene enrichment analysis. All authors contributed to the article and approved the submitted version.

FUNDING

This work was supported by JSPS KAKENHI Grant Numbers, JP20H03823, JP20K09666, and JP20K16886, and AMED under Grant Number JP20gm1310009.

ACKNOWLEDGMENTS

The authors thank Mrs. Miuta Sawai, Yumiko Yamamoto, Naoko Kondo, and Kazuko Sugiyama for their secretarial or technical assistance.

SUPPLEMENTARY MATERIAL

The Supplementary Material for this article can be found online at: https://www.frontiersin.org/articles/10.3389/fendo.2022.818064/full#supplementary-material

REFERENCES

1. Swinburn BA, Sacks G, Hall KD, McPherson K, Finegood DT, Moodie ML, et al. The Global Obesity Pandemic: Shaped by Global Drivers and Local Environments. *Lancet* (2011) 378(9793):804–14. doi: 10.1016/S0140-6736(11)60813-1
2. Caballero B. Humans Against Obesity: Who Will Win? *Adv Nutr* (2019) 10 (suppl_1):S4–9. doi: 10.1093/advances/nmy055
3. Huang PL. A Comprehensive Definition for Metabolic Syndrome. *Dis Model Mech* (2009) 2(5-6):231–7. doi: 10.1242/dmm.001180
4. Itoh H, Kanayama N. Developmental Origins of Health and Diseases (DOHaD). In: I Konishi, editor. *Perspective Toward Preemptive Medicine*. Singapore: Springer Nature (2017).
5. Fleming TP, Watkins AJ, Velazquez MA, Mathers JC, Prentice AM, Stephenson J, et al. Origins of Lifetime Health Around the Time of Conception: Causes and Consequences. *Lancet* (2018) 391(10132):1842–52. doi: 10.1016/S0140-6736(18)30312-X
6. Eriksson J, Forsen T, Tuomilehto J, Osmond C, Barker D. Size at Birth, Childhood Growth and Obesity in Adult Life. *Int J Obes Relat Metab Disord* (2001) 25(5):735–40. doi: 10.1038/sj.ijo.0801602
7. Ong KK. Size at Birth, Postnatal Growth and Risk of Obesity. *Horm Res* (2006) 65 Suppl 3:65–9. doi: 10.1159/000091508
8. Ekelund U, Ong KK, Linne Y, Neovius M, Brage S, Dunger DB, et al. Association of Weight Gain in Infancy and Early Childhood With Metabolic Risk in Young Adults. *J Clin Endocrinol Metab* (2007) 92(1):98–103. doi: 10.1210/jc.2006-1071
9. Martin A, Connelly A, Bland RM, Reilly JJ. Health Impact of Catch-Up Growth in Low-Birth Weight Infants: Systematic Review, Evidence Appraisal, and Meta-Analysis. *Matern Child Nutr* (2017) 13(1):10.1111/mcn.12297. doi: 10.1111/mcn.12297
10. Singhal A. Long-Term Adverse Effects of Early Growth Acceleration or Catch-Up Growth. *Ann Nutr Metab* (2017) 70(3):236–40. doi: 10.1159/000464302
11. Gluckman PD, Hanson MA. *Mismatch Why Our World No Longer Fits Our Bidies*. Oxford: Oxford University Press (2006).
12. Gluckman PD, Hanson MA, Beedle AS. Early Life Events and Their Consequences for Later Disease: A Life History and Evolutionary Perspective. *Am J Hum Biol* (2007) 19(1):1–19. doi: 10.1002/ajhb.20590
13. Yura S, Itoh H, Sagawa N, Yamamoto H, Masuzaki H, Nakao K, et al. Role of Premature Leptin Surge in Obesity Resulting From Intrauterine Undernutrition. *Cell Metab* (2005) 1(6):371–8. doi: 10.1016/j.cmet.2005.05.005
14. Kawamura M, Itoh H, Yura S, Mogami H, Suga S, Makino H, et al. Undernutrition *In Utero* Augments Systolic Blood Pressure and Cardiac Remodeling in Adult Mouse Offspring: Possible Involvement of Local Cardiac Angiotensin System in Developmental Origins of Cardiovascular Disease. *Endocrinology* (2007) 148(3):1218–25. doi: 10.1210/en.2006-0706
15. Kawamura M, Itoh H, Yura S, Mogami H, Fujii T, Kanayama N, et al. Angiotensin II Receptor Blocker Candesartan Cilexetil, But Not Hydralazine Hydrochloride, Protects Against Mouse Cardiac Enlargement Resulting From Undernutrition. *utero Reprod Sci* (2009) 16(10):1005–12. doi: 10.1177/1933719109345610
16. Kohmura YK, Kanayama N, Muramatsu K, Tamura N, Yaguchi C, Uchida T, et al. Association Between Body Weight at Weaning and Remodeling in the Subcutaneous Adipose Tissue of Obese Adult Mice With Undernourishment. *utero Reprod Sci* (2013) 20(7):813–27. doi: 10.1177/1933719112466300
17. Muramatsu-Kato K, Itoh H, Kohmura-Kobayashi Y, Ferdous UJ, Tamura N, Yaguchi C, et al. Undernourishment *In Utero* Primes Hepatic Steatosis in Adult Mice Offspring on an Obesogenic Diet; Involvement of Endoplasmic Reticulum Stress. *Sci Rep* (2015) 5:16867. doi: 10.1038/srep16867
18. Urmi JF, Itoh H, Muramatsu-Kato K, Kohmura-Kobayashi Y, Hariya N, Jain D, et al. Plasticity of Histone Modifications Around Cidea and Cidec Genes With Secondary Bile in the Amelioration of Developmentally-Programmed Hepatic Steatosis. *Sci Rep* (2019) 9(1):17100. doi: 10.1038/s41598-019-52943-7
19. Kawamura M, Itoh H, Yura S, Mogami H, Fujii T, Makino H, et al. Isocaloric High-Protein Diet Ameliorates Systolic Blood Pressure Increase and Cardiac Remodeling Caused by Maternal Caloric Restriction in Adult Mouse Offspring. *Endocr J* (2009) 56(5):679–89. doi: 10.1507/endocrj.K08E-286
20. Ashburner M, Ball CA, Blake JA, Botstein D, Butler H, Cherry JM, et al. Gene Ontology: Tool for the Unification of Biology. The Gene Ontology Consortium. *Nat Genet* (2000) 25(1):25–9. doi: 10.1038/75556
21. Zhou Q, Zhang F, He Z, Zuo MZ. E2F2/5/8 Serve as Potential Prognostic Biomarkers and Targets for Human Ovarian Cancer. *Front Oncol* (2019) 9:161. doi: 10.3389/fonc.2019.00161
22. Lee BC, Kim MS, Pae M, Yamamoto Y, Eberle D, Shimada T, et al. Adipose Natural Killer Cells Regulate Adipose Tissue Macrophages to Promote Insulin Resistance in Obesity. *Cell Metab* (2016) 23(4):685–98. doi: 10.1016/j.cmet.2016.03.002
23. Wensveen FM, Jelencic V, Valentic S, Sestan M, Wensveen TT, Theurich S, et al. NK Cells Link Obesity-Induced Adipose Stress to Inflammation and Insulin Resistance. *Nat Immunol* (2015) 16(4):376–85. doi: 10.1038/ni.3120
24. Gregor MF, Hotamisligil GS. Inflammatory Mechanisms in Obesity. *Annu Rev Immunol* (2011) 29:415–45. doi: 10.1146/annurev-immunol-031210-101322
25. Egger G, Dixon J. Beyond Obesity and Lifestyle: A Review of 21st Century Chronic Disease Determinants. *BioMed Res Int* (2014) 2014:731685. doi: 10.1155/2014/731685
26. Hotamisligil GS. Endoplasmic Reticulum Stress and the Inflammatory Basis of Metabolic Disease. *Cell* (2010) 140(6):900–17. doi: 10.1016/j.cell.2010.02.034
27. Hotamisligil GS. Inflammation, Metaflammation and Immunometabolic Disorders. *Nature* (2017) 542(7640):177–85. doi: 10.1038/nature21363
28. Lauterbach MA, Wunderlich FT. Macrophage Function in Obesity-Induced Inflammation and Insulin Resistance. *Pflugers Arch* (2017) 469(3-4):385–96. doi: 10.1007/s00424-017-1955-5
29. Mass E, Gentek R. Fetal-Derived Immune Cells at the Roots of Lifelong Pathophysiology. *Front Cell Dev Biol* (2021) 9:648313. doi: 10.3389/fcell.2021.648313
30. Chen T, Liu HX, Yan HY, Wu DM, Ping J. Developmental Origins of Inflammatory and Immune Diseases. *Mol Hum Reprod* (2016) 22(8):858–65. doi: 10.1093/molehr/gaw036
31. Christ A, Lauterbach M, Latz E. Western Diet and the Immune System: An Inflammatory Connection. *Immunity* (2019) 51(5):794–811. doi: 10.1016/j.immuni.2019.09.020
32. Troger B, Muller T, Faust K, Bendiks M, Bohlmann MK, Thonnissen S, et al. Intrauterine Growth Restriction and the Innate Immune System in Preterm Infants of </=32 Weeks Gestation. *Neonatology* (2013) 103(3):199–204. doi: 10.1159/000343260
33. Gotz AA, Stefanski V. Psychosocial Maternal Stress During Pregnancy Affects Serum Corticosterone, Blood Immune Parameters and Anxiety Behaviour in Adult Male Rat Offspring. *Physiol Behav* (2007) 90(1):108–15. doi: 10.1016/j.physbeh.2006.09.014
34. Zhu Q, An YA, Kim M, Zhang Z, Zhao S, Zhu Y, et al. Suppressing Adipocyte Inflammation Promotes Insulin Resistance in Mice. *Mol Metab* (2020) 39:101010. doi: 10.1016/j.molmet.2020.101010
35. Cottam DR, Mattar SG, Barinas-Mitchell E, Eid G, Kuller L, Kelley DE, et al. The Chronic Inflammatory Hypothesis for the Morbidity Associated With Morbid Obesity: Implications and Effects of Weight Loss. *Obes Surg* (2004) 14 (5):589–600. doi: 10.1381/096089204323093345
36. Rahman SU, Huang Y, Zhu L, Chu X, Junejo SA, Zhang Y, et al. Tea Polyphenols Attenuate Liver Inflammation by Modulating Obesity-Related Genes and Down-Regulating COX-2 and iNOS Expression in High Fat-Fed Dogs. *BMC Vet Res* (2020) 16(1):234. doi: 10.1186/s12917-020-02448-7
37. Dali-Youcef N, Vix M, Costantino F, El-Saghire H, Lhermitte B, Callari C, et al. Interleukin-32 Contributes to Human Nonalcoholic Fatty Liver Disease and Insulin Resistance. *Hepatol Commun* (2019) 3(9):1205–20. doi: 10.1002/hep4.1396
38. Tolosano E, Altruda F. Hemopexin: Structure, Function, and Regulation. *DNA Cell Biol* (2002) 21(4):297–306. doi: 10.1089/104454902753759717
39. Duncan JA, Canna SW. The NLRC4 Inflammasome. *Immunol Rev* (2018) 281 (1):115–23. doi: 10.1111/imr.12607

40. Man SM, Karki R, Briard B, Burton A, Gingras S, Pelletier S, et al. Differential Roles of Caspase-1 and Caspase-11 in Infection and Inflammation. *Sci Rep* (2017) 7:45126. doi: 10.1038/srep45126
41. Sanada Y, Yamamoto T, Satake R, Yamashita A, Kanai S, Kato N, et al. Serum Amyloid A3 Gene Expression in Adipocytes Is an Indicator of the Interaction With Macrophages. *Sci Rep* (2016) 6:38697. doi: 10.1038/srep38697
42. Riuzzi F, Chiappalupi S, Arcuri C, Giambanco I, Sorci G, Donato R. S100 Proteins in Obesity: Liaisons Dangereuses. *Cell Mol Life Sci* (2020) 77(1):129–47. doi: 10.1007/s00018-019-03257-4
43. Simard JC, Cesaro A, Chapeton-Montes J, Tardif M, Antoine F, Girard D, et al. S100A8 and S100A9 Induce Cytokine Expression and Regulate the NLRP3 Inflammasome *via* ROS-Dependent Activation of NF-Kappab(1.). *PloS One* (2013) 8(8):e72138. doi: 10.1371/journal.pone.0072138
44. Lizarraga-Mollinedo E, Carreras-Badosa G, Xargay-Torrent S, Remesar X, Mas-Pares B, Prats-Puig A, et al. Catch-Up Growth in Juvenile Rats, Fat Expansion, and Dysregulation of Visceral Adipose Tissue. *Pediatr Res* (2021) 91(1):107–55. doi: 10.1038/s41390-021-01422-9

Conflict of Interest: The authors declare that the research was conducted in the absence of any commercial or financial relationships that could be construed as a potential conflict of interest.

Publisher's Note: All claims expressed in this article are solely those of the authors and do not necessarily represent those of their affiliated organizations, or those of the publisher, the editors and the reviewers. Any product that may be evaluated in this article, or claim that may be made by its manufacturer, is not guaranteed or endorsed by the publisher.

frontiers | Frontiers in Endocrinology

ORIGINAL RESEARCH
published: 12 May 2022
doi: 10.3389/fendo.2022.860286

Vitamin D Deficiency During Development Permanently Alters Liver Cell Composition and Function

Kassidy Lundy[1], *John F. Greally*[2], *Grace Essilfie-Bondzie*[1], *Josephine B. Olivier*[1], *Reanna Doña-Termine*[1], *John M. Greally*[1] *and Masako Suzuki*[1]*

[1] Department of Genetics, Albert Einstein College of Medicine, Bronx, NY, United States, [2] Retired, Galway, Ireland

Vitamin D, a fat-soluble vitamin, plays a critical role in calcium homeostasis, the immune system, and normal development. Many epidemiological cohort studies globally have found high prevalence rates of vitamin D deficiency and insufficiency, recognized as an important health issue that needs to be solved. In particular, reproductive age and pregnant women low in vitamin D status may confer risks of diseases like obesity on their offspring. While observational studies have suggested associations between prenatal vitamin D deficiency and metabolic phenotypes in offspring, not yet determined is whether prenatal vitamin D deficiency permanently alters the development of the liver, a major metabolic organ. We tested the histopathology and the transcriptomic profiles of livers from male C57BL/6J mice exposed to prenatal vitamin D deficiency through a maternal dietary intervention model. We found that prenatal vitamin D deficiency increases the prevalence of histopathological changes in the liver, and alters its gene expression profile. Cell subtype proportion analysis showed that the liver of prenatal vitamin D deficiency alters non-parenchymal cells of the liver, specifically macrophages, a subset of endothelial cells, and dendritic cells. Our results indicate the long-term memory of prenatal vitamin D deficiency exposure in the adult liver, a potential contributor to offspring health risks.

Keywords: vitamin D deficiency, prenatal environment, liver, transcriptional alterations, DOHaD (developmental origins of health and disease)

OPEN ACCESS

Edited by:
Takahiro Nemoto,
Nippon Medical School, Japan

Reviewed by:
Nobuaki Shiraki,
Tokyo Institute of Technology, Japan
Satoru Ikenoue,
Keio University School of Medicine, Japan

***Correspondence:**
Masako Suzuki
masako.suzuki@einsteinmed.edu

Specialty section:
This article was submitted to Experimental Endocrinology, a section of the journal Frontiers in Endocrinology

Received: *22 January 2022*
Accepted: *21 March 2022*
Published: *12 May 2022*

Citation:
Lundy K, Greally JF, Essilfie-Bondzie G, Olivier JB, Doña-Termine R, Greally JM and Suzuki M (2022) Vitamin D Deficiency During Development Permanently Alters Liver Cell Composition and Function. Front. Endocrinol. 13:860286. doi: 10.3389/fendo.2022.860286

INTRODUCTION

Vitamin D is a crucial micronutrient that plays many physiologic functions in mammals. Humans create vitamin D from the action of sunlight on the skin, with the consequence that limiting sun exposure, covering skin with clothes, or darker skin pigmentation reduces vitamin D production and may cause its deficiency. The serum 25-hydroxyvitamin D concentration is the marker of vitamin D nutritional adequacy. Serum 25-hydroxyvitamin D concentrations in the range of 50-125 nmol/L indicate adequate vitamin D intake, 30-49 nmol/L is inadequate, and less than 30 nmol/L is classified as deficient, while greater than 125 nmol/L represents excess (1, 2). Many countries provide recommended daily vitamin D intake values and fortified foods such as milk, margarine, flours, cereals, and juices to reduce the prevalence rate of vitamin D deficiency (VDD), but VDD remains highly prevalent worldwide (3–6). In particular, the prevalence of VDD in reproductive-age

women and pregnant women is recognized to be an urgent issue that needs to be addressed in low- and mid-income countries, and in high-income countries within the specific race and ethnicity groups (6–8).

While a major role of vitamin D is in regulating calcium homeostasis [reviewed in (9)], it has broader physiological effects. The bioactive metabolite of vitamin D, 1,25(OH)2D3 (calcitriol), is a steroid hormone, influencing transcriptional regulation through interaction with the high-affinity nuclear vitamin D receptor (VDR), a member of the nuclear receptor superfamily of ligand-activated transcription factors. The VDR pathway regulates the transcription of many genes, including genes with essential roles in fetal development and ensures the fetal supply of calcium for bone development (10–13). Intriguingly, epidemiological studies exploring the effects of maternal vitamin D deficiency revealed that offspring exposed to vitamin D deficiency in the uterus increased not only the risk of infantile rickets (4) but also the risk of childhood obesity (14–17) later in adulthood, suggesting long-term memories of the deficiency while developing *in utero*.

A mouse dietary intervention study revealed that mice born to mothers fed a vitamin D deficient diet had rapid weight gain after weaning and were more susceptible to high-fat diet-induced adipocyte hypertrophy than those born to mothers fed a vitamin D sufficient diet (18). In addition, a study of mice exposed to prenatal VDD found that prenatal VDD alters the DNA methylation status of the liver and sperm of two generations of offspring (19). These findings suggest that prenatal vitamin D deficiency predisposes offspring to long-term metabolic phenotypic alterations. However, little is known if prenatal vitamin D deficiency permanently alters the physiology of the liver, a major metabolic organ. To fill this knowledge gap, we assessed the effects of prenatal vitamin D deficiency on liver physiology and gene expression at the adult stage.

MATERIALS AND METHODS

Maternal Vitamin D Deficiency Mouse Model

Five week old C57Bl/6J (Strain #000664) female mice (F0) purchased from the Jackson Laboratory were fed vitamin D deficient (VDD) or sufficient (VDS) diets for five weeks before mating to the control diet-fed male mice. The assigned diets were maintained throughout the subsequent pregnancy. VDD (0.0 IU/g vitamin D) and nutrient-matched VDS (1.0 IU/g vitamin D, D12450J) diets were obtained from Research Diets Inc. (10 kcal% fat, 20 kcal%Protein, and 70 kcal%Carbonate). VDD-fed females were supplemented with 1.5% calcium gluconate to maintain calcium homeostasis (20). Vitamin D deficiency of the F0 animals was confirmed by measuring serum 25-OH vitamin D levels using the Mouse Rat 25-OG Vitamin D ELISA kit (Eagle BIOSCIENCES) before mating and postnatal day 1 offspring (**Supplementary Figure 1A**). After delivery, all F0 mice were fed VDS diets. After weaning, the offspring (F1) were fed a VDS diet that was maintained until animal sacrifice. All animal studies were approved by the Institutional Animal Care and Use Committee at the Albert Einstein College of Medicine.

Histopathological Study

After dissection, the liver samples were fixed in 4% paraformaldehyde solution at 4°C for overnight and processed for paraffin embedding. The paraffin-embedded tissue slides were stained with hematoxylin and eosin (HE), trichrome, and Gomori Reticulin stainings. We assessed 10 VDS-F1 and 19 VDD-F1 male mice.

Transcription Analysis

We used male offspring for gene expression studies (n=6 VDD-F1 and n=6 VDS-F1). Total RNA was extracted from mouse livers at 16 weeks of age using the AllPrep DNA/RNA Micro Kits (QIAGEN). The RNA-seq libraries were generated using KAPA RNA HyperPrep with RiboErase kit (Roche) and sequenced on an Illumina NovaSeq sequencer (Novogene Co., Ltd., USA). After removing reads that failed the quality check and trimming adapter sequences, the resulting sequences were aligned to the mouse mm10 reference genome, quantifying gene expression by transcript counting (GENECODE release M15, GRCm38) using the STAR aligner (21). Differential expression as a result of dietary manipulation was determined using the Bioconductor package DESeq2 (22). We eliminated genes with fewer than the mean read counts per sample per gene is less than 12 from the analysis. Significantly differentially expressed genes (DEGs) were determined based on a $\log_2$-fold change of less than -1 or greater than 1 and a false discovery rate (FDR) adjusted p-value less than 0.05. DEGs were further assessed for their biological properties by Gene Ontology (GO) enrichment analysis using a Bioconductor package, clusterProfiler (23, 24). Quantitative reverse transcription PCR (qRT-PCR) was performed on the same RNA samples to verify the results. We used SuperScript III with random hexamer priming to synthesize cDNA and LightCycler FastStart Universal SYBR Green Master Mix for quantitative PCR. The measurement was performed using the LightCycler 480 system. The primers used in this study are listed in **Supplementary Table 1**.

Cell Subtype Deconvolution

We used CIBERSORTx, a web interface-based tool, for quantifying the proportion of cell types in the RNA-seq data (25). A publicly available mouse liver (parenchymal and non-parenchymal liver cells isolated by a two-step collagenase perfusion) single-cell RNA-seq data (GSE134134) (26, 27) was used to generate a custom signature from single-cell liver gene expression data that represents the gene expression signatures of liver cell and immune cell subtypes. We combined four datasets of single-cell RNA seq libraries listed under GSE134134, 1000 (GSM3937757), 2000 (GSM3937758), 5000 (GSM3937759), and 10000 (GSM3937760) (26, 27). We used the Seurat R package for the single-cell RNA-seq analysis (28). We excluded cells with the

detected number of genes were less than 1000 and reads from mitochondrial were greater than 10% before the analysis. We performed normalization and variance stabilization using the sctransform algorism (29), and the sctransformed datasets were merged using integration functions and identified clusters based on the gene expression profiles (29). We identified cell subtype clusters based on the expression status of maker genes (**Supplementary Figure 4**).

Statistical Analysis

All statistical analyses were performed using R version 4.1.1 (https://www.r-project.org/). The Student's *t*-test was used to analyze continuous variables between VDS and VDD unless otherwise stated, and Fisher's exact test to analyze categorical variables. P-values of <0.05 or FDR-adjusted p-values in multiple testing analyses were considered significant.

RESULTS

Prenatal Vitamin D Deficiency Is Associated With Histopathological Changes of the Livers of Offspring

The growth trajectory of offspring was comparable in VDD-F1 and VDS-F1 (**Supplementary Figure 1B**). We dissected F1 male mice at 16 weeks of age to assess the long-term effects of prenatal vitamin D deficiency. We found histopathological alterations of the livers including hydropic degenerations, steatosis, and fibrosis in VDD-F1 offspring (**Figure 1**). While the prevalence rates were not statistically significant due to the small sample numbers, steatosis and fibrosis were only observed in the VDD-F1 offspring. The sizes of lipid droplets were varied between the individuals, but the morphology of the nuclei remained unaltered. We summarize the histopathological alterations in **Table 1**.

Prenatal Vitamin D Deficiency Is Associated With Permanently Altered Gene Expression of the Liver

The histopathological analyses suggested that prenatal vitamin D deficiency alters liver physiology. We, therefore, conducted a transcriptional analysis using bulk RNA-seq to assess the gene expression alterations linked to prenatal vitamin D deficiency. We extracted total RNA from the left lateral lobes of the liver and prepared libraries (n=6 per group, **Supplementary Figure 2**). We sequenced libraries at the depth of at least 26 million paired reads per library. After the quality check of the sequences and removal of low-quality reads, we performed a principal components analysis to compare the expression pattern between the individual F1 mice (**Figure 2A**, **Supplementary Table 2**). We observed three large clusters that consist of only VDS samples, VDD samples, and both VDS and VDD. There were no significant histopathological differences between VDD samples in different clusters. Next, we performed a differential expression analysis and identified 281 significant differentially expressed genes (DEGs) when comparing samples from mice who were exposed to prenatal VDD versus those exposed to prenatal VDS. 249 of DEGs were upregulated and 32 of DEGs

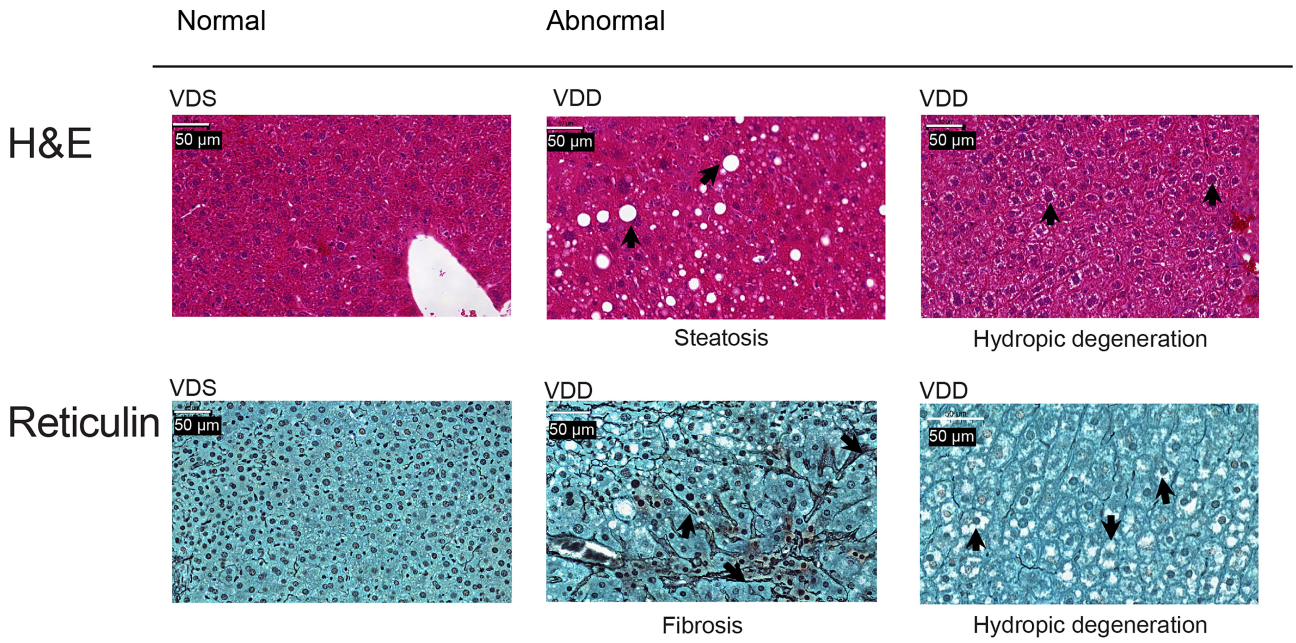

FIGURE 1 | Representative histopathological alterations in the liver of VDD-F1 offspring. Top, hematoxylin-eosin stain; bottom, Gomori's reticulin stain. The arrows indicate the described changes.

TABLE 1 | A summary of histopathological alterations in liver.

	VDD-F1 (n=19)	VDS-F1 (n=10)	p-values*
Hydropic degeneration	11	4	0.675
Steatosis	1	0	0.063
Steatosis and Fibrosis	5	0	–
No alterations observed	8	6	0.562

Fisher's exact test.

were downregulated (**Figure 2B**, **Supplementary Table 3**). We verified the results using the same RNA samples and confirmed significant alterations or the same trends of DEGs by quantitative RT-PCR (**Figure 2C**, **Supplementary Figure 3**).

The DEGs Are Enriched in Pathways for the Extracellular Structural Organization and Lipid Catabolism

We performed gene ontology (GO) enrichment analyses on upregulated and downregulated DEGs respectively to test if the DEGs are enriched in specific gene pathways. We found that lipid metabolism-related pathways such as lipid catabolic process, xenobiotic metabolism, and linoleic acid metabolic process are enriched in down-regulated DEGs. 249 upregulated DEGs were enriched in extracellular structure organization, nuclear division, and mitosis-related pathways (**Figure 3**, **Supplementary Table 4**).

Cell Subtype Proportion Analysis of Bulk RNA-Seq Data Revealed That Prenatal Vitamin D Deficiency Alters Cell Subtype Composition of Non-Parenchymal Liver Cells

We next tested if the proportions of cell subtypes are affected based on prenatal exposure to VDS or VDD. To perform cell subtype proportion analysis, we generated reference expression signatures of each liver cell subtype using publicly available adult liver single-cell RNA-seq data. We segregated 21 clusters of the adult liver cells, as shown in **Figure 4A** and **Supplementary Figure 4**. Based on the relative expression of well-known marker genes of liver cell subtypes identified by the mouse cell atlas, we identified the cell subtypes of each cluster. The cluster information was then used to generate a custom signature of gene expression in liver cells using CIBERSORTx. The generated reference expression signature was used to perform deconvolution of bulk RNA-seq data of each sample (**Supplementary Table 5**). As we expected, the hepatocyte proportion was the highest among the cell subtypes (80.6% VDD and 81.4% VDS, p=0.39) (**Supplementary Table 6**). While the proportions of hepatocytes were not significantly altered, we observed significant alterations in non-parenchymal liver cell subtypes, macrophages, endothelial cells, and dendritic cells (**Figure 4B**). Interestingly, while Cd163-positive macrophages were reduced in prenatal VDD offspring liver, Ccr2-positive macrophages were increased compared to that of VDS offspring. We previously reported that cell subtype composition significantly contributes to the gene expression profile (30). We therefore tested if the DEGs we identified were attributable to the cell subtype proportion differences between samples. We did not observe significant contributions of cell subtype proportion variations to the gene expression profile (**Supplementary Figure 5**). This result indicates that the identified DEGs were independent of the cell subtype proportion variations.

DISCUSSION

In this study, we found that prenatal vitamin D deficiency alters liver histology and transcription profiles in offspring adulthood. We observed livers with varying ranges of cytoplasmic clearing, hydropic changes, and fibrosis in histopathological analysis. Transcriptional analysis showed that lipid metabolism-related genes, mitosis-related genes, and extracellular structure organization-related genes were enriched in DEGs. Moreover, cell subtype deconvolution analysis indicates alterations of non-parenchymal liver cell proportions. These findings suggest that prenatal vitamin D deficiency permanently alters the physiological and metabolic properties of offspring livers.

Herrick et al. reported that more than 23% of Americans equal or older than 1 year are at risk of vitamin D inadequacy or deficiency and the prevalence of the risk of deficiency is at its highest among adults among 20-39 years old using 2011-2014 National Health and Nutrition Examination Survey (NHANES) data sets (1). They also reported that the risk of deficiency was higher among non-Hispanic Black than non-Hispanic Asian, non-Hispanic White, and Hispanic participants. Moreover, the high prevalence of vitamin D deficiency and inadequacy is associated with obesity (5, 31, 32). These findings suggest that reproductive-age women with obesity have a higher risk of vitamin D deficiency during pregnancies, specifically women of the vitamin D deficiency vulnerable ethnic/race groups.

The associations between maternal vitamin D deficiency and adverse maternal and fetal outcomes have been well reported (33–37). A systematic review of 3357 studies revealed that maternal vitamin D deficiency increases the risks of gestational diabetes, preeclampsia, and small for gestational age infants (35). In addition, prior studies have implicated associations between maternal vitamin D deficiency and offspring obesity later in life in both human observation studies (14–17, 38) and dietary manipulation studies in rodents (18, 39). We did not observe an obese phenotype; however, we found that mice exposed to prenatal vitamin D deficiency showed transcriptional alterations in lipid metabolism-related pathways. Moreover, the

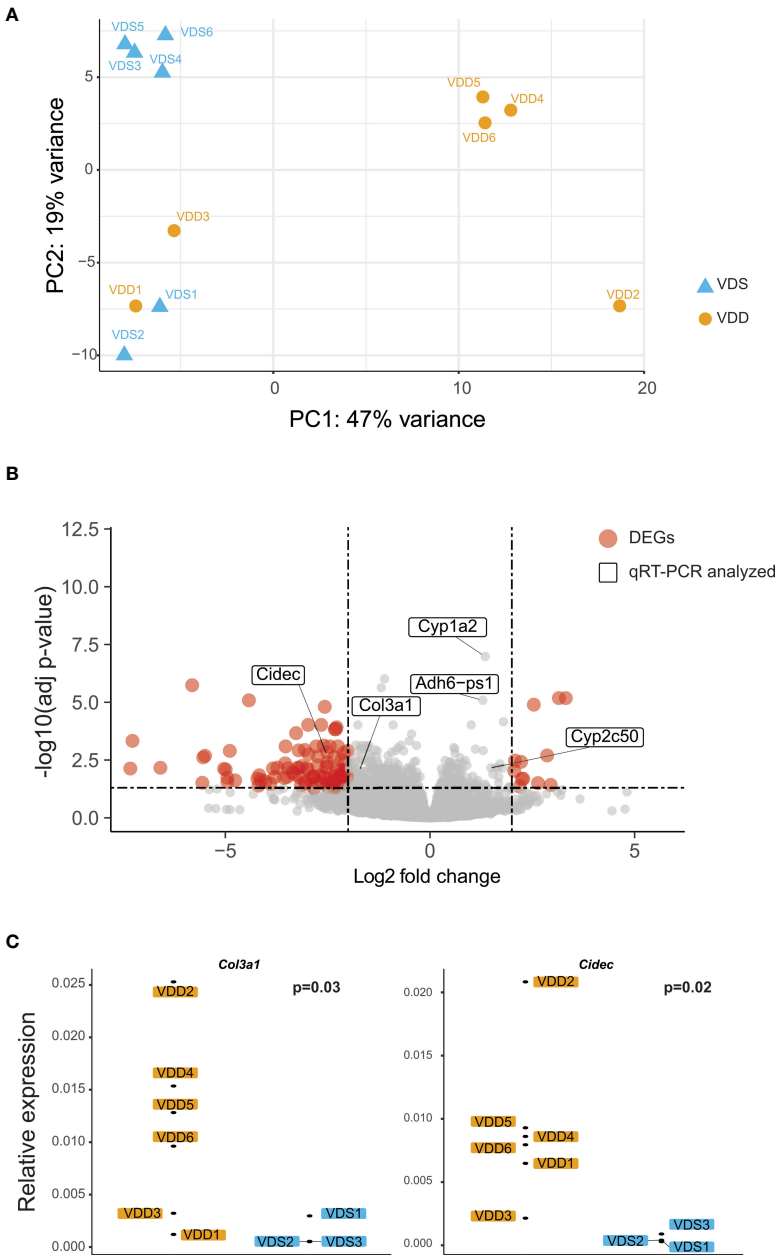

FIGURE 2 | Prenatal vitamin D deficiency leads to altered gene expression in adult mouse liver. **(A)** PCA demonstrates variation in expression patterns between VDD and VDS offspring. **(B)** A volcano plot shows differentially expressed genes (DEGs) found in the analysis comparing mouse offspring exposed to a prenatal vitamin D deficiency versus mice exposed to a vitamin D sufficient diet. Genes are significantly differentially expressed if they have a p adjusted value less than 0.05 and -2 < fold change < 2. **(C)** qRT-PCR using cDNA generated from offspring liver samples validates the upregulation of the collagen, type III, alpha I (*Col3a1*), and *Cidec* genes.

histopathological analysis suggested that exposure to a prenatal vitamin D deficiency affects the physiology of the liver at the adult stage. Our results suggest the existence of long-term memory of prenatal vitamin D deficiency exposure in the liver.

The association between vitamin D deficiency in adulthood and chronic liver diseases (CLD) (40), including cirrhosis (41), non-alcoholic fatty liver disease (NAFLD, recently been proposed to rename as metabolic-associated fatty liver disease [MAFLD) (42)] (43–45), and non-alcoholic steatohepatitis (NASH) (44, 45), have been identified in many cross-sectional studies. Stokes et al. reviewed the associations between CLD and vitamin D deficiency (46). We fed a vitamin D sufficient diet to all offspring after weaning, finding that the serum vitamin D concentration of mice exposed to prenatal VDD became normal by 5 weeks of age. Therefore, the pathogenesis of the liver phenotype we observed in the liver of prenatal VDD offspring was not by deficiency at the

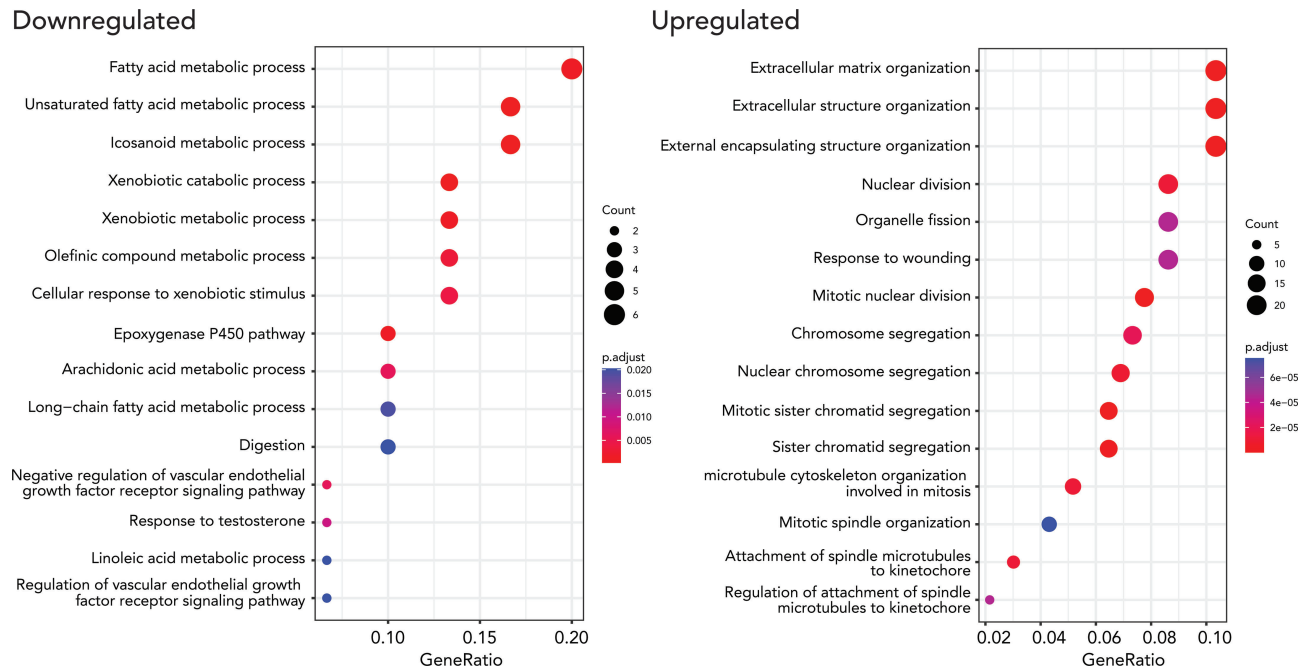

FIGURE 3 | Results from GO enrichment analysis (biological processes) using a Bioconductor package, *clusterProfiler*, for up and down-regulated DEGs. The top 15 up (right) and downregulated (left) terms were. The size of the dots represents the number of the genes, and the color indicates the significance of the enrichment.

time, likely by a long-term memory of VDD exposure. However, there are several similarities that exist. For instance, the infiltration and activation of macrophages is a key feature of endoplasmic reticulum stress-induced inflammation in liver injury, with VDR signaling regulating the inflammatory response in macrophages (47). We found that two distinct macrophage proportions, Cd163-positive, the anti-inflammatory (M2 phenotype) macrophages (48), and Ccr2-positive macrophages had distinct patterns of alteration in prenatal VDD offspring. Associations between the Ccr2-positive Kupffer cells (hepatic residential macrophage) and choline-deficient amino acid-defined diet-induced hepatic steatosis and fibrosis have been identified (49, 50). Several studies reported that a high-fat diet-induced hepatic steatosis increases bone-marrow (BM)-derived macrophages, which predominantly express Ccr2 (51, 52). The cell subtype reference expression signatures of both Cd163-positive and Ccr2-positive macrophages in this study showed higher expression of *Emr1* (F4/80) but low expression of *Itgam* (Cd11b) (52), indicating that they may be tissue-resident macrophages. Ccr2 expression in Kupffer cells contributes to BM-derived macrophage recruitment (49). The resident macrophages are derived from multiple anatomical locations during development suggesting developmental origin cell subtype proportion alterations may exist in the liver that is associated with a predisposing condition of prenatal VDD to the liver phenotype at the adult stage. The GO enrichment analyses on DEGs in this study showed enrichment of biological processes GO terms including extracellular matrix organization, regulation of vascularized development, and regulation of angiogenesis, processes which occur with liver fibrosis. Our study provides new insight into how prenatal VDD affects the liver phenotype and physiology as well as how this results in changes in the proportions of liver-resident immune cell subtypes in adult offspring.

There are several limitations of the current study that we would like to address in the future. First, we performed dietary manipulation on F0 female mice for five weeks prior to mating until the delivery. Belenchia et al. reported that it takes at least two weeks for serum vitamin D levels to return to normal after switching the diet to VDS from long-term VDD feeding (53). Thus, the F1 offspring were exposed to vitamin D deficient and insufficient conditions for the first two weeks of life. Using foster mothers would help us dissociate the effects between prenatal and neonatal periods. Second, while we observed cell subtype proportion changes in the prenatal VDD offspring, we cannot conclude if this alteration contributes to prenatal VDD exposure or results from liver damage. We believe testing cell subtype proportions in the liver before liver injury started would resolve this question.

Moreover, we estimated cell subtype proportion changes by the bulk RNA-seq results; therefore, the estimated proportion may be affected by the expression changes in specific cell subtypes. Testing the expression profiles at the single-cell levels will test if the alterations we observed in this study are attributed to the gene expression alterations between the same cell subtypes. Lastly, Wang et al. estimated the relationship between mice and humans at stages of growth and reported that the age range of 10 to 64.29 weeks of age in mice corresponds to the adult stage in

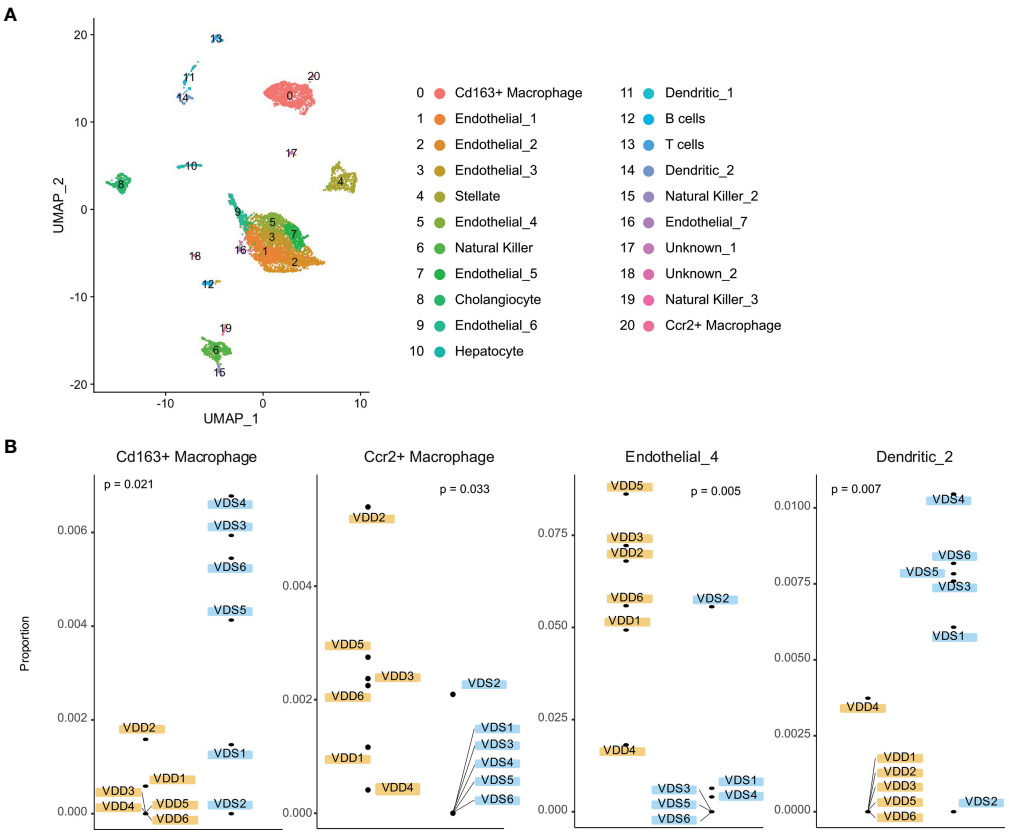

FIGURE 4 | Liver cell subtypes were found in different cell subtype proportions in prenatal VDD compared to VDS offspring. **(A)** Publicly available single-cell RNA-seq data was processed and clustered as shown in the UMAP plot. Gene expression patterns of clusters were used to define cell identities. **(B)** The proportions of Cd163+ macrophages and Ccr2+macrophages were inversely related between prenatal VDD and VDS offspring. Dendritic cells were found in a significantly lower proportion in VDD samples while a subset of endothelial cells was found in a higher proportion in VDD samples.

humans (20 to 51 years old) (54), suggesting 16 weeks of age is at the early adult stage. The prevalence of NAFLD increases after age 30 (55) and age older than 40 is a risk factor of NAFLD (56). This study could be improved by maintaining the mice for longer than 16 weeks of age following prenatal VDD in order to observe more changes related to prenatal VDD and at the adulthood stage.

In summary, we found that prenatal vitamin D deficiency alters gene expression profiles of the liver and cell subtype proportions of non-parenchymal cells at the adult stage. The prevalence of at risk of vitamin D deficiency and insufficiency is high among reproductive-age women, and a significant association of obesity to low vitamin D status has been implicated. Childhood obesity in the world is rising in frequency, with the prevalence of overweight/obesity among children aged 5-18 in the world rising from 4% in 1974 to 18% in 2016 (57). Epidemiological studies have identified significant associations between excess weight during childhood and the risk of adulthood obesity (58–62). Moreover, the incidence of NASH and NAFLD/MAFLD in young people has increased to 1.52 times between 1990 and 2017, and the prevalence of NAFLD/MAFLD in children varies by ethnicity (56). Prenatal and neonatal vitamin D deficiency may be contributing to this increase in prevalence rates. Reducing maternal vitamin D deficiency could reduce the adverse health outcome of the next generation, while understanding mechanisms of how our body remembers prenatal vitamin D status over the lifespan should help us to find interventions and treatments to prevent developmental origins of health and diseases in the liver.

DATA AVAILABILITY STATEMENT

The original contributions presented in the study are publicly available. This data can be found here: GEO, GSE194417.

ETHICS STATEMENT

The animal study was reviewed and approved by Institutional Animal Care and Use Committee at the Albert Einstein College of Medicine.

AUTHOR CONTRIBUTIONS

Conceptualization, MS. Methodology, KL, RD-T, and MS. Formal analysis, KL and GE-B. Histopathological analysis support, JO. Histopathological analysis, JFG. Data curation, KL and MS. Writing—original draft preparation, KL and MS. Writing—review and editing, KL, JFG, RD-T, JMG, and MS. Visualization, KL, GE-B, and MS. Supervision, JFG, JMG, and MS. Funding acquisition, MS. All authors have read and agreed to the published version of the manuscript.

FUNDING

This work was supported by the Human Genome Project Pilot Grant of the Department of Genetics at Albert Einstein College of Medicine and partially supported by the National Institutes of Health under award number R01HL145302 (MS).

ACKNOWLEDGMENTS

We thank to Analytical Imaging Facility (AIF) of Albert Einstein College of Medicine for their support. All histology slides were scanned with a P250 slide scanner supported by Shared Instrumentation Grant, 1S10OD019961-01. The AIF is partially funded by Cancer Center Support Grant of National Cancer Institutes (P30CA013330).

SUPPLEMENTARY MATERIAL

The Supplementary Material for this article can be found online at: https://www.frontiersin.org/articles/10.3389/fendo.2022.860286/full#supplementary-material

REFERENCES

1. Herrick KA, Storandt RJ, Afful J, Pfeiffer CM, Schleicher RL, Gahche JJ, et al. Vitamin D Status in the United States, 2011-2014. *Am J Clin Nutr* (2019) 110:150–7. doi: 10.1093/ajcn/nqz037
2. AC Ross, CL Taylor, AL Yaktine, HB Del Valle, eds. Institute of Medicine (US) Committee to Review Dietary Reference Intakes for Vitamin D and Calcium. In: *Dietary Reference Intakes for Calcium and Vitamin D*. Washington, DC): National Academies Press (US. doi: 10.17226/13050
3. Lips P. Worldwide Status of Vitamin D Nutrition. *J Steroid Biochem Mol Biol* (2010) 121:297–300. doi: 10.1016/j.jsbmb.2010.02.021
4. Özdemir AA, Ercan Gündemir Y, Küçük M, Yıldıran Sarıcı D, Elgörmüş Y, Çağ Y, et al. Vitamin D Deficiency in Pregnant Women and Their Infants. *J Clin Res Pediatr Endocrinol* (2018) 10:44–50. doi: 10.4274/jcrpe.4706
5. Liu X, Baylin A, Levy PD. Vitamin D Deficiency and Insufficiency Among US Adults: Prevalence, Predictors and Clinical Implications. *Br J Nutr* (2018) 119:928–36. doi: 10.1017/S0007114518000491
6. Roth DE, Abrams SA, Aloia J, Bergeron G, Bourassa MW, Brown KH, et al. Global Prevalence and Disease Burden of Vitamin D Deficiency: A Roadmap for Action in Low- and Middle-Income Countries. *Ann N Y Acad Sci* (2018) 1430:44–79. doi: 10.1111/nyas.13968
7. Kanatani KT, Nakayama T, Adachi Y, Hamazaki K, Onishi K, Konishi Y, et al. High Frequency of Vitamin D Deficiency in Current Pregnant Japanese Women Associated With UV Avoidance and Hypo-Vitamin D Diet. *PloS One* (2019) 14:e0213264. doi: 10.1371/journal.pone.0213264
8. Johnson DD, Wagner CL, Hulsey TC, McNeil RB, Ebeling M, Hollis BW. Vitamin D Deficiency and Insufficiency is Common During Pregnancy. *Am J Perinatol* (2011) 28:7–12. doi: 10.1055/s-0030-1262505
9. DeLuca HF. Evolution of Our Understanding of Vitamin D. *Nutr Rev* (2008) 66:S73–87. doi: 10.1111/j.1753-4887.2008.00105.x
10. Yu S, Bruce D, Froicu M, Weaver V, Cantorna MT. Failure of T Cell Homing, Reduced CD4/CD8alphaalpha Intraepithelial Lymphocytes, and Inflammation in the Gut of Vitamin D Receptor KO Mice. *Proc Natl Acad Sci USA* (2008) 105:20834–9. doi: 10.1073/pnas.0808700106
11. Yoshizawa T, Handa Y, Uematsu Y, Takeda S, Sekine K, Yoshihara Y, et al. Mice Lacking the Vitamin D Receptor Exhibit Impaired Bone Formation, Uterine Hypoplasia and Growth Retardation After Weaning. *Nat Genet* (1997) 16:391–6. doi: 10.1038/ng0897-391
12. Li YC, Pirro AE, Amling M, Delling G, Baron R, Bronson R, et al. Targeted Ablation of the Vitamin D Receptor: An Animal Model of Vitamin D-Dependent Rickets Type II With Alopecia. *Proc Natl Acad Sci USA* (1997) 94:9831–5. doi: 10.1073/pnas.94.18.9831
13. Dardenne O, Prud'homme J, Glorieux FH, St-Arnaud R. Rescue of the Phenotype of CYP27B1 (1alpha-Hydroxylase)-Deficient Mice. *J Steroid Biochem Mol Biol* (2004) 89–90:327–30. doi: 10.1016/j.jsbmb.2004.03.026
14. Morales E, Rodriguez A, Valvi D, Iñiguez C, Esplugues A, Vioque J, et al. Deficit of Vitamin D in Pregnancy and Growth and Overweight in the Offspring. *Int J Obes (Lond)* (2015) 39:61–8. doi: 10.1038/ijo.2014.165
15. Gale CR, Robinson SM, Harvey NC, Javaid MK, Jiang B, Martyn CN, et al. Maternal Vitamin D Status During Pregnancy and Child Outcomes. *Eur J Clin Nutr* (2008) 62:68–77. doi: 10.1038/sj.ejcn.1602680
16. Daraki V, Roumeliotaki T, Chalkiadaki G, Katrinaki M, Karachaliou M, Leventakou V, et al. Low Maternal Vitamin D Status in Pregnancy Increases the Risk of Childhood Obesity. *Pediatr Obes* (2018) 13:467–75. doi: 10.1111/ijpo.12267
17. Tint MT, Chong MF, Aris IM, Godfrey KM, Quah PL, Kapur J, et al. Association Between Maternal Mid-Gestation Vitamin D Status and Neonatal Abdominal Adiposity. *Int J Obes (Lond)* (2018) 42:1296–305. doi: 10.1038/s41366-018-0032-2
18. Belenchia AM, Johnson SA, Ellersieck MR, Rosenfeld CS, Peterson CA. *In Utero* Vitamin D Deficiency Predisposes Offspring to Long-Term Adverse Adipose Tissue Effects. *J Endocrinol* (2017) 234:301–13. doi: 10.1530/JOE-17-0015
19. Xue J, Schoenrock SA, Valdar W, Tarantino LM, Ideraabdullah FY. Maternal Vitamin D Depletion Alters DNA Methylation at Imprinted Loci in Multiple Generations. *Clin Epigenet* (2016) 8:107. doi: 10.1186/s13148-016-0276-4
20. Nicholas C, Davis J, Fisher T, Segal T, Petti M, Sun Y, et al. Maternal Vitamin D Deficiency Programs Reproductive Dysfunction in Female Mice Offspring Through Adverse Effects on the Neuroendocrine Axis. *Endocrinology* (2016) 157:1535–45. doi: 10.1210/en.2015-1638
21. Dobin A, Davis CA, Schlesinger F, Drenkow J, Zaleski C, Jha S, et al. STAR: Ultrafast Universal RNA-Seq Aligner. *Bioinformatics* (2013) 29:15–21. doi: 10.1093/bioinformatics/bts635
22. Love MI, Huber W, Anders S. Moderated Estimation of Fold Change and Dispersion for RNA-Seq Data With Deseq2. *Genome Biol* (2014) 15:550. doi: 10.1186/s13059-014-0550-8
23. Yu G, Wang L-G, Han Y, He Q-Y. Clusterprofiler: An R Package for Comparing Biological Themes Among Gene Clusters. *OMICS* (2012) 16:284–7. doi: 10.1089/omi.2011.0118
24. Wu T, Hu E, Xu S, Chen M, Guo P, Dai Z, et al. Clusterprofiler 4.0: A Universal Enrichment Tool for Interpreting Omics Data. *Innovation (NY)* (2021) 2:100141. doi: 10.1016/j.xinn.2021.100141
25. Newman AM, Steen CB, Liu CL, Gentles AJ, Chaudhuri AA, Scherer F, et al. Determining Cell Type Abundance and Expression From Bulk Tissues With Digital Cytometry. *Nat Biotechnol* (2019) 37:773–82. doi: 10.1038/s41587-019-0114-2
26. Baier FA, Sánchez-Taltavull D, Yarahmadov T, Castellà CG, Jebbawi F, Keogh A, et al. Loss of Claudin-3 Impairs Hepatic Metabolism, Biliary Barrier Function, and Cell Proliferation in the Murine Liver. *Cell Mol Gastroenterol Hepatol* (2021) 12:745–67. doi: 10.1016/j.jcmgh.2021.04.003
27. Sanchez-Taltavull D, Perkins TJ, Dommann N, Melin N, Keogh A, Candinas D, et al. Bayesian Correlation Is a Robust Gene Similarity Measure for Single-

Cell RNA-Seq Data. *NAR Genom Bioinform* (2020) 2:lqaa002. doi: 10.1093/nargab/lqaa002
28. Satija R, Farrell JA, Gennert D, Schier AF, Regev A. Spatial Reconstruction of Single-Cell Gene Expression Data. *Nat Biotechnol* (2015) 33:495–502. doi: 10.1038/nbt.3192
29. Hafemeister C, Satija R. Normalization and Variance Stabilization of Single-Cell RNA-Seq Data Using Regularized Negative Binomial Regression. *Genome Biol* (2019) 20:296. doi: 10.1186/s13059-019-1874-1
30. Kong Y, Rastogi D, Seoighe C, Greally JM, Suzuki M. Insights From Deconvolution of Cell Subtype Proportions Enhance the Interpretation of Functional Genomic Data. *PloS One* (2019) 14:e0215987. doi: 10.1371/journal.pone.0215987
31. Burris HH, Thomas A, Zera CA, McElrath TF. Prenatal Vitamin Use and Vitamin D Status During Pregnancy, Differences by Race and Overweight Status. *J Perinatol* (2015) 35:241–5. doi: 10.1038/jp.2014.198
32. Turer CB, Lin H, Flores G. Prevalence of Vitamin D Deficiency Among Overweight and Obese US Children. *Pediatrics* (2013) 131:e152–61. doi: 10.1542/peds.2012-1711
33. Bodnar LM, Catov JM, Simhan HN, Holick MF, Powers RW, Roberts JM. Maternal Vitamin D Deficiency Increases the Risk of Preeclampsia. *J Clin Endocrinol Metab* (2007) 92:3517–22. doi: 10.1210/jc.2007-0718
34. Wei SQ, Audibert F, Hidiroglou N, Sarafin K, Julien P, Wu Y, et al. Longitudinal Vitamin D Status in Pregnancy and the Risk of Pre-Eclampsia. *BJOG* (2012) 119:832–9. doi: 10.1111/j.1471-0528.2012.03307.x
35. Aghajafari F, Nagulesapillai T, Ronksley PE, Tough SC, O'Beirne M, Rabi DM. Association Between Maternal Serum 25-Hydroxyvitamin D Level and Pregnancy and Neonatal Outcomes: Systematic Review and Meta-Analysis of Observational Studies. *BMJ* (2013) 346:f1169. doi: 10.1136/bmj.f1169
36. van der Pligt P, Willcox J, Szymlek-Gay EA, Murray E, Worsley A, Daly RM. Associations of Maternal Vitamin D Deficiency With Pregnancy and Neonatal Complications in Developing Countries: A Systematic Review. *Nutrients* (2018) 10(5):640. doi: 10.3390/nu10050640
37. Gilani S, Janssen P. Maternal Vitamin D Levels During Pregnancy and Their Effects on Maternal-Fetal Outcomes: A Systematic Review. *J Obstet Gynaecol Can* (2019) 42(9):1129–37. doi: 10.1016/j.jogc.2019.09.013
38. Boyle VT, Thorstensen EB, Thompson JMD, McCowan LME, Mitchell EA, Godfrey KM, et al. The Relationship Between Maternal 25-Hydroxyvitamin D Status in Pregnancy and Childhood Adiposity and Allergy: An Observational Study. *Int J Obes (Lond)* (2017) 41:1755–60. doi: 10.1038/ijo.2017.182
39. Wen J, Hong Q, Wang X, Zhu L, Wu T, Xu P, et al. The Effect of Maternal Vitamin D Deficiency During Pregnancy on Body Fat and Adipogenesis in Rat Offspring. *Sci Rep* (2018) 8:365. doi: 10.1038/s41598-017-18770-4
40. He X, Xu C, Lu Z-H, Fang X-Z, Tan J, Song Y. Low Serum 25-Hydroxyvitamin D Levels are Associated With Liver Injury Markers in the US Adult Population. *Public Health Nutr* (2020) 23:2915–22. doi: 10.1017/S1368980020000348
41. Kubesch A, Quenstedt L, Saleh M, Rüschenbaum S, Schwarzkopf K, Martinez Y, et al. Vitamin D Deficiency Is Associated With Hepatic Decompensation and Inflammation in Patients With Liver Cirrhosis: A Prospective Cohort Study. *PloS One* (2018) 13:e0207162. doi: 10.1371/journal.pone.0207162
42. Eslam M, Sanyal AJ, George J. International Consensus Panel. MAFLD: A Consensus-Driven Proposed Nomenclature for Metabolic Associated Fatty Liver Disease. *Gastroenterology* (2020) 158:1999–2014.e1. doi: 10.1053/j.gastro.2019.11.312
43. Park E, Park EY. Inverse Association Between Serum 25-Hydroxyvitamin D Levels and Risk of Suspected Non-Alcoholic Fatty Liver Disease in Obese Population. *Int J Environ Res Public Health* (2021) 18(16):8682. doi: 10.3390/ijerph18168682
44. Livadariu R, Timofte D, Trifan A, Danila R, Ionescu L, Sîngeap AM, et al. Vitamin D Deficiency, a Noninvasive Marker of Steatohepatitis in Patients With Obesity and Biopsy Proven Nonalcoholic Fatty Liver Disease. *Acta Endocrinol (Buchar)* (2018) 14:76–84. doi: 10.4183/aeb.2018.76
45. Targher G, Bertolini L, Scala L, Cigolini M, Zenari L, Falezza G, et al. Associations Between Serum 25-Hydroxyvitamin D3 Concentrations and Liver Histology in Patients With Non-Alcoholic Fatty Liver Disease. *Nutr Metab Cardiovasc Dis* (2007) 17:517–24. doi: 10.1016/j.numecd.2006.04.002
46. Stokes CS, Volmer DA, Grünhage F, Lammert F. Vitamin D in Chronic Liver Disease. *Liver Int* (2013) 33:338–52. doi: 10.1111/liv.12106
47. Zhou Y, Dong B, Kim KH, Choi S, Sun Z, Wu N, et al. Vitamin D Receptor Activation in Liver Macrophages Protects Against Hepatic Endoplasmic Reticulum Stress in Mice. *Hepatology* (2020) 71:1453–66. doi: 10.1002/hep.30887
48. Wang H, Zhang C-S, Fang B-B, Hou J, Li W-D, Li Z-D, et al. Dual Role of Hepatic Macrophages in the Establishment of the Echinococcus Multilocularis Metacestode in Mice. *Front Immunol* (2020) 11:600635. doi: 10.3389/fimmu.2020.600635
49. Miura K, Yang L, van Rooijen N, Ohnishi H, Seki E. Hepatic Recruitment of Macrophages Promotes Nonalcoholic Steatohepatitis Through CCR2. *Am J Physiol Gastrointest Liver Physiol* (2012) 302:G1310–21. doi: 10.1152/ajpgi.00365.2011
50. Seki E, de Minicis S, Inokuchi S, Taura K, Miyai K, van Rooijen N, et al. CCR2 Promotes Hepatic Fibrosis in Mice. *Hepatology* (2009) 50:185–97. doi: 10.1002/hep.22952
51. Klein I, Cornejo JC, Polakos NK, John B, Wuensch SA, Topham DJ, et al. Kupffer Cell Heterogeneity: Functional Properties of Bone Marrow Derived and Sessile Hepatic Macrophages. *Blood* (2007) 110:4077–85. doi: 10.1182/blood-2007-02-073841
52. Obstfeld AE, Sugaru E, Thearle M, Francisco A-M, Gayet C, Ginsberg HN, et al. C-C Chemokine Receptor 2 (CCR2) Regulates the Hepatic Recruitment of Myeloid Cells That Promote Obesity-Induced Hepatic Steatosis. *Diabetes* (2010) 59:916–25. doi: 10.2337/db09-1403
53. Belenchia AM, Johnson SA, Kieschnick AC, Rosenfeld CS, Peterson CA. Time Course of Vitamin D Depletion and Repletion in Reproductive-Age Female C57BL/6 Mice. *Comp Med* (2017) 67:483–90.
54. Wang S, Lai X, Deng Y, Song Y. Correlation Between Mouse Age and Human Age in Anti-Tumor Research: Significance and Method Establishment. *Life Sci* (2020) 242:117242. doi: 10.1016/j.lfs.2019.117242
55. Estes C, Razavi H, Loomba R, Younossi Z, Sanyal AJ. Modeling the Epidemic of Nonalcoholic Fatty Liver Disease Demonstrates an Exponential Increase in Burden of Disease. *Hepatology* (2018) 67:123–33. doi: 10.1002/hep.29466
56. Amarapurkar D, Kamani P, Patel N, Gupte P, Kumar P, Agal S, et al. Prevalence of Non-Alcoholic Fatty Liver Disease: Population Based Study. *Ann Hepatol* (2007) 6:161–3. doi: 10.1016/S1665-2681(19)31922-2
57. Le Garf S, Nègre V, Anty R, Gual P. Metabolic Fatty Liver Disease in Children: A Growing Public Health Problem. *Biomedicines* (2021) 9(12):1915. doi: 10.3390/biomedicines9121915
58. Whitaker RC, Wright JA, Pepe MS, Seidel KD, Dietz WH. Predicting Obesity in Young Adulthood From Childhood and Parental Obesity. *N Engl J Med* (1997) 337:869–73. doi: 10.1056/NEJM199709253371301
59. Venn AJ, Thomson RJ, Schmidt MD, Cleland VJ, Curry BA, Gennat HC, et al. Overweight and Obesity From Childhood to Adulthood: A Follow-Up of Participants in the 1985 Australian Schools Health and Fitness Survey. *Med J Aust* (2007) 186:458–60. doi: 10.5694/j.1326-5377.2007.tb00997.x
60. Evensen E, Wilsgaard T, Furberg A-S, Skeie G. Tracking of Overweight and Obesity From Early Childhood to Adolescence in a Population-Based Cohort - The Tromsø Study, Fit Futures. *BMC Pediatr* (2016) 16:64. doi: 10.1186/s12887-016-0599-5
61. Wang LY, Chyen D, Lee S, Lowry R. The Association Between Body Mass Index in Adolescence and Obesity in Adulthood. *J Adolesc Health* (2008) 42:512–8. doi: 10.1016/j.jadohealth.2007.10.010
62. Llewellyn A, Simmonds M, Owen CG, Woolacott N. Childhood Obesity as a Predictor of Morbidity in Adulthood: A Systematic Review and Meta-Analysis. *Obes Rev* (2016) 17:56–67. doi: 10.1111/obr.12316

Author Disclaimer: The content is solely the responsibility of the authors and does not necessarily represent the official views of the National Institutes of Health.

Conflict of Interest: The authors declare that the research was conducted in the absence of any commercial or financial relationships that could be construed as a potential conflict of interest.

Publisher's Note: All claims expressed in this article are solely those of the authors and do not necessarily represent those of their affiliated organizations, or those of the publisher, the editors and the reviewers. Any product that may be evaluated in

this article, or claim that may be made by its manufacturer, is not guaranteed or endorsed by the publisher.

frontiers | Frontiers in Endocrinology

ORIGINAL RESEARCH
published: 23 May 2022
doi: 10.3389/fendo.2022.882532

Thrifty-Eating Behavior Phenotype at the Food Court – Programming Goes Beyond Food Preferences

*Roberta Dalle Molle[1,2,3], Euclides José de Mendonça Filho[2,4], Luciano Minuzzi[5], Tania Diniz Machado[3], Roberta Sena Reis[3,6], Danitsa Marcos Rodrigues[7], Amanda Brondani Mucellini[8], Alexandre Rosa Franco[9,10,11], Augusto Buchweitz[9,10,12], Rudineia Toazza[7], Andressa Bortoluzzi[7], Giovanni Abrahão Salum[8], Sonia Boscenco[4], Michael J. Meaney[13], Robert D. Levitan[14], Gisele Gus Manfro[7,8] and Patricia Pelufo Silveira[2,4]**

[1] Programa de Pós-Graduação em Ciências da Nutrição, Universidade Federal de Ciências da Saúde de Porto Alegre, Porto Alegre, Brazil, [2] Ludmer Centre for Neuroinformatics and Mental Health, Douglas Hospital Research Center, Montreal, QC, Canada, [3] Programa de Pós-Graduação em Saúde da Criança e do Adolescente, Faculdade de Medicina, Hospital de Clínicas de Porto Alegre, Universidade Federal do Rio Grande do Sul, Porto Alegre, Brazil, [4] Department of Psychiatry, McGill University, Montreal, QC, Canada, [5] Department of Psychiatry and Behavioural Neurosciences, McMaster University, Hamilton, ON, Canada, [6] Faculdade de Nutrição, Universidade Federal de Goiás, Goiânia, Brazil, [7] Programa de Pós-Graduação em Neurociências, Instituto de Ciências Básicas da Saúde, Universidade Federal do Rio Grande do Sul, Porto Alegre, Brazil, [8] Programa de Pós-Graduação em Ciências Médicas: Psiquiatria, Faculdade de Medicina, Hospital de Clínicas de Porto Alegre, Universidade Federal do Rio Grande do Sul, Porto Alegre, Brazil, [9] Instituto do Cérebro (InsCer), Pontifícia Universidade Católica do Rio Grande do Sul (PUCRS), Porto Alegre, Brazil, [10] Faculdade de Medicina, Programa de Pós-Graduação em Medicina e Ciências da Saúde, Pontifícia Universidade Católica do Rio Grande do Sul (PUCRS), Porto Alegre, Brazil, [11] Faculdade de Engenharia, Programa de Pós-Graduação em Engenharia Elétrica, PUCRS, Porto Alegre, Brazil, [12] Faculdade de Letras, Programa de Pós-Graduação em Letras, Linguística, Pontifícia Universidade Católica do Rio Grande do Sul (PUCRS), Porto Alegre, Brazil, [13] Singapore Institute for Clinical Sciences, Agency for Science, Technology and Research (A*STAR), Singapore, Singapore, [14] Department of Psychiatry, University of Toronto and Centre for Addiction and Mental Health, Toronto, ON, Canada*

OPEN ACCESS

Edited by:
Tomoko Aoyama, University of Auckland, New Zealand

Reviewed by:
Patricia Cristina Lisboa, Rio de Janeiro State University, Brazil
Yuko Nakamura, The University of Tokyo, Japan
Takahiro Osada, Juntendo University, Japan

***Correspondence:**
Patricia Pelufo Silveira
patricia.silveira@mcgill.ca

Specialty section:
This article was submitted to Pediatric Endocrinology, a section of the journal Frontiers in Endocrinology

Received: *23 February 2022*
Accepted: *14 April 2022*
Published: *23 May 2022*

Citation:
Dalle Molle R, de Mendonça Filho EJ, Minuzzi L, Machado TD, Reis RS, Rodrigues DM, Mucellini AB, Franco AR, Buchweitz A, Toazza R, Bortoluzzi A, Salum GA, Boscenco S, Meaney MJ, Levitan RD, Manfro GG and Silveira PP (2022) Thrifty-Eating Behavior Phenotype at the Food Court – Programming Goes Beyond Food Preferences. Front. Endocrinol. 13:882532. doi: 10.3389/fendo.2022.882532

Introduction: Prenatal growth impairment leads to higher preference for palatable foods in comparison to normal prenatal growth subjects, which can contribute to increased body fat mass and a higher risk for developing chronic diseases in small-for-gestational-age (SGA) individuals throughout life. This study aimed to investigate the effect of SGA on feeding behavior in children and adolescents, as well as resting-state connectivity between areas related to reward, self-control, and value determination, such as orbitofrontal cortex (OFC), dorsolateral prefrontal cortex (DL-PFC), amygdala and dorsal striatum (DS).

Methods: Caregivers and their offspring were recruited from two independent cohorts in Brazil (PROTAIA) and Canada (MAVAN). Both cohorts included anthropometric measurements, food choice tasks, and resting-state functional magnetic resonance imaging (fMRI) data.

Results: In the Brazilian sample (17 ± 0.28 years, n=70), 21.4% of adolescents were classified as SGA. They exhibited lower monetary-related expenditure to buy a snack compared to controls in the food choice test. Decreased functional connectivity (n=40) between left OFC and left DL-PFC; and between right OFC and: left amygdala, right DS,

and left DS were observed in the Brazilian SGA participants. Canadian SGA participants (14.9%) had non-significant differences in comparison with controls in a food choice task at 4 years old (± 0.01, n=315). At a follow-up brain scan visit (10.21 ± 0.140 years, n=49), SGA participants (28.6%) exhibited higher connectivity between the left OFC and left DL-PFC, also higher connectivity between the left OFC and right DL-PFC. We did not observe significant anthropometric neither nutrients' intake differences between groups in both samples.

Conclusions: Resting-state fMRI results showed that SGA individuals had altered connectivity between areas involved in encoding the subjective value for available goods and decision-making in both samples, which can pose them in disadvantage when facing food options daily. Over the years, the cumulative exposure to particular food cues together with the altered behavior towards food, such as food purchasing, as seen in the adolescent cohort, can play a role in the long-term risk for developing chronic non-communicable diseases.

Keywords: small for gestational age (SGA), feeding behavior, resting state fMRI, functional connectivity, orbitofrontal cortex

1 INTRODUCTION

According to the Developmental Origins of Health and Disease (DOHaD) framework, maternal conditions and environmental cues during pregnancy may impact health and disease in adulthood. Adversities experienced during embryonic and fetal development may program the offspring for increased predisposition to non-communicable chronic diseases (1). The most common outcome that reflects fetal adversity is birth weight. A recent meta-analysis found associations between being born with low birth weight or small for gestational age (SGA) and incidence of cardiometabolic disease, glucidic metabolism disorders, and metabolic syndrome (2).

In developing countries, poor gestational nutrition and low pre-pregnancy weight are the main determinants of intrauterine growth restriction (IUGR), whereas in developed countries the main risk factor is cigarette smoking (3). DOHaD emerged from epidemiological studies conducted in developed countries (4), however in developing countries the association between fetal adversity and the development of non-communicable chronic diseases has also been observed (5). This suggests that independently of the cause of insufficient fetal growth, scarcity of nutrients activates a process of physiological adaptation in the fetus to guarantee survival (6). The literature of underlying mechanisms of prenatal programming is still scarce but may include prenatal structural defects, metabolic (mitochondrial dysfunction, oxidative stress, protein modification), epigenetic and glucocorticoid signaling-related mechanisms (1).

A body of clinical and experimental evidence shows that the exposure to intrauterine adverse events, often culminating with IUGR, alters the individuals' feeding preferences and eating behaviors, increasing their intake of foods rich in carbohydrates and/or fat (7). The increased preference for palatable foods may lead to subtle but persistent nutritional imbalances and contribute to the development of adult chronic non-communicable diseases in individuals who did not grow as much as expected in the uterus. Awareness and deep comprehension about these behavioral peculiarities and their neuropsychological basis may open an important venue for disease prevention in these subjects. Therefore, childhood and adolescence are important life stages characterized by sensitive periods of development that need further investigation, since the cumulative effects of such nutritional imbalances might not be established yet.

Eating behavior is regulated by three interconnected central hubs: the hypothalamus, involved in the homeostatic control; the "appetitive network", which consists of four regions (insula, medial temporal lobe, OFC/vmPFC, and striatum) responsible to encode the current incentive salience of sensed and available food rewards; and the ventromedial, dorsomedial, and dorsolateral prefrontal cortices, which control goal-oriented and self-regulated behavior (8). The OFC plays a critical role in the choice evaluation; it encodes the value of goals in decision-making (9), and is more frequently activated to current energy balance information in response to food cues (10). According to Suzuki et al. (11), the information about the nutritive attributes of foods is represented in the lateral OFC, which integrates this information with the medial OFC to compute an overall value. Interestingly, obese individuals may have a relative inability to down-regulate the OFC response to high-calorie food cues following satiation (12) and after bariatric surgery OFC resting-state connectivity to mesolimbic areas is reduced (13).

This study was designed to contribute to the literature regarding fetal adversity programming of eating behavior throughout life by replicating the analyses in two independent cohorts. More specifically, we examined the effect of being born SGA on feeding behavior in children and adolescents, as well as on resting-state functional connectivity between areas related to reward, self-control, and value determination. Based on previous studies, we hypothesized that SGA individuals from the two sites would have: i) altered behavior towards food in different

situations presented to them (e.g. when buying a snack or exposed to a buffet), in comparison to normal birth weight individuals; and ii) altered brain functional tonic connectivity between the OFC and brain regions involved in encoding the subjective value for available goods and decision-making.

2 MATERIALS AND METHODS

2.1 Participants and Measurements

2.1.1 PROTAIA

The adolescents and young adults selected for the study originated from a community sample selected from six schools that belong to the service area of the Santa Cecilia Health Unit, located in Porto Alegre, Rio Grande do Sul, Brazil. The students were invited to participate in the PROTAIA project (The multidimensional evaluation and treatment of anxiety in children and adolescents), which included psychiatric and nutritional assessment (14). Two-hundred-and-forty-two participants completed the first assessment; out of which 229 were eligible for the current study (six were excluded due to intellectual disability; seven due to kinship with another participant). The study design was to carry out a detailed reevaluation, five years later, in approximately 30% of the eligible sample, as the present study is the fourth wave of a long-term follow-up study [as suggested by Barbieri et al. (15)]. The reevaluation included: (1) psychiatric assessment; (2) anthropometric and feeding behavior assessment; and (3) functional neuroimaging scans. In the current study we focused on anthropometric, feeding behavior and brain resting-state connectivity data as the outcomes. Socioeconomic and psychiatric data were used to describe the sample. Data collection was performed in two laboratory visits both conducted during the morning. Seventy-five participants attended the first laboratory visit (behavioral data collection) in the Clinical Research Center of the Hospital de Clínicas de Porto Alegre (CPC - HCPA) and 43 attended the second laboratory visit, at the Brain Institute of Rio Grande do Sul - PUCRS (InsCer), when a functional magnetic resonance imaging (fMRI) protocol was performed.

The psychiatric evaluation was carried out using: (1) a structured clinical interview - Schedule for Affective Disorders and Schizophrenia for School-Age Children-Present and Lifetime Version (K-SADS-PL) (16), held with the adolescents and (2) the Brazilian version of the MINI instrument (International Neuropsychiatric Interview) (17), applied in the over-18s. These instruments were applied by medical and psychology students trained for such activity and supervised by a child/adolescent psychiatrist.

The socioeconomic classification was based on the ABEP score (Brazilian Association of Research Companies), which ranks the socioeconomic status according to the possession of certain items and the educational level of the head of the family: Class A – 35 to 46; Class B – 23 to 34; Class C - 14 to 22; Class D - 8 to 13 and Class E – 0 to 7. Maternal education was collected in years of schooling and classified using the cut-off point of eight years of education.

The study was approved by the Institutional Ethics Committee of the HCPA (GPPG/HCPA, project number 12-0254) and followed national and international guiding principles for research involving humans, including the Resolution 196/96 from the National Health Council. Ethics committee approval and a subsequent written informed consent were obtained from all participants prior to the study.

2.1.2 MAVAN

Data from the Maternal Adversity, Vulnerability, and Neurodevelopment (MAVAN) prospective birth cohort (18) were used. Eligibility criteria for mothers included age 18 years old or older, singleton pregnancy, and fluency in French or English. Mothers were excluded from the study if they had severe chronic illness, placenta previa, a history of incompetent cervix, impending delivery, or had a fetus/infant born at gestational age <37 weeks or born with a major anomaly. Six hundred and thirty mother-child dyads were recruited during pregnancy in Montreal, QC and Hamilton, ON. They were assessed longitudinally, with multiple evaluations of both mother and child in-home and laboratory across the child's development. In the current study, we focused on the feeding behavior assessment performed at 4 years old with 315 participants. Moreover, functional neuroimaging scans performed at the Montreal site at 10 years of age with 49 participants were analyzed. Socioeconomic data were used to describe the sample. The socioeconomic classification was based on household total gross income, being the cut-off point CAD 40,000 per year. Maternal education was classified according to the completion of high school.

The study was approved by the institutional review boards at hospitals and university affiliates: McGill University, l'Universite de Montreal, the Royal Victoria Hospital, Jewish General Hospital, Centre Hopitalier de l'Universite de Montreal, Hôpital Maisonneuve-Rosemont, St Joseph's Hospital, and McMaster University. Informed consent was obtained from the parents/guardians of the participants.

2.2 Small for Gestational Age (SGA) Determination

Birth weight and gestational age data were collected from the child's health record. The SGA classification was based on the birth weight ratio (BWR), which is the ratio between the infant birth weight and the sex-specific mean birth weight for each gestational age for the local population (19, 20). Participants were classified as SGA if they have a BWR of <0.85 (21).

2.3 Anthropometric Assessment

The anthropometric assessment was performed by trained researchers. Weight and height were measured using accurate and calibrated equipment (Filizola®, Harpenden®, TANITA® and Perspective Enterprises®), and the participants were without shoes and in light clothing. The measures were performed in duplicate, and the average value was adopted. Body mass index (BMI) was calculated as weight in kilograms divided by height in meters squared (kg/m^2). Z-scores for BMI were calculated according to World Health Organization (WHO) standards (22). Children from 0 to 5 years of age with

BMI-for-age Z-scores above +2 were classified as overweight and +3 as obese. Children above 5 years old and adolescents were classified as overweight when the BMI-for-age Z-scores were above +1 and as obese when above +2 (23).

2.4 Feeding Behavior Assessment

2.4.1 PROTAIA

Anthropometric measures were performed in the morning while participants were fasting. Afterwards, they received a voucher to purchase snacks of their choice in the cafeteria of the HCPA Clinical Research Center (CPC-HCPA); the voucher offered had the same monetary value for all participants, and was sufficient to purchase different items (e.g. the voucher would be enough to purchase a sandwich plus a small soft drink or coffee, plus a small desert) (**Supplementary Figure S1**). Participants were free to choose any snack on the cafeteria, as long as it did not cost more than the voucher. If the participant did not use the full value of the voucher, the remaining value was returned to the researcher. Participants were requested to eat the snack before continuing the behavioral tests. Food choices were photographed before and after the consumption and all the participants ate the snack. The receipt which included the selected products and the amount spent was saved and attached to the participant's protocol. Subsequently, the amount spent, non-industrialized snacks recipes, and food choices were entered into an Excel® data spreadsheet (Microsoft). For each participant, the nutritional composition of the selected snack was calculated with the aid of a table of household measures (24) and the USDA National Nutrient Database (25).

2.4.2 MAVAN

Children and mothers were offered a test meal in the laboratory at approximately 10:30 a.m. including different types of foods in pre-weighed portions for 30 minutes. Pre-weighed plates of the different foods, chosen with the assistance of a nutritionist to represent local habitual snack items and to have similar colors, were displayed in a buffet to which the child had total access (26, 27). A table with two sets of plates was placed in the center of the room, with chairs for mother and child on both sides (facing each other) (**Supplementary Figure S2**). A cushion was placed on the child's chair to facilitate accessibility of the different foods. Mothers were instructed to offer a light breakfast to participants at home beforehand and not to share plates or influence children's choices. At the end of the session, the remaining foods were weighed again to measure the intake. Based on the nutritional content of each food and the amount eaten, we calculated the amount of fat, carbohydrates, and protein ingested (28).

2.5 Resting-State fMRI Acquisition and Data Processing

In both sites, the scan protocol included anatomical and resting-state fMRI acquisition. In the Brazilian sample, participants were scanned with at least 4 hours of fasting. About 30 minutes prior to the scan, they received a standardized snack [a cereal bar + one box juice = 174 kcal, carbohydrates 39g (90% of total calories), protein 0.9 g (2% of total calories) and 1.6 g of lipids (8% of total calories)]. Structural and functional images were collected on a 3.0T MRI scanner (GE Healthcare Signa HDxT) with an eight-channel head coil used for signal reception. Structural T1 weighted images were acquired for the whole cerebrum (1 mm^3 isotropic voxels, 170 contiguous slices, 256 x 256 mm grid, TR=6.1ms, TE=2.18ms) during the first five minutes of the imaging session. Resting-state functional MRI was carried out by acquiring T2* Echo Planar Images (EPI) on a 7-minute-long run with the following parameters: TR=2000ms, TE=30ms, flip angle=90 degrees with 240mm x 240mm FOV with 26 interleaved axial slices of 4 mm on a 80x64 matrix.

In the Canadian sample, data were acquired using a 3T Trio Siemens scanner. High resolution T1-weighted images for the whole cerebrum (1 mm isotropic 3D MPRAGE, sagittal acquisition, 256 x 256 mm grid, TR=2300ms, TE=4ms, FA=9degrees) were obtained in an approximately five-minute scan. Resting-state fMRI was obtained on a 6-minute-long run of blood oxygenation level-dependent (BOLD) signal at rest using a gradient echo-planar imaging sequence with the following parameters: TR=2000 ms, TE=30 ms, flip angle=90 degrees with 3x3 mm in-plane resolution with 33 slices of 4 mm on a 64x64 matrix. During the resting-state functional MRI acquisition participants in both cohorts were instructed to stay with their eyes open and fixating on a "+" at the center of a screen. Participants were instructed to relax and avoid thinking about anything in particular.

Images were pre-processed using Statistical Parametric Mapping (SPM, v.8 for PROTAIA and v.12 for MAVAN, University College London, UK; http://www.fil.ion.ucl.ac.uk/spm in conjunction with the default processing pipeline using the CONN Functional Connectivity Toolbox (CONN toolbox; www.nitrc.org/projects/conn, RRID : SCR_009550).

First, the images were converted from DICOM (scanner format) to Nifti-1 format for processing. In order to compensate for different temporal offsets between slices during acquisition, temporal data interpolation (slice-timing correction) was applied to the functional images (29). After slice-timing correction, the images were processed to correct movement-related artifacts, the preprocessing pipeline developed by CONN (https://web.conn-toolbox.org/fmri-methods/preprocessing-pipeline) involves an outlier identification process *via* calculation of a framewise displacement each timepoint with a 140x180x115mm bounding box. If the framewise displacement exceeds 0.9mm, then this acquisition frame is flagged as a potential outlier. Furthermore, the global BOLD signal change is computed at each timepoint, and if the average BOLD signal changes greater than 5 s.d. then this is also flag the acquisition as an outlier. Each image was transformed *via* a 6-parameter rigid-body transformation, and then an autoregressive-moving average model was applied to correct for changes in head positions (30). Functional slice-time, motion corrected images were then co-registered to the individual raw T1 anatomical images (PROTAIA: Ashburner & Friston, 1997; MAVAN: Montreal Neurological Institute; MNI152). High-resolution anatomical images were segmented into grey matter, white matter and cerebrospinal fluid (CSF) (31); the smoothed

gray matter images were then transformed into a standard space using a 12-parameter affine transformation and a 6-parameter three-dimensional quadratic deformation (32, 33). The parameters for the normalization to the standard space were applied to both anatomical and functional images for each subject. Following normalization, the functional data were smoothed using 8x8x8 mm Full Width at Half Maximum (FWHM) Gaussian kernel for statistical analysis (34). In PROTAIA, three subjects were excluded due to excess of movement during the resting-state fMRI, while in MAVAN five subjects were excluded due to excess movement and two for missing T1 data resulting in 40 and 49 total participants respectively.

Resting-state fMRI analysis was processed using CONN functional connectivity toolbox (35). Functional connectivity analysis was performed using a seed-driven approach with orbitofrontal cortex (OFC, right and left – Brodmann area 11) as seed points and adjusted for multiple comparisons. Functional imaging signal was filtered using a temporal band-pass filter of 0.01 Hz to 0.08 Hz. Residual motion correction parameters were used as regressors in the model according to the method described by Behzadi et al. (36) to mitigate motion-related artifacts in the seed-based connectivity analysis. The aCompCor method, part of the CONN pipeline, identifies confounding effects with noise from cerebral white matter and cerebrospinal components as well as head motion. Factors that are identified as confounds were then removed from volumes using Ordinary Least Square regression. Regions of interest (ROIs) corresponding to the ventral striatum, dorsal striatum, amygdala, medial prefrontal cortex, and dorsolateral prefrontal cortex were used to determine whether they were positively or negatively correlated with the OFC seed points (37). ROIs for seed points and target regions were extracted from Desikan et al. (38) and from the Harvard-Oxford subcortical structural atlases and comprehended only grey matter tissue (**Supplementary Figure S3**). For description of the OFC mask anatomic definition, including lateral and medial OFC, please see Desikan et al. (38). Individual Fisher's Z scores from the OFC to the anticorrelated or positive correlated ROIs were calculated according to Weissenbacher et al. (39).

Seed points and ROIs were chosen based on the "appetitive network" (8) and on literature search. The OFC is a brain area related to motivation and compulsive behavior (40), its hyperactivity has been observed in individuals with obsessive compulsive disorder (41, 42). Bracht et al. (43) found that an increased OFC-NAcc functional connectivity is associated with craving in alcohol use disorder, and Black et al. (44) demonstrated greater resting-state functional connectivity between left middle frontal gyrus and left lateral OFC in obese children when compared to healthy weight children. Moreover, activity in the OFC and in the DL-PFC encodes subjects' willingness to pay for food items (9). Therefore, it was assumed that SGA individuals would present connectivity changes between reward and self-control brain regions.

2.6 Statistical Analysis

Data were entered and analyzed in the Statistical Package for the Social Sciences (SPSS) 20.0 software (SPSS Inc., Chicago, IL, USA). Quantitative variables were described as mean ± standard error of the mean (SEM), whereas categorical data were described using absolute (n) and relative (%) frequencies. Comparisons between two groups were performed using Student's t-test for parametric continuous variables or Kruskal-Wallis for non-parametric continuous variables and Chi-square test for categorical variables. The food choice-related data were analyzed by one-way ANOVA using BMI Z-Score and sex as covariates. The resting-state fMRI data were analyzed using the Student's t-test in order to compare the connectivity between SGA individuals (BWR <0.85) and controls. Exploratory significance levels for all measures were set at $p<0.05$. To ensure reliability and robustness of exploratory significant mean differences we undertook further analyses to sample composition using 2,000 non-parametric bootstrapping with replacement and random resampling, in which 95% confidence intervals (Bootstrap CI) are reported. We also calculated false discovery rate (FDR) corrected q-values for each set of p-values from each resting-state fMRI seed points (45).

3 RESULTS

3.1 Sample Description

In the PROTAIA cohort, 75 healthy youths attended the behavioral data collection, however four could not inform birth data and one did not participate in the snack test, totaling 70 adolescents (SGA = 21.4%). Forty-three attended the fMRI visit, but data from 40 subjects (SGA = 17.5%) were processed and analyzed because three subjects had head excess movement. In the MAVAN cohort, 315 participated in the behavioral tests (SGA = 14.9%) and 49 were scanned for the fMRI analysis (SGA = 28.5%). **Figure 1** describes the sample sizes from both cohorts.

Table 1 shows the participants' characteristics from both cohorts. SGA and controls were not different regarding sex, color, maternal education, socioeconomic status, BMI, gestational age and prevalence of anxiety. As expected, the SGA group had a mean birth weight lower than the control group in both cohorts.

3.2 Feeding Behavior Assessment

Snack test data are shown in **Table 2**. In the PROTAIA cohort, a difference between groups was observed in the amount of the financial resource used to buy the snack. The SGA group used a smaller quantity, although the total caloric intake was comparable between groups [$F(1,65)=1.91$; $p=0.172$]. In both cohorts, the macronutrients' intake in grams and percentage of total calories were not different between SGA and controls. The same comparisons were performed dividing the energy and nutrients' consumption per body weight in kg and no differences between groups were observed in both cohorts (**Supplementary Table S1**).

Exploratory analyses of the snack test according to sociodemographic data, as well as the correlations between snack test results (original data and divided per body weight) and resting-state fMRI connectivity are presented in the Supplemental data (**Tables S2A–D**, **S3A–F** and **S4A–F**).

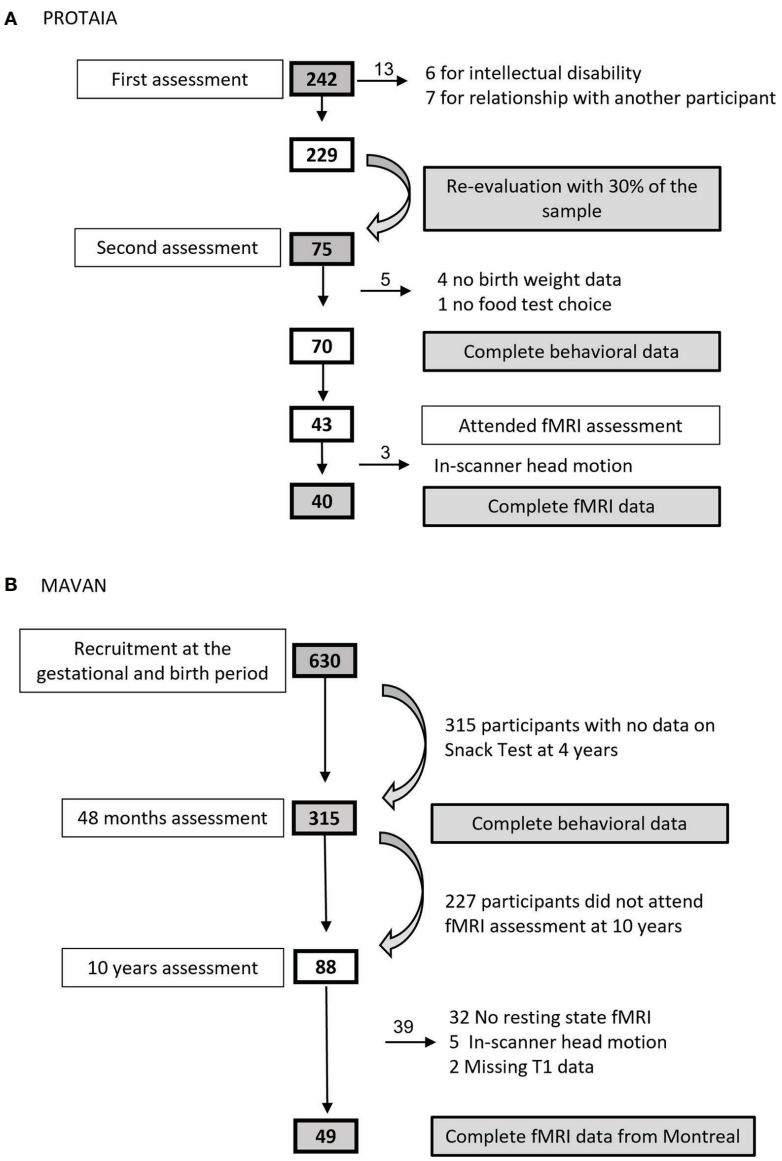

FIGURE 1 | Sample size flowcharts from **(A)** PROTAIA and **(B)** MAVAN.

3.3 Resting-State fMRI Connectivity

The brain imaging results are shown in **Table 3** and **Figure 2**.

In the PROTAIA cohort, the SGA group exhibited predominately negative resting-state functional connectivity (rs-FC) between a network of areas that included the right OFC and the left (mean difference = 0.159, Bootstrap CI = 0.05: 0.30, FDR q = 0.048) and right dorsal striatum (mean difference = 0.204, Bootstrap CI = 0.09: 0.32, FDR q = 0.018), and the left amygdala (mean difference = 0.230, Bootstrap CI = 0.12: 0.35, FDR q = 0.024), while in controls the rs-FC between these areas was predominately positive. Also, the SGA group compared to controls showed lower connectivity between the left OFC and the left DL-PFC (mean difference = 0.225, Bootstrap CI = 0.10: 0.36, FDR q = 0.024).

In the MAVAN cohort, the differences in functional connectivity were found between left OFC and both sides of the DL-PFC. The SGA group had higher levels of connectivity between left OFC and left DL-PFC in comparison to controls. This difference was significant according to the bootstrap procedure (mean difference =0.15, Bootstrap CI = 0.01: 0.30), but it was not significant when adjusting for multiple testing (FDR q = 0.12). Furthermore, the SGA group also showed higher connectivity between the left OFC and the right DL-PFC in relation to the control group but this result did not met the Bootstrap and FDR thresholds (mean difference =0.15, Bootstrap CI = -0.03: 0.30, FDR q = 0.12).

TABLE 1 | Participants' characteristics, according to the birth weight for gestational age groups (SGA vs. controls).

	Behavioral tests samples			
	PROTAIA		MAVAN	
	Controls[$] (n=55)	SGA[$] (n=15)	Controls (n=268)	SGA (n=47)
Male[a]	21 (38.2%)	6 (40.0%)	142 (52.98%)	23 (48.93%)
White color[a]	36 (66.7%)	11 (73.3%)	189 (76.20%)	35 (77.77%)
Anxious[a]	24 (43.6%)	9 (60.0%)	————	————
Age (years)[b]	17.62 ± 0.32	17.08 ± 0.60	4.06 ± 0.01	4.05 ± 0.01
Birth weight (g)[b]	3286.55 ± 59.80	2457.33 ± 89.63*	3495.83 ± 24.18	2735.95 ± 36.38**
BMI[b]	23.62 ± 0.62	21.71 ± 1.10	16.09 ± 0.09	16.09 ± 0.32
BMI Z score[b]	0.60 ± 0.16	0.03 ± 0.32	0.53 ± 0.06	0.48 ± 0.19
Gestational age[c]	40.0 (38.0-40.0)	40.0 (37.0-40.0)	39.0 (38.0-40.0)	39.0 (39.0-40.0)
SES[d]	16.71 ± 0.66	18.39 ± 1.57	65 (24.8%)	11 (24.4%)
Maternal education[a,e]	11 (30.6%)	3 (33.3%)	55 (20.52%)	9 (19.56%)
	Resting-state fMRI connectivity samples			
	Controls[&] (n=33)	SGA[&] (n=7)	Controls (n=35)	SGA (n=14)
Male[a]	15 (45.5%)	4 (57.1%)	17 (48.6%)	6 (42.9%)
White color[a]	20 (62.5%)	5 (71.4%)	27 (79.41%)	11 (78.57%)
Anxious[a]	11 (33.3%)	4 (57.1%)	————	————
Age (years)[b]	17.72 ± 0.41	17.91 ± 0.99	10.1 ± 0.18	10.5 ± 0.17
Birth weight (g)[b]	3344.39 ± 62.15	2631.43 ± 63.75*	3363 ± 57.6	2624 ± 69.0**
BMI[b]	23.12 ± 0.64	21.67 ± 1.85	17.23 ± 0.55	17.89 ± 1.05
BMI Z score[b]	0.50 ± 0.17	-0.10 ± 0.56	-0.01 ± 0.16	0.19 ± 0.31
Gestational age[c]	40.0 (37.0-40.0)	40.0 (40.0-40.0)	39.0 (38.0-40.0)	39.0 (39.0-40.0)
SES[d]	17.75 ± 0.91	16.00 ± 1.98	8 (25%)	2 (16.6%)
Maternal education[a,e]	10 (45.5%)	0 (0.0%)	9 (25.7%)	4 (28.6%)

[a]*Chi-square. Data expressed as absolute (n) and relative (%) frequencies.*
[b]*Student's t-test. Data expressed as mean ± SEM.*
[c]*Kruskal-Wallis test. Data expressed as median and interquartile range.*
[d]*Mean ± SEM ABEP score in PROTAIA and absolute (n) and relative (%) frequencies for household total gross income ≤ 40k a year in MAVAN.*
[e]*PROTAIA: ≤ 8 years of schooling; MAVAN: high school diploma or less.*
**p<0.05; **p<0.001.*
[$]*Color: 54 controls, 15 SGA; Maternal education: 36 controls, 9 SGA.*
[&]*Color: 32 controls, 7 SGA; Maternal education: 22 controls, 4 SGA.*

4 DISCUSSION

The current study showed that SGA individuals have altered connectivity between the OFC and the DL-PFC in the two samples, and between the OFC, dorsal striatum and amygdala in the adolescent sample. The direction of the association between SGA and the OFC-DL-PFC connectivity was different in children and adolescents. Although there were no differences between SGA and controls regarding anthropometric measures and snack nutrients' consumption in both cohorts, SGA adolescents exhibited a different behavior when buying a snack, spending less money without eating less calories. The results confirm the hypothesis that SGA is associated with changes in food-related behaviors, and introduces the idea that SGA individuals, when compared to controls, have a different brain resting-state connectivity in areas related to reward and decision-making.

In both samples, the food choice test showed no differences in food preference between SGA and controls, since the percentage of calories from carbohydrates, proteins and lipids did not differ between groups. In the current study, the food preference was assessed by the spontaneous choice of food in a single meal in a controlled environment (laboratory or clinical center cafeteria), which may not have been able to detect broader differences in food preference as described in the literature in different ages (46–51).

Confirming our hypothesis, altered rs-FC between the OFC and brain regions involved in encoding the subjective value for available goods and decision-making was observed in SGA groups when compared to controls. SGA adolescents exhibited decreased rs-FC between the OFC and the DL-PFC, a circuit encoding subjects' willingness to pay for food items (9). Interestingly, at the behavioral level, SGA adolescents spent less money on food than controls (even being informed that they would need to return the non-used money), but no significant differences between the quantity of calories consumed was found. This suggests that they choose cheaper (and usually nutritionally poorer) foods, as previously proposed (52, 53). The functional connectivity between the DL-PFC and the other frontal-lobe regions is associated with attribution of value at the time of a behavioral choice (54). It has been suggested that these areas are involved in foreseeing potential outcomes from not chosen actions (55), an ability that may be

TABLE 2 | Food choice tests' data, according to birth weight for gestational age group.

	PROTAIA		MAVAN	
Variables	**Controls (n=55)**	**SGA (n=15)**	**Controls (n=268)**	**SGA (n=47)**
Amount spent (R$)	8.54 ± 0.27	7.22 ± 0.52 *	————	————
Energy (kcal)	554.89 ± 27.16	480.01 ± 52.61	334.86 ± 9.1	301.55 ± 12.35
CHO (g)	69.91 ± 3.75	63.37 ± 7.27	40.40 ± 1.26	37.33 ± 2.09
CHO (% total kcal)	51.12 ± 1.50	52.65 ± 2.91	49.00 ± 1.00	50.00 ± 2.00
Sugar (g)	31.37 ± 2.95	30.16 ± 5.71	22.31 ± 0.72	20.4 ± 1.15
Fiber (g)	2.74 ± 0.24	2.37 ± 0.46	1.93 ± 0.11	1.93 ± 0.18
PTN (g)	17.76 ± 1.31	12.65 ± 2.53	12.21 ± 0.38	11.09 ± 0.54
PTN (% total kcal)	12.35 ± 0.67	10.57 ± 1.30	15.00 ± 0.00	15.00 ± 1.00
FAT (g)	23.15 ± 1.31	19.91 ± 2.54	13.62 ± 0.49	11.86 ± 0.63
FAT (% total kcal)	37.18 ± 1.17	37.24 ± 2.26	36.00 ± 1.00	35.00 ± 1.00

One-way ANOVA with BMI Z-Score and sex as covariates; data expressed as mean ± SEM.
**p<0.05. CHO, carbohydrate; PTN, protein.*

impaired in SGA individuals. Surprisingly, the same pattern of decreased connectivity between the OFC, DL-PFC and amygdala, observed in SGA adolescents, is seen in schizophrenia patients (56). Lower connectivity in schizophrenic patients is associated with executive function social cognition deficits – a deficit that has also been described in the SGA population (57).

However, the altered associations between OFC - DL-PFC rs-FC in SGA were in the opposite way in children and adolescents. SGA children exhibited higher rs-FC between the OFC and the DL-PFC than controls, while SGA adolescents showed lower rs-FC. The differences could be related to the demographic dissimilarities in the two populations (see **Table 1**). In addition, studies with preterm children and children exposed to early life stress have also identified positive correlations between frontal and dorsolateral regions. For example, in an independent component analysis higher correlations of the left motor cortex and the bilateral posterior temporal cortex were observed in pre-term infants at 18 and 36 months of age, while early stress was positively associated with temporal similarity of a cluster of voxels in the left middle frontal gyrus (56, 57). Alterations of connectivity strength and direction from childhood to adolescence could be reflecting the maturation of cognitive networks. For example, the connectivity of important networks like the lateral frontoparietal network and the default mode network can be positively correlated in childhood, anti-correlated in adolescence, and negatively correlated in young adults (58). The differences observed for SGA children could be altering the fine-tuning of networks that are dynamic, highly dependent on the interaction between the genetic substrate and quality of the prenatal and early environment resulting in weaker connectivity in adolescence (59–61). Longitudinal studies are therefore necessary to test this hypothesis.

In addition, other altered rs-FC networks were observed in SGA adolescents, who exhibited food-related altered behavior. The rs-FC between right OFC and left amygdala was predominately negative in SGA, while predominately positive

TABLE 3 | SGA versus controls rs-FC between orbitofrontal cortex (left and right) and ROIs with significant results in one of the cohorts.

	PROTAIA		MAVAN	
	left OFC	**right OFC**	**left OFC**	**right OFC**
left DS	SGA: 0.028 ± 0.055 Controls: 0.059 ± 0.034 p=0.689	SGA: -0.098 ± 0.060 Controls: 0.061± 0.030 p=0.024*	SGA: 0.25 ± 0.06 Controls: 0.20 ± 0.03 p= 0.345	SGA: 0.18 ± 0.06 Controls: 0.19 ± 0.03 p=0.839
right DS	SGA: -0.051 ± 0.066 Controls: 0.004 ± 0.036 p=0.521	SGA: -0.101 ± 0.050 Controls: 0.103 ± 0.030 p=0.003*	SGA: 0.07 ± 0.08 Controls: 0.04 ± 0.04 p=0.725	SGA: 0.22 ± 0.05 Controls: 0.23 ± 0.03 p=0.939
left AMY	SGA: -0.066 ± 0.051 Controls: 0.033 ± 0.040 p=0.283	SGA: -0.129 ± 0.050 Controls: 0.101 ± 0.040 p= 0.008*	SGA: 0.30 ± 0.06 Controls: 0.20 ± 0.04 p=0.128	SGA: 0.10 ± 0.04 Controls: 0.13 ± 0.03 p=0.682
right AMY	SGA: -0.006 ± 0.072 Controls: -0.027 ± 0.033 p=0.790	SGA: 0.038 ± 0.042 Controls: 0.095 ± 0.040 p=0.528	SGA: 0.28 ± 0.07 Controls: 0.14 ± 0.04 p=0.061	SGA: 0.22 ± 0.07 Controls: 0.18 ± 0.04 p=0.642
left DL-PFC	SGA: 0.004 ± 0.060 Controls: 0.229 ± 0.040 p=0.019*	SGA: -0.162 ± 0.091 Controls: -0.007 ± 0.041 p=0.119	SGA: 0.21 ± 0.06 Controls: 0.06 ± 0.04 p=0.036*	SGA:0.19 ± 0.07 Controls: 0.08 ± 0.04 p=0.161
right DL-PFC	SGA: -0.056 ± 0.052 Controls: 0.092 ± 0.045 p=0.147	SGA: -0.031 ± 0.060 Controls: 0.011 ± 0.052 p=0.719	SGA:0.01 ± 0.09 Controls: -0.14 ± 0.03 p=0.045*	SGA:0.17 ± 0.08 Controls:0.12 ± 0.04 p=0.531

*Student's t-test. Data expressed as mean ± SEM (*p<0.05). OFC, orbitofrontal cortex; DL-PFC, dorsolateral prefrontal cortex; AMY, amygdala; DS, dorsal striatum.*

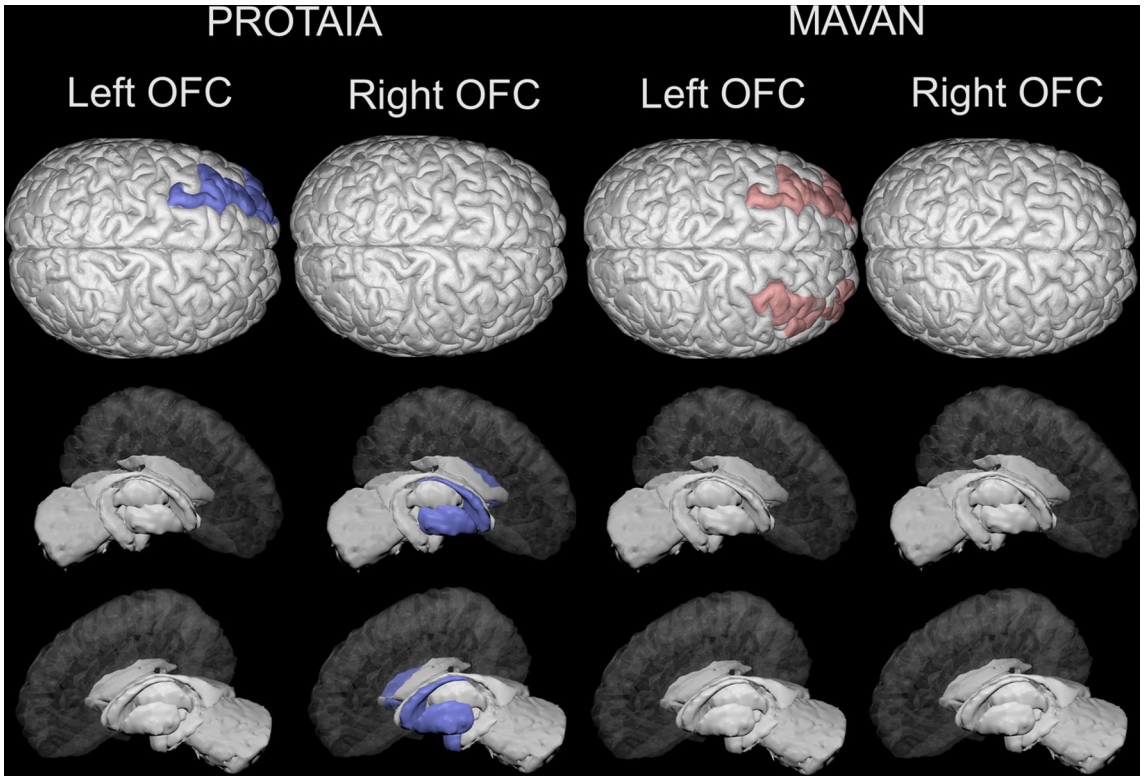

FIGURE 2 | Brain areas depicting statistically significant differences in resting-state functional connectivity (rsFC) with the left and right orbital frontal cortex between SGA and controls in the PROTAIA and MAVAN cohorts. Blue color (left DL-PFC, left amygdala and right and left dorsal striatum) represents lower rsFC in SGA versus Controls. Red color (right and left DL-PFC) represents higher rsFC in SGA versus Controls.

in controls. It is interesting to note that it is described in the literature a negative association between the OFC-amygdala functional connectivity and impulsivity scores in healthy subjects (62). As impulsivity seems to be an important behavioral feature linking impaired fetal growth to altered feeding behavior and preferences over the life-course (63, 64), the diminished connectivity between these two areas described in the current study could indeed characterize this group and be involved in the way they behave towards food. Finally, considering the proposed view of overeating palatable foods as a "food addiction" (65), the altered brain connectivity between the OFC, striatum and amygdala seen in our SGA adolescent group resembles the pattern previously seen in alcohol abusers (66, 67), cocaine users (68) and Internet Gaming Disorder (IGD) youths (69, 70).

Although our study has identified neurobehavioral changes in individuals who were born SGA, they had normal BMI both in childhood and adolescence. This suggests that the neurobehavioral changes precede the development of the well described increased adiposity and its metabolic consequences in these individuals (71, 72). More evident anthropometric and metabolic disturbances may arise over the years in this population with the cumulative exposure to particular food cues, altered behavior towards food (e.g. when purchasing foods), and consequent intake of energy-dense foods with low nutritional quality.

Our study was able to look for similarities in feeding behavior and rs-FC in two cohorts of SGA individuals, bringing results from different life stages. Our objective of having the two samples in the study was not to have a comparison between them, but rather pursuing a replication of the findings in an independent cohort. We understand that replication may be challenging, and perfect harmonization of the samples age, predictors and outcomes is virtually impossible. Even with these limitations, the effort for replication of the findings within the same study is aligned with the best methodological practices and we believe this is a strength of our study, considering the replication crisis in research (73, 74). Also, at first glance, the SGA groups seem to have a small sample size, however our study reflects the percentage of SGA in the population (10-20%). Despite this, we were still able to find brain rs-FC differences between groups in both cohorts. We suggest that the specific pattern of brain rs-FC observed could be leaving SGA individuals in a vulnerable position when facing food options on a daily basis. The increased vulnerability may affect food-related behaviors, as seen here, and food preferences reported in many other studies (46–51, 75–79), and play a role in the long-term risk for developing chronic non-communicable diseases. Therefore, the current study adds to the

literature demonstrating that while SGA individuals are more prone to future impairments in both physical and mental health in the adult years, they may represent an important populational group for targeted, well-matched intervention.

DATA AVAILABILITY STATEMENT

The datasets presented in this article are not readily available because they contain sensitive information. Requests to access the datasets should be directed to Patricia P. Silveira.

ETHICS STATEMENT

The studies involving human participants were reviewed and approved by PROTAIA: Comitê de Ética em Pesquisa do Hospital de Clínicas de Porto Alegre (HCPA). MAVAN: Institutional Review Boards at hospitals and university affiliates: McGill University, l'Universite de Montreal, the Royal Victoria Hospital, Jewish General Hospital, Centre Hopitalier de l'Universite de Montreal, Hôpital Maisonneuve-Rosemont, St Joseph's Hospital, and McMaster University. Written informed consent to participate in this study was provided by the participants' legal guardian/next of kin.

AUTHOR CONTRIBUTIONS

RDM, GS, MM, RL, GM, and PS were responsible for the study concept and design. RDM, TM, RR, DR, AM, RT, and ABo contributed to the acquisition of clinical data. RMD, EM, LM, AF, ABu, and SB assisted with fMRI data acquisition and/or analysis. RMD, EM, and PS contributed to the statistical analysis of the study. RDM and EM drafted the manuscript and PS and MM provided critical revisions on the manuscript for important intellectual content. All authors contributed to the article and approved the submitted version.

FUNDING

Universal National Counsel of Technological and Scientific Development (CNPq) (Silveira PP, 478820/2010-0); Foundation for the Coordination of Higher Education and Graduate Training (PNPD/CAPES, 3024/2010); Fundo de Incentivo à Pesquisa (FIPE/HCPA), Canadian Institutes of Health Research (CIHR) [PJT-166066 and PJT - 173237 to PI PPS], and the JPB Foundation through a grant to the JPB Research Network on Toxic Stress: A Project of the Center on the Developing Child at Harvard University. Dr. Levitan acknowledges support from the Cameron Holcombe Wilson Chair in Depression studies, CAMH and University of Toronto.

ACKNOWLEDGMENTS

We thank the MAVAN and PROTAIA study groups and all staff. The voluntary participation of all participants is greatly appreciated.

SUPPLEMENTARY MATERIAL

The Supplementary Material for this article can be found online at: https://www.frontiersin.org/articles/10.3389/fendo.2022.882532/full#supplementary-material

REFERENCES

1. Grilo L, Tocantins C, Diniz M, Gomes R, Oliveira P, Matafome P, et al. Metabolic Disease Programming: From Mitochondria to Epigenetics, Glucocorticoid Signalling and Beyond. *Eur J Clin Invest* (2021) 51(10): e13625. doi: 10.1111/eci.13625
2. de Mendonça E, Macêna M, Bueno N, de Oliveira A, Mello C. Premature Birth, Low Birth Weight, Small for Gestational Age and Chronic Non-Communicable Diseases in Adult Life: A Systematic Review With Meta-Analysis. *Early Hum Dev* (2020) 149:105154. doi: 10.1016/j.earlhumdev.2020.105154
3. Black RE, Victora CG, Walker SP, Bhutta ZA, Christian P, de Onis M, et al. Maternal and Child Undernutrition and Overweight in Low-Income and Middle-Income Countries. *Lancet* (2013) 382:427–51. doi: 10.1016/s0140-6736(13)60937-x
4. Barker DJP, Osmond C, Winter PD, Margetts B, Simmonds SJ. Weight in Infancy and Death From Ischaemic Heart Disease. *Lancet (London England)* (1989) 2:577–80. doi: 10.1016/S0140-6736(89)90710-1
5. Uauy R, Kain J, Corvalan C. How can the Developmental Origins of Health and Disease (DOHaD) Hypothesis Contribute to Improving Health in Developing Countries? *Am J Clin Nutr* (2011) 94:1759s–64s. doi: 10.3945/ajcn.110.000562
6. Salam RA, Das JK, Bhutta ZA. Impact of Intrauterine Growth Restriction on Long-Term Health. *Curr Opin Clin Nutr Metab Care* (2014) 17:249–54. doi: 10.1097/mco.0000000000000051
7. Dalle Molle R, Bischoff AR, Portella AK, Silveira PP. The Fetal Programming of Food Preferences: Current Clinical and Experimental Evidence. *J Dev Orig Health Dis* (2016) 7(3):222–30. doi: 10.1017/S2040174415007187
8. Neseliler S, Han J-E, Dagher A. "The Use of Functional Magnetic Resonance Imaging in the Study of Appetite and Obesity," In: H RBS, editor. *Appetite and Food Intake: Central Control*. Boca Raton, FL: CRC Press/Taylor & Francis (2017). doi: 10.1201/9781315120171-6
9. Plassmann H, O'Doherty J, Rangel A. Orbitofrontal Cortex Encodes Willingness to Pay in Everyday Economic Transactions. *J Neurosci* (2007) 27:9984–8. doi: 10.1523/JNEUROSCI.2131-07.2007
10. van der Laan L, de Ridder D, Viergever M, Smeets P. The First Taste Is Always With the Eyes: A Meta-Analysis on the Neural Correlates of Processing Visual Food Cues. *Neuroimage* (2011) 55(1):296–303. doi: 10.1016/j.neuroimage.2010.11.055
11. Suzuki S, Cross L, O'Doherty J. Elucidating the Underlying Components of Food Valuation in the Human Orbitofrontal Cortex. *Nat Neurosci* (2017) 20 (12):1780–6. doi: 10.1038/s41593-017-0008-x
12. Dimitropoulos A, Tkach J, Ho A, Kennedy J. Greater Corticolimbic Activation to High-Calorie Food Cues After Eating in Obese vs. Normal-Weight Adults. *Appetite* (2012) 58(1):303–12. doi: 10.1016/j.appet.2011.10.014
13. Duan S, Ji G, Li G, Hu Y, Zhang W, Wang J, et al. Bariatric Surgery Induces Alterations in Effective Connectivity Between the Orbitofrontal Cortex and Limbic Regions in Obese Patients. *Sci China Inf Sci* (2020) 63:1–11. doi: 10.1007/s11432-019-2817-x

14. Salum GA, Isolan LR, Bosa VL, Tocchetto AG, Teche SP, Schuch I, et al. The Multidimensional Evaluation and Treatment of Anxiety in Children and Adolescents: Rationale, Design, Methods and Preliminary Findings. *Rev Bras Psiquiatr* (2011) 33:181–95. doi: 10.1590/S1516-44462011000200015
15. Barbieri MA, Bettiol H, Silva AA, Cardoso VC, Simoes VM, Gutierrez MR, et al. Health in Early Adulthood: The Contribution of the 1978/79 Ribeirao Preto Birth Cohort. *Braz J Med Biol Res* (2006) 39:1041–55. doi: 10.1590/s0100-879x2006000800007
16. Kaufman J, Birmaher B, Brent D, Rao U, Flynn C, Moreci P, et al. Schedule for Affective Disorders and Schizophrenia for School-Age Children-Present and Lifetime Version (K-SADS-PL): Initial Reliability and Validity Data. *J Am Acad Child Adolesc Psychiatry* (1997) 36:980–8. doi: 10.1097/00004583-199707000-00021
17. Amorim P. Mini International Neuropsychiatric Interview (MINI): Validação De Entrevista Breve Para Diagnóstico De Transtornos Mentais. *Rev Bras Psiquiatr* (2000) 22:106–15. doi: 10.1590/s1516-44462000000300003
18. O'Donnell KA, Gaudreau H, Colalillo S, Steiner M, Atkinson L, Moss E, et al. The Maternal Adversity, Vulnerability and Neurodevelopment Project: Theory and Methodology. *Can J Psychiatry* (2014) 59(9):497–508. doi: 10.1177/070674371405900906
19. Pedreira CE, Pinto FA, Pereira SP, Costa ES. Birth Weight Patterns by Gestational Age in Brazil. *Acad Bras Cienc* (2011) 83:619–25. doi: 10.1590/s0001-37652011005000008
20. Kramer MS, Platt RW, Wen SW, Joseph KS, Allen A, Abrahamowicz M, et al. A New and Improved Population-Based Canadian Reference for Birth Weight for Gestational Age. *Pediatrics* (2001) 108:E35. doi: 10.1542/peds.108.2.e35
21. Kramer MS, Platt R, Yang H, McNamara H, Usher RH. Are All Growth-Restricted Newborns Created Equal(Ly)? *Pediatrics* (1999) 103:599–602. doi: 10.1542/peds.103.3.599
22. de Onis M, Onyango AW, Borghi E, Siyam A, Nishida C, Siekmann J. Development of a WHO Growth Reference for School-Aged Children and Adolescents. *Bull World Heal Organ* (2007) 85:660–7.doi: 10.2471/blt.07.043497
23. De Onis M, Lobstein T. Defining Obesity Risk Status in the General Childhood Population: Which Cut-Offs Should We Use? *Int J Pediatr Obes* (2010) 5:458–60. doi: 10.3109/17477161003615583
24. Pinheiro ABV, Lacerda EMA, Benzecry EH, Gomes MCS, Costa VM. Tabela Para Avaliação De Consumo Alimentar Em Medidas Caseiras. *Rio Janeiro: Atheneu* (2005).
25. USDA. *USDA National Nutrient Database for Standard Reference, Release*, Vol. 26. (2013). U.S. Department of Agriculture, Agricultural Research Service. 2013. USDA National Nutrient Database for Standard Reference, Release 26. Nutrient Data Laboratory Home Page, http://www.ars.usda.gov/ba/bhnrc/ndl.
26. Levitan RD, Rivera J, Silveira PP, Steiner M, Gaudreau H, Hamilton J, et al. Gender Differences in the Association Between Stop-Signal Reaction Times, Body Mass Indices and/or Spontaneous Food Intake in Pre-School Children: An Early Model of Compromised Inhibitory Control and Obesity. *Int J Obes* (2015) 39:614–9. doi: 10.1038/ijo.2014.207
27. Silveira PP, Portella AK, Kennedy JL, Gaudreau H, Davis C, Steiner M, et al. Association Between the Seven-Repeat Allele of the Dopamine-4 Receptor Gene (DRD4) and Spontaneous Food Intake in Pre-School Children. *Appetite* (2014) 73:15–22. doi: 10.1016/j.appet.2013.10.004
28. Vozzo R, Wittert G, Cocchiaro C, Tan WC, Mudge J, Fraser R, et al. Similar Effects of Foods High in Protein, Carbohydrate and Fat on Subsequent Spontaneous Food Intake in Healthy Individuals. *Appetite* (2003) 40:101–7. doi: 10.1016/s0195-6663(03)00003-5
29. Sladky R, Friston KJ, Trostl J, Cunnington R, Moser E, Windischberger C. Slice-Timing Effects and Their Correction in Functional MRI. *Neuroimage* (2011) 58:588–94. doi: 10.1016/j.neuroimage.2011.06.078
30. Friston KJ, Williams S, Howard R, Frackowiak RS, Turner R. Movement-Related Effects in fMRI Time-Series. *Magn Reson Med* (1996) 35:346–55. doi: 10.1002/mrm.1910350312
31. Ashburner J, Friston KJ. Unified Segmentation. *Neuroimage* (2005) 26:839–51. doi: 10.1016/j.neuroimage.2005.02.018
32. Ashburner J, Friston KJ. Voxel-Based Morphometry–the Methods. *Neuroimage* (2000) 11:805–21. doi: 10.1006/nimg.2000.0582
33. Wright IC, McGuire PK, Poline JB, Travere JM, Murray RM, Frith CD, et al. A Voxel-Based Method for the Statistical Analysis of Gray and White Matter Density Applied to Schizophrenia. *Neuroimage* (1995) 2:244–52. doi: 10.1006/nimg.1995.1032
34. Mikl M, Marecek R, Hlustik P, Pavlicova M, Drastich A, Chlebus P, et al. Effects of Spatial Smoothing on fMRI Group Inferences. *Magn Reson Imaging* (2008) 26:490–503. doi: 10.1016/j.mri.2007.08.006
35. Whitfield-Gabrieli S, Nieto-Castanon A. Conn: A Functional Connectivity Toolbox for Correlated and Anticorrelated Brain Networks. *Brain Connect* (2012) 2:125–41. doi: 10.1089/brain.2012.0073
36. Behzadi Y, Restom K, Liau J, Liu TT. A Component Based Noise Correction Method (CompCor) for BOLD and Perfusion Based fMRI. *Neuroimage* (2007) 37:90–101. doi: 10.1016/j.neuroimage.2007.04.042
37. Fox MD, Snyder AZ, Vincent JL, Corbetta M, Van Essen DC, Raichle ME. The Human Brain Is Intrinsically Organized Into Dynamic, Anticorrelated Functional Networks. *Proc Natl Acad Sci USA* (2005) 102:9673–8. doi: 10.1073/pnas.0504136102
38. Desikan RS, Segonne F, Fischl B, Quinn BT, Dickerson BC, Blacker D, et al. An Automated Labeling System for Subdividing the Human Cerebral Cortex on MRI Scans Into Gyral Based Regions of Interest. *Neuroimage* (2006) 31:968–80. doi: 10.1016/j.neuroimage.2006.01.021
39. Weissenbacher A, Kasess C, Gerstl F, Lanzenberger R, Moser E, Windischberger C. Correlations and Anticorrelations in Resting-State Functional Connectivity MRI: A Quantitative Comparison of Preprocessing Strategies. *Neuroimage* (2009) 47:1408–16. doi: 10.1016/j.neuroimage.2009.05.005
40. Volkow ND, Fowler JS. Addiction, a Disease of Compulsion and Drive: Involvement of the Orbitofrontal Cortex. *Cereb Cortex* (2000) 10:318–25. doi: 10.1093/cercor/10.3.318
41. Pauls D, Abramovitch A, Rauch S, Geller D. Obsessive-Compulsive Disorder: An Integrative Genetic and Neurobiological Perspective. *Nat Rev Neurosci* (2014) 15(6):410–24. doi: 10.1038/nrn3746
42. Robbins T, Vaghi M, Banca P. Obsessive-Compulsive Disorder: Puzzles and Prospects. *Neuron* (2019) 102(1):27–47. doi: 10.1016/j.neuron.2019.01.046
43. Bracht T, Soravia L, Moggi F, Stein M, Grieder M, Federspiel A, et al. The Role of the Orbitofrontal Cortex and the Nucleus Accumbens for Craving in Alcohol Use Disorder. *Transl Psychiatry* (2021) 11:1–10. doi: 10.1038/s41398-021-01384-w
44. Black WR, Lepping RJ, Bruce AS, Powell JN, Bruce JM, Martin LE, et al. Tonic Hyper-Connectivity of Reward Neurocircuitry in Obese Children. *Obes (Silver Spring)* (2014) 22:1590–3. doi: 10.1002/oby.20741
45. Fox J, Weisberg S. *An R Companion to Applied Regression*, *3rd*. Thousand Oaks CA: Sage (2019).
46. Barbieri MA, Portella AK, Silveira PP, Bettiol H, Agranonik M, Silva AA, et al. Severe Intrauterine Growth Restriction Is Associated With Higher Spontaneous Carbohydrate Intake in Young Women. *Pediatr Res* (2009) 65:215–20. doi: 10.1203/PDR.0b013e31818d6850
47. Crume TL, Scherzinger A, Stamm E, McDuffie R, Bischoff KJ, Hamman RF, et al. The Long-Term Impact of Intrauterine Growth Restriction in a Diverse U.S. Cohort of Children: The EPOCH Study. *Obes (Silver Spring)* (2014) 22:608–15. doi: 10.1002/oby.20565
48. Kaseva N, Wehkalampi K, Hemio K, Hovi P, Jarvenpaa AL, Andersson S, et al. Diet and Nutrient Intake in Young Adults Born Preterm at Very Low Birth Weight. *J Pediatr* (2013) 163:43–8. doi: 10.1016/j.jpeds.2012.12.076
49. Lussana F, Painter RC, Ocke MC, Buller HR, Bossuyt PM, Roseboom TJ. Prenatal Exposure to the Dutch Famine Is Associated With a Preference for Fatty Foods and a More Atherogenic Lipid Profile. *Am J Clin Nutr* (2008) 88:1648–52. doi: 10.3945/ajcn.2008.26140
50. Perala MM, Mannisto S, Kaartinen NE, Kajantie E, Osmond C, Barker DJ, et al. Body Size at Birth Is Associated With Food and Nutrient Intake in Adulthood. *PloS One* (2012) 7:e46139. doi: 10.1371/journal.pone.0046139
51. Kampmann FB, Grunnet LG, Halldorsson TI, Bjerregaard AA, Granstrøm C, Pires SM, et al. Being Born Small-for-Gestational-Age Is Associated With an Unfavourable Dietary Intake in Danish Adolescent Girls: Findings From the Danish National Birth Cohort. *J Dev Orig Health Dis* (2019) 10:488–96. doi: 10.1017/S2040174418000910
52. Portella AK, Silveira PP. Neurobehavioral Determinants of Nutritional Security in Fetal Growth-Restricted Individuals. *Ann N Y Acad Sci* (2014) 1331:15–33. doi: 10.1111/nyas.12390

53. Portella AK, Silveira PP. Parenting: Roots of the Sweet Tooth. *Sci (80-)* (2014) 345:1571–2. doi: 10.1126/science.345.6204.1571-c
54. Rudorf S, Hare TA. Interactions Between Dorsolateral and Ventromedial Prefrontal Cortex Underlie Context-Dependent Stimulus Valuation in Goal-Directed Choice. *J Neurosci* (2014) 34:15988–96. doi: 10.1523/JNEUROSCI.3192-14.2014
55. Abe H, Lee D. Distributed Coding of Actual and Hypothetical Outcomes in the Orbital and Dorsolateral Prefrontal Cortex. *Neuron* (2011) 70:731–41. doi: 10.1016/j.neuron.2011.03.026
56. Gruber O, Chadha Santuccione A, Aach H. Magnetic Resonance Imaging in Studying Schizophrenia, Negative Symptoms, and the Glutamate System. *Front Psychiatry* (2014) 5:32. doi: 10.3389/fpsyt.2014.00032
57. Pyhälä R, Hovi P, Lahti M, Sammallahti S, Lahti J, Heinonen K, et al. Very Low Birth Weight, Infant Growth, and Autism-Spectrum Traits in Adulthood. *Pediatrics* (2014) 134:1075–83. doi: 10.1542/PEDS.2014-1097
58. Grayson D, Fair D. Development of Large-Scale Functional Networks From Birth to Adulthood: A Guide to the Neuroimaging Literature. *Neuroimage* (2017) 160:15–31. doi: 10.1016/j.neuroimage.2017.01.079
59. Demir-Lira ÖE, Voss JL, O'Neil JT, Briggs-Gowan MJ, Wakschlag LS, Booth JR. Early-Life Stress Exposure Associated With Altered Prefrontal Resting-State fMRI Connectivity in Young Children. *Dev Cognit Neurosci* (2016) 19:107–14. doi: 10.1016/J.DCN.2016.02.003
60. Damaraju E, Phillips JR, Lowe JR, Ohls R, Calhou VD, Caprihan A. Resting-State Functional Connectivity Differences in Premature Children. *Front Syst Neurosci* (2010) 4:23. doi: 10.3389/FNSYS.2010.00023
61. Hoff GEAJ, Van den Heuvel MP, Benders MJNL, Kersbergen KJ, De Vries LS. On Development of Functional Brain Connectivity in the Young Brain. *Front Hum Neurosci* (2013) 7:650. doi: 10.3389/FNHUM.2013.00650
62. Xie C, Li SJ, Shao Y, Fu L, Goveas J, Ye E, et al. Identification of Hyperactive Intrinsic Amygdala Network Connectivity Associated With Impulsivity in Abstinent Heroin Addicts. *Behav Brain Res* (2011) 216:639–46. doi: 10.1016/J.BBR.2010.09.004
63. Reis RS, Bernardi JR, Steiner M, Meaney MJ, Levitan RD, Silveira PP. Poor Infant Inhibitory Control Predicts Food Fussiness in Childhood - A Possible Protective Role of N-3 PUFAs for Vulnerable Children. *Prostaglandins Leukot Essent Fat Acids* (2015) 97:21–5. doi: 10.1016/j.plefa.2015.03.004
64. Silveira PP, Agranonik M, Faras H, Portella AK, Meaney MJ, Levitan RD. Preliminary Evidence for an Impulsivity-Based Thrifty Eating Phenotype. *Pediatr Res* (2012) 71:293–8. doi: 10.1038/pr.2011.39
65. Volkow N, Wang G, Baler R. Reward, Dopamine and the Control of Food Intake: Implications for Obesity. *Trends Cogn Sci* (2011) 15(1):37–46. doi: 10.1016/j.tics.2010.11.001
66. Lee S, Lee E, Ku J, Yoon KJ, Namkoong K, Jung YC. Disruption of Orbitofronto-Striatal Functional Connectivity Underlies Maladaptive Persistent Behaviors in Alcohol-Dependent Patients. *Psychiatry Investig* (2013) 10:266–72. doi: 10.4306/pi.2013.10.3.266
67. Zhu X, Cortes CR, Mathur K, Tomasi D, Momenan R. Model-Free Functional Connectivity and Impulsivity Correlates of Alcohol Dependence: A Resting-State Study. *Addict Biol* (2017) 22(1):206–17. doi: 10.1111/adb.12272
68. Contreras-Rodríguez O, Albein-Urios N, Vilar-López R, Perales JC, Martínez-Gonzalez JM, Fernández-Serrano MJ, et al. Increased Corticolimbic Connectivity in Cocaine Dependence Versus Pathological Gambling Is Associated With Drug Severity and Emotion-Related Impulsivity. *Addict Biol* (2016) 21(3):709–18. doi: 10.1111/adb.12242
69. Jin C, Zhang T, Cai C, Bi Y, Li Y, Yu D, et al. Abnormal Prefrontal Cortex Resting State Functional Connectivity and Severity of Internet Gaming Disorder. *Brain Imaging Behav* (2016) 10:719–29. doi: 10.1007/S11682-015-9439-8
70. Zeng N, Wang M, Dong H, Du X, Dong G-H. Altered Dynamic Interactions Within Frontostriatal Circuits Reflect Disturbed Craving Processing in Internet Gaming Disorder. *CNS Spectr* (2022) 27(1):109–17. doi: 10.1017/S1092852920001832
71. Pilgaard K, Hammershaimb Mosbech T, Grunnet L, Eiberg H, Van Hall G, Fallentin E, et al. Differential Nongenetic Impact of Birth Weight Versus Third-Trimester Growth Velocity on Glucose Metabolism and Magnetic Resonance Imaging Abdominal Obesity in Young Healthy Twins. *J Clin Endocrinol Metab* (2011) 96:2835–43. doi: 10.1210/jc.2011-0577
72. Ravelli AC, van der Meulen JH, Osmond C, Barker DJ, Bleker OP. Obesity at the Age of 50 Y in Men and Women Exposed to Famine Prenatally. *Am J Clin Nutr* (1999) 70:811–6. doi: 10.1093/ajcn/70.5.811
73. Moonesinghe R, Khoury MJ, Janssens ACJW. Most Published Research Findings are False-But a Little Replication Goes a Long Way. *PloS Med* (2007) 4:e28. doi: 10.1371/JOURNAL.PMED.0040028
74. Zadvinskis IM, Melnyk BM. Making a Case for Replication Studies and Reproducibility to Strengthen Evidence-Based Practice. *Worldviews Evidence-Based Nurs* (2019) 16:2–3. doi: 10.1111/WVN.12349
75. Hill C, Saxton J, Webber L, Blundell J, Wardle J. The Relative Reinforcing Value of Food Predicts Weight Gain in a Longitudinal Study of 7–10-Y-Old Children. *Am J Clin Nutr* (2009) 90:276–81. doi: 10.3945/ajcn.2009.27479
76. Ayres C, Agranonik M, Portella AK, Filion F, Johnston CC, Silveira PP. Intrauterine Growth Restriction and the Fetal Programming of the Hedonic Response to Sweet Taste in Newborn Infants. *Int J Pediatr* (2012) 2012:657379. doi: 10.1155/2012/657379
77. Migraine A, Nicklaus S, Parnet P, Lange C, Monnery-Patris S, Des Robert C, et al. Effect of Preterm Birth and Birth Weight on Eating Behavior at 2 Y of Age. *Am J Clin Nutr* (2013) 97:1270–7. doi: 10.3945/ajcn.112.051151
78. Oliveira A, de Lauzon-Guillain B, Jones L, Emmett P, Moreira P, Ramos E, et al. Birth Weight and Eating Behaviors of Young Children. *J Pediatr* (2015) 166:59–65. doi: 10.1016/j.jpeds.2014.09.031
79. Stein AD, Rundle A, Wada N, Goldbohm RA, Lumey LH. Associations of Gestational Exposure to Famine With Energy Balance and Macronutrient Density of the Diet at Age 58 Years Differ According to the Reference Population Used. *J Nutr* (2009) 139:1555–61. doi: 10.3945/jn.109.105536

Conflict of Interest: The authors declare that the research was conducted in the absence of any commercial or financial relationships that could be construed as a potential conflict of interest.

Advantages of publishing in Frontiers

OPEN ACCESS
Articles are free to read for greatest visibility and readership

FAST PUBLICATION
Around 90 days from submission to decision

HIGH QUALITY PEER-REVIEW
Rigorous, collaborative, and constructive peer-review

TRANSPARENT PEER-REVIEW
Editors and reviewers acknowledged by name on published articles

Frontiers
Avenue du Tribunal-Fédéral 34
1005 Lausanne | Switzerland

Visit us: www.frontiersin.org
Contact us: frontiersin.org/about/contact

REPRODUCIBILITY OF RESEARCH
Support open data and methods to enhance research reproducibility

DIGITAL PUBLISHING
Articles designed for optimal readership across devices

FOLLOW US
@frontiersin

IMPACT METRICS
Advanced article metrics track visibility across digital media

EXTENSIVE PROMOTION
Marketing and promotion of impactful research

LOOP RESEARCH NETWORK
Our network increases your article's readership